Molecular Profiling of Acquired Resistance to Chemotherapy in Triple Negative Breast Cancer Cell Lines

Elaheh Ahmadzadeh

Division of Experimental Medicine

Faculty of Medicine

McGill University, Montreal

August 2015

A thesis submitted to McGill University in partial fulfillment of the requirements of the degree of Doctor of Philosophy

Table of Contents

List of Figures

List of Tables

Abbreviations

2-ME2	2-methoxyoestradiol
ABC	ATP binding cassette
ABCB1	ATP binding cassette B1
aCGH	Array comparative genomic hybridization
AREG	Amphiregulin
ATCC	American Type Culture Collection
BL1	Basal-like 1
BL2	Basal-like 2
BLBC	Basal-like breast cancer
BSA	Bovine serum albumin
BTC	Betacellulin
Cep7	Chromosome-7 centromeric probe
CNA	Copy number alteration
EGF	Epidermal growth factor
EGFR	Epidermal growth factor receptor
EMT	Epithelial to mesenchymal transition
EPGN	Epigen
ER	Estrogen receptor
EREG	Epiregulin
FISH	Fluorescence in situ hybridization
GAPDH	Glyceraldehyde-3-phosphate dehydrogenase
GO MF	Gene ontology molecular function
HB-EGF	Heparin-binding EGF
HER	Human epithelial receptor
HER2	Human epidermal receptor 2
HPRT1	Hypoxanthine phosphoribosyl-transferase 1
HR	Homologous recombination
IC50	Half maximal inhibitory concentration
IDC NOS	Invasive ductal carcinoma not otherwise specified
IHC	Immunohistochemistry
IL6	Interleukin 6
IM	Immunomodulatory
KD	Knock down
LAR	Luminal androgen receptor
LPS	Lipopolysaccharide
M	Mesenchymal
MAP	Microtubule-associated proteins

MAPK	Mitogen activated protein kinase
MDR1	Multi-drug resistance 1 gene
miRNA	MicroRNAs
MSL	Mesenchymal stem-like
NBD	Nucleotide-binding domain
NF-KB	Nuclear Factor-Kappa B
NF-ϰB	Nuclear factor-ϰB
NHEJ	Non-homologous end joining
NRG1	Neuregulin 1
P-gp	P-glycoprotein
PARP	Poly(ADP-ribose) polymerase
PBS	Phosphate buffer saline
PCA	Principal component analysis
pCR	Pathologic complete response
PEI	Polyethylenimine
PR	Progesterone receptor
PTB	Phospho-tyrosine binding
PTX	Paclitaxel
qRT-PCR	Quantitative Reverse transcription polymerase chain reaction
ROS	Reactive oxygen species
RTK	Receptor tyrosine kinases
SH2	Src homology 2
shRNA	Small hairpin RNA
TGF-α	Transforming growth factor alpha
TK	Tyrosine kinase
TKI	Tyrosine kinase inhibitor
TMD	Trans-membrane domain
TNBC	Triple negative breast cancer
TNF-α	tumour necrosis factor alpha
UTR	Untranslated region
ΔCNA	Differential copy number alteration

Abstract

Triple-negative breast cancer (TNBCs), characterized by tumours that do not express estrogen receptor (ER), progesterone receptor (PR), or HER-2 genes, shows one of the most aggressive clinical behaviors with distinctive metastatic patterns and very poor prognosis. Since no targeted therapy is available, chemotherapy and, in particular, taxane-based therapy (e.g. paclitaxel) is the treatment of choice for patients with TNBC. TNBCs are initially highly responsive to PTX, however the majority of advanced TNBC patients acquire resistance and develop progressive disease. Here we developed five *in vitro* models of resistance to better understand and characterize the biological mechanisms underlying resistance to PTX. We used an integrative analysis of array CGH and gene expression data to gain insights into the functional genomic changes in PTX-resistant TNBC cell lines. The results of integrative analysis of array CGH and gene expression identified ABCB1 as the most highly up-regulated gene in all 5 resistant cell lines. This up-regulation was accompanied by gene amplification in three resistant cell lines: BT20R, SUM149R and MDA-468 but not in 2 other lines, MDA-MB-231 and MDA-MB-436. Further analysis of the 7q21.12 chromosome fragment containing the ABCB1 gene in BT20R, SUM149R and MDA-468R revealed similar, but not identical, intra-genic breakpoints in ABCB1. RNAseq analysis identified novel inter-chromosomal translocations of ABCB1 in 2 drug resistance cell lines

containing ABCB1 breakpoints. These genomic rearrangements occurred in the 5' un-translated region (UTR) of ABCB1. We hypothesize that the deletion of the 5'UTR of ABCB1 in these resistant cell lines may serve to overcome a translation initiation block, which would then favor the expression of ABCB1. The overexpression of ABCB1 at protein level was confirmed only in the three resistant cell lines with the ABCB1 genomic rearrangement, suggesting that the deletion of 5'UTR of ABCB1 may be a candidate biomarker to predict resistance to paclitaxel in triple negative breast cancers.

In order to better understand the biological significance of the observed changes we performed pathway analysis and identified enriched molecular function of deregulated genes common in resistant cell lines. We found that the molecular function "growth factor activity", including several epidermal growth factor receptor (EGFR) ligands was consistently up-regulated in all 5 resistant cell line models. Considering the importance of EGFR ligands and given the up-regulation of EGFR signaling pathway, we examined the sensitivity of all five cell line models to two EGFR inhibitors, lapatinib and neratinib in combination with PTX. Our results revealed that the addition of 100nM of lapatinib or neratinib partially re-sensitized resistant cell lines to PTX to various degrees, with one exception: BT20R did not show sensitivity to the addition of 100nM lapatinib to increasing concentration of PTX. These results suggest that anti-EGFR therapies can

re-sensitize PTX-resistant TNBC cells to PTX and that up-regulation of EGFR ligands in PTX resistant cell lines may be a biomarker of sensitivity to EGFR inhibitors.

Résumé

Le cancer du sein triple-négatif (TNBC), caractérisé par des tumeurs qui n'expriment ni le récepteur aux estrogènes (RO), ni le récepteur à la progestérone (PR) ou ni les gènes HER-2, constitue une évolution des plus agressive avec des profils métastatiques particuliers et un très sombre pronostic. Puisqu'aucune thérapie ciblée n'est à ce jour disponible, la chimiothérapie, et en particulier la thérapie à base de Taxanes (Placlitaxel), représente le traitement de référence pour les patientes atteint de TNBC. Les TNBC répondent initialement fortement au paclitaxel (PTX), cependant la majorité des patientes aux stades avancés développent des résistances et la maladie progresse. *In vitro*, nous avons développé cinq modèles de résistance dans le but de mieux comprendre et caractériser les mécanismes biologiques sous-tendant la résistance. Nous avons utilisé une analyse intégrée de array-CGH et des données d'expression de gènes pour comprendre les changements génomiques fonctionnels dans des lignées cellulaires TNBC résistantes au PTX. Les résultats de ces analyses ont identifié ABCB1 comme étant le gène plus fortement sur-exprimé parmi les cinq lignées cellulaires résistantes. Cette sur-expression était accompagnée d'une amplification du gène dans trois lignées résistantes : BT20R, SUM149R et MDA-468, mais pas dans les deux autres lignées, MDA-MB-231 et MDA-MB-436. Des analyses complémentaires d'un fragment du chromosome 7q21.12 contenant le gène ABCB1 dans BT20R, SUM149R et

MDA-468R révèlent des cassures intra-géniques similaires mais non identiques. Une analyse RNAseq a identifié de nouvelles translocations intra-chromosomiques de ABCB1 dans deux lignées cellulaires résistantes contenant les cassures de ABCB1. Ces réarrangements génomiques se localisaient dans la région «5' non-traduite region» (UTR) de ABCB1.

Notre hypothèse est que la délétion de la région 5'UTR de ABCB1 dans ces lignées cellulaires résistantes pourrait servir à surmonter un blocage initial de la traduction et pourrait ensuite favoriser l'expression de la protéïne Abcb1. La surexpression de ABCB1 à un niveau protéique a été confirmée seulement dans les trois lignées résistantes contenant les réarrangements génomiques ABCB1, suggérant que la délétion de la région 5'UTR dans ABCB1 serait un bio-marqueur potentiel pour prédire la résistance au Paclitaxel dans les TNBC. Dans le but de mieux comprendre la signification biologique des changements observés, nous avons pratiqué des analyses de voies moléculaires et avons identifié une fonction moléculaire enrichie chez les gènes dérégulés dans les lignées résistantes. Nous avons trouvé que la fonction moléculaire d'« activité de facteur de croissance », incluant plusieurs ligands du récepteur « Epidermal Growth Factor Receptor » (EGFR), étaientsystématiquement sur-exprimés dans les cinq modèles de lignées cellulaires résistantes. Considérant l'importance des ligands au EGFR et étant donné leur sur-expression, nous avons examiné la sensibilité des cinq modèles cellulaires à deux inhibiteurs de EGFR, Lapatinib et Neratinib en association avec le PTX. Nos résultats ont révélé que l'ajout de

100nM de Lapatinib ou Neratinib re-sensibilisait partiellement les lignées résistantes au PTX à des degrés variables, avec une exception : BT20R n'a pas montré de sensibilisation à l'addition de 100nM de Lapatinib à des concentrations croissantes de PTX. Ces résultats suggèrent que des thérapies anti-EGFR pourraient re-sensibiliser les cellules de TNBC résistantes au PTX ; et cette sur-expression des ligands du EGFR dans les cellules résistantes au PTX pourrait constituer un bio-marqueur de sensibilité aux inhibiteurs du EGFR.

Acknowledgements

I would like to thank my supervisor, Dr. Mark Basik, for accepting me as a PhD student and for giving me the opportunity to learn cutting-edge techniques used in his laboratory. His invaluable insight and broad clinical vision helped me grow as a student, researcher and as a person.

I would like to express my sincere gratitude to the members of my PhD advisory committee for their kind advice and support: Dr. Martine Raymond, Dr. Sylvie Mader, Dr. Raquel Aloyz and Dr. Josie Ursini-Siegal. It is my pleasure to acknowledge my external examiner, Dr. Amadeo Parissenti, for his critical appraisal of my PhD dissertation. I also want to thank the division of Experimental Medicine and specifically Dominique Besso and Marylin Linhares for their understanding and their support.

I wish to thank Dr. Ivan Topisirovic and Dr. Léon van Kempen for their constructive suggestions. I am exceptionally grateful to Dr. Mounib Elchebly for kindly teaching me the techniques required for my research, and for selflessly sharing his knowledge and experience with me. I would also like to thank Dr. Ewa Przybytkowski, Dr. Anke van Rijk, Dr. Naciba Benlimame, Christian Young and Chris Polykandriotis for their unwavering support and their patience.

I had the privilege of being motivated by exceptionally talented friends and colleagues, in particular, Dana Keilty, Alicia Bolt, Sanne Janssen, Samuel Lagabrielle, Laura Hulea, and Valentina Gandin. Thank you, my friends, for your companionship and abundantly helpful feedback.

Finally, but most importantly, I would like to express gratitude beyond words to my family, especially my father, Seyed Ahmad Ahmadzadeh, and my mother, Bibi Ozra Nabavi, who have always valued education and taught me perseverance, honesty, and integrity. I am eternally grateful for your unconditional love, and it gives me great pleasure to dedicate this thesis to you.

Preface and contribution of authors

The work presented in this thesis encompasses our investigation into the genomic landscape of drug resistance in triple negative breast cancer (TNBC) and constitutes novel contributions to the field of drug resistance. Over the years, more and more research has emerged surrounding the identification of new biomarkers of resistance in TNBCs, yet no validated biomarker currently exists for appropriate selection of patients for chemotherapy treatment. To address this issue, this thesis embarks on studying the mechanisms underlying paclitaxel-resistance, one of the main obstacles in treatment of TNBCs. The molecular changes during the development of drug resistance to paclitaxel is explored in depth in this thesis using in vitro models in conjunction with high resolution array comparative genomic hybridization, gene expression profiling and RNA seq. We identified novel genomic amplifications and rearrangements responsible for paclitaxel resistance in drug-resistant TNBC cell lines generated as part of this project. Furthermore, we showed that up-regulation of a set of EGFR ligands may be a biomarker of sensitivity to EGFR inhibitors in combination with PTX.

The work presented in this thesis was mainly performed by myself. I developed the PTX-resistant TNBC cell lines used in this study and performed gene expression and array CGH profiling in TNBC cell lines. The analysis of gene expression data was carried out in collaboration with

François Lefebvre and the bioinformatic analysis of RNA seq data was performed by Eric Bareke. Anke Van rijk performed the optimization of FISH for ABCB1. All other experiments and analyses were done by myself. All the figures in this manuscript are based on experiments that I performed. I constructed all the figures and wrote the first draft of the manuscript.

Chapter 1

Introduction

1.1. Cancer

Cancer is caused by the accumulation of randomly occurring mutations and epigenetic alterations of DNA that modulate the expression of genes controlling cell proliferation, survival and other traits associated with neoplastic transformation [1]. This multistep process has been linked to Darwinian evolution, in which beneficial genetic changes, conferring growth advantages, leads to the progressive transformation of normal human cells into highly malignant derivatives. There is a number of molecular, biochemical and cellular traits that are commonly shared by most types of cancer.

Hanahan and Weinberg described six key processes, which must be deregulated in the cell for progression to malignancy. These hallmarks of cancer include "sustaining proliferative signaling, evading growth suppressors, resisting cell death, enabling replicative immortality, inducing angiogenesis and activating invasion and metastasis" [1, 2]. Each of these essential alterations in cell physiology "represent the successful breaching of an anticancer defense mechanism hardwired into cells and tissues" [2]. Recently, Hanahan and Weinberg have suggested two additional hallmark features that contribute to the tumour development including reprogramming of energy metabolism and evading immune destruction. In addition, they proposed two enabling characteristics crucial to the acquisition of the described hallmark capabilities, including tumour-

promoting inflammation and genomic instability [1]. These capabilities are mostly acquired, directly or indirectly, through changes in the genome, which generates the genetic diversity that expedites their acquisition. Since I am primarily interested in breast cancer, I will focus on the details of some of these characteristics in breast cancer.

1.2. The breast

The mature female breast is composed of skin and subcutaneous tissue, fibroglandular tissue, and a supporting stroma. The fibroglandular component consists of lobules, which produce milk during lactation, and ducts, which are tubular structures that transport milk from the lobules to the nipple (Figure 1). In most women, there are 15-20 lobes in each breast arranged in a radial pattern emanating from the nipple area. The breast stroma contains fat, ligaments, nerves, arteries, veins, and lymphatics. The lymph vessels are thin walled, valved structures that filter and transfer lymph fluid away from the breast into lymph nodes. The breast lymphatics drain primarily to the axillary nodes, and also to the internal mammary nodes [3].

Histologically, the normal duct-lobular system of the breast is composed of two epithelial cell types, the inner layer of luminal epithelial cells and an outer layer of contractile myoepithelial cells. These structures are separated from the interstitial stroma by an intact basement membrane. The luminal epithelial cells are polarized glandular cells, which are potential milk secreting cells.

The myoepithelial cells form the basement membrane and are responsible for the contractile phenotype of the breast [4, 5].

The luminal epithelial compartments of the breast ductal network are the origin of the majority of malignant breast cancers. However, 2-18% of all invasive ductal carcinomas arise from myoepithelial cells [6].

1.3. Breast Cancer

Breast cancer is the most commonly diagnosed cancer in women worldwide and is the leading cause of cancer related death among women in both developed and developing countries. It is estimated that more than 1.4 million women are diagnosed with breast cancer every year, of whom approximately one-third die of the disease [7]. Several risk factors have been identified for breast cancer including age, family history of heritable gene mutations and factors that involve prolonged hormonal exposure, such as early menarche, low parity, older age at first live birth, late menopause, and hormone replacement therapy [8].

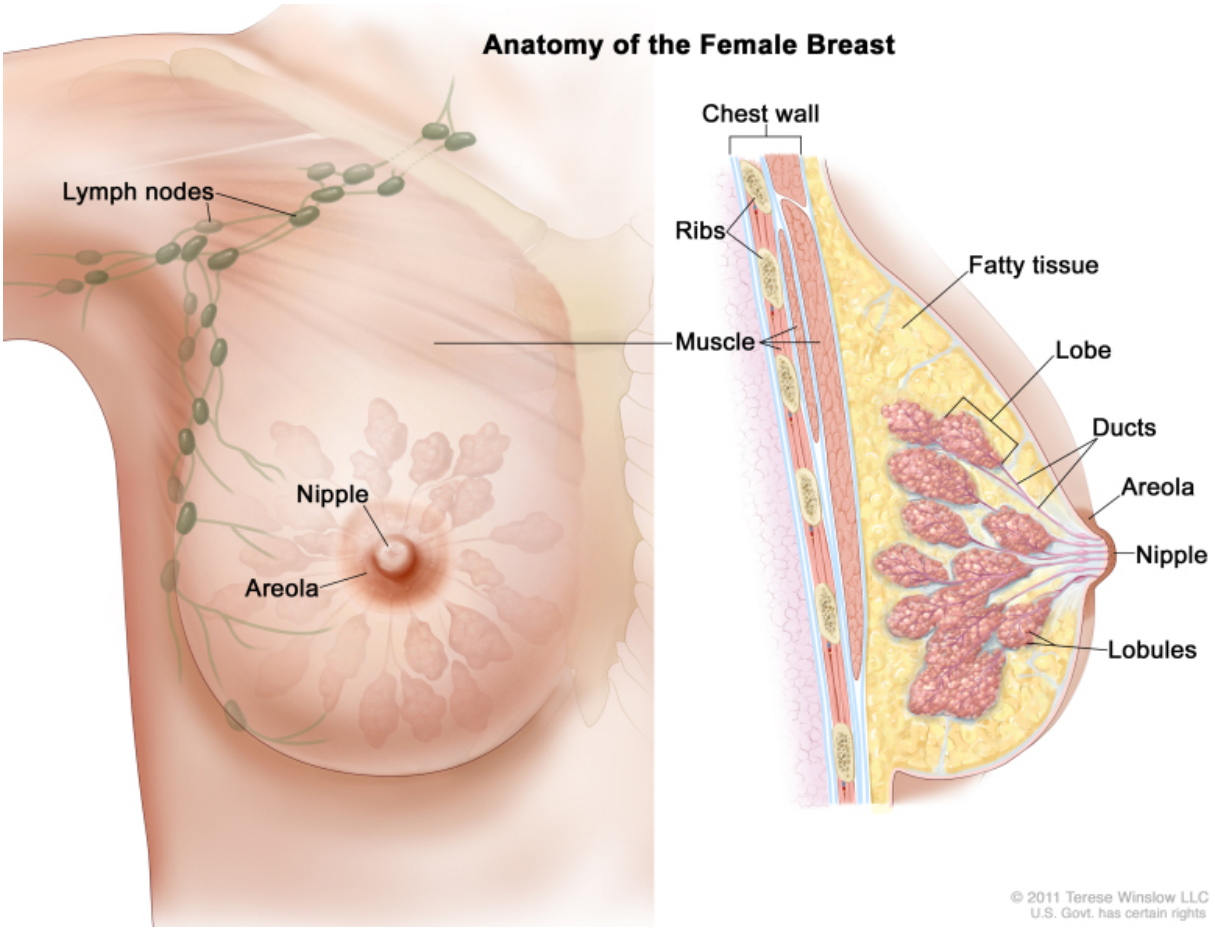

Figure 1.1. Anatomy of the female breast. The figure depicts the anatomical structure of the breast including the nipple and areola on the outside of the breast, the lymph nodes, lobes, lobules, ducts, and other parts on the inside of the breast. This figure was reproduced from Terese Winslow LLC Medical Illustration, For the National Cancer Institute ©2012. Available from: http://www.teresewinslow.com [9].

1.3.1. Breast cancer classification

Breast cancer is a heterogeneous disease that exhibits several histological and biological features, various clinical outcome and different responses to systemic interventions. These differences in breast cancer have served as the basis for disease classification.

Clinical pathology has segregated breast carcinomas into 18 different subtypes based on the diversity of the morphological features and structural organization. The most common histopathological types are 'invasive ductal carcinoma not otherwise specified' (IDC NOS) and invasive lobular carcinoma, which collectively represent the vast majority of breast carcinomas [4]. This classification is adopted worldwide, and is reasonably reproducible and together with tumour grade and stage has prognostic implications. However, it is unable to mirror the heterogeneity of breast cancer and has minimal predictive implications [10].

While histopathological classification provides prognostic value, the lack of a molecular component to the classification limits its ability to predict a response to targeted therapies. In the last decades, intense research efforts have led to the identification of molecular markers to categorize breast cancer patients, in order to assess prognosis and determine the most appropriate therapy with standard pathological techniques such as immunohistochemistry (IHC). These markers include estrogen receptor (ER), progesterone receptor (PR), and human epidermal

receptor 2 (HER2). Combinations of these markers allow for the assignment of individual cases to specific categories including, ER^+ ($ER^+/HER2^-$), $HER2^+$ ($ER^-/HER2^+$), triple negative (TN; $ER^-/PR^-/HER2^-$), and triple positive ($ER^+/PR^+/HER2^+$). Recent guidelines include that a threshold of >1% positive tumour nuclei in the sample on ER and PgR assays should be considered as hormone-receptor positive.

The ER expression provides an index for sensitivity to endocrine treatments, including ER antagonists or aromatase inhibitors, which target ER dependent signaling. ER^+ breast cancer is the most common type of breast cancer and patients with ER^+ tumour exhibit the best overall outcome. Breast cancers with amplification and overexpression of HER2, seen in approximately 15-20% of invasive breast cancers, benefit from HER2 targeted therapies. HER2 amplification, assessed in case of equivocal protein expression levels, is detected by fluorescence in situ hybridization (FISH) [4, 11]. TN tumours, on the other hand, are linked to the worst prognosis and do not respond to endocrine therapy or treatments against HER2.

1.3.1.1. Intrinsic Molecular subtype of breast cancer

Based on comprehensive gene expression profiling and hierarchical clustering, Perou and his colleagues identified molecular subtypes of breast cancer that reflected the original immunopathological classes to some extent [12]. The intrinsic molecular subtype provided

biological information and allowed for the classification of breast cancer into four intrinsic subtypes: luminal, HER2, basal-like and normal-like. The subsequent expansion of this work in a larger cohort of patients showed that the luminal subgroup could be divided into luminal A and B; both contain principally ER cases and are distinguished by the presence of genes regulated by the ER signaling pathway, however they were associated with different prognosis. The ErbB2$^+$ subtype generally overlaps with IHC-defined HER2$^+$ tumours and is associated with poor prognosis.

Basal-like subtype, representing 10–20% of all breast carcinomas, broadly corresponds to the TN (ER$^-$/PR$^-$/HER2$^-$) tumours. Basal-like was referred to as basal-like because of the unique expression of high molecular weight cytokeratins (CK5, CK14, CK17), which are associated with normal myoepithelial cells of the outer layer of breast duct and are typically expressed in the basal epithelial layer of the skin and airways [13, 14]. These tumours also express high levels of smooth muscle markers, P-cadherin and EGFR, along with caveolin 1, meosin, and β4 integrin [15-17]. By contrast, they express low RNA levels of *ESR1*, *PGR* and *ERBB2*. Basal-like tumours have a worse prognosis than do luminal ones with a higher relapse rate in the first 3 years [18].

Normal-like molecular subtype, which resembles normal epithelial tissue, accounts for about 5–10% of all breast carcinomas [4, 12]. These tumours express genes characteristic of adipose tissue,

presenting an intermediate prognosis between luminal and basal-like and usually lack the expression of ER, PR and HER2, so these tumours can also be classified as TN, without being considered basal-like as they are negative for CK5 and EGFR. The existence and clinical significance of these tumours remains to be determined since no cases of normal breast subtype were found in a large series of samples isolated by micro-dissection, supporting the hypothesis that this tumour subtype is a technical artefact from contamination of samples with normal tissue during microarray experiments [19].

After the initial molecular classification into subtypes of breast cancer, unsupervised clustering analysis of the combined gene expression data for 232 human breast tumours revealed a new intrinsic subtype which is referred to as claudin-low. The claudin-low subtype is characterized by a low expression of many claudin genes including claudin-3, -4, -7 cingulin, ocludin, and E-cadherin. The claudin-low tumours are also triple negative, and therefore can be classified as another subtype of triple-negative disease [14].

The immunohistochemically and molecularly defined classes do not completely overlap. For example TN breast cancer (TNBC) and basal-like breast cancer (BLBC) breast cancer definitions have been used interchangeably to identify breast cancers that lack expression of the hormone receptors and overexpression and/or amplification of HER2. The majority of basal-like breast

cancers do exhibit low levels of ER and PR and lack HER2 protein overexpression and ErbB2 gene amplification, however, there is 30% discordance between the basal-like and triple negative breast cancer subtype. Some basal-like breast cancers do not show the expected TN immunophenotype, and vice versa not all the immunohistochemically triple-negative breast cancer are classified as basal-like by gene expression profiling [12].

Gene expression profiling of cell lines has identified two distinct basal groups (A and B). Basal A cell lines display epithelial characteristics and are keratin 5 and 14 positive. On the other hand, Basal B are more invasive and display mesenchymal features including vimentin expression [20]. Supporting the argument that the Basal B subtype is not a cell culture artifact, this sub-classification and the existence of mesenchymal tumours was supported by immunohistochemical studies detecting the expression of vimentin in basal like primary breast tumours [21].

The term, TNBC, is used in this study to refer to any breast cancers that do not express the genes for ER, PR or Her2.

1.3.2. Triple Negative Breast Cancer

Triple negative breast cancers (TNBC) represent approximately 15%-20% of all breast cancers; however, it is responsible for a disproportionate number of breast cancer deaths. TNBCs more

frequently affect women of younger age, and are more prevalent in African-American women [22, 23]. Morphologically, TNBC are highly cellular tumours characterized by solid architecture with little or no tubule formation, high nuclear grade, high mitotic count, and necrosis. Patients with TNBC are more likely to have grade III tumours, larger in size and a higher rate of lymph node involvement at diagnosis [22]. TNBCs are characterized by aggressive tumour biology resulting in a poor prognosis. This aggressiveness is best exemplified by the fact that the peak risk of recurrence is between the first and third years after diagnosis and the majority of deaths occur in the first 5 years [22, 24]. Women with TNBC have higher risk of recurrence and significantly shorter overall survival following the first metastatic event compared to women with other types of breast cancer [22, 25, 26].

1.3.2.1. Molecular aspects of Triple negative

A predominant characteristic of TNBC is genomic instability, which refers to an increased rate of genomic alteration, and is believed to be necessary for cells to accumulate the multiple mutations required for cancer to develop. TNBCs show a high degree of genomic instability resulting in a high rate of aneuploidy; chromosomal changes, translocations, gains and losses [13].

One copy number alteration (CNA) frequently reported in BLBC is loss of chromosome 5q11, where important genes involved in *BRCA1*-dependent DNA repair, such as *RAD17*, *RAD50* and

RAP80, are located [27, 28]. In fact, Weigman et al. observed that a great majority of tumours with 5q11 loss, harbour 13q14.2 (RB1) deletion and more than half of those tumours 17p13.1 (*TP53*) loss co-occurs [29]. Although TNBCs do not exhibit many frequent recurrent structural rearrangements, CNA of *PARK2*, *RB1*, *PTEN* and *EGFR* is frequently observed [30].

Mutation or loss of *TP53* tumour suppressor gene is one of the most common recurrent genetic abnormalities observed in TNBC. TP53 is a master caretaker that mediates cellular response to DNA damage. Mutations in *PIK3CA*, *USH2A*, *MYO3A*, *PTEN* and *RB1* are frequently observed in basal breast cancers [13, 30]. The most deleterious DNA damage is double stranded breaks, which are repaired by either homologous recombination (HR) or with non-homologous end joining (NHEJ). An important mediator in HR repair is BRCA1. In the context of *BRCA1* mutation, DSBs cannot be efficiently repaired by HR. The dysfunction of HR repair would lead to activation of NHEJ, the alternative highly error-prone repair pathway, which results in chromosomal rearrangements and copy-number changes [25, 31]. There is a strong association of *BRCA1* germline mutations, one of the most important types of hereditary breast cancer, with TNBC. The majority of tumours arising in women carrying a germline *BRCA1* mutation, in particular those that are diagnosed under the age of 50, possess TNBC morphological features. The morphological features of BRCA1 tumours, including high histological grade, atypical medullary features, high

proliferation indices, pushing borders and conspicuous lymphocytic infiltrate, are remarkably similar to TNBCs [21, 32].

1.3.2.2. Triple negative breast cancer stratification

TNBC, itself, is a highly heterogeneous disease that exhibits distinct molecular subtypes with differential response to chemotherapy and targeted agents. It has been shown that a subset of patients who respond to treatment and achieve pathological complete response, have higher survival rate compare to patients with residual disease after chemotherapy [33]. To better understand the molecular basis of heterogeneity within TNBC, Lehmann and his colleagues, performed gene expression data analysis of 587 TNBC tumours, obtained from publicly available datasets, to identify distinct molecular subtypes displaying unique biology and drug sensitivity. Cluster analysis of TNBC revealed six distinct molecular subtypes including two basal-like (BL1 and BL2), an immunomodulatory (IM), a mesenchymal (M), a mesenchymal stem-like (MSL), and a luminal androgen receptor (LAR) subtype (Figure 2) [34].

The BL1 subtype is heavily enriched in cell cycle and cell division pathway components including increased RNA expression of *AURKA*, *AURKB*, *CENPA*, *CENPF*, *BUB1*, *TTK*, *CCNA2*, *PRC1*, *MYC*, *NRAS*, *PLK1*, and *BIRC5*. High expression of genes associated with proliferation is accompanied by decreased expression of genes regulating cell cycle checkpoints and elevated

DNA damage response (ATR/BRCA) pathways. The BL2 subtype is enriched in active growth factor signaling pathways including EGF, MET, and Wnt/β-catenin pathways. In addition it is also enriched for genes involved in energy metabolism including glycolysis and gluconeogenesis, and the expression of myoepithelial markers (TP63 and MME). The IM subtype displays transcriptomic gene ontologies involved in immune cell processes, immune signal transduction pathways and cytokine signaling. Both the M and MSL subtypes have high expression of genes associated with epithelial to mesenchymal transition (EMT) accompanied by genes involved in cell motility and cell differentiation. The LAR subtype includes tumours that are characterized by genes involved in androgen receptor signaling [34, 35].

Because the limited number of known biomarkers and absence of common molecular alterations in TNBC tumours have limited the development of therapeutic strategies, this stratification of TNBC tumours may lead to better biomarker selection, drug discovery, and clinical trial design that will enable more appropriate treatment.

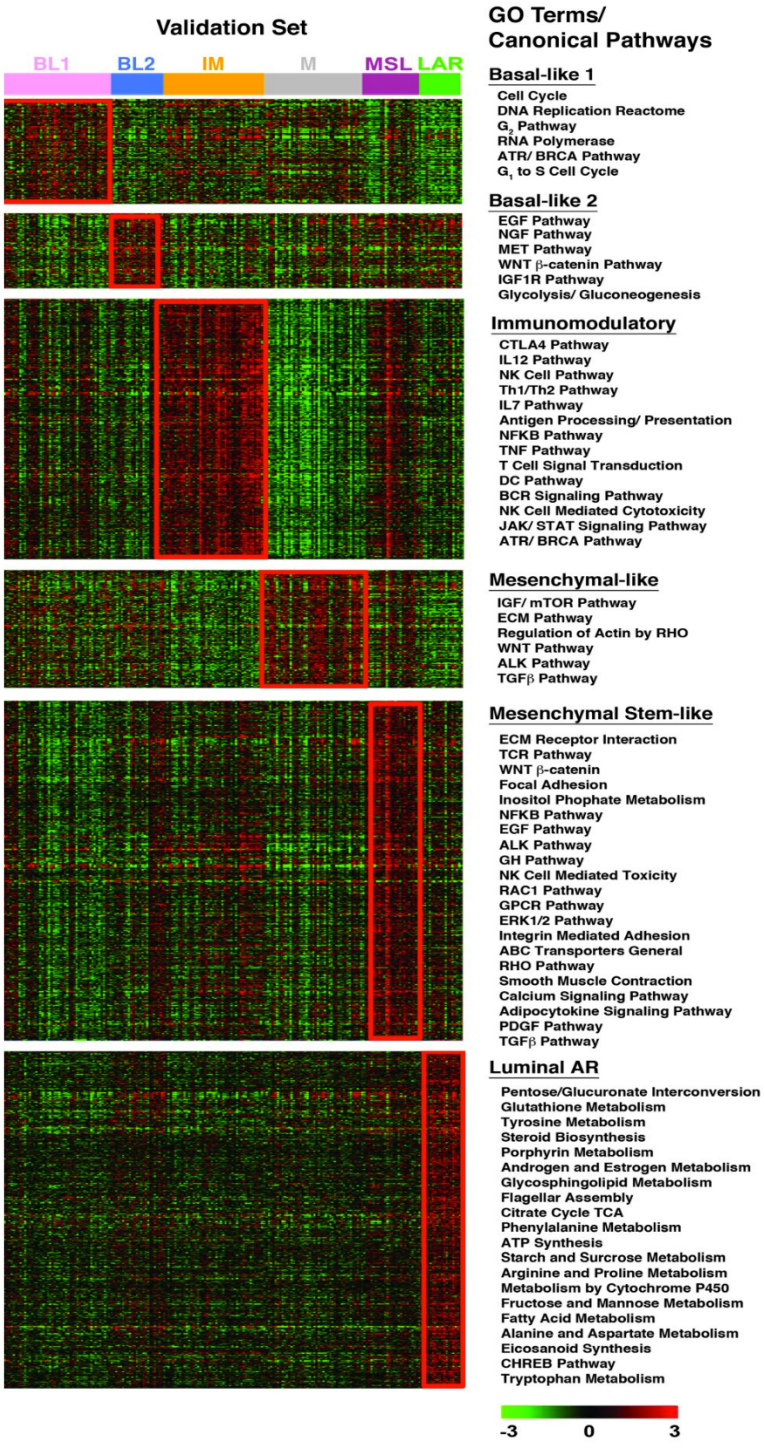

Figure 1.2. TNBC molecular classification. Heat map analysis of TNBC showing the relative gene expression of differentially expressed genes in each subtype. This figure was reproduced from "Lehmann, B.D., et al., J Clin Invest, 2011" [34].

1.3.3. Treatment Strategies for TNBC

To date, there is currently no accepted molecularly targeted agents against TNBC and no specific treatment guidelines for TNBCs published. Due to the lack of ER, PR and HER2 expression, TNBCs are not amenable to hormone therapy or therapies against HER2, making treatment options limited to standard chemotherapy including anthracyclines, taxanes and cyclophosphamide.

TNBCs are characterized by the high expression of the proliferation markers, including Ki-67 and therefore highly chemosensitive [12]. Numerous studies have demonstrated the effectiveness of chemotherapy in the treatment of TNBC in the neoadjuvant, adjuvant and metastatic settings. Patients with TNBC achieve higher rates of complete pathologic response (pCR) compared to hormone positive subtypes of breast cancer [36-38]. A prospective study of 1,118 patients, recruited at the MD Anderson Cancer Center, demonstrated a higher response to neoadjuvant chemotherapy resulting in significant improvements in pCR; a pCR was seen in 22% of patients with TNBC compared with 11% of patients with non-TNBC. Among all types of TNBCs, patients with a high proliferative index, as measured by Ki-67, exhibit a higher pCR and those who achieved a pCR had an excellent long term outcome [39]. However, patients with residual disease

after neoadjuvant chemotherapy had significantly worse survival if they had TNBC compared with non-TNBC, particularly in the first 3 years [40].

Current standard, systemic chemotherapy consists largely of Anthracycline/taxane-based adjuvant or neoadjuvant regimens, which have been shown to be highly effective in TNBC. The most widespread approved therapeutic regimens are based on combinations of an anthracycline, a taxane, and/or an alkylating agent (typically cyclophosphamide). Several studies have demonstrated that the addition of taxanes to anthracycline-based chemotherapy increases pCR rate as well as disease-free survival in breast cancer patients [41-43].

The interesting association of TNBC tumours with BRCA1 germline mutations has attracted attention to platinum-based regimens as an emerging option for their treatment. Platinum agents act through the formation of DNA crosslinks, resulting in double-stranded DNA breaks. A BRCA1 mutation disrupts the ability of the cells to recover from DNA damaging agents by reducing its repair DNA capacity through homologous recombination [42, 44, 45]. This leads to activation of more error prone repair pathways, which rely on Poly (ADP-ribose) polymerase (PARP). Drugs that inhibit PARP activity lead to the accumulation of structural DNA lesions, which results in genomic catastrophe and finally apoptotic cell death [46]. Several PARP inhibitors are in clinical trials as mono- or combination therapies to assess the toxicities, the

efficacies and the benefit of the drugs. Preliminary clinical evidence with BRCA mutant patients supports the efficacy of PARP inhibitor, Olaparib. [47].

The response of TNBCs to taxanes and the mechanisms of resistance to taxanes are the main focus of my PhD project. Hence, I will focus on the mechanism of action of taxanes and then mechanisms of resistance to taxane.

1.4. Microtubules

Microtubules are filamentous protein polymers that play essential roles in development and maintenance of cell structure, protein trafficking, chromosomal segregation, and mitosis. They are composed of α-tubulin and β-tubulin heterodimers, along with other proteins such as microtubule-associated proteins (MAPs). Different isotypes of tubulin (6 isotypes of α- tubulin and 8 isotypes of β-tubulin) have been identified in humans that are expressed at varying levels in different cells and tissues [48]. Head-to-tail association of αβ-tubulin heterodimers forms linear protofilaments and the lateral association of 13 protofilaments leads to formation of cylindrical microtubules that can be many micrometers long (Figure 3).

Both α- and β-tubulin possess a GTP-binding region that can accommodate one molecule of GTP. During the association of α/β-tubulin heterodimers to the ends of microtubules, GTP in β-tubulin

is hydrolyzed to GDP, resulting in conformational changes that lock the tubulin–GDP into the microtubule core. In contrast, the α-tubulin subunit is always bound to the GTP molecule, at the nonexchangeable site, and is never hydrolyzed or exchanged [49]. Microtubules are polar structures with dynamic plus and minus ends that can frequently switch between phases of growth and rapid de-polymerization. This polarity arises from the arrangement of α- and β-tubulin heterodimers in the protofilaments with the α-tubulin subunit localized towards the minus end and the β-tubulin subunit exposed at the plus end [49].

The coexistence of assembly and disassembly, defined as "dynamic instability", is one of the important properties of microtubules. This dynamic state is characterized by four parameters: the rate of microtubule growth, rate of shortening, frequency of transition from a growing or paused state to a shortening state (an event referred to as ''catastrophe''), and conversely the frequency of transition from a shortening state to a growing or paused state (termed ''rescue'') [50]. Another important dynamic behaviour of microtubules is treadmilling, which involves the flux of tubulin dimers from the minus end of the microtubule to the plus end. During treadmilling, which occurs during metaphase and anaphase, the polymer length stays constant [48, 50].

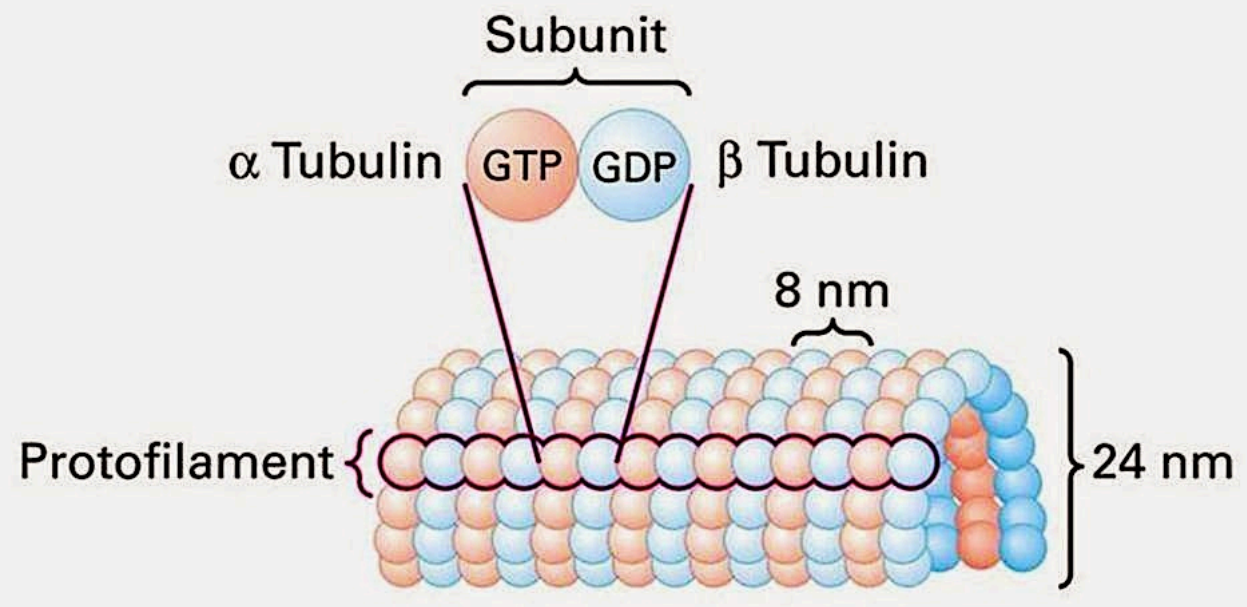

Figure 1.3. Microtubule structure and polymerization. Heterodimers of α- and β-tubulin assemble to form protofilaments. Side by side packing of protofilaments forms the cylindrical microtubules. Each microtubule has a plus end and a minus end. This figure was reproduced from "Molecular Cell Biology by Lodish, H.F. and J.E. Darnell, 2000" [51].

Dynamic instability is coordinated by either positively, by increasing the frequency or speed, or negatively, by suppressing transitions or reducing the speed. This dynamicity is tightly regulated by MAPs, which bind to tubulin heterodimers or the microtubule surfaces and ends, by expression of different tubulin isotypes, and by post-translational modifications of tubulin such as acetylation, polyglycylation and polyglutamylation, tyrosination, phosphorylation and palmitoylation [49, 52].

Microtubules and their innate dynamics are vital for the cell division process. At the onset of mitosis, microtubule dynamics dramatically increase and the entire microtubule network undergoes remodelling of interphase arrays to assemble specialized, highly dynamic mitotic spindles nucleated from the centrosomes. These specialized microtubule structures are required for all stages of mitosis, from correct attachment of chromosomes at their kinetochores, to the spindle during pro-metaphase, to the synchronous separation and segregation of the chromosomes after the metaphase–anaphase checkpoint is complete [48].

1.4.1. Microtubule interacting proteins

A rich panel of protein partners interact with tubulin and modulate the dynamics of microtubules. Some promote microtubule polymerization by suppression of catastrophe, rescuing a depolymerizing microtubule, and reduction of shrinkage, while others induce depolymerisation by inducing catastrophe, preventing rescue, or increasing shrinkage speeds.

One major group of microtubule interacting proteins are MAPs, which bind to the C-terminal region of tubulin along the microtubule wall and stabilize microtubules. Most MAPs including MAP1, MAP2, MAP4, Tau, and DCX (doublecortin) are post-translationally regulated by phosphorylation of the KXGS motif. The phosphorylation of MAPs reduces their affinity for microtubules and attenuates their capacity to stabilize microtubules [50, 53]. Tau and MAP2 share

microtubule-binding repeats at their C-terminal and are mostly expressed in neurons. MAP2 expression is restricted to cell bodies and dendrites in mature neurons whereas Tau is mainly present in axons [53]. However, expression of Tau in non-neuronal tissues, including epithelial cells has been reported. Tau is also implicated in Alzheimer's disease and some malignancies including breast cancer [54]. Tau contains an imperfect estrogen response element, upstream of its promoter, and is induced by estrogen in cultured neurons and MCF-7 cells [55].

Another group of microtubule interacting proteins are Microtubule destabilizers, which act as negative regulator of microtubule stability. Stathmin/Oncoprotein 18 (Op18) is the founding member of this group that plays a critical role in the regulation of mitosis [56]. Stathmin is a mitotic regulator and acts as a tubulin-sequestering protein and a catastrophe promoter. The activity of stathmin is regulated by phosphorylation at multiple sites. High levels of stathmin expression in human malignancies, including breast cancer are linked to disease progression. Stathmin expression in breast cancer patients correlates negatively with estrogen receptor (ER) expression and positively with proliferating cell nuclear antigen expression, tumour size and histopathological grade [57].

1.5. Microtubule Binding Agents

The presence of a single chromosome that is unable to attach to the spindle is sufficient to block mitosis and prevent the cell from progressing beyond the checkpoint, resulting in an arrested pro-metaphase/metaphase state that eventually leads to induction of apoptosis. The critical role that microtubules play in cell division makes them an ideal target for the development of chemotherapeutic drugs against rapidly dividing cancer cells. Microtubule disrupting compounds are divided into two distinct categories: 1. Microtubule stabilizing agents, which inhibit microtubule polymerization, such as taxanes (paclitaxel and docetaxel) and epothilones, and 2. Microtubule destabilizing agents, which disrupt microtubule function by promoting polymerization, includes vinca alkaloids, 2-methoxyoestradiol (2-ME2), dolastatin, and the combretastatins. Most of these compounds bind to the β-tubulin subunit of α/β-tubulin heterodimer at either of the three well established drug binding sites on β-tubulin, the vinca domain, the taxane site and the colchicine site.[58] The vinca domain is located adjacent to the exchangeable GTP binding site in β-tubulin at the plus end; the taxane site is located in a hydrophobic pocket, within the lumen of the microtubule at the lateral interface between adjacent protofilaments; and the colchicine site resides at the intra-dimer interface between β-tubulin and

α-tubulin. The effectiveness of microtubule-targeting drugs has been validated by the successful use of taxanes for the treatment of a wide variety of human cancers [48, 58].

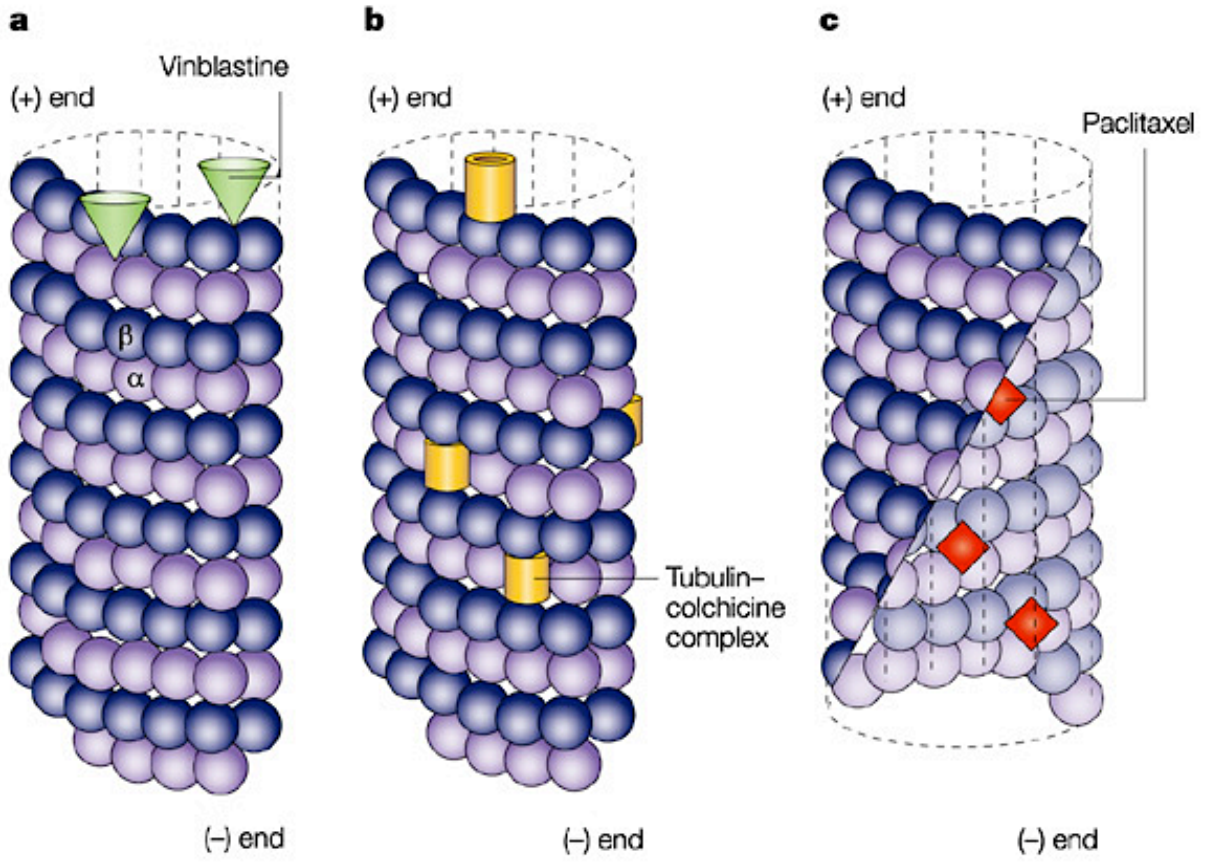

Figure 1.4. Microtubule binding agents. Most microtubule binding agents bind to the β-tubulin subunit of α/β-tubulin heterodimer at either of the three well established drug binding sites on β-tubulin, the vinca domain, the taxane site and the colchicine site. **A.** Vinblastine binds to high-affinity sites at the microtubule plus end and promotes polymerization. **B**. Colchicine forms complexes with tubulin dimers and suppresses microtubule dynamics. **C.** The interior surface of a microtubule is shown. Paclitaxel inhibits microtubule dynamics by binding to the inside surface of the microtubule. This figure was reproduced from "Jordan, M.A. and L. Wilson, Nat Rev Cancer, 2004" [48].

1.5.1. Paclitaxel

Paclitaxel (Taxol) was first isolated in the 1960s from the bark of the Pacific yew, *Taxus brevifolia*, by Monroe Wall and Mansukh Wani [59]. The mechanism of action of this natural compound was not reported until 1979, when Susan Horwitz made the surprising discovery that, unlike the Vinca alkaloids, paclitaxel stimulated microtubule polymerization [60]. Limited supplies of the natural compound impeded the development of paclitaxel for clinical use, until procedures for its semi-synthetic form made its production feasible. Paclitaxel was primarily FDA-approved in 1992 for the treatment of ovarian cancer. It is now widely used to treat breast and ovarian cancer, non-small-cell lung cancer and Kaposi's sarcoma [48]. The clinical success of paclitaxel revolutionized the treatment of adult solid malignancies and led to the discovery and clinical development of numerous other classes of microtubule stabilizers such as docetaxel and epothilones [50].

Paclitaxel binds to βIII-tubulin isotype located on the luminal side of the microtubule wall, along the length of the polymerized microtubules[61]. Unpolymerized, soluble tubulin has no significant affinity for paclitaxel, but it binds strongly to β-tubulin, indicating that the binding site is formed during the polymerization process [62]. Paclitaxel promotes tubulin assembly under different reaction conditions, including decreased protein concentrations, lower temperature, lack of MAPs,

and lack of GTP, leading to the formation of resistant tubulin polymers with highly polymerized microtubules. It exerts its effect by binding to GDP-bound β-tubulin molecules and changing their conformation to the more stable GTP-bound β-tubulin structure. This change increases the incorporation of β-tubulin into the microtubule and results in an equilibrium shift from the soluble to the polymerized form of tubulin [61].

Paclitaxel suppresses microtubule dynamic instability according to the stoichiometry of paclitaxel binding to the microtubules. At lower concentrations (< or = 100 nM), substoichiometric binding of paclitaxel to tubulin suppresses the rate and extent of shortening of microtubules and increases the microtubule polymer mass. However, at this concentration, paclitaxel retains its capability to induce mitotic arrest and subsequent apoptotic cell death. At intermediate paclitaxel concentrations (between 100 nM and 1 μM), the binding of additional paclitaxel molecules to the microtubules inhibits both growing and shortening events at both plus and minus ends of microtubule, with no additional increase in mass of microtubule polymer. At paclitaxel concentrations greater than 1 μM, paclitaxel binding to microtubules approaches saturation, microtubule mass increases significantly and microtubule dynamics is almost completely suppressed [63].

It is thought that the main mechanism of paclitaxel-induced cytotoxicity is through disruption of normal spindle formation at metaphase of cell division, which results in mitotic arrest. Following mitotic arrest, cells can either undergo apoptosis or exit mitosis without cell division (mitotic slippage), forming multinucleated tetraploid (4C DNA content) cells. In flow cytometry results of cell cycle distribution, both mitotic and postmitotic tetraploid cells are seen in the same 4C DNA peak, traditionally called 'G2/M arrest'. PTX does not induce G2 arrest and the G2/M peak in PTX-treated cells consists of both mitotic cells and tetraploid cells, which escape mitotic arrest without division [64-67]. Although paclitaxel mediates its effects by interaction with the cytoskeleton, its effect varies depending on cell type and drug concentration. At high concentrations, paclitaxel causes cell cycle arrest in G2/M and hence induces apoptosis, whereas low doses of paclitaxel can induce apoptosis after an aberrant mitosis, without a G2/M-phase arrest [68].

The molecular mechanism underlying the apoptotic response to paclitaxel is still not fully understood, and the role of intact *p53* in the intrinsic sensitivity of human cancer cells to paclitaxel remains controversial. *p53* is a tumour-suppressor gene that plays pivotal roles in the regulation of many critical cellular functions, including cell cycle arrest and apoptosis [67, 69]. Functional *p53* causes cell cycle arrest in the G1 phase in cases of DNA damage, thereby allowing DNA repair and enhanced survival in normal cells. It has been shown that, although a wild-type

p53 protein contributes to the paclitaxel-induced G2/M arrest, inactivation of *p53* in cells that express dominant negative *p53*, mutated *p53*, or in cells treated with the p53 inhibitor, does not suppress paclitaxel-induced apoptosis and these cells remain extremely sensitive to paclitaxel [67, 70]. It is suggested that paclitaxel induces apoptosis through two different pathways: a *p53*-independent pathway, occurring in cells blocked in prophase, which is observed both in cells with intact *p53* and in cells with abnormal *p53;* and a *p53*-dependent mechanism, which occurs in cells that accumulate in G1 and require functional *p53* [69]. Therefore, the efficacy of paclitaxel may not be limited to its microtubule-stabilizing activity, but its ability to activate and modulate other cellular intermediates [70].

The action of paclitaxel on cells can initiate a cascade of cell death pathways and induce a spectrum of genes involved in proliferation, apoptosis, inflammation; activate transcriptional pathways leading to inhibition of cell growth, apoptosis and angiogenesis. Paclitaxel induces the production of cytokines and interleukins, such as IL-1β, IL-6, and IL-8, increases tyrosine phosphorylation of proteins, including mitogen activated protein kinase (MAPK) and modulates the expression of cyclin dependent kinases and protein kinase C isoforms. Paclitaxel can interact and induce cytotoxicity via phosphorylation of Bcl-2 family, apoptosis regulator proteins, including Bcl-xl and Bcl-2/BAX. It also induces high level of ROS (reactive oxygen species),

activates Raf-1 kinase, a mediator of apoptosis, and modulates the expression of the proto-oncogene c-myc [68, 71]. Although Raf-1 activation is not a requirement for cell death at low concentration of paclitaxel, at higher doses paclitaxel-induced apoptosis is accompanied by Raf-1 activation [72]. Raf-1 activation coincides the accumulation of cells in G2/M, suggesting that Raf-1 activation may be a component of the signal cascade activated during the mitotic checkpoint [72]. It has been shown that paclitaxel mimics LPS (bacterial lipopolysaccharide) by inducing the translocation of NF-KB (Nuclear Factor-Kappa B) from cytoplasm to nucleus that leads to secretion of TNF-α and interleukin IL-1β [71, 73]. This effect is independent of paclitaxel's ability to stabilize microtubules, because some derivatives of paclitaxel retain microtubule-stabilizing activity, but do not stimulate cytokine secretion [74].

1.6. Mechanisms of drug resistance

While microtubule stabilizers have had great success in the clinic, the major limiting factors for their clinical applicability includes tumour resistance, dose-limiting side effects causing various toxicities, and possible hypersensitivity [50]. Of these, the most important unsolved question is the development of drug resistance that, in a simplified view, can be divided into intrinsic resistance, inherent insensitivity, and acquired resistance, which is the emergence of resistant populations upon exposure to the drug. Intrinsic resistance appears at the early stages of

carcinogenesis and involves the lack of response to the first-line systemic treatment whereas acquired resistance results from genetic and epigenetic changes in the cells, previously sensitive to the treatment [75]. The emergence of acquired resistance to paclitaxel is potentially a result of several alterations in the tumour including mutations in drug binding sites on tubulin or alterations in tubulin isotype distribution, altered expression of microtubule regulatory proteins, aberrant expression of microRNAs (miRNAs), overexpression of the multi-drug resistance 1 gene (MDR-1/ABCB1), which encodes the P-glycoprotein (P-gp) drug transporter, and impairment of apoptotic pathways [49].

1.6.1. β-tubulin isotypes and mutations

Tubulin isotypes, which share a high degree of homology, are expressed in a tissue specific manner. Some are exclusively expressed in certain tissues (β II, β IVa and β III isotypes in the brain and βVI in hematopoietic tissues), whereas others (βI and βIVb) are expressed constitutively in all tissues. Altered expression of β-tubulin isotypes is found in cells that have been selected for resistance to antimitotic agents [49, 76]. Microtubule dynamics, and the effects of paclitaxel on this process, can be modulated by the β-tubulin isotype composition [77]. While βIII-isotype expression is normally restricted to neuronal tissues, its aberrant expression in tumours has been associated with paclitaxel resistance in lung, ovarian, breast, prostate and

pancreatic cancer. In fact, elevated βIII-tubulin levels confer resistance to a broad spectrum of drug classes, including tubulin targeted agents and non-tubulin-targeted agents, in solid and hematological tumours and are associated with poor prognosis in a host of different epithelial cancers [78, 79]. It has been shown that overexpression of the βIII-isotype induces paclitaxel resistance, by inherent increase in dynamic instability of microtubules [80] or by decreasing the efficacy of paclitaxel binding to βIII-tubulin, resulting in a weaker suppressive effect on microtubule dynamics [81].

The regulation of tubulin isotype composition have been detected at both the gene and protein level and result from increased gene transcription and enhanced mRNA stability [78]. Several transcription factors including HIF1α, p53 and nuclear factor-κB (NF-κB) can induce the expression of *TUBB3* [82]. In addition, the tumour suppressor miR-100 and the miR-200 family of microRNAs are implicated in regulation of β-tubulin isotype expression [83, 84]. Restoring miR-200c expression in the Hec50 endometrial cancer cell line decreases the expression of βIII-tubulin and increases sensitivity to microtubule-targeting agents by 85% [83].

Additionally, several mutations in β-tubulin have been characterized that confer resistance to paclitaxel either by impairing paclitaxel binding to tubulin, including mutations occurring in the taxane-binding site, [85, 86] or by increasing microtubule stability [87].

1.6.2. Microtubule associated proteins

It is the coordinated action of microtubule interacting proteins that governs the dynamicity of the microtubule [50]. Microtubule associated proteins (MAPs) have been largely divided into two categories based on microtubule interaction motifs: Type I including MAP1 proteins and type II including MAP2, MAP4 and tau proteins [88]. Aberrant expression of MAPs has been shown to impact the sensitivity of tumour cells to microtubule stabilizers. Loss of Tau expression or overexpression of active stathmin, a microtubule stabilizer, decreases cancer cell sensitivity to paclitaxel by opposing the microtubule-stabilizing effect of the drug [50, 55]. Additionally, alterations in expression or phosphorylation of MAP4 modulate the microtubule-stabilizing activity of this protein and affect the dynamicity and stability of microtubules [56, 89]. Such changes in tumour cells could reduce the microtubule-stabilizing potency of paclitaxel.

1.6.3. Mechanisms of drug resistance by miRNAs

Increasing evidence indicates that alterations in miRNA expression are implicated in the acquisition of resistance to microtubule targeting agents. Although the exact mechanisms by which miRNAs confer resistance to drugs is not fully understood, it is likely that they exert their effect by providing cells with survival mechanisms including escape from apoptosis, decrease in drug uptake, and as mentioned before by overexpression of different β-tubulin isotypes [90]. Increased expression of miRNAs including miR-125b, miR-200c, miR-21, miR-155 and let-7a confers drug resistance by modulating the expression of apoptosis-related genes [91-93]. Other miRNAs such as miR-22 and miR-203 enhance paclitaxel-induced apoptosis by inhibition of Akt2 expression and altered expression of Bcl-xL, Bax and caspase-3 [90, 94, 95].

1.6.4. Multidrug Resistance

Development of drug resistance to chemotherapy is the major factor in the failure of chemotherapeutic agents for the successful treatment of many forms of malignancies. Cancer cells can develop resistance to individual cytotoxic agents by alteration in the targets of the drug, but can also exhibit a multidrug resistant (MDR) phenotype against multiple unrelated drugs with different chemical structures and different mechanisms of action. This phenotype was originally attributed to the overexpression of a 170 kDa MDR1/P-glycoprotein (P-gp), which was the first of

the membrane transporters that were later classified as ATP binding cassette (ABC) transporters. The ABC-transporters use energy from ATP hydrolysis to move a wide range of substrates across cellular membranes (plasma membrane, intracellular membranes of the endoplasmic reticulum, peroxisomes, and mitochondria) against their concentration gradients, thereby limiting the cellular accumulation of their substrates. To date, 48 ABC transporters have been identified in the human that have been classified into seven subfamilies, ABCA, ABCB, ABCC, ABCD, ABCE, ABCF, and ABCG based on sequence similarities [96-98]. All ABC transporters share a conserved ATP binding domain, however their domain structures are organized differently [96]. The human ABCB subfamily consists of 11 members, ABCB1 (MDR1/P-gp) through ABCB11 [98].

1.6.4.1. ATP binding cassette B1 (ABCB1)

ABCB1, the most extensively studied ABC transporter, is expressed in a variety of tissues including brain, intestine, liver and kidney, with the highest expression level found in the apical membranes of the blood-brain barrier. In normal tissues, ABCB1 removes a wide range of cytotoxic compounds by excretion into the bile and urine [99], however due to its broad range of substrate specificity, it plays a crucial role in limiting the absorption and effect of chemotherapeutic agents by decreasing their intracellular accumulation. A variety of pharmacologically distinct drugs indicated for the treatment of cancer, hypertension, allergy,

infection, immunosuppression, neurology, and inflammation are ABCB1 substrates [98]. ABCB1 has been demonstrated to be a promiscuous transporter of anticancer drugs (Vinca alkaloids, anthracyclines, etoposide, taxol) [100-102], calcium channel blockers (verapamil, diltiazem, azidopine) [103], Immunomodulators (cyclosporine A, FK-506) [104, 105], cardiac glycoside (digoxin) [106], steroids (cortisol, aldosterone) [107] , and fluorescent dyes (rhodamine 123, fluo-3) [108]. The expression of ABCB1 has been associated with drug resistance in many cancer types.

The ABCB1 protein has 1280 amino acids that are arranged as two tandem repeats of 610 amino acids joined by a linker region. Each repeat begins with a trans-membrane domain (TMD) containing six membrane-spanning α-helices followed by a nucleotide-binding domain (NBD) which can bind and hydrolyze ATP [96, 99]. The 12 trans-membrane segments are located in the apical part of the plasma membrane and the hydrophilic NBDs are localized at the cytoplasmic face of the membrane [98]. Drug substrates appear to bind at multiple drug-binding sites within a cavity at the interface between the TMDs. Co-expression of both TMDs is necessary to form a complex that can bind to drug substrates. A truncated ABCB1 molecule that lacks both NBDs retains the ability to interact with drug substrates, suggesting that the NBDs are not required for substrate binding [109]. However, both NBDs must be functional for drug efflux activity [110].

Each NBD consists of two core consensus motifs, referred to as the Walker A and B motifs, which are found in many proteins that bind and hydrolyze ATP, and a LSGGQ signature C motif, which is unique to the ABC superfamily [111]. These motifs are directly involved in the binding and hydrolysis of ATP.

The active efflux of drug substrate starts with the binding of the substrate to the interface between the two TMDs of ABCB1. Drug binding alters the structure of the nucleotide-sandwich dimer and can stimulate or inhibit the ATPase activity. ABCB1 has low basal ATPase activity in the absence of drug substrate. Drug binding can stimulate the ATPase activity up to 20 fold, suggesting a cross talk between the drug-binding pocket and the ATP-binding sites. The conformational changes in the TMDs upon binding the substrate, close the drug-binding pocket at the expense of ATP hydrolysis, facilitates release of drug substrate from ABCB1 and efflux the substrate into the extracellular medium [109, 110, 112].

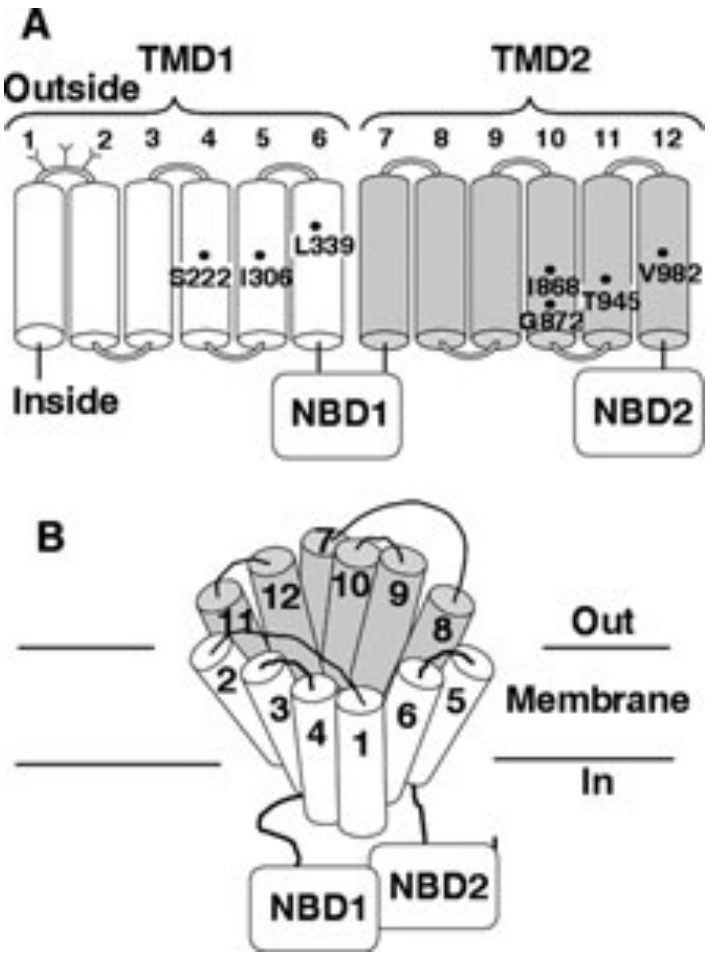

Figure 1.5. Schematic models of ABCB1. **A.** The cylinders represent the transmembrane domains (TMD) and the rectangles represent the nucleotide binding domains (NBD). The residues identified to be part of the drug-binding pocket are shown. **B** Model of the organization of the TMDs based on cross-linking and cysteine-scanning mutagenesis studies. The drug-binding pocket is at the interface between the TMDs. This figure was reproduced from "Loo, T.W. and D.M. Clarke, J Membr Biol, 2005" [99].

1.6.4.2. Mechanisms of drug efflux

The exact mechanism by which ABCB1 transports its substrate across the membrane is not fully understood, however several models have been proposed to explain the efflux mechanism, including the "hydrophobic vacuum cleaner" and "flippase" models [113, 114]. The ABCB1 protein recognizes hydrophobic compounds embedded in the inner leaflet of the plasma, and expel the non-polar molecules from the interior of the bilayer to the extracellular milieu, possibly via a flippase type of mechanism. This results in a concentration gradient across the plasma membrane, with a higher drug concentration in the external aqueous phase [114, 115]. The substrates partitioning into the lipid phase prior to interacting with the protein and the substrates access to the pore from the lipid phase of the membrane are necessary for both models. However, experimentally it is difficult to distinguish between the "hydrophobic vacuum cleaner" and "flippase" models [113] (Figure 6).

1.6.4.3. ABCB1 Gene Structure

The *ABCB1* gene, located on chromosome 7q21, contains 29 exons numbered –1 to 28. The two most 5' exons are un-translated. The gene can be transcribed from two different transcriptional start regions, a proximal promoter for constitutive expression, and a cryptic distal promoter. The proximal promoter drives the expression of *ABCB1* in most drug-selected cell lines and cancer

patient samples [98, 99, 116]. The upstream promoter is found at the beginning of exon –1, and the downstream promoter is located within exon 1. The downstream promoter is flanked by two parts of exon 1 that have been further named exon 1a and exon 1b. The portion of exon 1, proximal to 5' of the downstream promoter is designated exon 1a, and the other portion of exon 1 located at the 3' of the downstream promoter is designated exon 1b [117, 118].

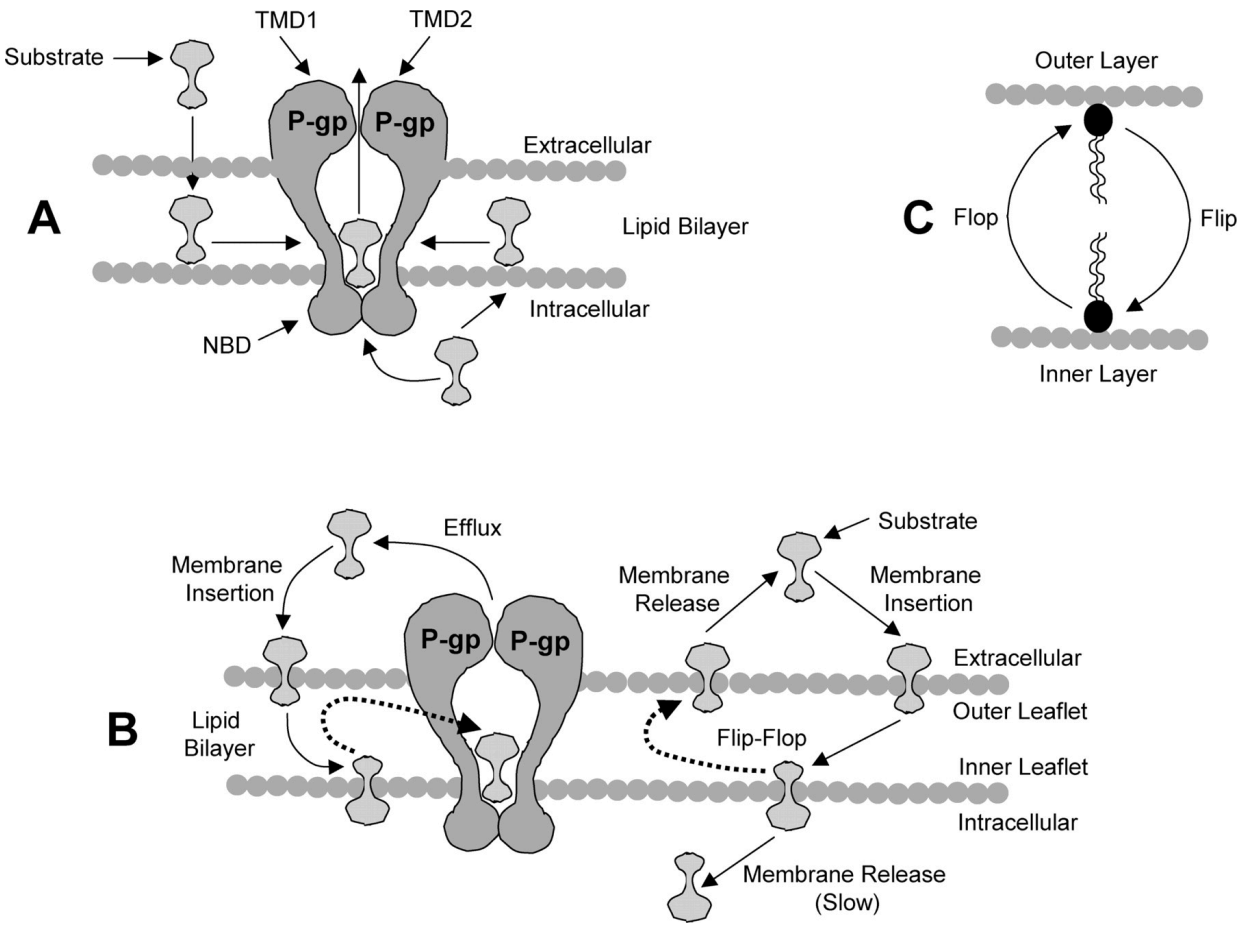

Figure 1.6. Representation of models of extrusion of ABCB1 substrates. A. Hydrophobic vacuum cleaner model. Substrates can be extruded from the intracellular side by recognizing them as foreign to the membrane. **B.** Flippase model. ABCB1 encounters the substrate on the inner leaflet of the lipid bilayer and flips it to the outer leaflet, against a concentration gradient. **C.** Phospholipid flip-flop within the lipid bilayer. The figure was reproduced from "Choudhuri, S. and C.D. Klaassen. Int J Toxicol, 2006" **[98].**

The *ABCB1* mRNA is 4872 base pairs in length (including the 5' untranslated region (5' UTR)), and it translates into a protein that is 1280 amino acids in length [117, 119]. The *ABCB1* gene does not have a TATA-box, however structural and functional analysis of the promoter has revealed that the *ABCB1* transcription initiation is governed by an initiator sequence (Inr). The proximal promoter contains a CAAT box, an inverted CCAAT element/Y-box upstream from the transcriptional start site, two GC boxes, and several important transcription binding sites which regulate its expression in response to external stimuli [116, 120-122].

The ATG translation initiation codon is located within exon 2 and thus the protein-coding sequence of *ABCB1* gene consists of 27 exons and 28 introns. The first half of the protein is encoded by 14 exons, the second half is encoded by 13 exons and there are 26 introns that interrupt the protein-coding sequence [98]. ABCB1 is post-translationally modified by phosphorylation, N-glycosylation, or ubiquitination [123].

1.6.4.4. Regulation of ABCB1 Expression

The mechanisms by which tumour cells overexpress ABCB1 to confer resistance have not been fully understood, however two models have been proposed. In the first model, ABCB1 overexpression results from drug selection of a small subset of ABCB1 overexpressing cells

within tumour that eventually outgrow and dominate the tumour cell population. Alternatively, the expression of *ABCB1* can be modulated by drug-induced activation of the gene [124].

The widespread expression of ABCB1 in tumour cells with both intrinsic and acquired multidrug resistance has been reported [124, 125]. Intrinsic expression of the ABCB1 is generally found in cancers subtypes derived from tissues that endogenously and in normal physiological conditions express ABCB1 including kidney, liver, colon, pancreas, and adrenal [100, 124-126]. However, the expression of ABCB1 in untreated cancers has also been reported in acute and chronic leukemia's of children and adults, non-Hodgkin's lymphoma, chronic myelogenous leukemia, non-small cell lung cancer with neuro-endocrine properties, neuroblastoma, sarcoma, and astrocytoma. The tissue of these tumour origins does not express ABCB1 [124, 125].

The intrinsic expression of ABCB1 in cancers derived from tissues that do not normally express ABCB1, has led to the hypothesis that ABCB1 expression may coincide with or play an active role in tumourigenesis. Evidence from several studies indicates that ABCB1 expression is modulated by genes associated with tumour progression such as *H-Ras*, *c-Raf* and mutant *p53* [125, 127-129]. Several *p53* mutants activate *ABCB1* expression, whereas wild-type *p53* has been shown to suppress *ABCB1* expression [127, 128]. In addition, increased expression of ABCB1 is commonly seen in relapsed/refractory patients with breast cancer, ovarian cancer, lymphoma,

leukemia, neuroblastoma, pheochromocytoma, rhabdomyosarcoma, and multiple myeloma, who have been treated with chemotherapeutic agents that are ABCB1 substrates [125, 130-132].

A myriad of factors may contribute to the expression and activity of ABCB1, which can be controlled either pre- or post-transcriptionally. Elevated expression of ABCB1 appears to be complex and is not always a function of gene dosage alone, but can occur as a result of increased protein stability, plasma membrane incorporation, mRNA stability and mRNA processing [100, 101, 133, 134].

The mechanisms responsible for *ABCB1* gene expression are complex and can be modulated by a variety of transcription factors such as HIF-1α, SP1, NF-Y, YB-1, AP-1, p53, and NF-IL6 [128, 135, 136]. Several studies have proposed that AP-1-mediated signals play an important role in *ABCB1* gene regulation. Co-expression of ABCB1 with Fos and Jun, components of the AP-1 transcription factor complex, have been reported [134, 137, 138]. However, contradictory results have also been reported suggesting that enhancement of c-jun and the JNK pathway can inhibit the expression of ABCB1 [139]. The overexpression of H-Ras, c-Raf, MEK1/2 and ERK1/2, show an additive effect on ABCB1 expression, whereas the overexpression of the regulatory subunit of PI3K, wild-type or mutant PTEN, or AKT1, all of which are involved in the PI3K-AKT

signaling pathway, do not affect ABCB1 expression, suggesting that the MAPK pathway, but not the PI3K-AKT pathway, positively controls ABCB1 expression [129].

ABCB1 protein levels can be modulated by post-translational modifications, including phosphorylation and glycosylation. Differential phosphorylation of ABCB1 by kinases has been shown to influence ABCB1 expression and activity. Phosphorylation of Ser683 protects the protein from degradation and allows its glycosylation and cell-surface expression. Glycosylation of ABCB1 promoted by Pim-1, a serine/threonine protein kinase, that stabilizes the under-glycosylated form of ABCB1 and prevents its proteasomal degradation [123].

Several polymorphic variants have been reported in the *ABCB1* gene, however most of *ABCB1*-coding polymorphisms do not show any modifications in cell-surface localization, expression level, or change in the transport function of ABCB1 [96, 98].

Also, epigenetic mechanisms are likely to play an important role in ABCB1 expression regulation. It has been reported that histone modifications and promoter methylation can modulate the expression of ABCB1 in prostate cancer cells [140, 141]. A number of microRNAs have been described to modulate the expression of ABCB1. Some of these, including miR-451, miR-27a, miR-508-5p, miR-331-5p, miR-298, and miR-145, are direct regulators of ABCB1 and regulate its expression by direct interaction with the 3'-untranslated region (UTR) of the *ABCB1* mRNA

region [142-144]. Other microRNAs, such as MiR-137, miR-200c, miR-122, and miR-138, indirectly modulate the transcription of *ABCB1* through intermediate proteins or transcription factors involved in *ABCB1* gene activation. It has been reported that mir-137 suppresses the expression of ABCB1 by targeting YB-1 [145]. In contrast, expression of miR-19a/b induces ABCB1 expression by regulating the PTEN-AKT pathway and confers resistance in gastric adenocarcinoma cell line by increasing the expression of ABCB1 and reducing the expression of anti-apoptotic factors Bcl-2 and Bax [146].

In many multidrug resistant cell lines, overexpression of ABCB1 is accompanied by gene amplification or chromosomal rearrangements such as translocations, inversions, insertions, and deletions [101, 126, 133, 147]. The gene copy number increase can occur intrachromosomally, forming homogenously staining regions, or extrachromosomally, forming double minutes. Both types have been reported in *ABCB1* regional amplifications in various resistant cancer cell lines, including breast cancer cell line (MCF7) [148, 149], ovarian cancer cell lines [150], lung cancer cell line (NCI-H460) [151, 152], osteosarcoma [153], colon carcinoma cell line (SW620) [154], leukemia [155, 156], hepatocellular carcinoma cell line (HKCI) [157], neuroblast [158], and. esophagus [159]. In patient's samples, the copy number increase of 7q21~q22 has been reported in head and neck squamous cell carcinoma, and glioma [160, 161] and leukemia [162].

In addition to amplification, *ABCB1* gene expression can be affected by more dramatic genomic alterations such as translocations. *ABCB1* gene activation driven by chromosomal translocation was first reported in an Adriamycin-selected human colon adenocarcinoma cell line [147]. The activation of ABCB1 occurred after a (4q;7q) translocation in this cell line, which resulted in juxtaposition of the *ABCB1* gene 3' to a transcriptionally active gene located on chromosome 4 [147]. Additional, *ABCB1* gene rearrangements, within active gene sequences of chromosomes 1, 4, or 16, have been identified [147, 152, 162]. Chromosomal rearrangement in the *ABCB1* gene region, resulting in formation of *ABCB1* hybrid mRNA has also been reported in leukemia patients refractory to therapy [162].

Despite the diversity of fusion partners, most of the cell lines and patient's samples share a similar, but not identical, pattern of chromosomal rearrangement, suggesting that chromosomal rearrangements lead to "capture" *ABCB1* by a, random, constitutively active promoter, resulting in aberrant activation of the *ABCB1* gene. Kitada *et al*. have proposed that *ABCB1* chromosomal translocations, mediated by breakage-fusion-bridge cycle, occur prior to amplification and activate the *ABCB1* gene placed downstream of a constitutively active gene promoter [152]. However, detailed activation mechanisms of ABCB1 by gene fusion remain to be elucidated.

1.7. Epidermal Growth Factor Signaling

Growth factors mediate diverse biologic responses by binding to and activating cell-surface receptors with intrinsic protein kinase activity. The first growth factor discovered was epidermal growth factor (EGF) [163]. Later studies have shown that this protein binds to a cell surface growth factor receptor, epidermal growth factor receptor (EGFR).

The EGFR is a member of the EGFR family of receptor tyrosine kinases (RTKs), also known as the HER (human epithelial receptor) or ERBB family. EGFR plays a vital role in the regulation of cell proliferation, survival and differentiation. The EGFR family consists of 4 members: EGFR, HER2, HER3, and HER4 (alternately known as ERBB1–4). All of these trans-membrane glycoproteins are within the 170-190 kilo Dalton (kDa) size range and are composed of three different domains; the extracellular ligand-binding domain, hydrophobic transmembrane domain, and intracellular tyrosine kinase (TK) domain [164]. HER3 is a distinctive member of the EGFR family because, unlike EGFR, HER2 and HER4, its kinase domain lacks certain residues that are essential for catalytic activity in other kinases [165].

The extracellular region of EGFR is divided into four domains; Domain I, II, III and IV (DI, DII, DIII and DIV) with domain III being responsible for ligand binding [166]. Various ligands responsible for the activation of EGFR have been identified including epidermal growth factor

(EGF), transforming growth factor alpha (TGF-α), amphiregulin (AREG), betacellulin (BTC), epigen (EPGN), epiregulin (EREG), and heparin-binding EGF (HB-EGF). The expression and release of EGFR ligands are tightly regulated as they represent a crucial point in regulation of EGFR signaling [167, 168] (Figure 7).

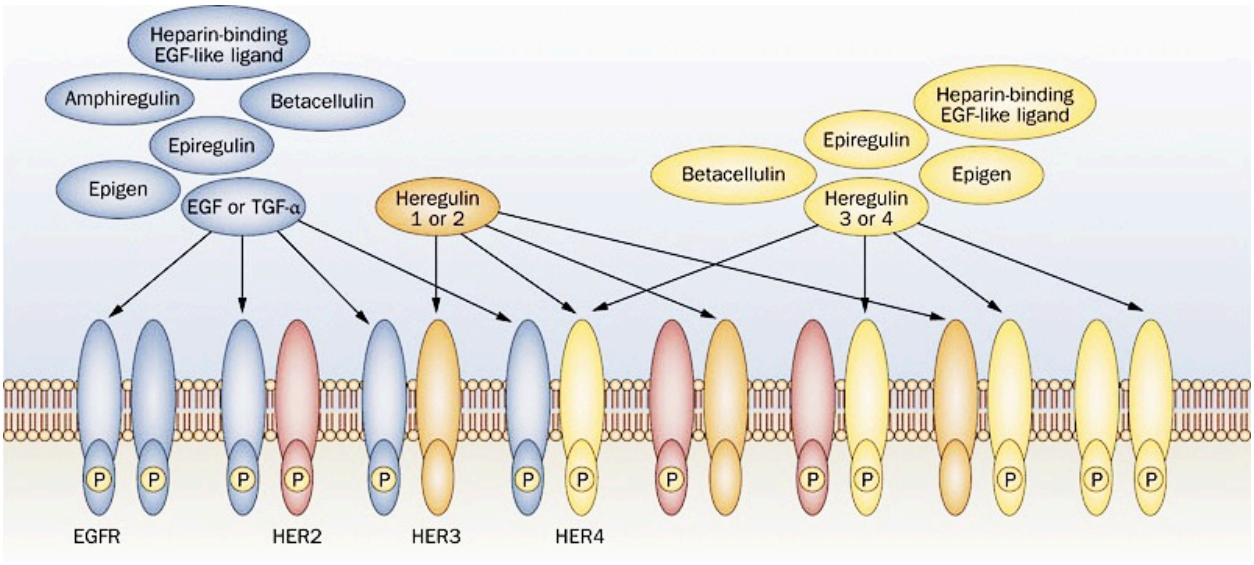

Figure 1.7. Heterodimerization and ligand binding in HER family. The four HER family members are able to form 28 homo and heterodimers. With the 11 growth factors in the EGF-like family and 28 possible dimers, there are 614 possible combinations of receptors. However, not all are biologically functional. This figure is adapted from "Okines, A., D. Cunningham, and I. Chau. Nat Rev Clin Oncol, 2011". [169].

Binding of ligand to the extracellular domain stabilizes EGFR in an extended conformation, triggers receptor homo- and/or heterodimerization, and promotes receptor autophosphorylation, which is essential for activation of the tyrosine kinase. Both the ligand and composition of the dimer determines which downstream signaling pathway is activated. Different ligands cause the phosphorylation of distinct sets of EGFR tyrosine residues and dictate the duration of signaling events and divergent cellular responses [166, 170]. These residues provide docking sites for several cytosolic proteins containing Src homology 2 (SH_2) domains or phospho-tyrosine binding (PTB) motifs [170, 171]. Autophosphorylation and transphosphorylation of the receptors through their tyrosine kinase domains lead to the recruitment of adapter proteins like GRB2, which in turn activates complex downstream signaling pathways. This includes the activation of STAT proteins, SRC family kinases, AKT protein, MAP kinases, PLCγ, PKC, and PI3-kinase, which induces the transcription of genes involved in cellular processes such as cell division and survival [170].

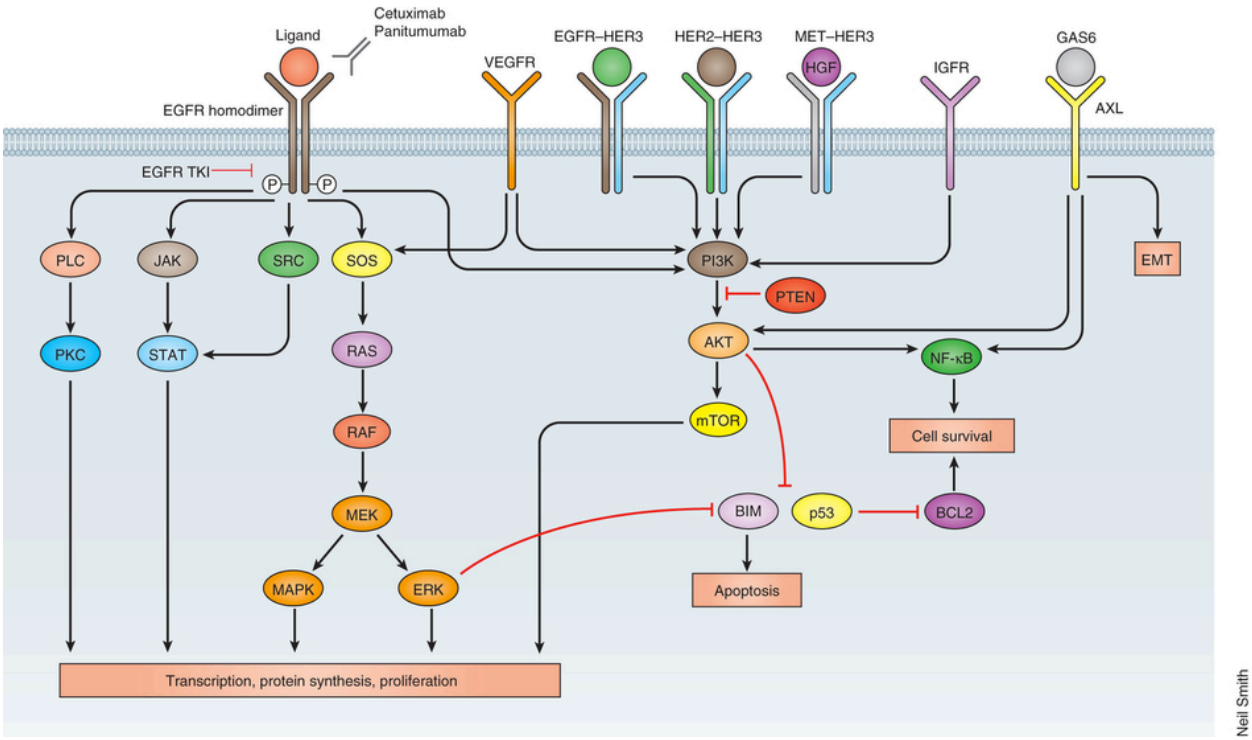

Figure 1.8. Overview of EGFR Signaling. The main downstream signaling modules include PI3K, Ras/Raf/MEK/ERK1/2, and PLC. This figure was reproduced from "Chong, C.R. and P.A. Janne, Nat Med, 2013" [172].

1.7.1. EGFR Sustaining Signaling in Cancer

Cell growth and cell division in normal cells is controlled by finely regulated production and release of growth-promoting signals, ensuring cell homeostasis. The most fundamental trait of cancer cells is their ability to proliferate without signaling input. This capability is acquired in a number of alternative mechanisms including producing growth factor ligands themselves,

stimulating normal cells in the microenvironment to supply the cancer cells with growth factors, increasing the number of receptors on the cell surface, structurally altering receptor molecules to facilitate the signaling, and activating components of downstream signaling pathways [2].

EGFR signaling is deregulated in several malignancies, including breast cancer, head and neck squamous cell carcinoma (HNSCC), non-small cell lung cancer (NSCLC), colorectal cancer (CRC), pancreatic cancer and brain cancer. EGFR activation via ligand binding results in signaling through various pathways, ultimately resulting in uncontrolled proliferation of tumour cells, conferring the ability to evade programmed cell death, enhancing their ability to migrate, and facilitating metastasis [164, 167]. Dysregulation of EGFR pathways by overexpression or constitutive activation is associated with poor prognosis [173]. High levels of EGFR in breast tumours is associated with poor overall survival and is positively correlated with cell proliferation markers, Ki67 and cyclin D1 [174].

1.7.2. EGFR Expression in TNBC

In the past few years, many studies have shown that the EGFR signalling is frequently activated in TNBC [175-177]. The overexpression of EGFR has been reported in 45% to 78% of TNBC cases [18, 175, 176] and is associated with a poor clinical outcome [178]. Although the underlying mechanism of EGFR gene activation has yet to be elucidated, there is little evidence that EGFR

gene amplification or EGFR-activating mutations is involved in the mechanisms leading to the overexpression of EGFR in TNBC [175, 176, 178]. Frequent EGFR overexpression in TNBC offers the potential for targeted molecular therapy in this breast cancer subtype.

1.7.3. EGFR Inhibitors

There are two predominant classes of EGFR inhibitors including monoclonal antibodies that are highly specific for EGFR, that target the extracellular domain of EGFR, such as cetuximab, and small molecule tyrosine kinase inhibitors that target the receptor catalytic domain of EGFR, such as gefitinib and erlotinib.

Tyrosine kinase inhibitors are synthetic, low molecular weight molecules that bind to the intracellular tyrosine kinase domain of EGFR and/or other members of the ErbB family of receptors and compete with ATP for receptor binding. They all exert their effect through inhibition of ligand-induced receptor phosphorylation. However they differ in their abilities to bind the EGFR ATP-binding pocket—either reversibly or irreversibly—or in their capacities to additionally inhibit other members of the ErbB family of receptors [179, 180].

Many breast cancers express multiple members of the EGFR signaling family. This has led to an interest in developing inhibitors of dual inhibitors, inhibiting EGFR and HER2, such as lapatinib, or pan-EGFR inhibitors, inhibitors of several ErbB receptors, such as neratinib.

1.7.3.1. Lapatinib

Lapatinib (Tykerb®) is a potent, orally bioavailable small molecule that reversibly binds the ATP-binding pocket of the intracellular domain of the EGFR and the HER2 and inhibits the phosphorylation and activation of the PI3K-Akt and Ras-Raf-MAPK signaling cascades, decreasing cell proliferation and increasing cell death. It was initially approved by the FDA for the treatment of patients with advanced or metastatic breast cancer whose tumours overexpress HER2 and who have received prior therapy including an anthracycline, a taxane and trastuzumab [181, 182]. Lapatinib causes moderate toxic effects in patients who receive up to 1500 mg of the drug per day with the adverse events being limited to diarrhea, rash, nausea, and fatigue [183].

Lapatinib has been used alone and in combination with both cytotoxic and molecularly targeted agents. Most responses have been seen in HER2 positive breast cancer patients. However, it is minimally effective as a monotherapy for chemotherapy-refractory TNBC or HER2-negative breast cancers [184]. It is possible that lapatinib in combination with another chemotherapeutic agent or targeted therapy may be effective [185, 186] (Figure 9).

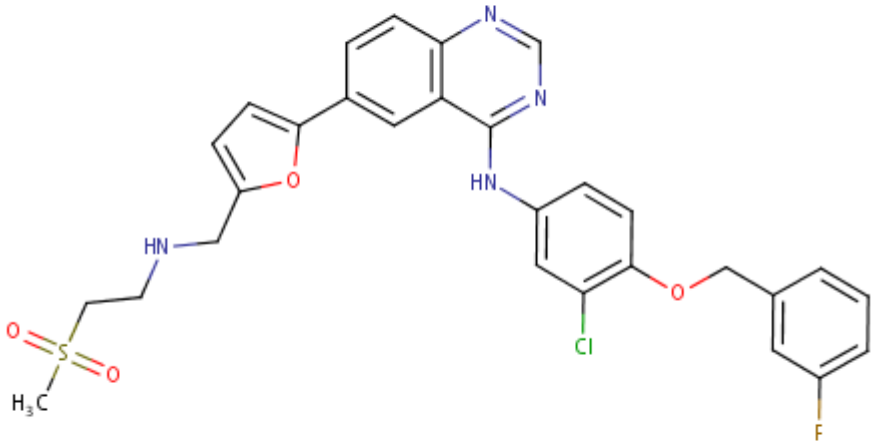

Figure 1.9: Chemical Structure of Lapatinib. The figure was reproduced from Drug Bank, Available at: http://www.drugbank.ca/drugs/db01259 [187] .

1.7.3.2. Neratinib

Neratinib (HKI-272) is a potent, orally administered irreversible tyrosine kinase inhibitor of the ErbB family of receptors (EGFR, HER2, and HER4) that interacts directly with the cytoplasmic domain of ErbB receptors and inhibits downstream signaling. It effectively inhibits the proliferation of EGFR- and HER2-expressing cells that are resistant to other ErbB receptor tyrosine kinase inhibitors [188].

In cell line models of acquired trastuzumab resistance HER2 positive breast cancer, both lapatinib and neratinib can overcome trastuzumab resistance and sensitize the cells to trastuzumab. However, neratinib shows cytotoxic activity in lapatinib resistant cell lines, which suggests that neratinib may have clinical benefits in patients who do not respond to trastuzumab and/or lapatinib alone [188] (Figure 10).

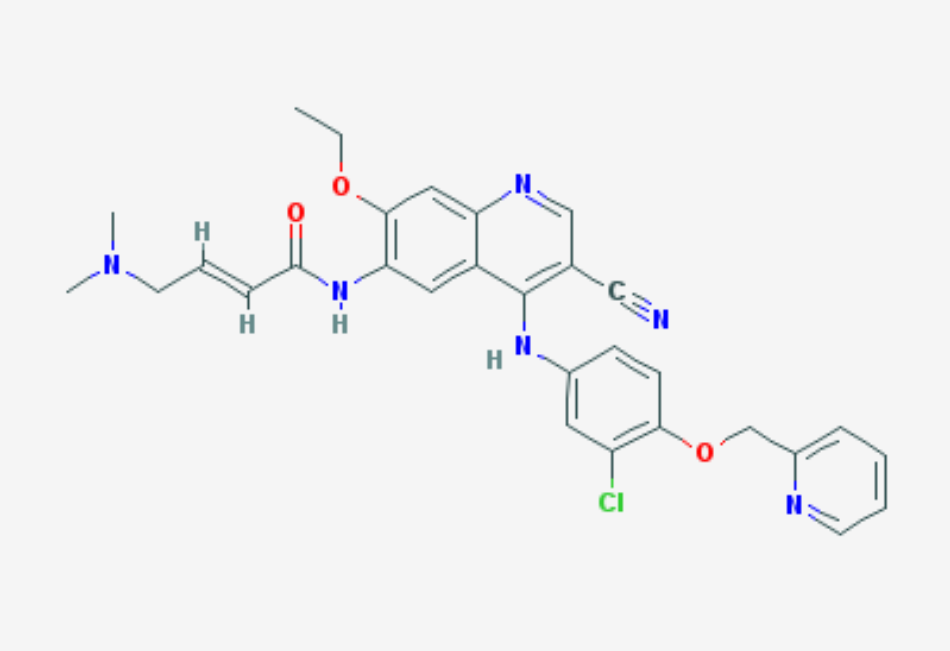

Figure 1.10: Structure of Neratinib. This figure was reproduced from Pubchem, Available at: http://pubchem.ncbi.nlm.nih.gov/compound/Neratinib#section=Top [189]

Several *in vitro* experiments and clinical trials have suggested that monotherapy of tyrosine kinase inhibitors are largely ineffective, and there is enough *in vitro* experimental evidence to support the use of combination therapy, targeting multiple tyrosine kinases [190].

1.8. Aims of the research

Paclitaxel (PTX), one of the most effective anti-cancer agents developed in the past decades, is widely used in the treatment of patients with locally advanced and metastatic breast cancer. PTX

exerts its effect by promoting microtubule polymerization and stabilization. Suppression of microtubule dynamic properties prior to cell division results in cell cycle arrest at G2/M and apoptosis. Due to their highly proliferating nature, TNBCs are initially very responsive to PTX. However, the majority of TNBC tumours acquire resistance, leading to progressive disease. Therefore, acquired resistance to paclitaxel has become one of the major obstacles in the successful treatment of patients with TNBC. This thesis focuses on understanding the molecular factors of resistance to PTX in a TNBC *in vitro* model.

In vitro studies on cell lines with acquired resistance provide models for characterization of the biological mechanisms of resistance. I first established *in vitro* models of PTX acquired resistance in TNBC cell lines. The emergence of resistance results from the acquisition or selection of genomic and epigenetic changes within TNBCs due to their genomically unstable characteristics. Therefore the aims of my PhD project were to i) identify genomic alterations associated with acquisition of PXL resistance in TNBC cell lines, and ii) to functionally validate the role of one or more genomic alterations in drug resistance in vitro.

Chapter 2

Materials and Methods

2.1. Cell culture

2.1.1. Sources

BT20, MDA-MB-231, MDA-MB-468 and HCC38 cell lines were purchased from ATCC for the purpose of this study. HCC1937 (previously purchased from ATCC) and SUM149 (originally from Dr. Stephen Ethier) were obtained from Dr. William Foulkes laboratory, McGill University. MDA-MB-436 and MCF10A were previously available in Dr. Basik's laboratory. The origin of cell lines used is given in table 1.

2.1.2. Cell Culture

The vials received from American Type Culture Collection (ATCC) were immediately thawed and culture was initiated upon receipt. The MDA-MB-231 and MDA-MB-468 cell lines were cultured initially in Leibovitz's L-15 medium, ATCC recommended medium, with 10% FBS. Since the Leibovitz's L-15 medium formulation is devised for use in 100% atmospheric air and CO2 is detrimental to cells cultured in this medium, the cells were gradually transferred to RPMI 1640 medium. The medium used for all cell lines is listed in table 2.

To freeze cells, cells in logarithmic phase were pelleted, and resuspended in 1.5ml of FBS with 10% DMSO in 2ml cryotubes. Tubes were frozen slowly at -80°C and stored in liquid nitrogen.

To thaw cryopreserved cells, the vial was rapidly thawed by placing the frozen tube in a 37°C water bath. Once the cells had thawed, the mixture was transferred to a T25 flask. Complete media consisting of 10% FBS and antibiotic was added drop-wise to restore physiologic osmolality. The cells were incubated overnight to allow adhesion and the medium containing DMSO was replaced by fresh medium.

Cell line	**Supplier**	**Disease**	**Patient Ethnicity**	**Patient Age**	**Reference**
BT20	ATCC	Advanced ductal carcinoma	Caucasian	74	Lasfargues, E. Y. et al. 1958
SUM149pt	Stephen Ethier (Asterand)	Inflammatory ductal carcinoma	Caucasian		
MDA-MB-231	ATCC	Metastatic pleural effusion	Caucasian	51	Cailleau, R. et al. 1978
MDA-MB-436	ATCC	Metastatic pleural effusion	Caucasian	43	Cailleau, R. et al. 1979
MDA-MB-468	ATCC	Metastatic pleural effusion	Black	51	Cailleau, R. et al. 1980
HCC38	ATCC	Primary ductal carcinoma	Caucasian	50	Gazdar, A. F. et al. 1998
HCC1937	ATCC	Primary ductal carcinoma	Caucasian	23	Gazdar, A. F. et al. 1999
MCF10A	ATCC	Fibrocystic disease	Caucasian	36	Soule, H. D. et al. 1986

Table 2.1. Origin of cell lines

Cell line	Supplier recommended medium	Culture Media	Supplement
BT20	EMEM	EMEM	10% FBS
SUM149pt		RPMI-1640	10% FBS+ IH
MDA-MB-231	Leibovitz's L15 Medium	RPMI-1640	10% FBS
MDA-MB-436	Leibovitz's L15 Medium	RPMI-1640	10% FBS
MDA-MB-468	Leibovitz's L15 Medium	RPMI-1640	10% FBS
HCC38	RPMI-1640	RPMI-1640	10% FBS
HCC1937	RPMI-1640	RPMI-1640	10% FBS
MCF10A	MEBM	RPMI-1640	10% FBS+ IHE

Table 2.2. List of medium used for each cell line. FBS: Fetal Bovine Serum, IH: 5µg/mL Insuline+100µg/mL Hydrochortisone, IHE: 5µg/mL Insuline+100µg/mL Hydrochortisone +20ng/mL EGF (part of MEGM kit, Lonza/Clonetics Corporation).

2.2. Cell viability assay.

The Alamar Blue Assay was employed to determine the sensitivity of cell lines to different chemotherapeutic drugs and inhibitors. Cells were plated at the density of $1X10^4$ cells per well, in 100 µl of medium, in 96-well plates, in quadruplicate. The cells were incubated for 24h at 37 °C to allow cell adhesion. The following day, 100µl of medium containing 2X-concentration drug

were added to each well. Some cells were left untreated in order to provide 100% cell viability (control). The cells were incubated for 72h and were subjected to the Alamar Blue assay. 20µl of Alamar Blue reagent were added to 200 µl medium in each well and the cells were incubated for 4h at 37 °C. The relative fluorescence was determined using a Fluostar Optima microplate reader (BMG LABTECH) at 590nm. The fluorescent readings were normalized to the untreated control and expressed as percentage and the values were plotted against the drug concentration in a logarithmic scale. The half maximal inhibitory concentration (IC_{50}) was calculated using the GraphPad Prism software employing the sigmoidal dose-response function.

2.3. Development of PTX-resistant cell lines.

The sensitivity of all cell lines to PTX was tested using Alamar Blue assay. Six cell lines that showed sensitivity to PTX at nano-molar concentrations were selected for the development of paclitaxel-resistant cell lines. Cells were cultured in T75 flasks and exposed to increasing concentrations of PTX in a stepwise fashion, starting from concentrations 100 times lower than their IC_{50}. The cells were kept in each drug concentration for two weeks and the confluence was assessed: for cell lines with confluence below 50%, the treatment was stopped, for confluence between 50–70%, the treatment was maintained and for those with a confluence over 70% the concentration was increased. A portion of the cells was frozen at every concentration. Alamar

Blue assay was performed to monitor sensitivity of the resistant cell lines as previously described. Additionally, untreated parental cell lines were kept in culture for the entire duration of the study and were used as control cell lines. The resistant cell lines are collections of drug-resistant clones and are not derived from an isolated single clone.

2.4. Cell Cycle Analysis

Cells were seeded at 1 x 10^5 cells per well in 6-well culture dishes and incubated overnight at 37°C to allow cell adhesion. After 24h of incubation, cells were treated with 100 nM PTX. Cells were harvested via trypsinization 24, 48h and 72h after treatment, washed with cold PBS, and processed for cell cycle analysis. The cells were fixed in 70% ethanol and stored at –20°C overnight. Prior to sorting, the fixed cells were centrifuged at 1000 rpm and re-suspended in PBS containing Propidium Iodide staining solution (50 μg/mL final concentration) and RNase A (20 μg/mL final concentration). The cells were incubated for 30 min at 37°C in the dark and were analyzed using a FACSCalibur instrument (BD Biosciences). For each condition, 10,000 events were collected and percentage of cells in G0/G1, S and G2/M phases was analyzed using Modfit software.

2.5. Apoptosis Assay

Apoptosis detection was performed using the AnnexinV-FITC Apoptosis Detection Kit according to the manufacturer's protocol (BD Biosciences, San Diego, USA). Briefly, 1 X 10^5 cells were seeded in 6-well plates and incubated overnight at 37°C to allow cell adhesion. After 24h of incubation, cells were exposed to 100 nM of drug. Cells were harvested 24h, 48h and 72h after treatment, washed twice in PBS, and then re-suspended in 1X Binding Buffer at a concentration of 1 x 10^6 cells/ml. 100 µl of cell suspension were transferred to FACS tubes, stained with 5 µl FITC Annexin V and 5 µl of Propidium Iodide and incubated for 15 minutes at room temperature in the dark. 400 µl of 1X Binding Buffer was added to each tube and the fluorescence was detected analyzed using a FACSCalibur instrument (BD Biosciences) and analyzed using FlowJo analysis software.

2.6. Nucleic Acid Extraction

Parental and resistant cells growing in drug or just thawed were seeded at a density of 0.8x10^6 per well in 6 well-plates and incubated without drug for 24 hours. Cells were harvested and genomic DNA and mRNA from parental and resistant cell lines were extracted simultaneously from the same pellet, using the AllPrep DNA/RNA Mini kit (Qiagen, Canada) according to manufacturer's instructions. Extraction procedures were modified to isolate total RNA that will contain miRNAs.

The cells were lysed directly in the well and the lysate was homogenized using QIAshredder spin columns and transferred into the ALLPrep DNA spin column for DNA to bind to the column. The column was centrifuged at 8000 g for 1 minute to collect the flow-through RNA extraction. The column was washed with 500 µl Buffer AW1 and AW2 and the DNA bound to the AllPrep DNA spin column was then eluted with 2 × 50 µl of H_2O so that the DNA could be concentrated and used for genome profiling. The flow-through RNA-containing fraction was mixed with an equal volume of 100% ethanol. The mixture was then transferred to an RNeasy MinElute spin column from the RNeasy Micro kit for RNA to bind to the column. The column was washed with 500 µl Buffer RPE and the RNA was diluted in 30µl of RNAse-free water. Quantity and quality of purified RNA and DNA was determined by ND-1000 spectrophotometer nanodrop. The RNA with A260/A280 ratio higher than 1.8 and DNA A260/A280 ratio higher than 2 were selected. The RNA integrity was measured with a 2100 bioanalyzer (Agilent Technologies) and RNA with RIN scores higher than 8 were qualified for the gene expression profiling. RNA was stored in −80°C and DNA was stored at −20°C.

2.7. Quantitative Real Time PCR (qRT-PCR)

qRT-PCR was carried out with the GoTaq qPCR Master Mix (Promega). All reactions were performed in triplicates in a 96-well plate with the CFX96 Touch™ Real-Time PCR Detection

System (Bio-Rad) and qRT-PCR analysis was performed using the Bio-Rad CFX Manager™ Software.

Prior to qRT-PCR analysis, 1µg of total RNA was converted into cDNA using the iScript™ cDNA Synthesis Kit (Bio-Rad). The reaction was performed according to the manufacturer's protocol. The qRT-PCR was carried out in a cycle of 25°C for 5 minutes, 42°C for 30 minutes, 85°C for 5 minutes. The cDNA was subsequently used for qRT-PCR analysis. Primers to amplify specific regions of genomic DNA or cDNA were designed using Ensembl (www.ensembl.org) and PrimerQuest (http://www.idtdna.com/primerquest/home/index). For ABCB1, the NM-000927 reference sequence from NCBI was used to design primers. The primers used in this study are listed in table 3.

qPCR was carried out using Gotaq® qPCR Master Mix (Promega) with the following reaction mix: 5µl of 2X GoTaq® qPCR Master Mix, 1µl each of forward and reverse primer (final concentration of 200nM), 2.5µl volume of 1:5 diluted cDNA and nuclease free water. Cycling parameters used were: 1 cycle 95°C 5 min; 39 cycles 95°C 10 s, 60°C 30s, and 65°C 30s and 1 cycle 65°C 1 min. All expression levels were normalized to relative HPRT1 expression.

The copy numbers of the ABCB1 gene were confirmed by Real-time Quantitative PCR experiments. qPCR was carried out using Gotaq® qPCR Master Mix using 50ng of genomic DNA

for copy number analysis. We used RNase P copy number as control since our aCGH results showed no amplification or deletion in RNase P gene in any of the cell lines. Cycling parameters used were: 1 cycle 95°C 5 min; 39 cycles 95°C 10 s, 60°C 30s, and 65°C 30s and 1 cycle 65°C 1 min. Experiments were done in triplicate.

Gene	Forward Reverse	Primer efficiency
ABCB1 5'UTR	Fwd: TTCGCTCTCTTTGCCACAGGAAG Rev: AAGACGTGAAATTTTGGAAGAAGATAC	118%
ABCB1 Coding sequence	Fwd: AAATTTGACACCCTGGTTGGAGAGAG Rev: TTATCCAGAGCCACCTGAACCACTG	110%
ABCB1 Coding sequence/cDNA	Fwd: TTTCTATTGCTACAGAATAAAAGATG Rev: CTCTCTCCAACCAGGGTGTCAAATTT	117%
AREG	Fwd: GAGAAGCTGAGGAACGAAAGA Rev: GGCAGTGACTCCAATGTGATA	98.7%
BTC	Fwd: CCACACAATCAAAGCGGAAAG Rev: CTCACACCTTGCTCCAATGTA	120%
HB-EGF	Fwd: TTCTCTAACTCCTGCCATTCTTC Rev: CCTGTTCCTTCTCAGCCTTT	83%
EGF	Fwd: ACACATGCTAGTGGCTGAAA Rev: GCATCCTCTCCCTCTGAAATAC	107%
EREG	Fwd: CTGGCATGTGCTAGGGTAAA Rev: TGCATGGATACACATGGAGAC	93%
IL-6	Fwd: CCAGGAGAAGATTCCAAAGATGTA Rev: CGTCGAGGATGTACCGAATTT	111%
HPRT1	Fwd: CGTCGTGATTAGTGATGATGAAC Rev: AAGACGTTCAGTCCTGTCCATAA	90%
RNASE P (RPP30)	Fwd: GCAAGAAGTTTCTCCGAATCC Rev: GCGCAGAGCCTTCAGGT	100%

Table 2.3. List of primers used in this study

2.8. Rhodamine Accumulation Assay

To determine the drug efflux properties of cells, $1x10^5$ cells were re-suspended in media containing 500 μM rhodamine 123 (Sigma-Aldrich, St. Louis, MO), with or without 100nM of one of the following inhibitors, verapamil (Sigma-Aldrich, St. Louis, MO), lapatinib (LC Laboratories, Woburn, MA, USA) or Neratinib (Selleckchem, Houston, TX, USA). Cells were incubated for 1 hour at 37 °C in the dark to absorb Rhodamine. After incubation, cells were centrifuged at 1400 rpm for 4 minutes, re-suspended in fresh media with or without 100nM of inhibitor and incubated for 30 min at 37°C in the dark. Cells were washed twice with ice-cold PBS and analyzed for green fluorescence (525 nm) intensity using a FACSCalibur instrument (BD Biosciences) and analyzed using FlowJo analysis software.

2.9. Gene Expression profiling

We performed gene expression microarray analysis using SurePrint G3 Human Gene Expression Microarray kit 8x60K (Agilent Technologies). For each hybridization, 100ng RNA was reverse transcribed into cRNA and labeled with Cy3 using the One-Color Low Input Quick Amp labeling kit (Agilent Technologies, Inc). Sample preparation and microarray hybridization were performed following the manufacturer's standard protocols. The amplified, labeled cRNA was purified using RNeasy Mini Kit (Qiagen, Canada) and assessed for dye incorporation and cRNA yield using the

nanodrop (ND-1000. spectrophotometer). Labeled cRNAs were denatured and hybridized onto Sure Print G3 Human GE 8X60K microarray (Agilent Technologies) at 65 °C for 17h in a rotating Agilent hybridization oven. Following hybridization, arrays were washed and scanned using Agilent Scanner G2505B. Microarray data were extracted and visualized using the Feature Extraction Software v8.1 and imported into GeneSpring GX 10.0 (Agilent Technologies, Inc.) for analysis.

Arrays were normalized using Quantile inter-array normalization, with the threshold set to intensity value of 1 and normalized to the 75th percentile. Gene expression profiles of parental and resistant pairs were compared using paired t-tests with Benjamini-hochberg correction to identify genes with significant differences in expression between parental and resistant pairs (adjusted p value < 0.05).

2.10. Array comparative genomic hybridization (aCGH)

Array CGH was performed on high-resolution human genome CGH 1M microarrays (Agilent Technologies, Inc.) containing 1 million oligonucleotide probes with a median resolution of 2kb. The experiments were performed based on the manufacturer's standard protocols. 3.0µg of genomic DNA from the experimental sample and from normal diploid DNA (pool of DNA obtained from 5 healthy individual, Promega, Madison, WI) were digested with 5 units of each

Alu1 and Rsa1 (New England Biolabs, Ipswich, MA) for 2 hours at 37°C, then at 65°C for 20 minutes. Labeling reactions were carried out according to Agilent's standard protocol using random primers and exo-Klenow from the Agilent Genomic DNA labeling kit where the experimental sample was labeled with Cy5-dUTP and the reference samples was labeled with Cy3-dUTP. The labeled DNA was subsequently purified using a Centricon YM-30 column (Millipore, Billerica, MA) according to manufacture protocol. Specific activities for labeled DNA were determined by ND-1000 spectrophotometer nanodrop (ND-1000. spectrophotometer). The Cy5-labled experimental and Cy3-labled reference DNA were pooled and mixed with 50µg of human Cot-1 DNA (Invitrogen), 52µl of 10× aCGH Blocking Agent (Agilent Technologies) and 260 µl of 2× HI-RPM Hybridization Buffer (Agilent Technologies) and incubated at 95°C for 3 minutes, at 37°C for 30 minutes. Probes were applied to the slide using an Agilent microarray hybridization station. Hybridization was performed at 65 °C for 40 h with constant rotation. The arrays were disassembled and washed according to manufacturer protocol with wash buffers supplied with the Agilent kit. The slides were scanned using an Agilent 2565AA DNA microarray scanner and data were extracted using the Feature Extraction Software v8.1. The data were visualized and analyzed with Agilent CGH Analytics software v3.2.25 usingADM-2 algorithm. The parameters used for aCGH data analysis are listed in table 4.

PARAMETERS	
Aberration Algorithm	ADM2
Threshold	6
GC Correction	ON
Window Size	10Kb
Centralization	ON
Bin Size	10
Centralization Threshold	6
Fuzzy Zero	OFF
Nesting Level	OFF
Combine Replicates (Intra Array)	ON
Combine Replicates (Inter Array)	OFF
Genome	hg19
Aberration Filters	minProbes = 5 AND minAvgAbsLogRatio = 0.3 AND maxAberrations = 10000 AND percentPenetrance = 0
Feature Level Filters	gIsSaturated = true OR rIsSaturated = true OR gIsFeatNonUnifOL = true OR rIsFeatNonUnifOL = true; Include matching values=false
Design Level Filters	NONE
Array Level Filters	NONE
Metric Set Filters	NONE
Genomic Boundaries	NOT APPLIED

Table 2.4. Parameters used for aCGH data analysis.

2.11. Fluorescent In Situ Hybridization.

2.11.1. Preparation of metaphase arrest slides

Cells were split in T75 flasks, one day prior to performing chromosome spread experiments to synchronise the cells. The medium was replaced with fresh medium 3 hours prior to harvesting and colcemid was added at a final concentration of 0.1μg/ml and cells were incubated for 1.5 hours. After incubation, cells were trypsinised and centrifuged at 1000 rpm for 10 minutes to pellet the cells. The supernatant was removed, leaving ~500μl of medium on the pellet, and cells were gently re-suspended in the remaining medium. 7 ml of pre-warmed hypotonic solution (0.075M KCl) was added drop by drop to the cells with agitation, and the cells were incubated at 37°C for 10 minutes. A few drops of ice cold, freshly prepared Carnoy's fixative (3 parts methanol to 1 part acetic acid) were added, gently mixed and centrifuged at 900 rpm for 10 minutes. The supernatant was removed and the cells were re-suspended in ~500μl of remaining fixative. 7 ml of fixative was added to cells while mixing and cells were incubated for 10 minutes at room temperature. The cells were centrifuged at 900 rpm for 10 minutes and were gently re-suspended in the remaining medium and stored at -20°C.

To prepare the slides, 10-20 µl of metaphase suspension were dropped from a height of ~40cm onto a wet slide that was placed horizontally at a 45° angle. The slides were air-dried and aged overnight at 65°C and stored until needed.

2.11.2. Hybridization

For fluorescence in situ hybridization (FISH) analysis, two FISH probes, RP11-91M13 and Cep7, were purchased from Empire Genomics and the hybridizations were carried out according to manufacturer's instructions. Probes were denatured at 73 °C for 5 minutes, cooled on ice for 2 minutes, and incubated at 37°C for 15 minutes. Slides were denatured for 5 minutes at 73 °C in pre-warmed denaturation buffer (70% formamide, 2x SSC, PH 7-8). Slides were then washed in a series of 70%, 85%, 100% ethanol solutions for 1m each and dried at 45°C using a slide warmer until ethanol evaporates. 10 µl of probe mixture (2 µl probes and 8 µl hybridization buffer) were pipetted onto a slide and covered with 22X22, clean coverslip and sealed with rubber cement. The slides were incubated at 37°C for 16 hours.

2.11.3. Detection

The coverslips were removed and slides were washed with pre-warmed WS1 solution (0.4xSSC/0.3% NP-40) for 10 seconds at 73°C and 1 minute in WS2 solution (2XSSC/0.1% NP-

40). Slides were allowed to air-dry in the dark. Nuclei and chromosomes were counterstained with 10 µl DAPI and the signals were visualized using a Jenco Epi-fluorescent Microscope (Jenco International Inc.) equipped with a CCD camera (Applied Imaging Diagnostic Instruments).

2.12. Cell Lysis/Western Blotting

Total cell lysates were prepared from parental and resistant cell lines. Exponentially growing cells were washed with cold phosphate buffer saline (PBS), pelleted and lysed in HMETG lysis buffer (50 mM HEPES/NaOH pH 7.5, 150 mM NaCl, 1.5 mM MgCl2, 1 mM EGTA, 1% Triton X-100, and 10% glycerol) supplemented with protease inhibitor cocktail (Complete Protease Inhibitor, Roche, Germany) and phosphatase inhibitors. The amount of protein in lysates was quantified using pierce BCA protein assay kit (Thermos Scientific) according to manufacturer's instruction. Samples were prepared by adding 4X lammeli sample buffer (Bio Rad, USA) and beta mercaptoethanol. Samples were applied on a 4–20% Mini-PROTEAN TGX precast gel (Bio-Rad). Protein transfer was carried out at 30 V overnight at 4 °C using nitrocellulose blotting membranes (Amersham Proteran supported 0.45 μm for high molecular weight protein and Bio Rad 0.2 μm for 4EBP). The membrane were blocked with 5 % bovine serum albumin (BSA) in TBST (137 mM Sodium Chloride, 20 mM Tris and 0.1% Tween-20) at room temperature for 1

hour and were further incubated with primary antibodies diluted in TBST. The list of the antibodies used in this study are listed in table 4.

Antibody	**Source**	**Clone**	**Host**	**Phosphorylation site**
ABCB1	Cell signaling	Monoclonal-E1Y7S	Rabbit/IgG	
ABCB1	Sigma Aldrich	Monoclonal-clone F4	Mouse/IgG	
4EBP1	Cell signaling	Monoclonal-53H11	Rabbit	
Phospho 4EBP	Cell signaling	Monoclonal	Rabbit	T37/46 and S65
RSP6	Santa Cruz Biotechnology	Monoclonal	Mouse	
EGFR	Cell signaling	Monoclonal	Rabbit	TYR 1068
Phospho EGFR	Cell signaling	Monoclonal	Rabbit	
ERK 1/2	Cell signaling	Monoclonal	Rabbit	T202/Y204
Phospho ERK	Cell signaling	Monoclonal	Rabbit	
AKT	Cell signaling	Monoclonal	Rabbit	
Phospho AKT	Cell signaling	Monoclonal	Rabbit	S473

Table 2.5. List of antibodies used in this study

The membranes were washed three times with TBST and incubated with either anti–rabbit or anti-mouse IgG secondary antibodies conjugated with horseradish peroxidase for 1 hour at room

temperature. Membranes were washed three times and protein expression was detected using Clarity™ western ECL substrate (Bio Rad, USA).

2.13. Gene knockdown by shRNA

The TRC and pGIPZ shRNA lentiviral constructs expressing a non-targeting negative control shRNA (scr) or shRNA against ABCB1 were purchased from Thermo Scientific. The sequence targeted by each shRNAs are listed in table 5. The shRNA targeting 4EBP1 and 4EBP2 were kind gifts from Dr. Ivan Toposirovic's laboratory. The shRNA clones were grown in 2X LB broth (LB-Broth-Lennox 20 g/L Peptone 10 g/L Yeast Extract 5 g/L) at 37 °C for 18-19 hours with vigorous shaking. The culture was pelleted and the plasmid DNA was isolated using GenElute™ HP Plasmid Maxiprep Kit following the manufactures protocol.

2.13.1. Transfection

Cells were seeded and grown to 60–80 % confluence. 10 μg of purified DNA was used for a 10 cm dish transfection. In tube A, DNA was mixed with 500 μl of opti-mem (serum free medium). In tube B, 30 μl of polyethylenimine was diluted in 500 μl of opti-mem (serum free medium) reagent. The contents of both tubes were mixed gently and incubated at room temperature for 20 minutes. The DNA-Lipid complex was then added to the cells and cells were incubated at 37 °C

for 3-4 h. After incubation, medium was replaced with fresh medium. 24 h post-transfection 5 μl of Puromycin (10 mg/ml). Transfected cells were pelleted and used for qRT-PCR and western blot analysis.

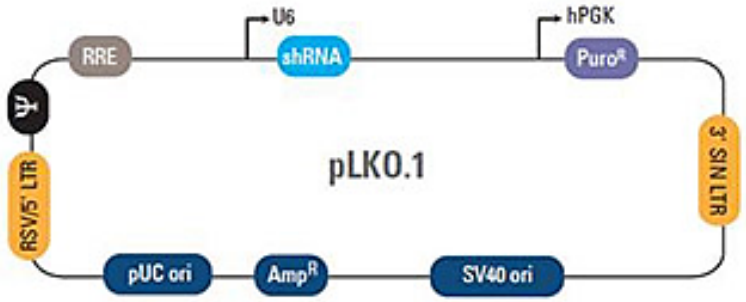

Figure 2.1 pLK0.1 vector element used in TRC lentiviral shRNA targeting ABCB1. This figure was reproduced from http://dharmacon.gelifesciences.com/

2.13.2. Transduction

HEK 293T cell lines were plated at a density of 3 x 10^6 in a T-75 culture flask 24 h before transfection. The plasmids were co-transfected with packaging plasmids into HEK 293T with polyethylenimine in a 2:1:2 ratios, respectively, to produce lentiviral particles. Virus-containing supernatant was collected 24 h after transfection, filtered through 0.45 µm syringe filter, aliquoted and stored at –80°C.

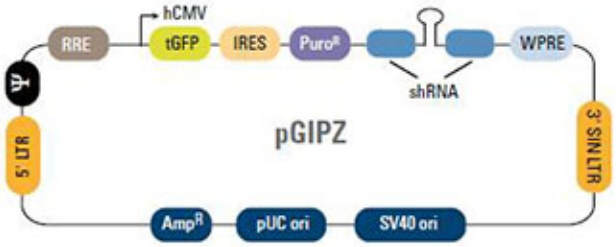

Vector Element	Utility
hCMV	Human cytomegalovirus promoter drives strong transgene expression
tGFP	TurboGFP reporter for visual tracking of transduction and expression
Puro^R	Puromycin resistance permits antibiotic-selective pressure and propagation of stable integrants
IRES	Internal ribosomal entry site allows expression of TurboGFP and puromycin resistance genes in a single transcript
shRNA	microRNA-adapted shRNA (based on miR-30) for gene knockdown
5' LTR	5' long terminal repeat
3' SIN LTR	3' self-inactivating long terminal repeat for increased lentivirus safety
Ψ	Psi packaging sequence allows viral genome packaging using lentiviral packaging systems
RRE	Rev response element enhances titer by increasing packaging efficiency of full-length viral genomes
WPRE	Woodchuck hepatitis posttranscriptional regulatory element enhances transgene expression in the target cells

Figure 2.2 pGIPZ vector structure and elements. This figure was reproduced from http://dharmacon.gelifesciences.com/

To infect the cell lines, virus-containing supernatant was supplemented with polybrene (8 μg/ml), and overlaid on the target cells. After overnight incubation with the viral supernatant, medium was replaced with fresh medium. Multiple clones of stably expressing shRNA from the same transfection were pooled and FACS sorted for GFP positive fraction.

ShRNA	Target Gene	Construct	Sequence
TRC Lentiviral	ABCB1	TRCN0000059686	GCTCATCGTTTGTCTACAG
TRC Lentiviral	ABCB1	TRCN0000059683	CCGAACACATTGGAAGGAAAT
TRC Lentiviral	ABCB1	TRCN0000059684	GCAGCAATTAGAACTGTGA
TRC Lentiviral	ABCB1	TRCN0000059685	CGACAGAATAGTAACTTGT
TRC Lentiviral	ABCB1	TRCN0000059687	GCTGCTTTCCTGCTGATCT
GIPZ Lentiviral	ABCB1	V2LHS_131347	AACTTGAGCAGCATCATTG
GIPZ Lentiviral	ABCB1	V2LHS_347173	AATCTTGGAGACATCATCT
GIPZ Lentiviral	ABCB1	V3LHS_347175	TTTGTGTATTTGTCTTCCA

Table 2.6. List of shRNAs and the targeted sequence used in this study

2.14. Immunohistochemistry

Exponentially growing cells were trypsinized, pelleted and washed with cold PBS. Cells were fixed by adding 3 ml of 3.7 % paraformaldehyde in PBS (or 10 % Buffered Formalin) drop by drop while gently vortexing cells. Cells were incubated at room temperature for 30 minutes. Cells were pelleted and washed with PBS twice. The pellet was re-suspended in 70 % ethanol and cells were paraffin embedded and sections were cut and placed on superfrost plus slides.

Immunohistochemistry was performed at the Segal Cancer Centre Research Pathology Facility (Jewish General Hospital). Tissue samples were cut at 4-μm, placed on SuperFrost/Plus slides (Fisher) and dried overnight at 37°C, before IHC processing.

The slides were then loaded onto the Discovery XT Autostainer (Ventana Medical System). All solutions used for automated immunohistochemistry were from Ventana Medical System unless otherwise specified. Slides underwent de-paraffinization, heat-induced epitope retrieval (CC1 prediluted solution Ref: 950-124, standard protocol). Immunostaining for P-glycoprotein was performed using a heat protocol. Briefly, rabbit polyclonal anti-ABCB1 antibody (Cells signaling technology, Inc.), diluted at 1:250 in antibody diluent (Ref: 251-018) was incubated on the slides for 32 min at 37 °C, then followed by incubation with the appropriate detection kit reagents (OmniMap anti-Rabbit-HRP, Ref: 760-4311 for 8 min, followed by ChromoMap-DAB (Ref: 760-159). A negative control was performed by the omission of the primary antibody. Slides were counterstained with hematoxylin for four minutes, blued with Bluing Reagent for four minutes. Slides were removed from the autostainer, washed in warm soapy water, dehydrated through a series of graded alcohol washes, cleared in xylene, and mounted with mounting medium (Eukit, E.M.S). Sections were analyzed by conventional light microscopy and scanned.

Chapter 3

Results: Molecular profiling of PTX resistant TNBC cell lines

3.1. Development of in vitro model of acquired resistance

3.2. Panel of TNBC cell lines

In vitro studies on cell lines with acquired resistance provide models for characterization of the biological mechanisms of resistance. In order to generate TNBC resistant cell lines, we first prepared a list of triple negative breast cancer cell lines that showed sensitivity to PTX at Nano Molar concentration in previous studies [191, 192]. Choosing a parental cell line is important, as it is the basis of the resistant cell lines and the basis of all the subsequent experiments. The parental cell line that can be easily maintained in cell culture is recommended, as resistant variants usually become more challenging to grow.

At the time we started this project, TNBC had been classified into two major subgroup, basal A and basal B [193]. To capture this heterogeneity we chose 3 cell lines that belong to basal A subtype including BT20, MDA-MB-468 and HCC1937 and 4 cell lines from basal B subtype including HCC38, SUM149, MDA-MB-231 and MDA-MB-436 (Table 3.1). These cell lines were chosen based on their mutation profile including p53 mutations, the most common mutation in TNBC, as well as PIK3CA, PTEN and BRCA1 mutations.

Cell line	Disease	Ethnicity	Age	Basal Subtype	TNBC subtype	Reference
BT20	Advanced ductal carcinoma	Caucasian	74	Basal A	Unclassified	Lasfargues, E. Y. et al. 1958
SUM149pt	primary inflammatory ductal carcinoma	Caucasian		Basal B	BL2	Ethier, S. P et al. 1993
MDA-MB-231	Metastatic pleural effusion	Caucasian	51	Basal B	MSL	Cailleau, R. et al. 1978
MDA-MB-436	Metastatic pleural effusion	Caucasian	43	Basal B	MSL	Cailleau, R. et al. 1979
MDA-MB-468	Metastatic pleural effusion	Black	51	Basal A	BL1	Cailleau, R. et al. 1980
HCC38	primary ductal carcinoma	Caucasian	50	Basal B	BL1	Gazdar, A. F. et al. 1998
HCC1937	primary ductal carcinoma	Caucasian	23	Basal A	BL1	Gazdar, A. F. et al. 1999

Table 3.1. Cell line characteristics and subtypes.

BT20 cells were derived from an advanced ductal carcinoma from a 74-year-old Caucasian female [194]. This cell line was established "by isolation and cultivation of cells spilling out of the tumour when it was cut in thin slices". BT20 is classified as basal A subgroup of basal breast cancer according to Kao et al. classification of TNBC cancer cell lines [193]. This cell line harbors mutation in TP53, PIK3CA and CDKN2A genes as well as EGFR gene amplification [195].

The SUM149pt cell line (a kind gift from Dr. William Foulke's laboratory, McGill University) was developed in Dr. Stephen Ethier's laboratory. This cell line was derived from an invasive ductal carcinoma from a Caucasian female patient with inflammatory breast cancer. The cell line

is classified as basal B and harbors a mutant BRCA1 gene and expresses cytokeratin 8, 18 and 19 [196].

The MDA-MB-231 cell line, derived from a metastatic pleural effusion from a 51 year-old Caucasian, was obtained from ATCC. This cell line is highly invasive, exhibiting features of epithelial-mesenchymal transition (EMT) and is classified as Basal B subtype. It harbors KRAS and BRAF mutation in addition to TP53 missense mutation[192].

MDA-MB-468 was isolated by Dr. R Cailleau in 1977 from a pleural effusion of a black female patient with metastatic adenocarcinoma at the age of 51. This cancer cell line harbors mutations in TP53 and PTEN genes. MDA-MB-468 expresses high level of EGFR, which is attributable to the amplification of the *EGFR* gene locus [197]. It is categorized as Basal A subtype.

MDA-MB-436 was developed by Dr. R Cailleau from a Metastatic pleural effusion from a 43-year-old female Caucasian. This cell line belongs to Basal B and carries a BRCA1 mutation. *TP53* gene in this cell line harbors a frame-shift insertion.

The HCC38 cell line was initiated from a 50 year-old Caucasian white female with grade III primary ductal carcinoma. The patient had prior history of leiomyosarcoma and family history of breast cancer. The cell line carries a wild type BRCA1, however, it exhibits BRCA1 promoter

hypermethylation and minimal expression of the BRCA1 RNA transcript [198]. HCC38 is categorized as Basal B subtype

The HCC1937 cell line was isolated from a 23 year-old female Caucasian with grade III ductal carcinoma. This cell line was classified as Basal A. It harbors a TP53 mutation and is homozygous for the BRCA1 5382C mutation.

Recent work from Dr. Jennifer Pietenpol's laboratory published in the Journal of Clinical Investigation used cluster analysis to examine gene expression data from 587 TNBC cases and identified six distinct subtypes of TNBCs [34]. Based on this classification, the cell lines I chose reflect some of the reported heterogeneity of TNBCs. SUM149 and MDA-MB-468 are basal-like, MDA-MB-436 and MDA-MB-231 are mesenchymal-like and BT-20 cells are unclassified (Table 3.1).

3.3. Development of PTX resistant cell lines

3.3.1. Cell lines sensitivity to PTX

The cell line sensitivity to PTX was determined using Alamar blue cytotoxicity assay. In order to detect significant differences in drug sensitivity in the assay, we allowed time for at least 3 cell divisions after drug treatment. The concentration of paclitaxel required to inhibit the growth of

50% of resistant cells (the IC_{50}) was determined using Graph Pad Prism software. All the experiments were performed in triplicates and were repeated at least three times. We observed a broad spectrum of paclitaxel sensitivity across the panel of cell lines with IC_{50} ranging from pM to more than10 μM (Figure 3.1). SUM149 cell line was the most sensitive of the cell lines to PTX with an IC_{50} of 0.00002 μM, whereas HCC1937 did not show sensitivity to micro molar concentrations of PTX. The intrinsic resistance observed in HCC1937 can be justified by the low proliferation rate and the long doubling time of this cell line (69.2 h).

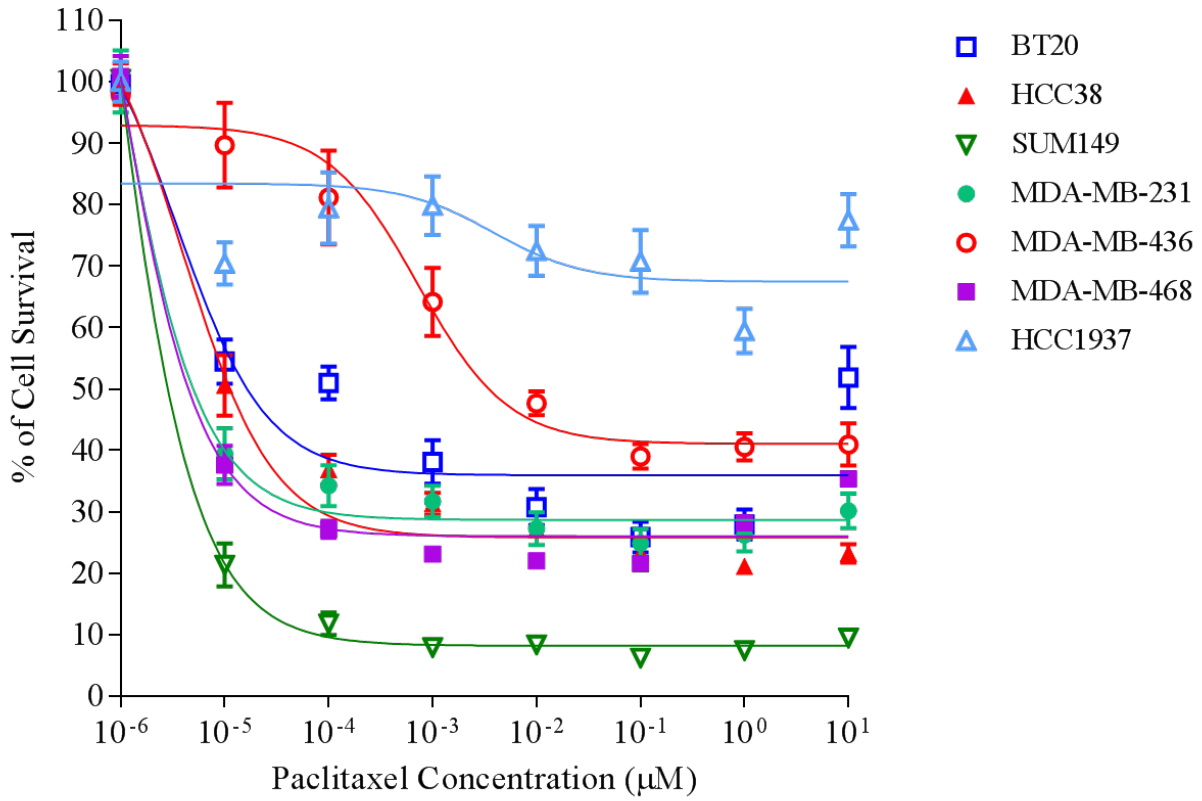

Figure 3.1 Determination of PTX sensitivity of the panel of TNBC cell lines, using cell viability assay. The curves were created using sigmoidal equation in GraphPad Prism.

3.3.2. Development of PTX-resistant cell lines

The first acquired drug resistant cell line was established in 1970 using a stepwise increase in treatment dose with actinomycin D [199]. This was one of the first reports describing the use of cell line models with in vitro-derived chemo-resistance. The development of drug resistant cell lines can be carried out using 2 approaches: a clinically relevant model and a high-level laboratory model. Clinically relevant drug-resistant cell lines are developed, mostly by pulsed treatment strategy, to mimic the conditions cancer patients experience during chemotherapy. Resistant cell lines developed with this aim display less resistance compared to high-level laboratory models. However this method can result in the development of unstable, low-level resistance, with few molecular changes to detect and analyze. On the other hand, high-level laboratory models can provide a more stable model of resistance. We aimed to develop a high-level in vitro model of acquired resistance, which is developed by increasing concentration of drug over time [200].

To develop the resistant cell lines, the cells were seeded in a T75 flask at 20% density. 24h later the cells were treated with 1/100 dose of IC_{50} and were maintained in the same dose for two passages. The drug concentration was increased two fold each time until a dramatic lethal effect was observed; this concentration was defined as the desired level of resistance. The dead cells were removed and the media was replaced with fresh media with no treatment and the individual

cells that survived were allowed to recover and form growing colonies. No antibiotic was used while establishing drug resistant cell lines, as resistance mechanisms developed in the presence of antibiotics may not reflect clinical drug resistance [200]. All drug treatments were begun 24h following the passage of the culture.

Once the desired level of resistance was achieved, the selected resistant cells were pooled and were maintained in the presence of final concentration of drug. The SUM149R and MDA-MB-436R cells were maintained in 100nM PTX and MDA-231R, BT20R and MDA-436R cells were maintained in 50nM, 40nM and 40nM PTX, respectively. The sensitivity of the surviving population was determined using alamar blue and the fold resistance was calculated by following equation:

Fold resistance = IC_{50} of resistant cell lines / IC_{50} of parental cell lines

The fold resistance was in the range of 10^2-10^4 in resistant cells compared to the parental cells from which they were derived (Table 3.2). We successfully developed 5 resistant cell lines, which will be referred to as BT20R, SUM149R, MDA-231R, MDA-436R and MDA-468R in this thesis (Figure 3.2). During the development of drug resistant cell lines, a non-treated flask of the parental cell lines was kept in culture. A duplicate flask was prepared and the IC_{50} of these cells were determined frequently to assess whether the long-term culture of the parental cells altered

the PTX sensitivity. Although we detected an increase in IC_{50} of the parental cell lines over time, this increase was not comparable to the IC_{50} of resistant cell lines **(Figure 3.3)**. Throughout the development of resistant cell lines, both parental cells and resistant cells were frozen down in liquid nitrogen at each step and the cell pellet was collected for further studies.

Cell lines	IC50	Fold Resistance
BT20 P	1.8x 10-5	39548
BT20 R	0.7	
SUM149 P	1.3 x 10-6	268848
SUM149 R	0.3	
MDA-MB-231 P	1.7 x 10-6	21756
MDA-MB-231 R	0.03	
MDA-MB-436 P	N/A	N/A
MDA-MB-436 R	N/A	
MDA-MB-468 P	8.2 x 10-6	9713
MDA-MB-468 R	0.08	

Table 3.2. The IC_{50} values of parental and resistant cell lines and the fold resistance. N/A; not applicable. We were unable to reach the IC_{50} for the MDA-MB-436 cell lines despite increasing PTX concentrations in the μM range.

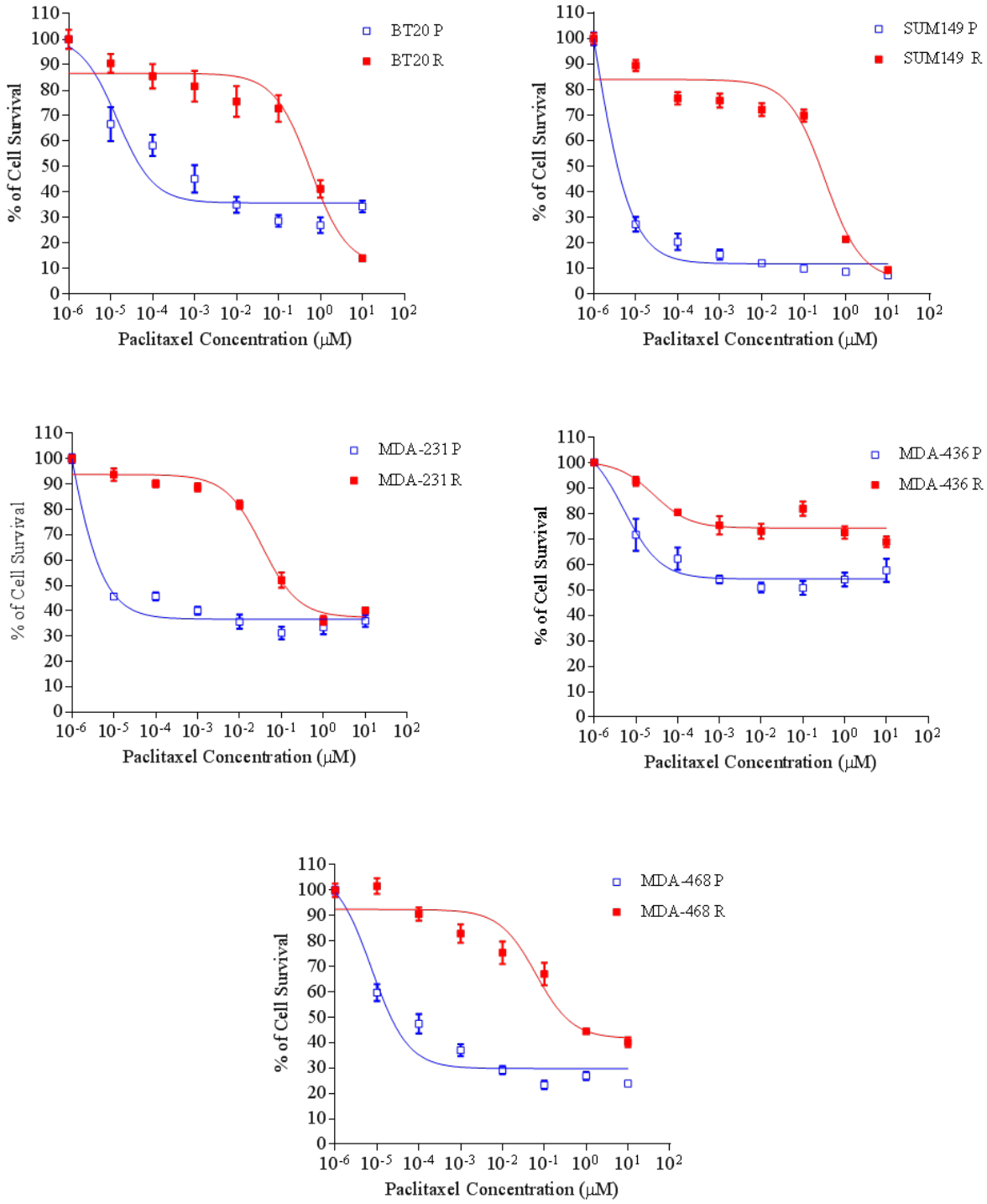

Figure 3.2. PTX sensitivity of resistant cell lines and their sensitive counterparts. A significant increase in IC_{50} concentration was determined for each PTX resistant cell line relative to that for the corresponding parental cell line.

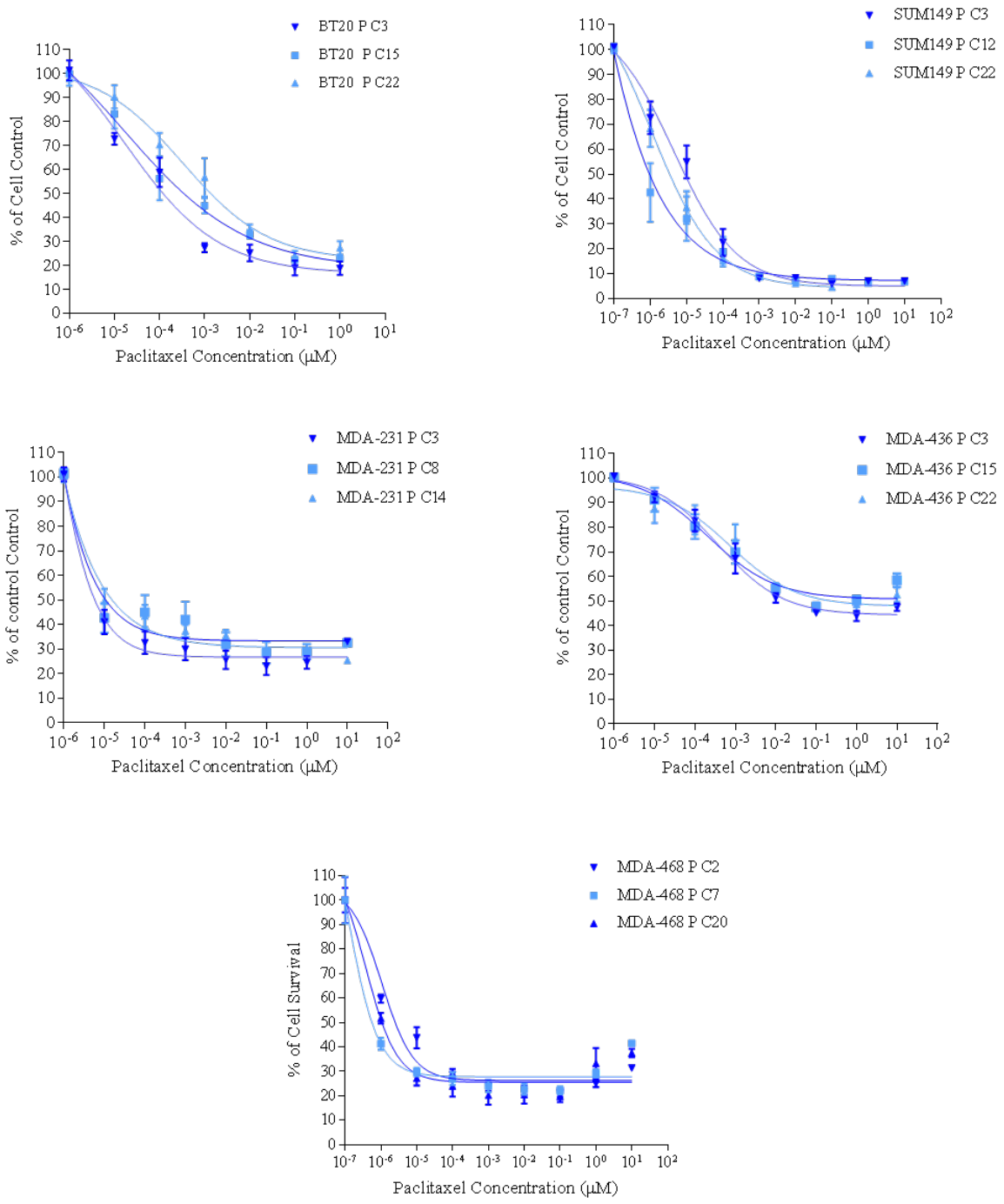

Figure 3.3. Parental cells exhibit slight increases in IC_{50} following long-term culture.

3.3.3. Assessment of stably resistance phenotype in PTX resistant cell lines

To assess whether the resistance phenotype in newly generated resistant cell lines is stable, the MDMB-436R and SUM149R cell lines were maintained in media without drug for 3 passages and the sensitivity of the cells was determined using the alamar blue assay. The result of the cytotoxicity assay confirmed that resistance phenotype in MD-MB-436R and SUM149R cell lines persisted throughout several passages without continuous PTX exposure, suggesting a stably resistant phenotype in resistant cell lines (**Figure 3.4).**

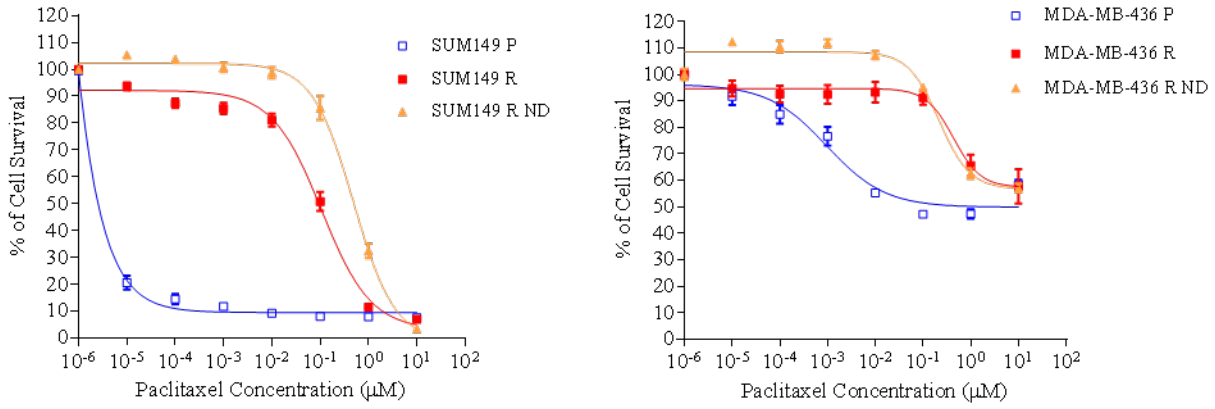

Figure 3.4. Assessment of stably resistance phenotype in PTX resistant cell lines. Following maintenance of PTX resistant cell lines in culture for 3 passages without PTX, IC_{50} concentrations were re-assessed for SUM149R and MDA-MB-436R cell line using dose-response curves generated by GraphPad Prism software ND: No Drug., cells were maintained in medium without PTX for several passages.

3.3.4. PTX-Resistant cell lines display extended doubling time

PTX, like most anticancer agents, primarily targets proliferating cancer cells. It stabilizes microtubule formation, affecting the assembly and disassembly of cytoskeletons and thus leading to cell cycle blockage in G2/M and subsequently cell death. Passage through mitosis is a definite requirement for PTX-induced death and the quiescent cancer cells blocked at G0/G1 phase show less sensitivity to PTX [201]. It's been shown that in PTX-resistant cells the proliferation rate is significantly lower, the population doubling time is extended, and most cells are blocked in G0/G1 phase [202]. Therefore, we compared the doubling time and cell cycle parameters in resistant cell lines and their matching parental cell lines. The doubling times of all the resistant cell lines were longer than that of their matching parental cell lines (**Table 3.3**).

Cell lines	Doubling time (Hour)
BT20 P	21.8
BT20 R	26.1
SUM149 P	19.0
SUM149 R	24.6
MDA-MB-231 P	34.0
MDA-MB-231 R	48.0
MDA-MB-436 P	29.1
MDA-MB-436 R	46.3
MDA-MB-468 P	23.0
MDA-MB-468 R	28.0

Table 3.3. Cell lines doubling time in hours.

The decreased number of cells existing in the G2/M stage in the resistant cell lines may reduce the potency of PTX. Therefore, in order to further investigate the longer doubling times of the resistant cell lines we performed cell cycle analysis and compared the cell cycle compartments of resistant cell lines with their sensitive counterparts. The MDA-MB-436R cell lines displayed a higher proportion of cells existing in the G1 and S stages of the cell cycle and a reduced number of cells in the G2/M phase compared to the sensitive matching cell lines (p value < 0.05)We did not detect any significant changes in proportion of cells in different stages of cell cycle in other resistant cell lines **(Figure 3.5)**.

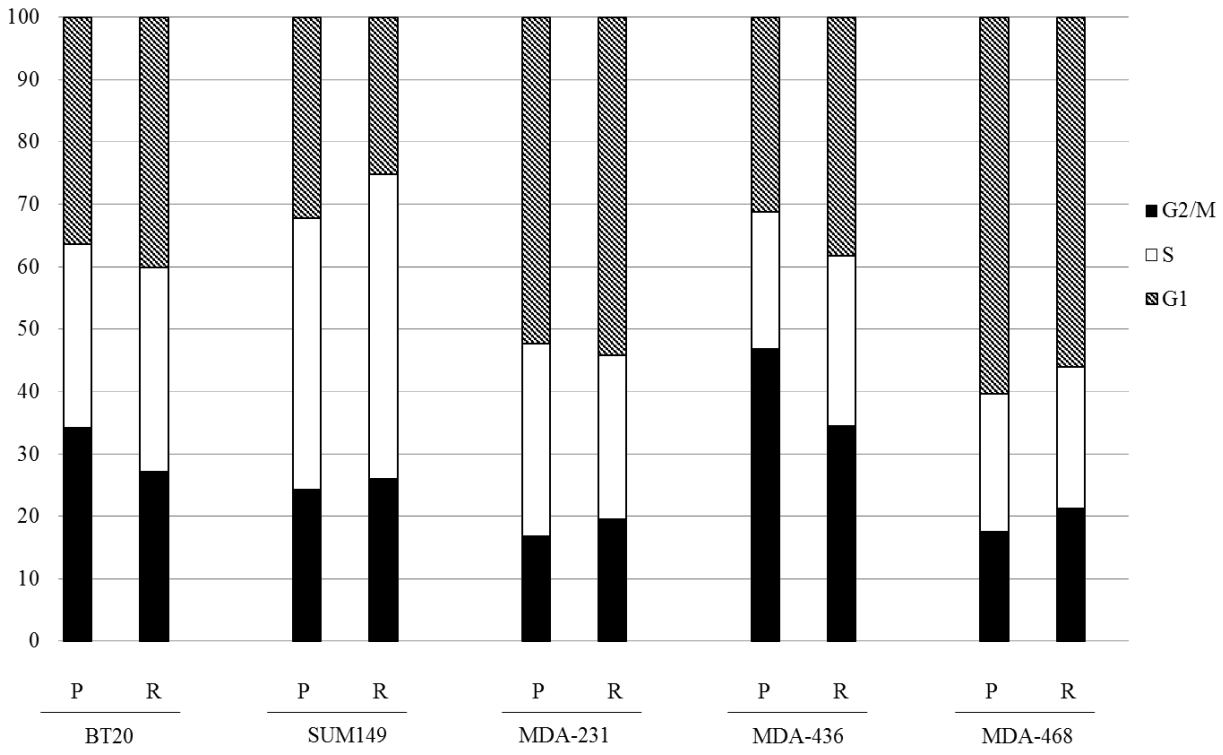

Figure 3.5. Flow cytometry analysis of cell cycle distribution of resistant cell lines and their sensitive counterparts. Cells were incubated for 48h, stained with propidium iodide and analyzed by flow cytometry. The number of cells in various stages of the cell cycle were quantified measuring the area under each compartments peak and are represented as percentage.

3.3.5. PTX-induced cell cycle arrest and apoptosis is decreased in resistant cells

We examined the effect of PTX on cell cycle distribution in resistant cell lines and their sensitive counterparts. Cells were treated with 100nM PTX for 24h, fixed in 70% ethanol and stained with propidium iodide and were analyzed using flow cytometry. We observed a significant reduction in the proportion of cells arrested at the G2/M checkpoint in resistant cells exposed to paclitaxel compared to parental cells **(Figure 3.6)**.

Next, we determined the susceptibility of the resistant cell lines to paclitaxel-induced apoptosis. Cells were treated with 100 nM PTX for 24, 48 and 72 h and viability was analyzed by propidium iodide and Annexin IV staining using flow cytometry. The drug-induced apoptosis in resistant cell lines compared to their parental counterparts was significantly reduced **(Figure 3.7)**. We noticed that the baseline apoptosis (in the absence of PTX) in drug resistant cell lines, BT20R, SUM149R and MDA-MB-468R, is significantly higher compared to parental cell lines.

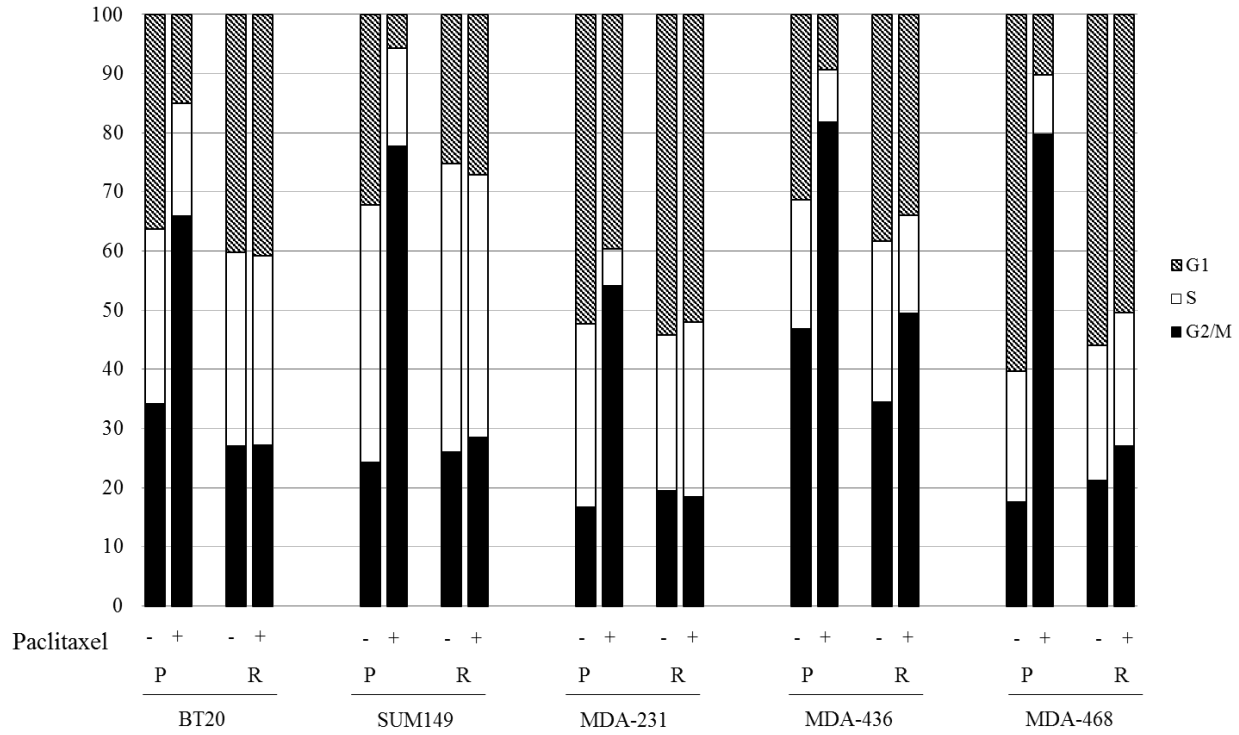

Figure 3.6. Flow cytometry analysis of the effect of PTX on cell cycle distribution of resistant cell lines and their sensitive counterparts. Cells were treated with or without 100nM PTX and incubated for 48h, stained with propidium iodide and analyzed by flow cytometry. The number of cells in various stages of the cell cycle were quantified measuring the area under each compartments peak and are represented as percentage. PTX treatment significantly induced cell cycle arrest at G2/M in all parental cell lines. The number of cell in resistant cell lines treated with PTX for 48h did not show a significant increase.

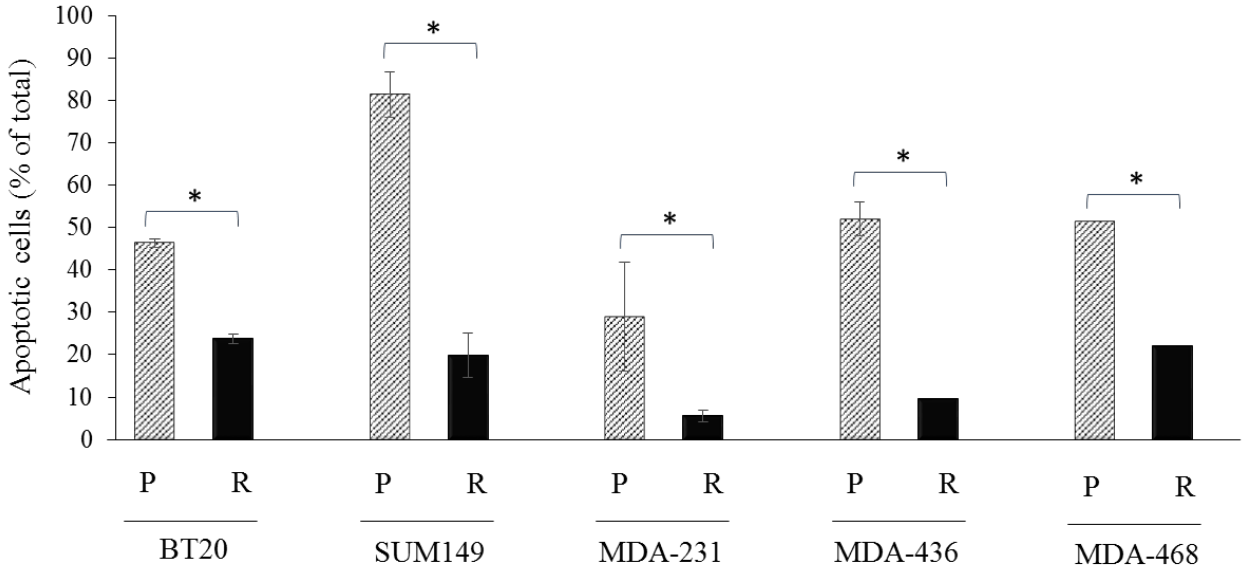

Figure 3.7 Apoptosis analysis of five pairs of resistant cell lines and their matching sensitive cell lines. Cells were treated with 100nM PTX for 72h and Total apoptosis level was measured by Annexin V-FITC assay. The results (mean ± SD) were determined from data generated in three independent tests. Student t test were performed to compare the PTX-induced apoptosis in resistant cell lines with their matching sensitive counterparts. *indicates significant p values ($p<0.05$)

3.4. Gene expression profiling of parental and resistant cell lines

In order to identify changes in gene expression associated with resistance to PTX, we performed gene expression profiling on parental and resistant cell lines. Parental and resistant cells were seeded in 6 well-plates and incubated without drug for 24 hours. Cells were harvested and mRNA from parental and resistant cell lines was extracted, reversed transcribed, labeled and hybridized to Agilent 60K SurePrint G3 Human Gene Expression Microarray. Microarray data were normalized using Quantile inter-array normalization with the threshold set to intensity value of 1 and normalized to 75th percentile. To eliminate the impact of systematic noise such as batch effect we performed two technical replicates for each sample.

The expression of ~22,000 transcripts was analyzed in parental and resistant cell lines. To assess the global landscape of expression and to visualize the impact of PTX resistance on gene expression pattern of resistant cell lines, we performed a principal component analysis (PCA), using GeneSpring GX 10.0 (Agilent Technologies, Inc.). PCA identifies transcriptional components, which each capture a part of the variance seen in gene expression across cell lines. The PCA analysis revealed a clear separation between the cell lines but no gathering were observed based on sensitivity to PTX (**Figure 3.8),** suggesting that there are only a small number of genes for which the expression is changed significantly during development of resistance.

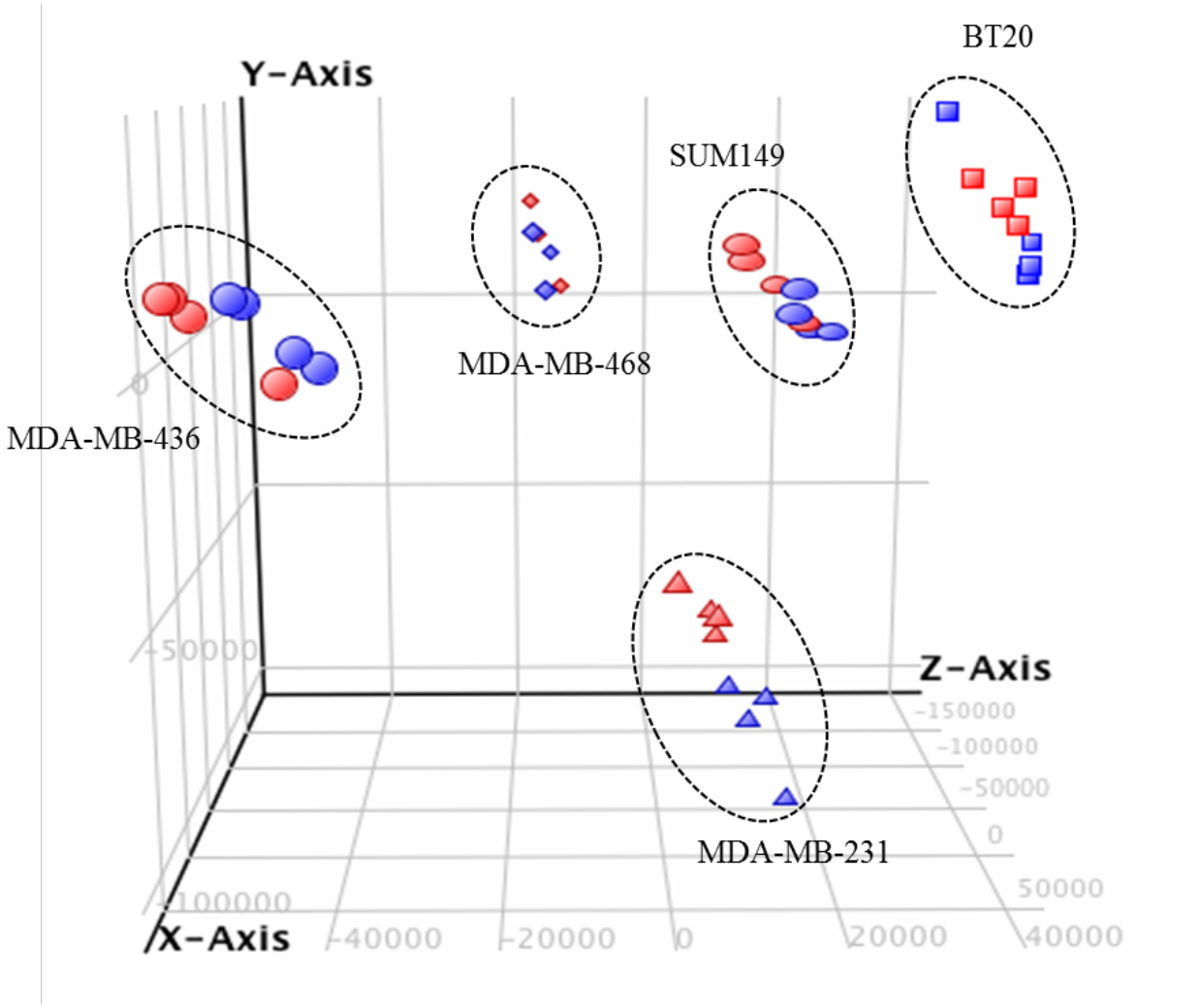

Figure 3.8. Principal components analysis for parental and resistant cell lines. Three-dimensional representation of the principal components analysis of all gene expression arrays consisting of: 4 for BT20P (blue square), 4 for BT20R (red square), 4 for SUM149P (blue oval), 4 for SUM149R (red oval), 4 for MDA-MB-231P (blue rectangle),4 for MDA-MB 231R (red rectangle), 4 for MDA-MB-436P (blue circle),4 for MDA-MB 436R (red circle), 3 for MDA-MB-468P (blue diamond),3 for MDA-MB 468R (red diamond). Proportion of variance explained: PC1, 31.84 %; PC2, 13.66 %; PC3, 11.67%. The PCA scores were computed and plot using GeneSpring version 10.0.

Using TNBCType (http://cbc.mc.vanderbilt.edu/tnbc/), an online subtyping tool for TNBC, we performed subtyping on gene expression data of both parental and resistant cell lines to determine whether the acquisition of PTX resistance influenced the molecular subtype of the resistant cell lines. According to Lehmann et al, SUM149 and MDA-MB-468 are basal-like, MDA-MB-436 and MDA-MB-231 are mesenchymal-like and BT-20 cells are unclassified [34]. These were validated with our own gene expression data for both parental and resistant cell lines, with the only difference with Lehmann et al being that BT-20 cells were classified as LAR or androgen responsive TNBCs.

Of ~22000 genes surveyed by microarray analysis, 5.0%, 3.7%, 9.0%, 7.3%, and 5.4% of the genes showed changes in expression of 2-fold or greater (p value < 0.05) in BT20, SUM149, MDA-MB-231, MDA-MB-436 and MDA-MB-468 cell lines, respectively. In order to identify differentially expressed genes in resistant cell lines compared to their sensitive counterparts, a comparative analysis were performed using paired t-tests with a Benjamini-Hochberg correction. The gene expression of parental cells was used as a baseline for up- or down-regulation of expression in resistant cell lines. All transcripts with no significant change in expression (FDR corrected p-value higher or equal to 0.05) or in linear fold change ($-2 < FC < 2$ for resistant vs parental) were excluded from the final gene list. Only genes passing these filters were retained to

improve the statistical relevance of our results. The top 15 up-regulated and down-regulated genes in each pairs are presented in **Table 3.4.**

According to our criteria, a total of 1094 differentially expressed genes were identified in BT20R cell lines, of which 630 genes were up-regulated and 464 genes were down-regulated compared to their parental counterparts. The fold changes of differentially expressed genes ranged from 2 to 176 for up-regulated genes and from -2 to -303 for down-regulated. However, more than 68% of differentially expressed genes did not show fold change higher than 3 or lower than -3. The most differentially expressed genes were *ABCB1* (+176 FC) and *FMR1NB*, Fragile X Mental Retardation 1 Neighbor, (-303 FC) (FC=fold change).

SUM149R cells showed the least number of differentially expressed genes with an equal number of up-regulated and down-regulated genes. More than 70% of these genes showed a fold change in the range of 2 to 3 and -2 to -3. The most differentially expressed genes were *ABCB1* (+221 FC) and *LTF*, Lactotransferrin (-35 FC).

In MDA-MB-231R, a list of 1977 differentially expressed genes was produced, containing 1205 up-regulated and 772 down-regulated genes, of which 1262 genes showed differential expression in the range of 2 to 3 or -2 to -3. MDA-MB-231R showed the most highly deregulated genes

compared to its parental counterpart. The differential expression of 58 genes was up-regulated in the range of +10 to +52 fold and 34 genes showed down-regulation of more than -10 fold.

The gene expression analysis of MDA-MB-436R cell line revealed 1598 differentially expressed genes, 1084 genes falls into low differentially expressed genes (-3< FC <3). The MDA-MB-436R cell lines showed the most highly differentially expressed genes, *CALB1*, Calbindin 1, with +519 fold increase in the resistant cell lines.

A total of 1186 differentially expressed genes were identified in the MDA-MB-468R cell lines, more than 68% of which were up-regulated. More than 66% of differentially expressed genes did not show fold change higher than 3 or lower than -3. The most differentially expressed genes were *H19*, long noncoding RNA H19, (+51 FC), *ABCB1* (+47 FC), and *ALDH1A*, Aldehyde dehydrogenase 1A, (+43 FC).

We next sought to identify a common gene signature across the panel of resistant cell lines. Our comparative analysis revealed that ABCB1 is the only common up-regulated gene across all resistant cell lines. However, a total of 86 genes were identified that were up-regulated (> 2 fold) in at least 3 of resistant cell lines compared to parental cells and not down-regulated in any. Of these, 13 genes were up-regulated in 4 resistant cell lines compare to their parental counterparts including *INHBA*, Inhibin, Beta A, (up-regulated in BT20R, MDA-231R, MDA-468R and

SUM149), *TRIM29*, Tripartite Motif Containing 29, *IFI27*, Interferon, Alpha-Inducible Protein 27, *SERPINB3*, Serpin Peptidase Inhibitor, Clade B (Ovalbumin) Member 3, *RASGRP2*, RAS Guanyl Releasing Protein 2, *IGF2*, Insulin-Like Growth Factor 2, *SERPINB4*, Serpin Peptidase Inhibitor, Clade B (Ovalbumin), Member 4 and *RTP4*, Receptor (Chemosensory) Transporter Protein 4 (up-regulated in BT20R, MDA-231R, MDA-436R, MDA-468R), *CLDN1*, Claudin 1, and *CTHRC1*, Collagen Triple Helix Repeat Containing 1 (up-regulated in MDA-231R, MDA-436R, MDA-468R and SUM149R). The up-regulation of ABCB1, the only common gene between all 5 resistant cell lines, was further investigated and the data are presented in the chapter 4 of this thesis.

		BT20		SUM149		MDA-MB-231		MDA-MB-436		MDA-MB-468	
		Gene	**FC**	**Gene**	**FC**	**Gene**	**FC**	**Gene**	**FC**	**Gene**	**FC**
Up- regulated Genes	1	ABCB1	176	ABCB1	222	PTGFRN	53	CALB1	519	H19	51
	2	IFI27	155	C4orf7	20	TRIM29	43	LY6D	107	ABCB1	47
	3	CSTA	37	PDIA2	13	CCL3	40	SERPINB5	96	ALDH1A1	43
	4	MX1	37	ANO1	9	C7orf29	37	KRT6A	75	TMPRSS11E	30
	5	XLOC002736	31	RNF144A	9	SORCS2	30	PCDHA1	31	WFDC2	26
	6	CALB2	30	CSF3	9	C3	28	KRT6C	26	FLG	21
	7	IFI44	28	OLAH	9	ABCB1	26	ABCB1	22	ALOX5	20
	8	ANXA1	26	IGFBP2	8	LAIR1	26	SFN	19	CALB2	17
	9	IFI44L	25	IL8	8	FLG	25	ZBTB32	15	MSX1	16
	10	IL13RA2	20	IL6	8	CHI3L2	24	KRT16P2	14	NNMT	16
	11	EREG	14	PTGER4	7	LCN2	22	LRRC38	14	SERPINB2	15
	12	OAS2	14	TLR4	7	RARRES2	22	KRT14	13	IFI27L2	14
	13	XAF1	13	HHIP	7	DMKN	19	SPANXA1	11	TNNT1	14
	14	IFI6	12	FST	7	FAP	18	KRT17	11	NGFR	14
	15	LOC201651	12	NFE2L3	6	GBP5	18	CASP10	11	DPYSL5	13
Down-regulated Genes	1	SH3BGRL	-10	C11orf86	-8	ADAMTS1	-17	PDE1C	-24	ADAMTS4	-6
	2	CXCR4	-11	FBXO32	-8	PDE1C	-22	TPM2	-29	MDGA2	-6
	3	KRT1	-14	SLC2A5	-8	SLCO4A1	-23	TNFRSF11B	-31	NR2F1	-7
	4	TAGLN	-14	S100A8	-8	CHRDL1	-23	C4orf7	-32	ITGBL1	-7
	5	MTMR1	-16	CCR2	-8	GALNT14	-24	AQP9	-32	CA9	-8
	6	SCGB2A2	-19	ABLIM3	-9	FAM155A	-25	BEX1	-35	CCDC160	-8
	7	DPYSL5	-21	DCN	-9	NRK	-25	CRABP1	-37	GLYATL2	-10
	8	RAMP1	-21	SPINK6	-11	LDOC1	-26	AHR	-49	RASIP1	-10
	9	MUCL1	-23	CYP4B1	-12	ZNF521	-28	IL1A	-50	LOC100131289	-10
	10	ZNF22	-33	SYT12	-17	PAGE2	-29	SNX13	-64	PDLIM3	-12
	11	SRGN	-33	WISP2	-18	CALHM2	-30	BZW2	-66	GSTA5	-14
	12	FAM107B	-106	CNR1	-18	PAGE2B	-34	CYP1B1	-68	MT1M	-14
	13	ACTG2	-127	MAP2	-18	P01115	-34	HIST1H4E	-70	DDC	-16
	14	PASD1	-152	IFI27	-21	COX7B2	-36	OCIAD2	-88	VAV1	-19
	15	FMR1NB	-304	EDN2	-27	MAGEC1	-45	IL1B	-92	ACN9	-21

Table 3.4. The list of up-regulated and down-regulated genes in resistant cell lines. The 15 top genes of all the up-regulated and down-regulated genes are presented. FC; fold change of the normalized expression value of resistant cell lines verses normalized expression value of their matching sensitive line

Analysis of down-regulated genes revealed that all the resistant cell lines do not share any down-regulated gene. However we identified 3 genes that were down-regulated in 4 resistant cell lines compared to their parental counterparts, including *SPDEF*, SAM Pointed Domain Containing ETS Transcription Factor, down-regulated in BT20R, MDA-MB-231R, MDA-MB-468R and SUM149R, *UGT1A6*, UDP Glucuronosyltransferase 1 Family, Polypeptide A6, and *CFI*, Complement Factor I, that showed down-regulation in BT20R, MDA-MB-436R, MDA-MB-468R and SUM149R (Figure 3.10).

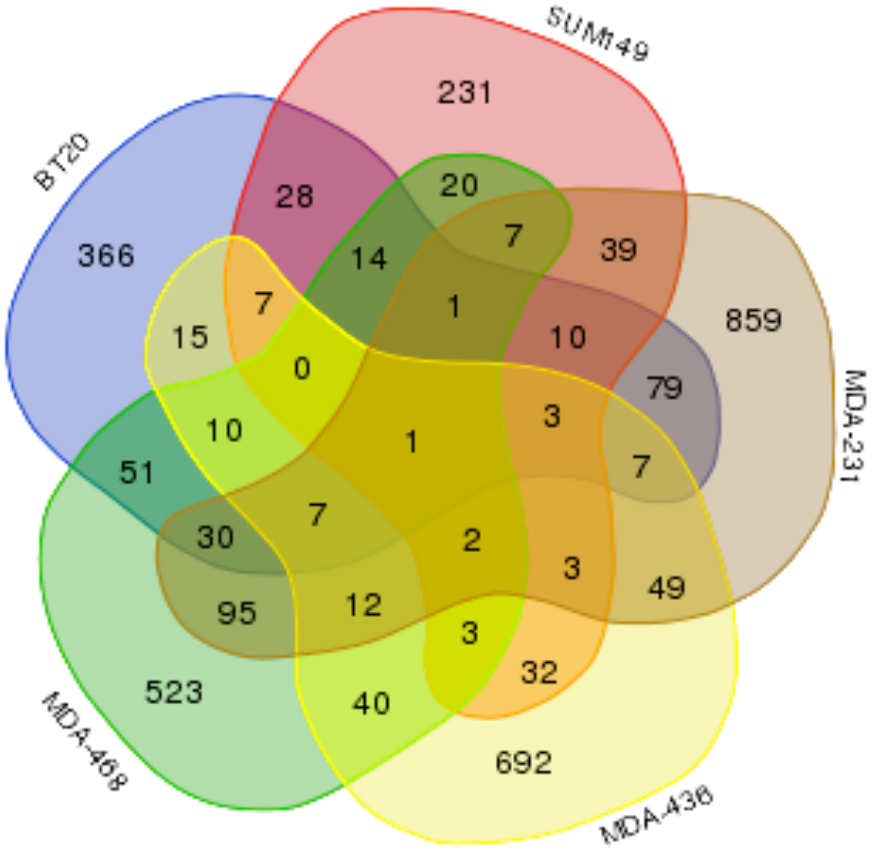

Figure 3.9. Five-way Venn Diagram comparing differentially up-regulated genes between five resistant cell lines. BT20R (blue), SUM149R (red), MDA-MB-231R (beige), MDA-MB-436R (yellow), and MDA-MB-468R (green). Numbers of up-regulated genes overlapping between all five resistant cell lines are given in their respective colors and encircled. The analysis was performed on transcripts with significant change in expression (FDR corrected p-value lower than 0.05) and linear fold change of higher than 2.

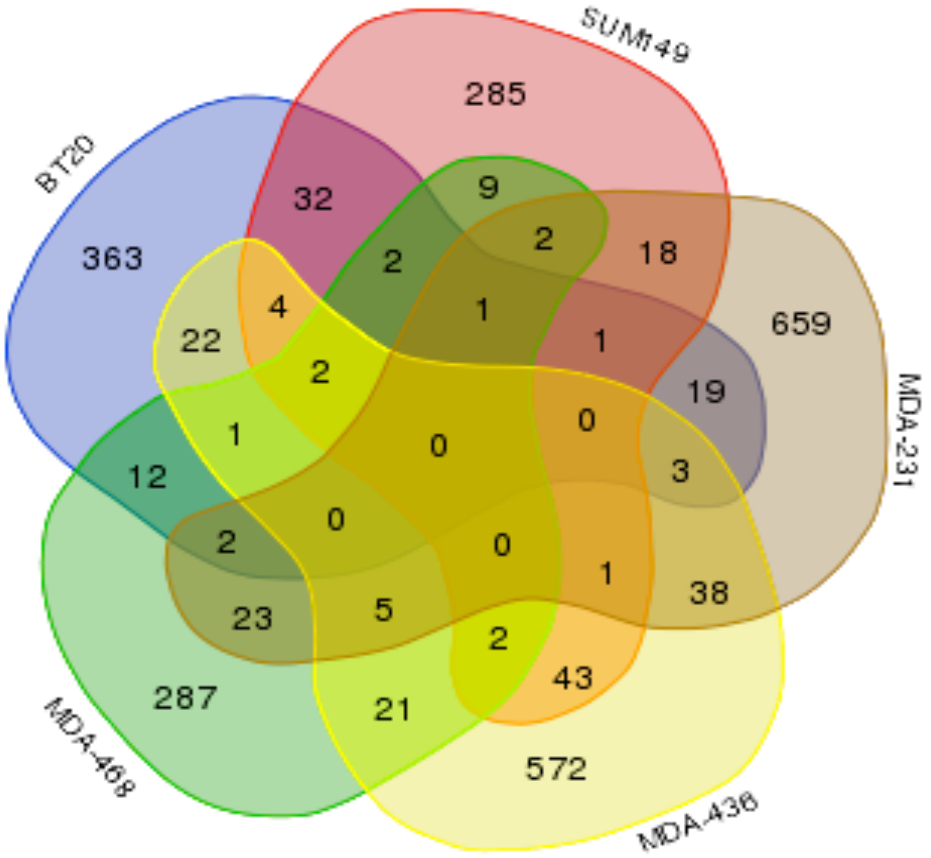

Figure 3.10. Five-way Venn diagram comparing differentially down-regulated genes between five resistant cell lines. BT20R (blue), SUM149R (red), MDA-MB-231R (beige), MDA-MB-436R (yellow), and MDA-MB-468R (green). Numbers of down-regulated genes overlapping between all five resistant cell lines are given in their respective colors and encircled. The analysis was performed on transcripts with significant change in expression (FDR corrected p-value lower than 0.05) and linear fold change of lower than -2.

3.5. Identification of pathways associated with PTX resistance

In order to gain insight into pathways involved in resistance to PTX in TNBC resistant cell lines and to understand the biological significance of the observed changes we analyzed the differentially expressed genes using the DAVID Bioinformatics Resources web tool that provides information on gene ontology classification, identifying significantly enriched themes. Only GO MF (Gene Ontology Molecular Function) categories with p values lower than 0.05 were considered for analysis.

The DAVID GO MF revealed similarities as well as clear differences between molecular functions over-represented in the resistant cell lines. Briefly, as shown in Table 3.5, we found 13, 17, 71, 11 and 50 significant GO MF categories of up-regulated genes in BT20R, SUM149R, MDA-231R, MDA-436R and MDA-468R respectively. We identified one enriched molecular function of up-regulated genes common to all 5 resistant cell line models, "growth factor activity". We noted that several epidermal growth factor receptor (EGFR) ligands were up-regulated in the "growth factor activity" list, including EGF, AREG, EREG, TGFA, BTC and HBEGF. The enrichment of genes with epidermal growth factor-related activity was further investigated and the data are presented in chapter 5 of this thesis. The set of genes up-regulated in BT20R, SUM149R, MDA-231R, and MDA-468R is functionally associated with cytokine

activity. Other commonly recurrent GO MF terms (in at least 3 cell line models) included insulin-like growth factor binding, peptidase inhibitor activity and PDZ domain binding.

To further elucidate the pathways affected in connection with PTX resistance in the cell lines, we also performed pathway analysis of genes exhibiting down-regulation in resistant cell lines. A total of 10, 12, 21, 27, and 4 GO MF categories of down-regulated genes were significantly represented in BT20R, SUM149R, MDA-231R, MDA-436R and MDA-468R respectively. Among the most enriched molecular functions of up-regulated genes that were recurrently down-regulated in at least two resistant cell lines were those related to cytoskeletal protein binding in BT20R and MDA-MB-436R and extracellular matrix structural and heparin binding constituent in MDA-MB-436R and MDA-MB-468R. MDA-MB-231 did not share any GO MF down-regulated genes with other resistant cell lines. The top ranked terms observed in MDA-MB-231 include DNA binding, nucleotide binding, ribonucleotide binding, nucleoside binding and transcription factor.

BT20

Term	Count
endopeptidase activity	19
growth factor activity	14
cytokine activity	13
peptidase inhibitor activity	10
cysteine-type endopeptidase activity	8
drug transporter activity	4

SUM149

Term	Count
cytokine activity	19
growth factor activity	17
enzyme inhibitor activity	13
glycosaminoglycan binding	10
heparin binding	8
PDZ domain binding	5

MDA-436

Term	Count
growth factor activity	15
growth factor binding	14
cytokine receptor activity	6
insulin-like growth factor binding	5

MDA-231

Term	Count
carbohydrate binding	41
endopeptidase activity	40
cytokine activity	33
enzyme inhibitor activity	32
growth factor binding	25
peptidase inhibitor activity	24
protein complex binding	24
glycosaminoglycan binding	21
growth factor activity	20
serine-type endopeptidase inhibitor activity	19
heparin binding	15
cytokine receptor activity	12
integrin binding	12
cysteine-type endopeptidase activity	12
insulin-like growth factor binding	7

MDA-468

Term	Count
endopeptidase activity	30
carbohydrate binding	25
enzyme inhibitor activity	23
peptidase inhibitor activity	18
protein complex binding	17
glycosaminoglycan binding	16
cytokine activity	16
heparin binding	14
growth factor binding	14
growth factor activity	14
serine-type endopeptidase inhibitor activity	12
insulin-like growth factor binding	7
integrin binding	7
PDZ domain binding	6
drug transporter activity	4

Table 3.5. Common Pathways/Terms found enriched in the indicated cell lines. Only pathways with $P<0.05$ were considered in analysis.

3.6. Identification of copy number alterations associated with resistance

Chromosomal aberrations due to genome instability are a characteristic of human solid tumours and are considered the primary drivers in the development and progression of cancer. Precise measurements of gene copy number alterations with high resolution are now possible with array CGH (aCGH) performed on BAC arrays, cDNA microarrays, or oligoCGH arrays. TNBCs display a high incidence of p53 mutation, frequent loss of pRB and BRCA1 inactivation, which are responsible for the high aneuploidy in these tumours, including frequent chromosomal changes, translocations, gains and losses [203]. Therefore we reasoned that these cells could acquire novel DNA copy number changes during the acquisition of drug resistance. We used the Agilent aCGH platforms with a million feature microarray resulting in a functional resolution of 4kb to identify novel amplicons or deletions that appear in the resistant cell lines compared to their matched parental cells.

In order to delineate genomic alterations specific to resistance we performed a comparative analysis of CGH data between each resistant cell line and its matched parental counterpart. We identified a significant number of novel genomic alterations (gains and losses) in resistant cells compared to their parental lines, suggesting an increased number of genetic alterations upon acquisition of drug resistance. The majority of chromosomal aberrations detected by aCGH

involved entire chromosome, chromosome arms or extended segments of chromosome arms. However, array CGH analysis also revealed focal aberrations that affect relatively small regions of genomic DNA, spanning from a few hundred kb to a couple of Mb.

The ADM-2 algorithm of CGH Analytics v3.4.40 software (Agilent) was used to identify DNA copy number alterations (CNA). The criteria used to identify CNAs by array CGH varies considerably between studies. Choosing a cut off for array data at a particular ratio is commonly used to determine significant copy number gains and losses. However, the cut off value often differs greatly ranging from a log2 ratio of 0.3 to 1.0 in different studies. In order to identify the genomic changes accompanying the resistance acquisition process, we used differential CNA (ΔCNA) which is defined as any deviation of fluorescence log2 ratio of resistant cell lines vs their matching parental cell lines. We selected a cutoff of 0.3 for the resistant/parental ratios, to define significant ΔCNA, log 2 ratio >0.3 for amplification and <-0.3 for deletion. In order to determine the threshold for high-level ΔCNAs, we calculated the averaged log2 ratio plus or minus the standard deviation of the averaged log2 ratio for each pair of cell lines. The threshold varied between the cell lines, 0.7 for BT20, 0.5 for SUM149, 0.8 for MDA-MB-231, 1.1 for MDA-MB-436 and 0.6 for MDA-MB-468. Therefore, we decided to set threshold of log2 ratio >0.7 for high-level gain or amplification and of log2 ratio <-0.7 for high level deletion for all cell lines.

The results of the comparative analysis in BT20R revealed copy number gains of the entire p arm of chromosome 20, and focal amplifications mainly within chromosomes 7q21, 10p12 and Xq23, which includes a total of 928 amplified genes. BT20 showed the least number of copy number gains amongst all resistant cell lines however; copy number losses in BT20R were more extensive. Our analysis detected more than 6000 deleted genes, of which more than 40% showed deletion ratio of higher than -0.4. The majority of deleted genes were located on chromosome 1, 2, 7 and 14. We identified two de novo high-level focal amplifications in BT20R including gain of 7q21 ΔCNA of higher than +1.8, which involved 16 genes, and gain of Xq22-23 (ΔCNA >+0.9) with which involved 48 genes. The whole genome views of the array CGH analysis of BT20P and BT20 R are depicted in Figure 3.11. The fold change values of parental (blue line) and resistant cell lines (red line) relative to the pool of DNA obtained from five healthy individuals are displayed using overlapped moving averages with a 200-kb window and visualized as lines on the genome sequence coordinate.

SUM149R showed the lowest number of high-level aberrations among all the resistant cell lines, with only 53 genes with ΔCNA > +0.7. The results of the comparative analysis in SUM149R vs SUM149P showed 2199 differentially amplified genes, of which more than 40% are located on chromosome 7, and 1028 genes with deletions, mostly located on chromosome 17. We did not

identify any high-level de novo focal amplification or deletion in SUM149R. However we identified a de novo break point within chromosome 7p, where ABCB1 gene is located (Figure 3.12).

The analysis of MDA-MB-231R showed alterations involving chromosome arms and extended chromosomal segments scattered across the genome. We identified copy number gains including gains of 2q, 5p, 6q and large portion of 1p and copy number losses of a small portion of distal 8q, a portion of 12q and all of 2p. The majority of genes in 2q, 6q and 7q in MDA-MB-231R were identified as differentially aberrant genes due to copy number losses in MDA-MB-231P. However, these regions do not show copy number gain in MDA-MB-231R cell line. The analysis also revealed a focal amplification in 8q and a focal deletion in 7q (Figure 3.13).

MDA-MB-436R cell line showed the highest number of genes with differential high-level aberrations including 1308 genes with differential amplifications of higher than 0.7 and 282 genes with differential deletions of lower than -0.7. The MDA-MB-436R cell lines exhibit gain of 8q and a large portion of chromosomal arm 14q and a loss of 7p. We identified several focal chromosomal aberrations including losses of 2q14 and 16p13 and gains of 14q32 and 18q (Figure 3.14).

The comparative analysis in MDA-MB-468 resistant and parental cell lines revealed alterations involving entire chromosomes and chromosome arms. We identified copy number gains including gains of chromosome 20, 22, and 5p and copy number losses of chromosome 6, 1q, 19p and a large portion of 7q. The differential analysis detected 438 genes that displayed high-level copy number gains (> +0.7) and 472 genes that showed high-level of copy number loss (< -0.7). We identified a high-level focal amplification in 7q21 in MDA-MB-468R (Figure 3.15.).

Figure 3.11. Whole genome frequency of distribution of chromosomal aberrations in BT20P and BT20R. The blue line represents the array CGH data obtained from parental cell line and the red line represents the data from resistant cell line. The extension of each blue or red line to the right side and left side of the bar depicts the chromosomal amplification and deletion, respectively. The arrows indicate the focal aberrations in resistant cell lines.

Figure 3.12. Whole genome frequency of distribution of chromosomal aberrations in SUM149P and SUM149R. The blue line represents the array CGH data obtained from parental cell line and the red line represents the data from resistant cell line. The extension of each blue or red line to the right side and left side of the bar depicts the chromosomal amplification and deletion, respectively. The arrows indicate the focal aberrations in resistant cell lines .

Figure 3.13. Whole genome frequency of distribution of chromosomal aberrations in MDA-MB-231P and MDA-MB-231R. The blue line represents the array CGH data obtained from parental cell line and the red line represents the data from resistant cell line. The extension of each blue or red line to the right side and left side of the bar depicts the chromosomal amplification and deletion, respectively. The arrows indicate the focal aberrations in resistant cell lines.

Figure 3.14. Whole genome frequency of distribution of chromosomal aberrations in MDA-MB-436P and MDA-MB-436R. The blue line represents the array CGH data obtained from parental cell line and the red line represents the data from resistant cell line. The extension of each blue or red line to the right side and left side of the bar depicts the chromosomal amplification and deletion, respectively. The arrows indicate the focal aberrations in resistant cell lines.

Figure 3.15. Whole genome frequency of distribution of chromosomal aberrations in MDA-MB-468P and MDA-MB-468R. The blue line represents the array CGH data obtained from parental cell line and the red line represents the data from resistant cell line. The extension of each blue or red line to the right side and left side of the bar depicts the chromosomal amplification and deletion, respectively. The arrows indicate the focal aberrations in resistant cell lines.

Accumulation of gains and/or losses in the genome during the acquisition of drug resistance can generate a pattern of chromosomal aberrations, which could constitute a molecular signature. Therefore we investigated whether such patterns of chromosomal aberrations could be observed in our PTX-resistant cell lines. We identified common chromosomal gains and losses in resistant cell lines. The most common DNA copy number variations in resistant cell lines included gains of 20p, detected in BT20R, MDA-MB-231R and MDA-MB-468R, gain within chromosomes 7q21 in BT20R, SUM149R and MDA-MB-468, and losses within chromosomes 2p and 5p. The majority of these common copy number changes are in the entire chromosome arms or extended segments of chromosome arms.

3.7. Integrative Analysis of Gene expression and Copy Number Alteration

We performed a correlation analysis to determine the effect of copy number alterations on gene expression deregulation in paired cell lines. Genes showing at least a 2 fold change or greater based on microarray analysis and >0.3 log 2 ratios for copy number alterations were included in the analysis. The result of integrative analysis illustrates a considerable influence of copy number on gene expression patterns, which indicates that copy number alterations lead to changes in gene expression levels in resistant cell lines that may have functional consequences. This effect was

more pronounced in genes with high-level copy number changes (-0.7 >CAN log 2 ratio> 0.7). **(Table 3.6).**

Our integrative analysis showed a positive correlation between copy number alteration and expression at the mRNA level (Gene expression fold change >2 and deltaCNA >0.3). The analysis revealed that 30% of the genes located on 8q in MDA-MB-436 with copy number gain are up-regulated and 26.2% of the genes located on chromosome X in BT20 with copy number gain or loss are up-regulated or down-regulated respectively. To investigate the level of concordance between copy number log 2 ratios and expression log 2 ratios for chromosome 8 in MDA-MB-436 and chromosome X in BT20, we calculated a Pearson correlation. The results showed moderate positive correlation in both chromosomes between copy number and expression values ($R2 > 0.43$ for chromosome 8 in MDA-MB-436 and $R2 > 0.41$ for chromosome X in BT20), Figure 3.6 is a representation of the positive association between copy number gain and increase in transcript level, in a high-level amplification.

The effect of copy number change on gene expression was not consistent across all the resistant cell lines. MDA-MB-436R showed the highest level of association between gene expression and copy number change whereas MDA-MB-468R showed the least positive correlation between gene

expression and copy number change (Table 3.6). Also, we identified a high degree of association between high-level amplification and gene expression in BT20R cell lines.

	Ratio	Number of Amplified genes	Number of Deleted genes	Total	Number of Amplified and Up-regulated genes	Number of Deleted and Down-regulated genes	Amplification/Up-regulation correlation %	Deletion/Down-regulation correlation%
BT20	**0.3**	928	6203	7131	131	236	14.1	3.8
	0.7	246	732	978	87	111	35.4	15.2
	1	91	190	281	37	47	40.7	24.7
SUM149	**0.3**	2199	1028	3227	69	25	3.1	2.4
	0.7	31	21	52	9	3	29.0	14.3
	1	2	12	14	0	1	0.0	8.3
MDA-MB-231	**0.3**	2910	4638	7548	318	326	10.9	7.0
	0.7	489	121	610	101	24	20.7	19.8
	1	194	3	197	39	1	20.1	33.3
MDA-MB-436	**0.3**	1984	947	2931	312	142	15.7	15.0
	0.7	1308	282	1590	263	87	20.1	30.9
	1	311	53	364	107	23	34.4	43.4
MDA-MB-468	**0.3**	2927	2704	5631	170	107	5.8	4.0
	0.7	438	472	500	37	61	8.4	12.9
	1	13	191	204	3	28	23.1	14.7

Table 3.6. Representation of the positive association between CNA and increase in transcript level, in low level CNAs (-0.3>CAN>0.3) and high level CAN (-0.7).

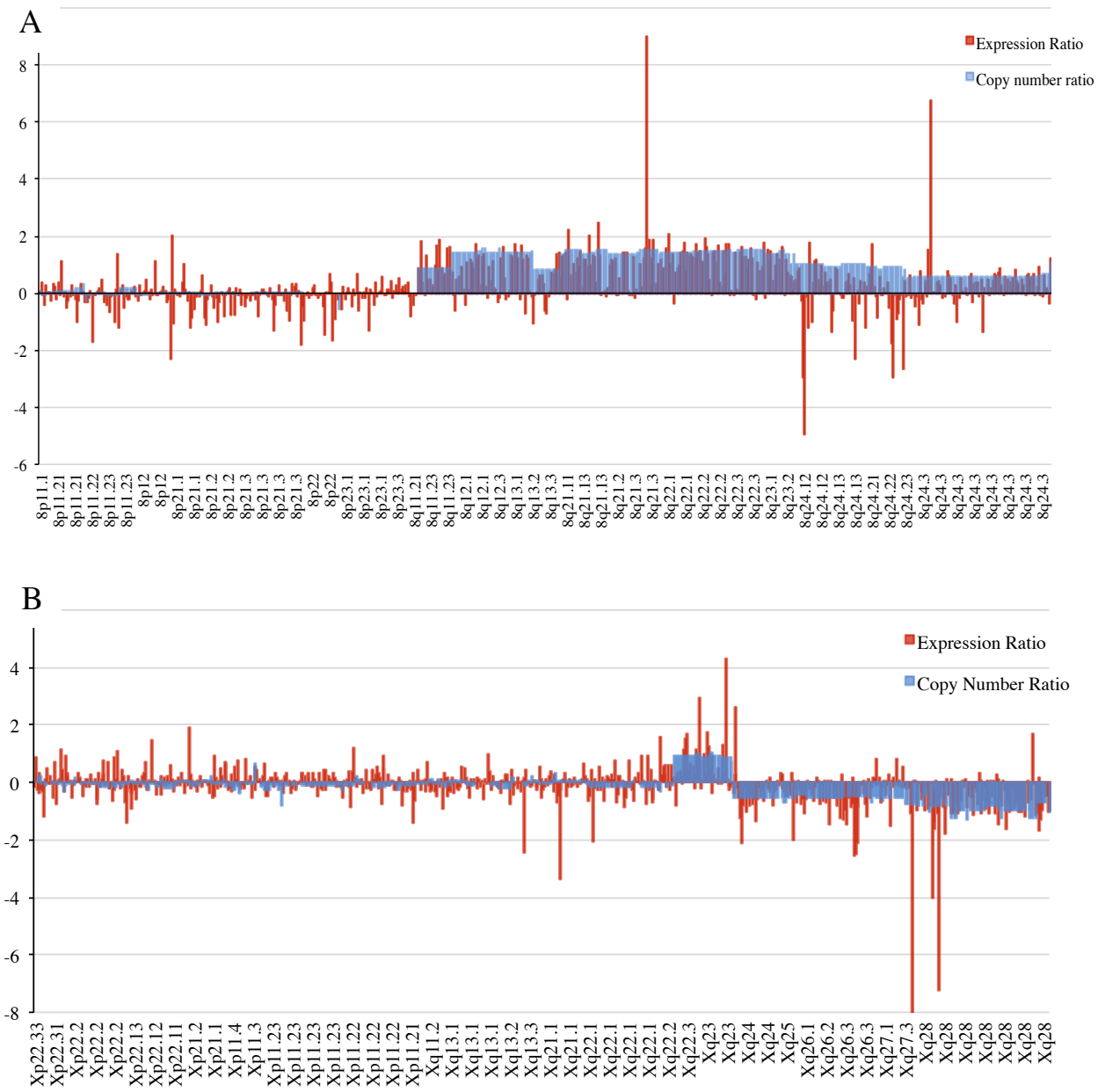

Figure 3.16. Influence of copy number on gene expression patterns. A. Association of copy number increase and transcript level in chromosome 8q of MDA-MB-436 Cell line. B. Correlation of high-level amplification and expression in chromosome X in BT20 cell line. The red columns represent the differential gene expression in each cell line and the blue represents the differential copy number aberrations.

We next sought to identify overexpressed genes with recurrent copy number gain shared in resistant cell lines. Identifying these recurrent changes is of great interest as it might shed light on the mechanism of resistance in these cell lines. We found a total 26 amplified and overexpressed genes common between at least two resistant cell lines (**Table 3.7**). Interestingly, ABCB1, ABCB4 and C7orf23, located alongside on 7q21.12, showed overexpression and amplification in 3 cell lines including BT20R, SUM149R and MDA-MB-468R. Among these 3 recurrently up-regulated and amplified genes, ABCB1 showed the highest expression. Our analysis revealed a total 15 genes with copy number loss and decrease in transcription level common between at least two resistant cell lines**.** Of these, SPDEF, a tumour suppressor gene [204], is deleted and down-regulated in BT20R, MDA-MB-436R and MDA-MB-468R cell lines (**Table 3.8**).

			BT20		SUM149		MDA-MB-231		MDA-MB-436		MDA-MB-468	
Gene Symbol	**Chromosome**	**Cytoband**	**GE FC**	**CN FC**	**GE FC**	**CN FC**	**GE FC**	**CN FC**	**GE FC**	**CN FC**	**GE FC**	**CN FC**
ABCB1	chr7	7q21.11	176.4	1.9	221.6	0.9	26.2	0.5	22.2	0.0	47.3	1.1
ABCB4	chr7	7q21.12	4.5	1.9	2.0	0.9	3.1	0.5	1.1	0.0	2.2	1.4
C7orf23	chr7	7q21.12	3.3	1.8	2.9	0.9	2.0	0.5	-1.0	0.0	1.1	0.0
ANKRD52	chr12	12q13.3	1.4	-0.4	1.1	0.0	1.0	-0.1	1.1	0.0	-1.0	0.0
C20orf3	chr20	20p11.21	2.1	1.1	-1.0	0.2	2.0	0.4	1.3	0.0	1.7	0.4
PYGB	chr20	20p11.21	2.0	1.1	1.0	-0.1	1.1	0.4	1.1	0.0	2.6	0.4
NINL	chr20	20p11.21	2.1	1.1	-1.8	-0.1	2.6	0.4	-1.0	0.0	1.1	0.4
PRNP	chr20	20p13	2.8	0.9	2.1	-0.1	2.3	0.4	1.1	0.0	-1.1	0.2
RASSF2	chr20	20p13	3.2	0.9	-1.1	-0.1	2.2	0.4	-1.3	0.0	1.2	0.2
SIRPA	chr20	20p13	3.5	0.9	1.5	0.0	7.3	0.3	-2.3	0.0	1.1	0.2
SIRPG	chr20	20p13	6.5	0.9	1.6	0.0	5.1	0.3	-6.4	0.0	1.4	0.2
VIM	chr10	10p13	2.7	0.9	3.6	0.5	-1.3	-0.5	1.3	0.0	-1.6	0.0
KALRN	chr3	3q21.2	2.2	0.4	1.2	0.0	5.0	-0.1	1.1	0.0	3.1	0.0
STEAP1	chr7	7q21.13	1.2	0.3	4.0	0.9	-2.3	0.5	-1.7	0.0	3.0	0.6
APOBEC3B	chr22	22q13.1	2.1	0.0	2.4	0.7	-2.3	0.0	-1.1	0.0	2.6	1.1
KCNJ12	chr17	17p11.2	1.8	0.0	3.1	0.4	1.1	0.0	-4.0	0.0	2.9	0.0
APOBEC3C	chr22	22q13.1	1.1	-0.3	2.3	0.4	1.4	-0.1	-1.2	0.2	3.3	0.4
LAMB1	chr7	7q31.1	-1.0	-0.1	2.1	0.4	2.6	0.5	-1.4	0.0	-1.2	-0.6
TPPP	chr5	5p15.33	2.0	-0.3	2.1	0.2	7.1	0.4	1.6	0.0	1.8	0.9
IGDCC4	chr15	15q22.31	1.3	0.0	1.5	0.0	2.4	0.5	6.1	0.8	1.9	0.0
CD24	chrY	Yq11.222	-2.5	0.0	-2.6	0.0	5.6	0.5	4.2	0.6	1.0	0.0
SLC12A7	chr5	5p15.33	-1.1	-0.3	1.7	0.2	2.8	0.4	1.2	0.0	2.5	0.6
FAM134B	chr5	5p15.1	2.2	-0.5	-1.2	-0.2	10.4	0.4	-1.4	0.0	3.8	0.5
ACSS1	chr20	20p11.21	-1.0	1.1	-4.0	0.2	3.2	0.4	1.1	0.0	9.3	0.4
IL7R	chr5	5p13.2	5.9	-0.9	3.2	-0.2	2.5	0.3	2.1	0.0	2.0	0.4
IFI27	chr14	14q32.12	155.2	0.0	-21.3	0.0	8.6	0.0	10.1	0.5	3.3	0.3

Table 3.7. List of amplified and overexpressed genes common between at least two resistant cell lines. Common amplification and expression in each cell line are highlighted in light blue. GE FC: gene expression ratio fold change. CN FC : Copy number ratio, fold change.

			BT20		SUM149		MDA-MB-231		MDA-MB-436		MDA-MB-468	
Gene Symbol	**Chromosome**	**Cytoband**	**GE FC**	**CN FC**	**GE FC**	**CN FC**	**GE FC**	**CN FC**	**GE FC**	**CN FC**	**GE FC**	**CN FC**
SSR4	chrX	Xq28	-2.1	-0.8	-2.4	-0.3	1.3	0.0	1.0	0.0	-1.2	-0.4
TMEM187	chrX	Xq28	-2.8	-1.0	-3.3	-0.3	1.5	0.0	-1.5	0.0	-1.3	-0.4
DYNLT1	chr6	6q25.3	-1.1	-0.5	-1.0	0.0	1.6	0.5	-2.2	-0.3	-2.2	-0.9
POLH	chr6	6p21.1	-2.0	-0.8	1.2	0.0	-2.0	-0.4	1.1	0.0	-1.7	-0.4
C6orf48	chr6	6p21.33	-2.0	-0.4	1.3	0.0	-2.3	-0.4	1.6	0.1	-1.3	-0.4
SPDEF	chr6	6p21.31	-3.0	-0.8	-2.7	0.0	-4.9	-0.4	1.1	0.0	-3.3	-0.4
CNN1	chr19	p13.2	-2.1	-0.4	1.1	-0.4	1.3	-0.3	-1.2	-0.1	-2.2	-0.4
C10orf114	chr10	10p12.31	1.4	0.9	-1.0	0.0	-3.1	-0.5	1.5	0.1	-2.2	0.0
UHRF1BP1L	chr12	12q23.1	-1.7	0.1	1.3	0.0	-1.3	-0.4	-1.1	0.0	-1.3	0.0
FAM161A	chr2	2p15	-2.5	-0.5	1.5	0.1	-2.3	-0.5	1.1	0.0	-1.0	0.0
RMND5A	chr2	2p11.2	-2.0	-0.5	1.3	0.0	-3.8	-0.8	1.7	0.0	-1.2	0.0
FKBP14	chr7	7p14.3	-2.0	-0.4	1.8	0.6	1.4	0.0	-2.2	-0.9	-1.2	-0.1
HIBADH	chr7	7p15.2	-2.4	-0.4	-1.3	0.5	1.5	0.0	-3.8	-0.9	-1.2	0.0
KLHL7	chr7	7p15.3	-2.4	-0.4	1.2	0.5	1.1	0.0	-3.8	-0.9	1.2	-0.1
CCDC77	chr12	12p13.33	-1.1	0.0	1.2	-0.1	-2.0	-0.5	-2.2	-0.8	-1.1	0.0

Table 3.8. List of deleted and downregulated genes common between at least two resistant cell lines. Common deletion and expression in each cell line are highlighted in light blue. GE FC: gene expression ratio fold change. CN FC : Copy number ratio, fold change.

3.8. Summary

The development of resistance to chemotherapeutic agents is the major obstacle in successful treatment of TNBC patients. In order to investigate the molecular mechanisms of resistance in TNBCs, we developed *in vitro* model of acquired resistance to PTX. Five TNBC cell lines (BT20, SUM149, MA-MB-231, MDA-MB-436 and MDA-MB-468) were cultured in the presence of increasing concentrations of paclitaxel until they acquired resistance. The established resistant cell lines showed significant decreased sensitivity to PTX as well as reduced susceptibility to paclitaxel-induced apoptosis and cell cycle arrest compared to their sensitive parental counterparts. These resistant cell lines with acquired resistance can provide models for characterization of the biological mechanisms of resistance.

In order to identify changes in gene expression occurring during selection for resistance to PTX, we carried out a genomic microarray analysis. Comparative data analysis of resistant cell lines and their sensitive counterparts revealed a small number of genes for which the expression is changed significantly during development of resistance including 5.0% in BT20, 3.7% in SUM149, 9.0% in MDA-MB-231, 7.3% in MDA-MB-436, and 5.4% in MDA-MB-468. We identified a total of 86 genes that were up-regulated (> 2 fold) in at least 3 of resistant cell lines compared to parental cells. Of these, ABCB1 was up-regulated in all five resistant cell lines and INHBA, TRIM29,

IFI27, SERPINB3, RASGRP2, IGF2, SERPINB4 and RTP4, CLDN1 and CTHRC1 were commonly up-regulated in 4 resistant cell lines compared to their parental counterparts. Future experiments dissecting these genes will potentially identify a biomarker for PTX resistance in TNBCs.

To better understand the biological significance of the observed changes in gene expression profile in resistant cell lines, we performed pathway analysis on differentially expressed genes. We found enriched molecular functions of up-regulated genes that were recurrently up-regulated in at least two resistant cell lines including growth factor activity, insulin-like growth factor binding, peptidase inhibitor activity and PDZ domain binding. We further investigated the role of up-regulation genes in "growth factor activity" function in PTX resistance in resistant cell lines.

Using array CGH, we identified chromosomal abnormalities associated with PTX resistance in all pairs of parental and resistant cell lines. We detected regions with significant DNA copy number changes and recurrent chromosomal alterations in resistant cell lines. The total number of genomic alterations (gains and losses) was found to be significantly higher in resistant cells compared to their parental lines, suggesting an increased number of genetic alterations under the drug condition. This analysis revealed a number of genes in whose genomic alterations could provide a selective advantage to resistant cells. The most common DNA copy number variations

in resistant cell lines included gains of 20p, detected in BT20R, MDA-MB-231R and MDA-MB-468R, gain within chromosomes 7q21 in BT20R, SUM149R and MDA-MB-468, and losses within chromosomes 2p and 5p.

We used an integrative analysis of array CGH and gene expression data to gain insights into the functional changes of the genome in TNBC resistant cell lines. Integrative analysis of aCGH and gene expression can reveal deregulated genes whose expression is correlated with their copy number alterations. The association of gene copy number with gene expression has been previously shown in different type of cancers, including breast cancer (cell lines and primary breast tumours), prostate cancer cell line and leukemia cell line.[205-207]. Pollack et al. showed that global DNA copy number alteration in breast cancer cell line or primary breast tumours lead directly to global deregulation of gene expression. They found that roughly, a 2-fold change in DNA copy number is associated with a corresponding 1.5-fold change in mRNA expression and at least 12% of all the variation in gene expression among the breast tumours is directly attributable to underlying variation in gene copy number. They showed that this association is more pronounced in highly amplified genes and that 62% of highly amplified genes show moderately or highly elevated expression [205]. Hyman et al. showed that 44% of highly amplified genes in breast cancer tumours tested were highly expressed [208]. Consistent with

these results, our data show a generally positive correlation between copy number alteration and expression at the mRNA level. We found a high degree of association between high-level CNA and differential gene expression in resistant cell lines.

Although both amplifications and deletions can affect gene function, the gain-of-function amplifications make them ideal targets for the development of biomarkers and strategies to overcome resistance. To identify regions of potential interest for follow up, we sought to identify up-regulated and amplified genes common in resistant cell lines. We identified 26 genes up-regulated (gene expression ratio >2) and amplified genes (delta CNA>0.3) in at least two resistant cell lines Our integrative analysis of gene expression and array CGH showed that the most highly up-regulated gene in all resistant cell lines, ABCB1, was accompanied by amplification in three resistant cell lines: BT20R, SUM149R and MDA-468. We decided to further investigate the role of ABCB1 amplification in PTX resistance in these cell lines.

Chapter 4

Results: ABCB1 gene rearrangement

4.1. PTX-resistant cell lines have elevated ABCB1 expression

The analysis of copy number profiles using high-resolution array CGH technique demonstrated copy number increases in the region of 7q11.21~q21.12 in 3 resistant cell lines, including BT20R, SUM149R and MDA-MB-468R. ABCB1, ABCB4 and C7orf23, located alongside on 7q21.12, showed overexpression in BT20R, SUM149R and MDA-MB-468R. Among these 3 recurrently up-regulated and amplified genes, ABCB1 showed the highest expression. The comparative analysis of gene expression profiling between resistant cell lines and their sensitive counterparts revealed that ABCB1 is differentially up-regulated in all resistant cell lines and is in the top most differentially up-regulated genes in BT20R, SUM149R and MDA-MB-468R cell lines. ABCB1, often referred to as P-glycoprotein (P-gp), is a member of the ATP binding cassette superfamily of transporter proteins and is a protein known to be associated with PTX resistance by efficiently transporting taxane out of the cell.

The mechanisms responsible for ABCB1 gene expression are complex and can occur as a result of changes in gene transcription, gene amplification and increased protein or mRNA stability [100, 101, 133, 134]. ABCB1 regional gene amplification and chromosomal rearrangement in various resistant cancer cell lines have been reported [148-153], as described in the introduction above.

However, to our knowledge, ABCB1 copy number increase in TNBC cell lines has not been reported.

The aim of this chapter is first, to validate the result of integrative analysis of gene expression and array CGH and second, to determine the impact of ABCB1 up-regulation in PTX resistance and third, to further investigate the effect of ABCB1 amplification in resistance to paclitaxel in the TNBC resistant cell lines.

4.2. Validation of ABCB1 expression and amplification

Our comparative gene expression analysis identified elevation of ABCB1 transcript level in all resistant cell lines (Table 4.1). We first performed quantitative real time PCR to validate the ABCB1 gene expression. To choose the endogenous reference gene for internal standardization of relative mRNA expression, several housekeeping genes were tested including beta-actin, glyceraldehyde-3-phosphate dehydrogenase (GAPDH), and hypoxanthine phosphoribosyl-transferase 1 (HPRT1). Of these, HPRT1 was moderately expressed and showed minimal variation in expression across all cell lines. The efficiency of both ABCB1 and HPRT1 primers was determined from analysis of a serial dilution of cDNA. Considering the results of gene expression microarray and high ABCB1 gene-abundance in resistant cell lines, and also the moderate expression of HPRT1, the cDNA was diluted 1:50 ratio. The result of quantitative RT-PCR confirmed the up-regulation of ABCB1 in all resistant cell lines. The expression of ABCB1 in the parental cell line in 1:50 dilution of cDNA was undetectable.

The comparative analysis of array CGH revealed ABCB1 differential copy number increases in BT20R, SUM149R, MDA-MB-231R and MDA-MB-468R cells. However, we did not identify an absolute copy number gain in ABCB1gene in MDA-MB-231R cells and the differential copy number alteration was due to deletion of 7q21 region in MDA-MB-231P cells not being observed

in the resistant cell line. The expression values, copy number values and differential expression and copy number aberration of ABCB1 for all cell lines are presented in Table 4.1.

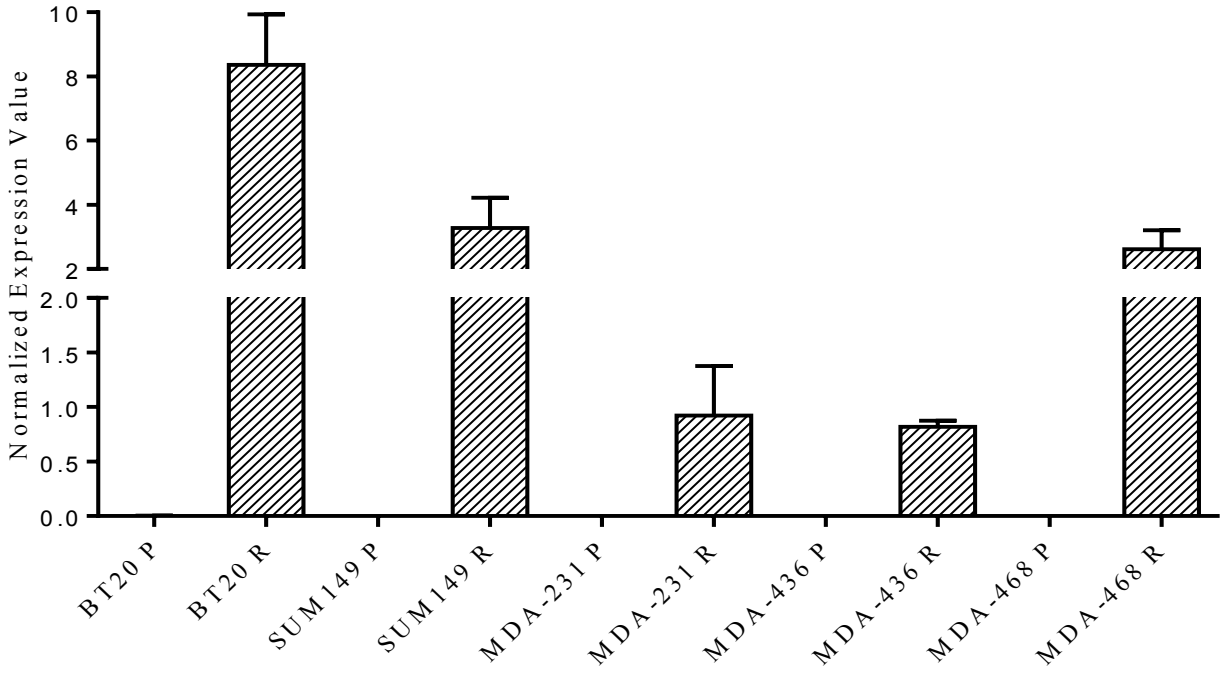

Figure 4.1. ABCB1 gene expression validation using quantitative RT-PCR. The mRNA level was tested using primers designed on coding sequence of ABCB1 gene. The expression values were normalized using HPRT1 gene. Results represent mean values of three independent biological replicates ± SD (experimental error).

Cell lines	BT20		SUM149		MDA-MB-231		MDA-MB-436		MDA-MB-468	
	P	R	P	R	P	R	P	R	P	R
Gene Expression value	52.0	9197.0	34.0	7656.0	41.0	1097.0	42.0	932.0	54.0	2593.0
Differential Expression	**176.4**		**221.6**		**26.8**		**22.2**		**48.0**	
CGH Value	-0.5	1.3	0.0	0.9	-0.5	0.0	0.0	0.0	0.0	1.1
Differential CGH	**1.8**		**0.9**		**0.5**		**0.0**		**1.1**	

Table 4.1. Comparative analysis of gene expression and array CGH of ABCB1 gene. P: Parental; R: Resistant. Gene expression: the normalized gene expression values for each cell line, CGH values: log 2 ratio of fluorescence values of samples / pooled DNA.

We performed a quantitative RT-PCR to validate ABCB1 gene copy number in parental and resistant cell lines. To normalize the copy number values, we used RNase P as reference gene since our aCGH results showed no amplification or deletion in RPP30 (RNase P) gene in any of the cell lines.

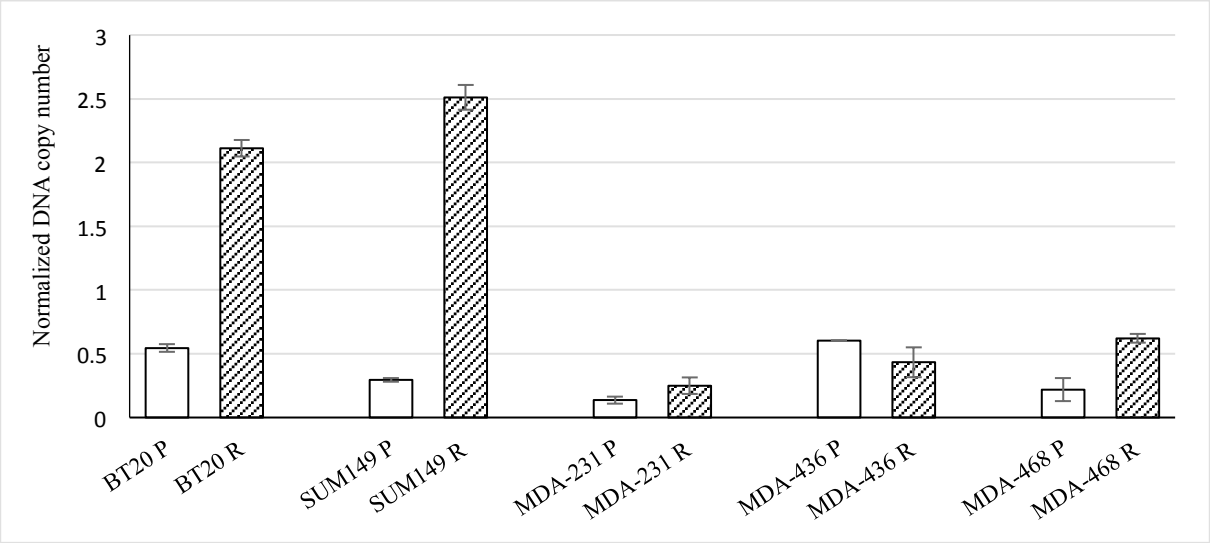

Figure 4.2. Analysis of ABCB1 copy number using quantitative RT-PCR. The copy number values were validated using 50ng of genomic DNA. The results were normalized using RPP30 gene. Results represent mean values of three independent replicates ± SD (experimental error).

4.3. ABCB1 protein expression

We evaluated the ABCB1 protein expression in all resistant cell lines using monoclonal antibodies specific to ABCB1. The majority of ABCB1 antibodies, in particular those developed using clone C219, are reported to detect other proteins including c-erbB2 protein (185KDa), or cross-react with human ABCB4 [209, 210]. To minimize the cross-reactivity of the ABCB1 antibody, we chose two different monoclonal antibodies specific to ABCB1, which do not recognize the ABCB4 protein including the ABCB1 monoclonal antibody clone F4 (Sigma Aldrich) and the ABCB1 monoclonal antibody E1Y7S (Cell Signaling).

The evaluation of protein expression showed an increase corresponding to the overexpression and amplification seen in BT20R, SUM149R, and MDA-MB-468R cell lines (Figure 4.3). Interestingly, although MDA-MB-231R and MDA-MB-436R showed significant ABCB1 gene up-regulation, we did not detect an increase in protein expression in these two resistant cell lines. A band around 170 kDa was detected on blots of cell lysates from BT20R, SUM149R, and MDA-MB-468R, but not from MDA-MB-231R and MDA-MB-436R. The size of the band agrees with the reported molecular weight of the ABCB1 protein.

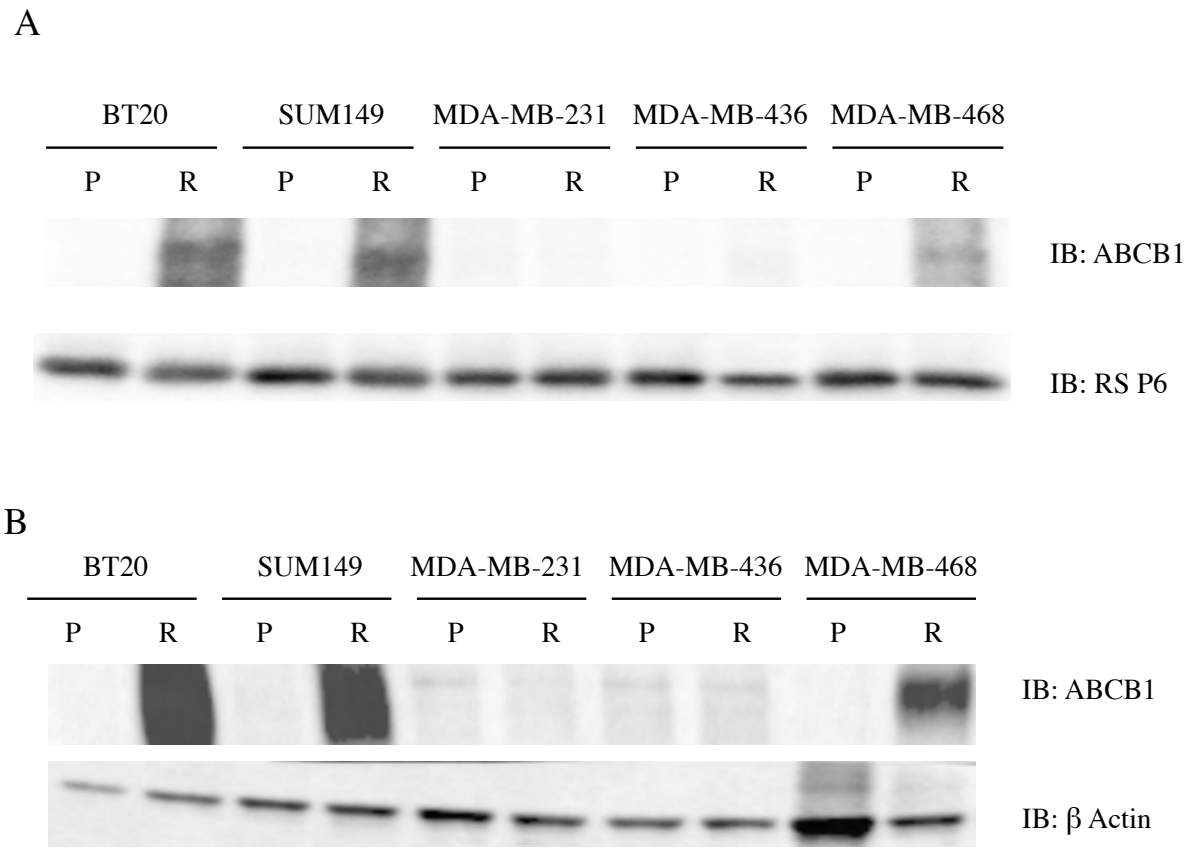

Figure 4.3. Evaluation of ABCB1 protein expression in parental and resistant cell lines. Cells were harvested and lysed and 20μg of total protein was loaded on 4-12% gradient SDS-PAGE gels, and analyzed by western blotting with A: ABCB1 monoclonal antibody, cell signaling, E1Y7S and RPS6, the loading control. B: ABCB1 monoclonal antibody, Sigma Aldrich, clone F4 Ascites fluid and beta Actin was used as an internal control. Both antibodies detected a band around 170 kDa from BT20R, SUM149R, and MDA-MB-468R, but not from MDA-MB-231R and MDA-MB-436R.

4.4. ABCB1 efflux activity

We tested the efflux activity of ABCB1 by measuring the accumulation of rhodamine 123 in parental and resistant cells. Rhodamine 123 is a member of the rhodamine family of flurone dyes and is routinely used to examine membrane transport by ABCB1. Rhodamine 123 is a substrate of ABCB1 and its uptake into cells is an indicator of ABCB1 transport activity. After 1 hour of incubation in media containing 500μM rhodamine 123, cells were centrifuged and re-suspended in fresh media without rhodamine 123 and were incubated for 30 minutes. The intracellular rhodamine 123 intensities were measured using flow cytometery at 525 nm. We found a significant reduction of intracellular rhodamine 123 accumulation in BT20R, SUM149R and MDA-468R cells compared to their parental counterparts (Figure 4.4). This effect was not seen in the MDA-231R and MDA-436R cells, congruent with their lack of ABCB1 amplification and protein overexpression (Figure 4.5).

We then tested the effect of verapamil on the ABCB1 over-expressing cells. Verapamil have been reported to reverse the MDR phenotype by directly competing with ABCB1 substrates as well as by interacting with the ABCB1 transporter and blocking drug efflux [103]. Treatment with 100nM verapamil reversed the extrusion of rhodamine in BT20R, SUM149R and MDA-468R cell lines, suggesting that the over-expressed ABCB1 transporters were functionally active (Figure 4.4).

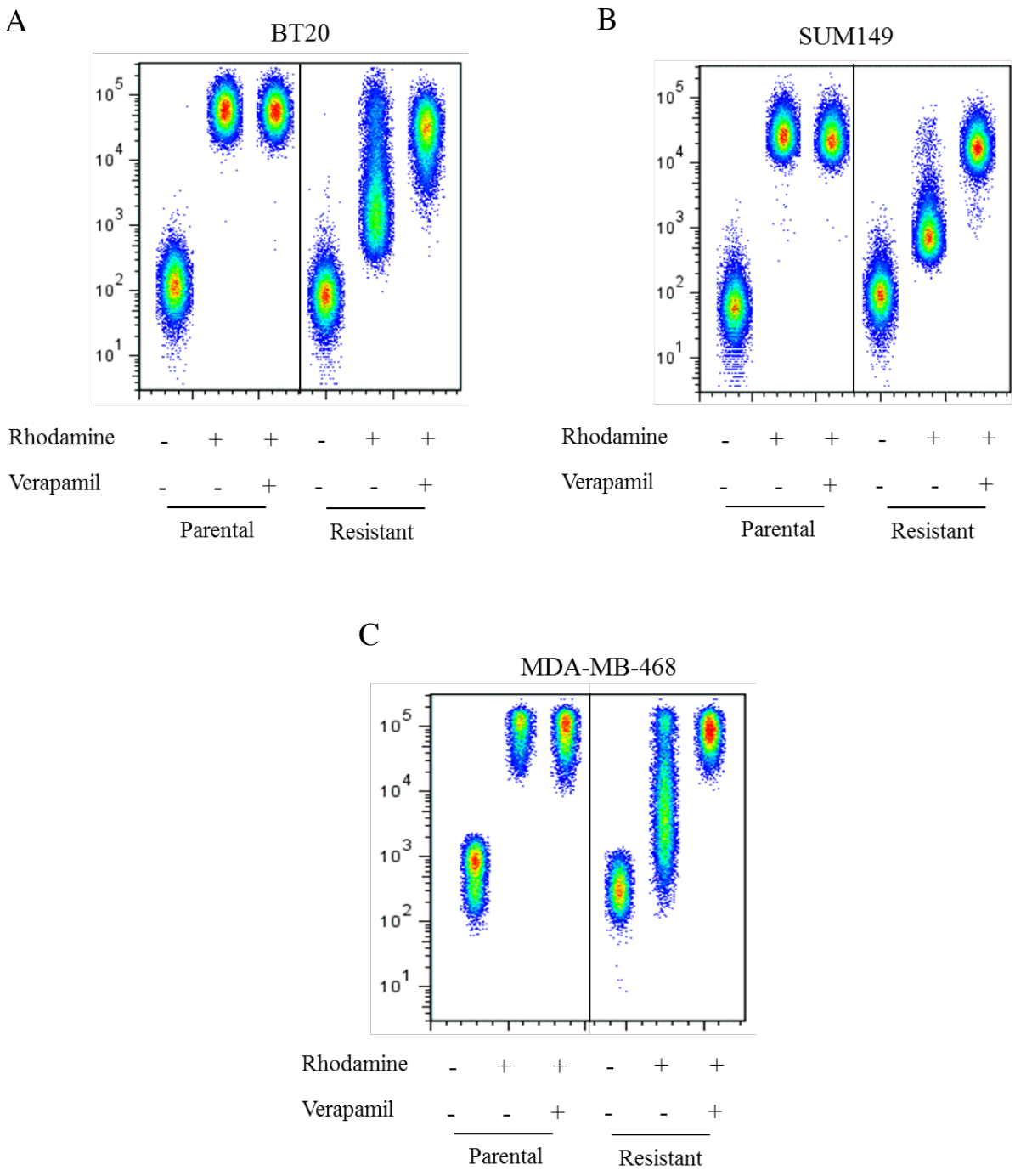

Figure 4.4. Flow cytometry analysis of rhodamine accumulation in ABCB1 over-expressing resistant cell lines and their parental counterparts. A: BT20, B: SUM149 and C: MDA-MB-468. The ability to export Rhodamine by ABCB1 activity was inhibited by 100nM verapamil.

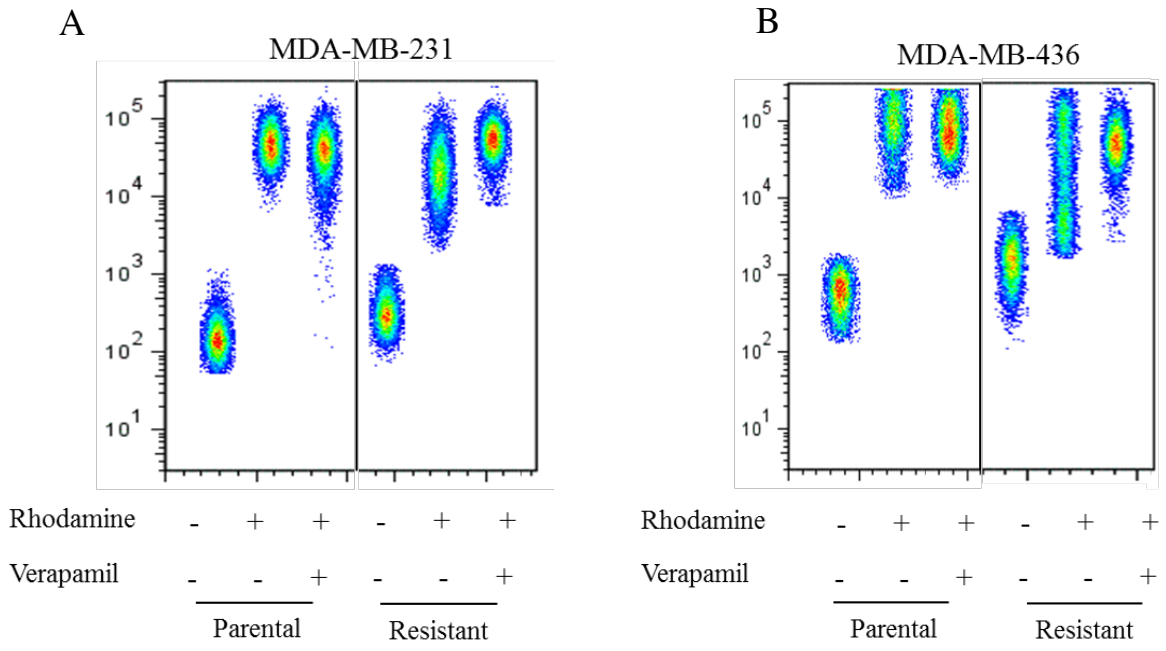

Figure 4.5. Flow cytometry analysis of rhodamine 123 accumulation in MDA-MB-231 and MDA-MB-436 resistant and parental cell lines. The fluorescent intensity of cells treated with or without rhodamine 123 were detected. Rhodamine accumulation was not altered after 30 min incubation of the cells in fresh medium. Treatment of the cells with100nM verapamil did not have any effect on rhodamine accumulation of the cells.

4.5. Verapamil re-sensitizes ABCB1 over-expressing resistant cell lines

To elucidate whether ABCB1 inhibition rescues the PTX sensitivity in BT20R, SUM149R and MDA-MB-468R, we tested the cytotoxicity of verapamil in combination with PTX. Cells were exposed to 100nM verapamil along with PTX in series of concentration ranging from10 pM to 10 μM. We observed that inhibition of ABCB1 efflux activity by verapamil partially reverses the sensitivity of these cell lines to PTX. Verapamil alone did not show any cytotoxic effect on ABCB1-over-expressing cell lines (Figure 4.6). This suggests that overexpression of ABCB1 contributes to PTX resistance in BT20R, SUM149R and MDA-468R.

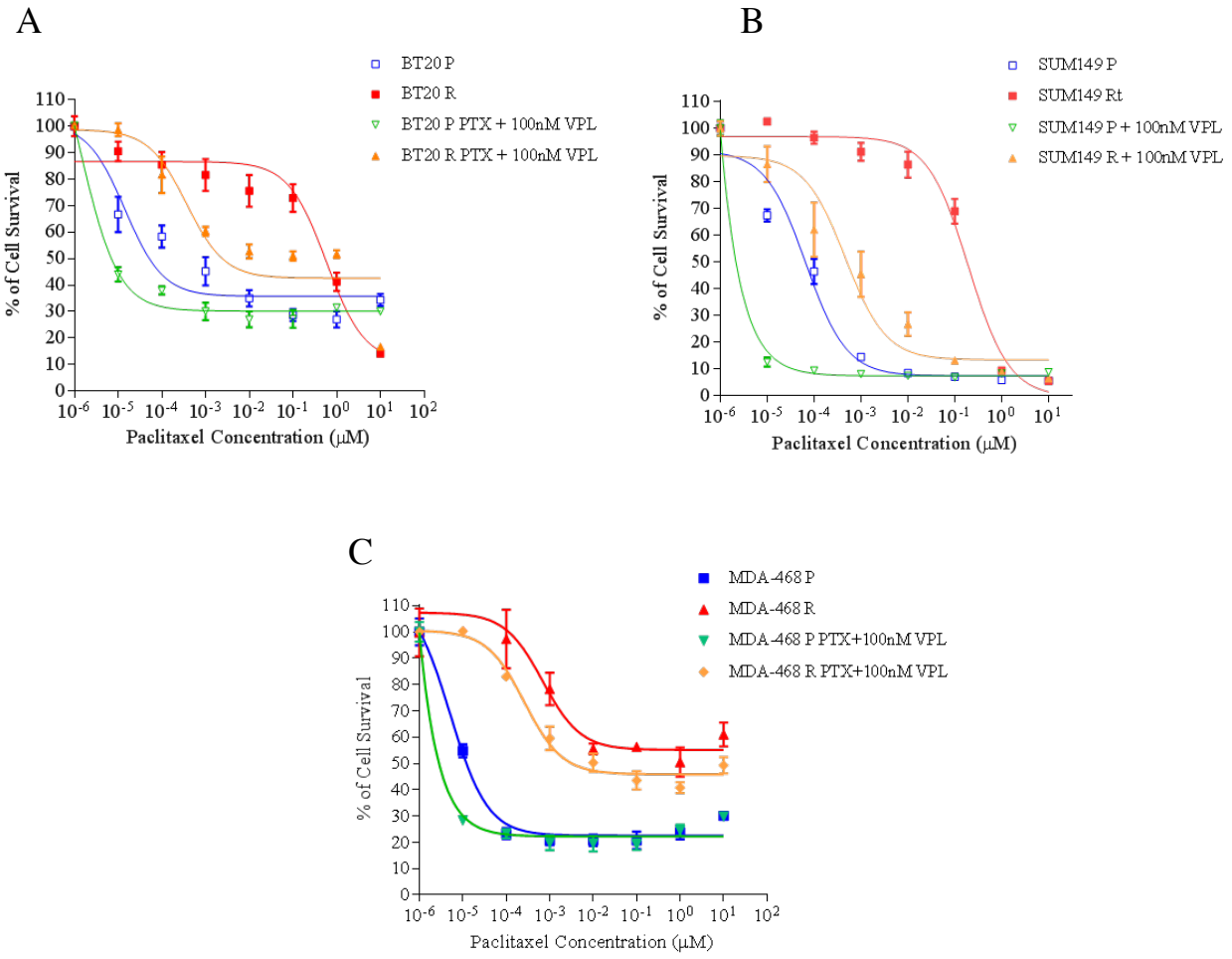

Figure 4.6. Effect of verapamil and PTX on viability of ABCB1 over-expressing cell lines. Cells were incubated for 72h with 100nM of verapamil in combination with increasing concentrations of PTX. Cell viability was measured by alamar blue assay. The data show the mean ± SD (n=3). Verapamil markedly enhanced the cytotoxic effect of PTX (not in 468R that much).

A

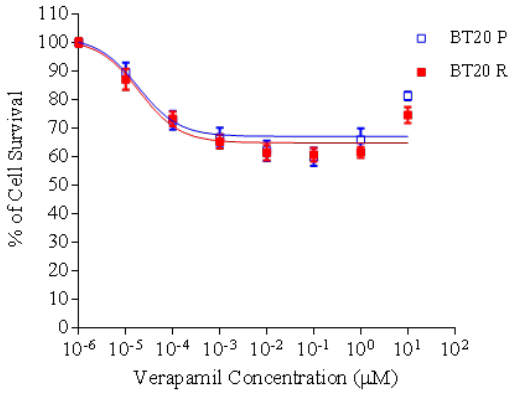

B

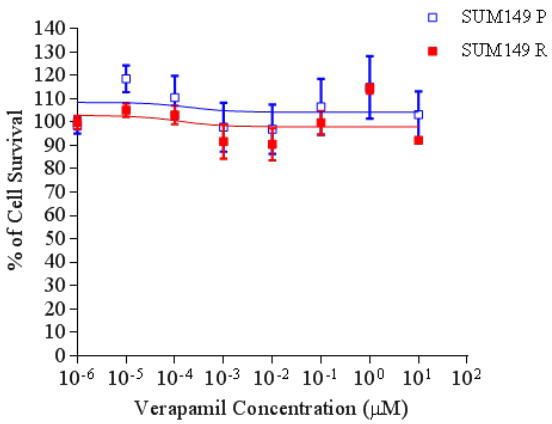

C

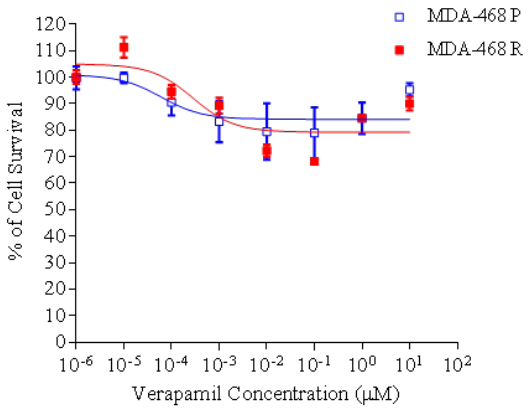

Figure 4.7. Effect of verapamil on viability of ABCB1 over-expressing cell lines. Cell viability was measured by alamar blue assay. The data show the mean ± SD (n=3). The ABCB1 over-expressing resistant cell lines are not sensitive to verapamil.

4.6. Knockdown of ABCB1 rescues the sensitivity of ABCB1_overexpressing resistant cell lines

To assess the role and impact of ABCB1 to PTX resistance in BT20R, SUM149R and MDA-468R we silenced ABCB1 gene expression by using a shRNA targeting ABCB1. Five different TRC lentiviral shRNAs specific to ABCB1 were tested. Cells were transfected using polyethylenimine (PEI) reagent and incubated for 24h in fresh media. After incubation, medium was replaced with fresh medium and 10 μg/ml Puromycin was added to the cells in order to select for transfected cells. ABCB1 expression in transfected cells were evaluated by qRT-PCR and western blot analysis and their sensitivity to PTX was determined by cytotoxicity assay. Much to our surprise, transfection of ABCB1 over-expressing cells with ABCB1 targeting shRNA not only did not decrease the expression of ABCB1 or the sensitivity of the cells to PTX, but it increased the ABCB1 mRNA and protein expression in these cell lines and it increased the efflux activity of the transfected cells (Figure 4.8). This increase was also observed in cells transfected with shRNA with scrambled construction, suggesting that the selection procedure has selected for cells with high expression of ABCB1. We hypothesized that the expression of ABCB1 confers puromycin resistance to transfected ABCB1 over-expressing cells. The results of cytotoxicity assay showed decreased sensitivity of resistant cells to puromycin compare to their sensitive counterparts.

Transfected cells with higher expression of ABCB1 displayed lower sensitivity to puromycin compared to non-transfected resistant cells. In support of our hypothesis, the result of efflux assay of the transfected cells showed decreased accumulation of rhodamine 123 in transfected cells compared to non-transfected resistant cell lines (Figure 4.9).

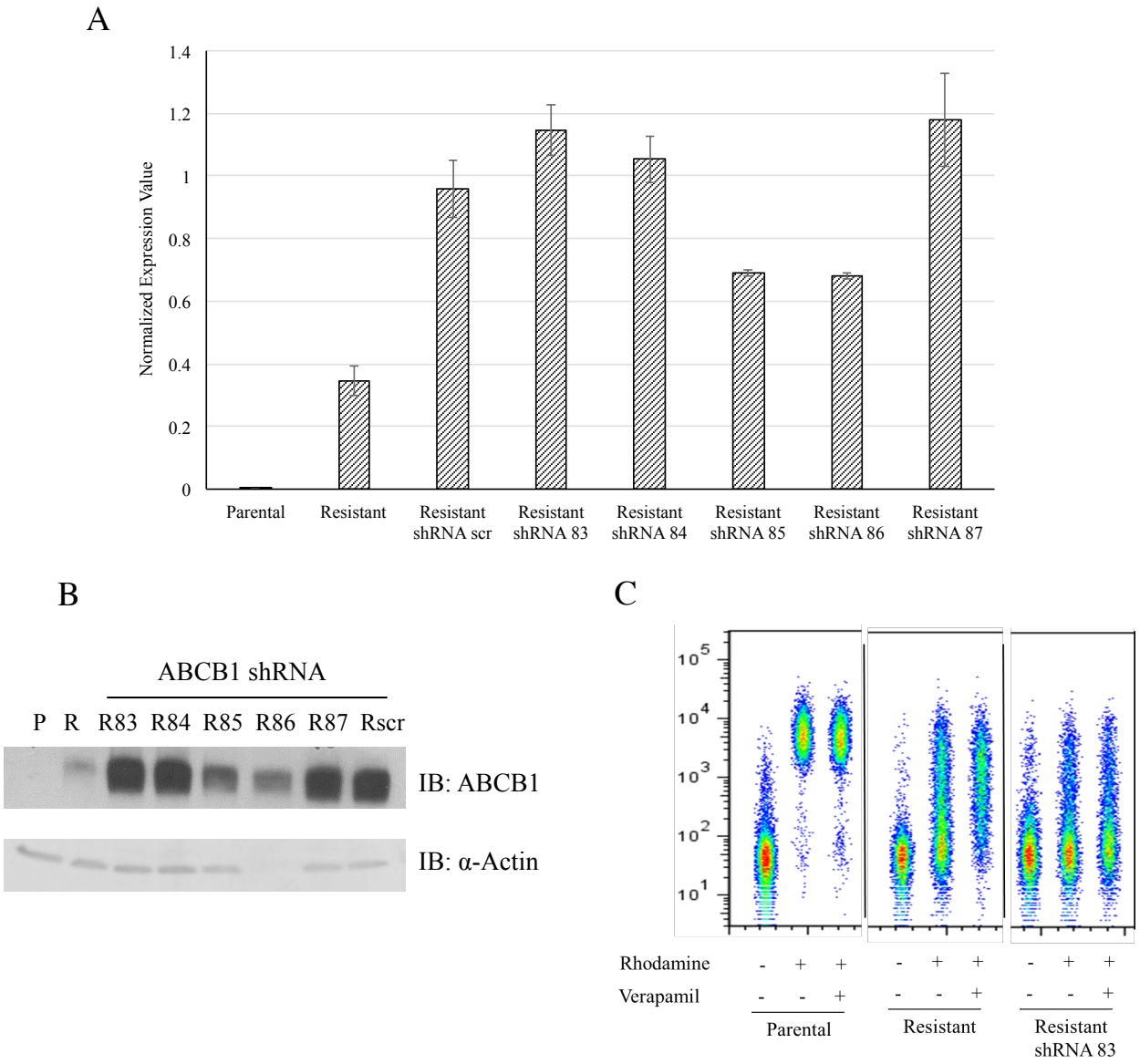

Figure 4.8. Analysis of ABCB1 expression in cells transfected with five different shRNA targeting ABCB1. A: Elevated ABCB1 transcript was observed in all transfected cells including cells transfected with scrambled shRNA construct and shRNA targeting ABCB1. B: The transfection procedure increased the ABCB1 protein expression. C: Increased efflux activity was observed in ABCB1 transfected cells.

A

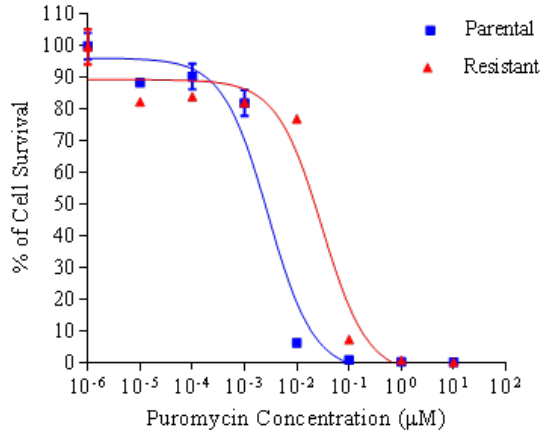

B

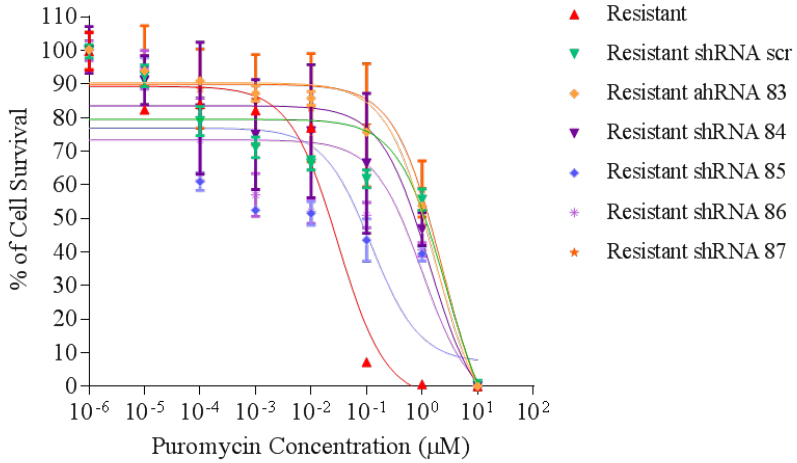

Figure 4.9. Puromycin sensitivity of the ABCB1 over-expressing cells. SUM149R cell line show decreased sensitivity to puromycin. The sensitivity to puromycin is decreased in transfected resistant cell line.

In order to avoid the use of selective markers after transfection, we aimed to silence the ABCB1 gene infecting the cells using a pGIPZ lentiviral-vector expressing shRNAs specific for ABCB1. The cells were infected with lentiviruses containing three different ABCB1 targeting shRNAs or non-targeting shRNA vector (scr) and FACS sorted for the GFP expressing fraction. The ABCB1 knockdown efficiency was then evaluated by qRT-PCR and western blotting. The results showed that ABCB1 mRNA and protein expression was significantly down-regulated in BT20R and MDA-468R expressing ABCB1 targeting shRNAs as compared to cells expressing non-targeting shRNA. We next determined the sensitivity of these cells to PTX by cytotoxicity assay. Knock down (KD) of ABCB1 re-sensitizes BT20R-KD and MDA-468R-KD to PTX (Figure 4.10).

To determine the degree to which ABCB1 up-regulation contributes to PTX resistance, we sorted transfected cells into fractions with low and high GFP expression. The ABCB1protein expression of each fraction was evaluated by western blotting and the sensitivity of cells to PTX were determined by cytotoxicity assay. We found that ABCB1 gene silencing re-sensitizes BT20R and MDA-468R to PTX in a gene dosage dependent manner (Figure 4.11). These data suggest that ABCB1 is the main mechanism of resistance to PTX in BT20R and MDA-468R. Transfection of SUM149R with ABCB1 targeting shRNA had no effect on ABCB1 mRNA or protein expression and it did not increase the sensitivity of SUM149R cells to PTX.

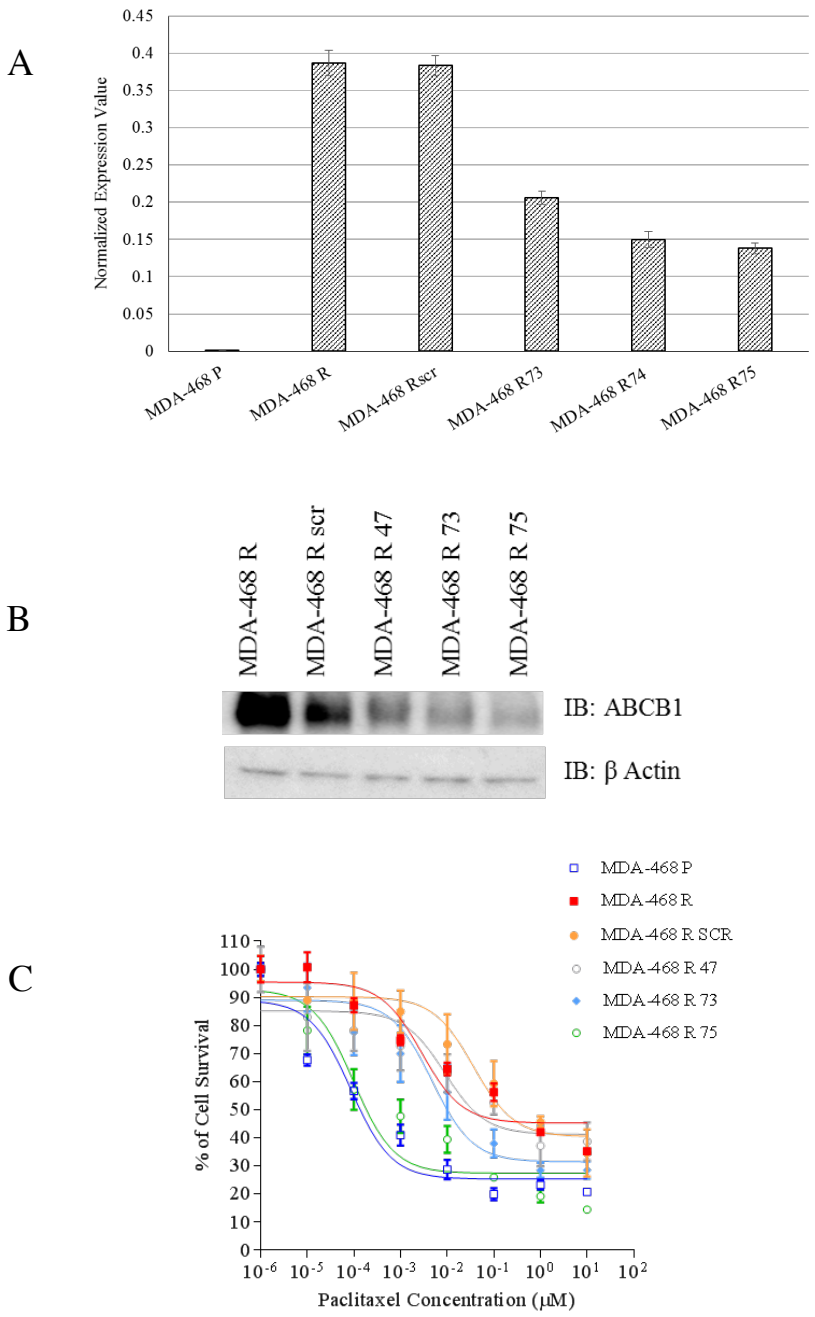

Figure 4.10. ABCB1 knock down restores the sensitivity of resistant cell lines to PTX. A: ABCB1 mRNA expression of MDA-MB-468P, MDA-MB-468R and MDA-MB-468R transfected with shRNA targeting ABCB1. B western blot analysis of ABCB1 protein expression. C: Cytotoxicity assay of ABCB1 KD cell lines.

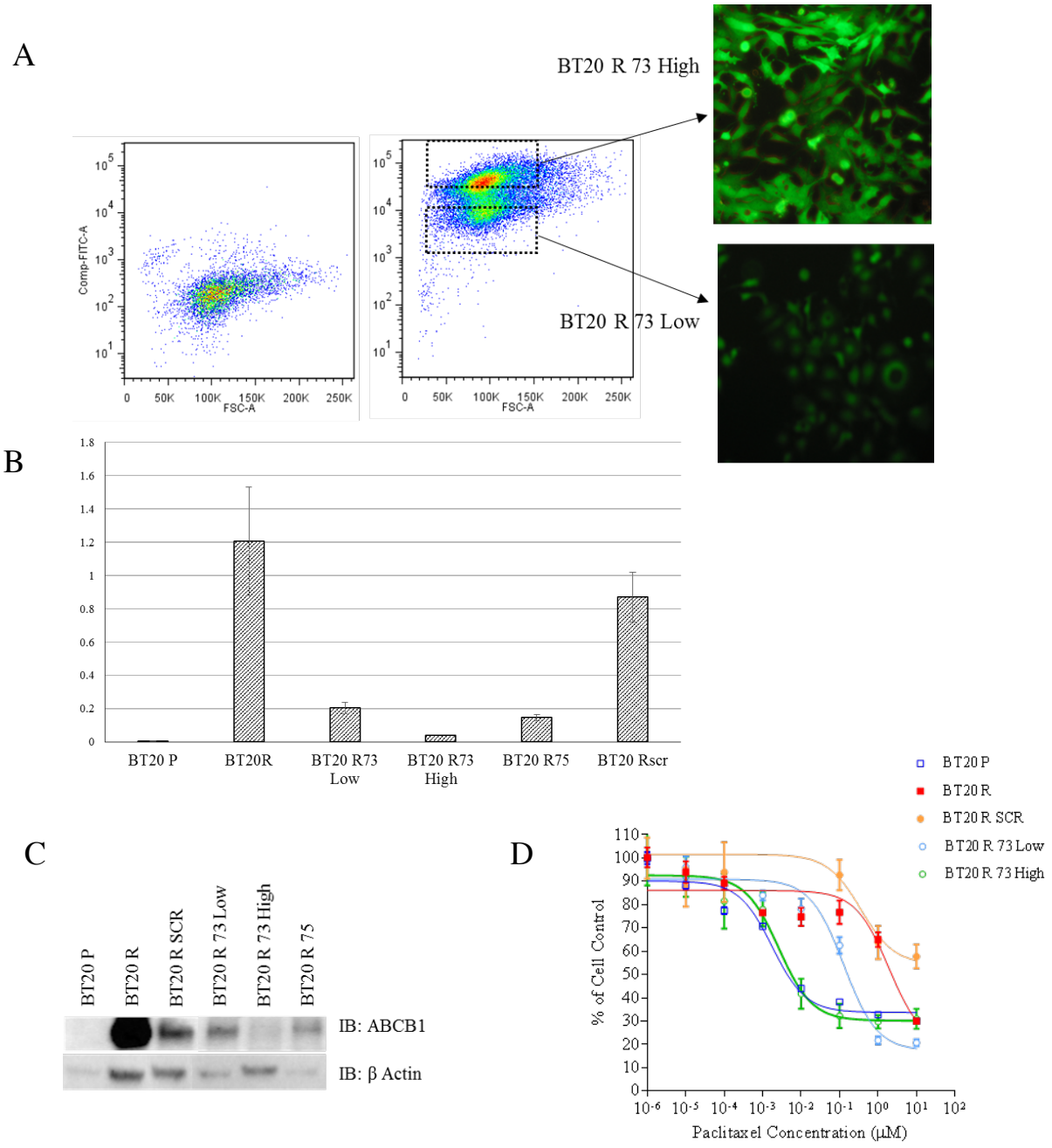

Figure 4.11. ABCB1 overexpression confers the sensitivity of the cell lines to PTX in gene dosage dependent manner. A: The flow cytometry analysis of ABCB1 shRNA transfected cells revealed 2 distinct populations with different levels of GFP expression. B and C: ABCB1 mRNA and Protein expression was markedly reduced in BT20 R 73 GFP-high cells. D: ABCB1 knock down restores PTX sensitive in a gene dose dependent manner.

4.7. ABCB1 amplification is accompanied by a distal sharp breakpoint

Closer analysis of array CGH results of the 7q21.12 chromosomal region in BT20R, SUM149R and MDA-468R cells revealed similar, but not identical, breakpoints in the 5'-untranslated region (UTR) of ABCB1 (Figure 4.12, 4.13, 4.14). To measure the effect of these DNA breaks on RNA expression, we measured the expression of exons on either side of the breaks with qRT-PCR. Two sets of primers were designed targeting the 5'-UTR and the coding sequence of the ABCB1 mRNA. We found a loss of RNA expression of exon 1 (5'-UTR) and high expression of exon 15 (coding sequence) (Figure 4.15).

To determine whether the ABCB1 copy number gain was due to the duplication in tandem, intra-chromosomal translocation or inter-chromosomal translocation with a FISH assay for ABCB1. Two FISH probes were purchased, one probe for the amplified region of ABCB1 and one for the centromeric region of chromosome 7 (Cep7). The parental cell lines were also subjected to FISH analysis to determine whether genomic aberrations found in the resistant cell lines were present in their sensitive counterparts. FISH analysis revealed de novo inter-chromosomal translocation in both BT20R and SUM149R cell lines (Figure 4.15). These results indicate that ABCB1 amplification in TNBC cells is associated with a deletion of the 5'UTR including exons 1 and 2 that may involve translocation events.

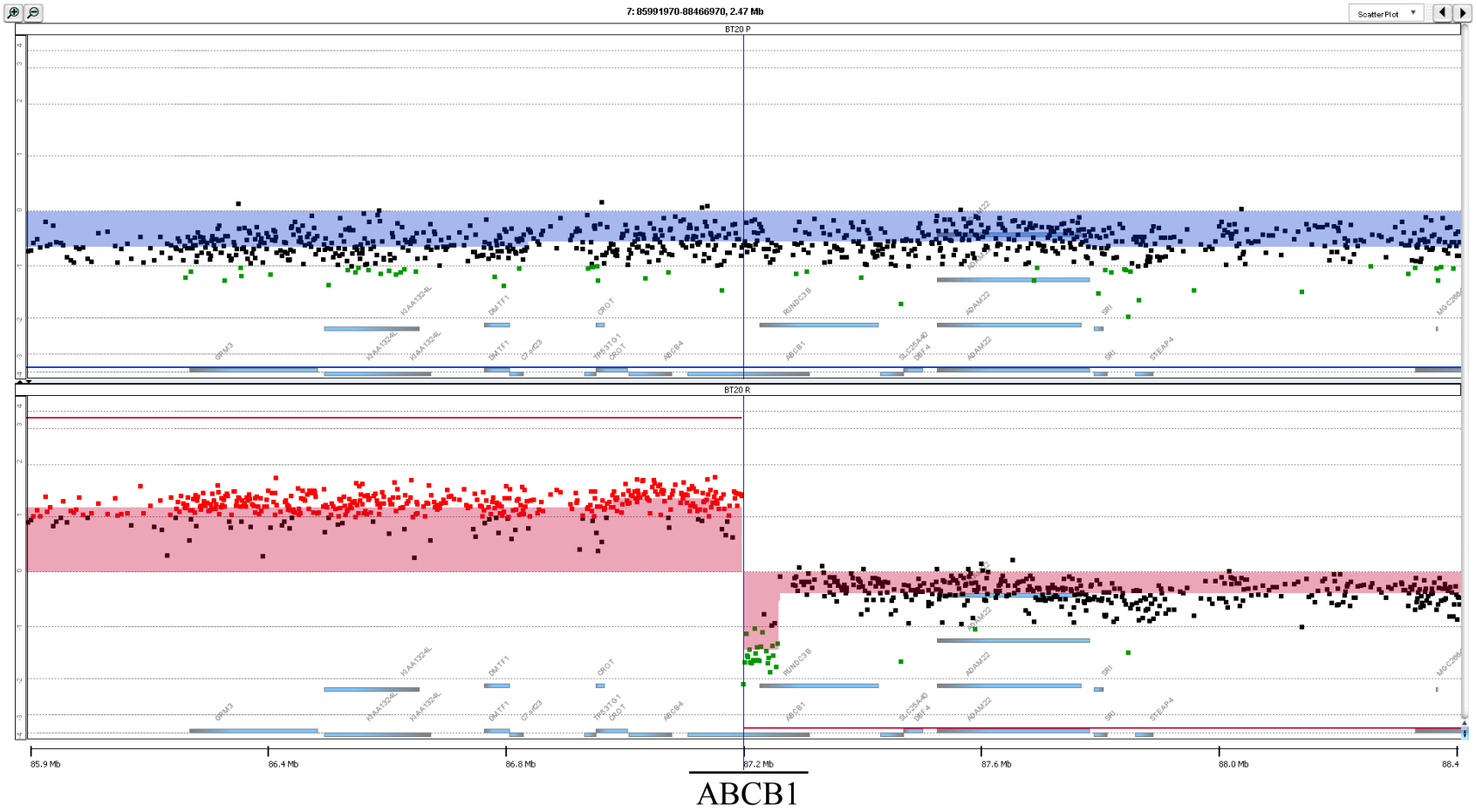

Figure 4.12. Array CGH analysis of 7q21 in BT20P and BT20R. The upper panel represents BT20P and the lower panel represents BT20R. The dots represent the Log2 fluorescence ratios of individual oligonucleotide probes on the microarrays. The red dots represent probes with Log2 fluorescence ratios higher than 1, and the green dots represent probes with Log2 fluorescence ratios lower than -1. The blue shaded areas denote ADM2 aberrant intervals in parental cell line and the red shaded areas denote ADM2 aberrant intervals in resistant cell line.

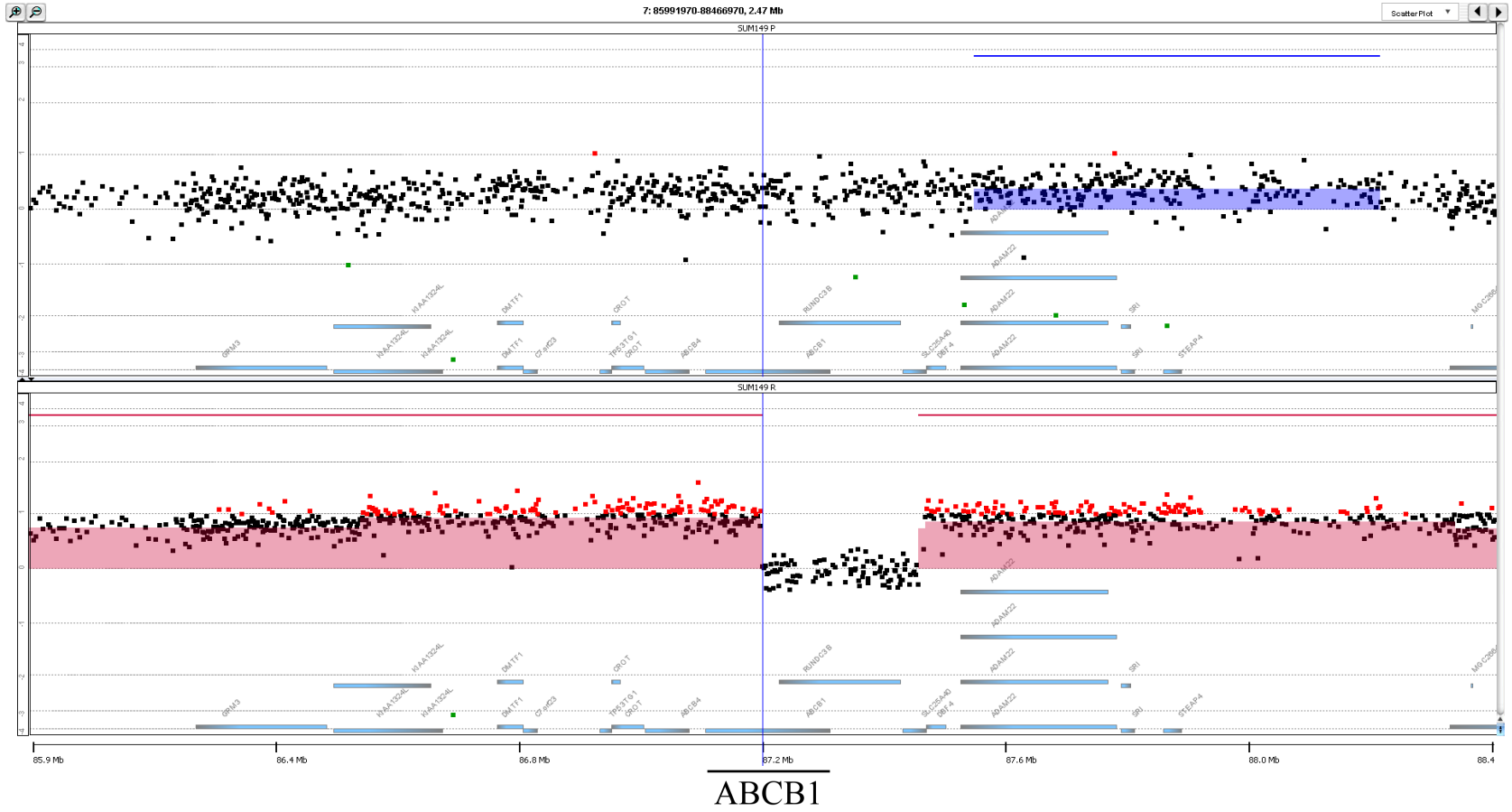

Figure 4.13. Array CGH analysis 7q21 in SUM149P and SUM149R. The upper panel represents SUM149P and the lower panel represents SUM149R. The dots represent the Log2 fluorescence ratios of individual oligonucleotide probes on the microarrays. The red dots represent probes with Log2 fluorescence ratios higher than 1, and the green dots represent probes with Log2 fluorescence ratios lower than -1. The blue shade in parental and the red shade in resistant cell line represent regions of copy number alterations determined statistically significant by the ADM2 software.

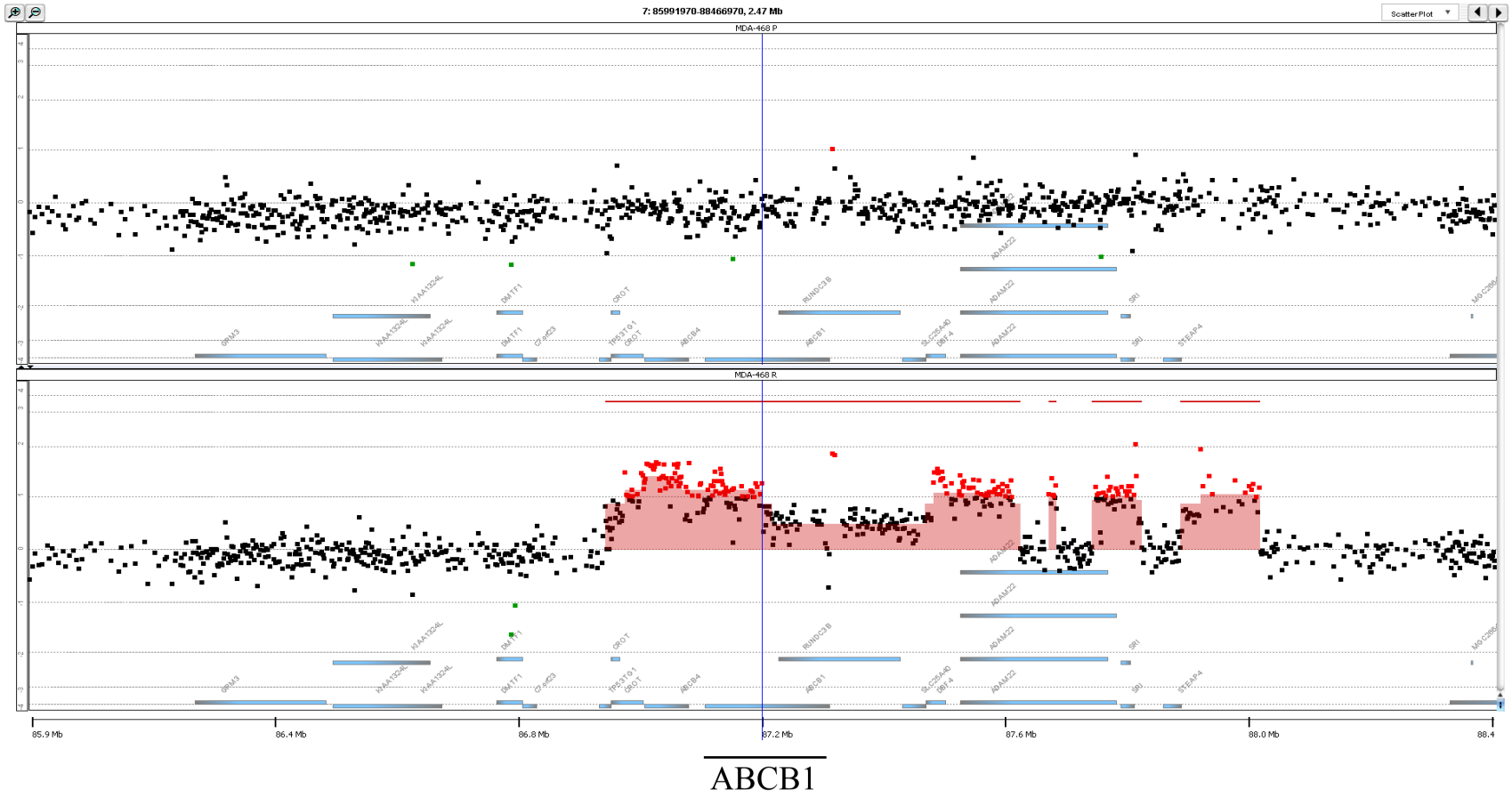

Figure 4.14. Array CGH analysis 7q21 in MDA-MB-468P and MDA-MB-468R. The upper panel represents MDA-MB-468P and the lower panel represents MDA-MB-468R. The dots represent the Log2 fluorescence ratios of individual oligonucleotide probes on the microarrays. The red dots represent probes with Log2 fluorescence ratios higher than 1, and the green dots represent probes with Log2 fluorescence ratios lower than -1. The blue shade in parental and the red shade in resistant cell line represent regions of copy number alterations determined statistically significant by the ADM2 software.

A

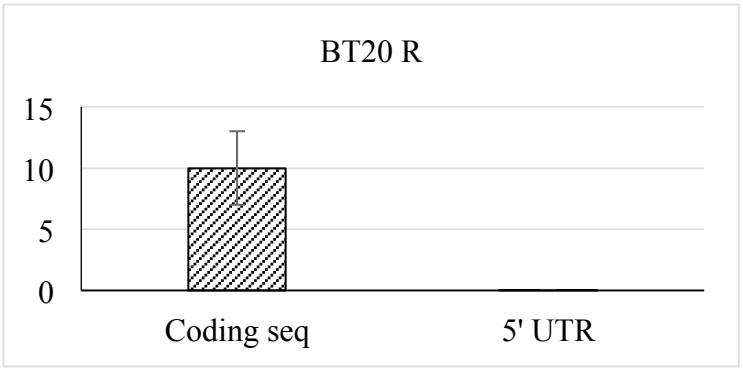

B

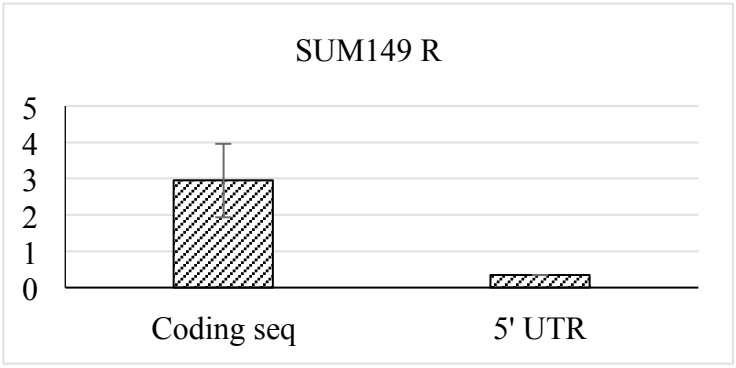

C

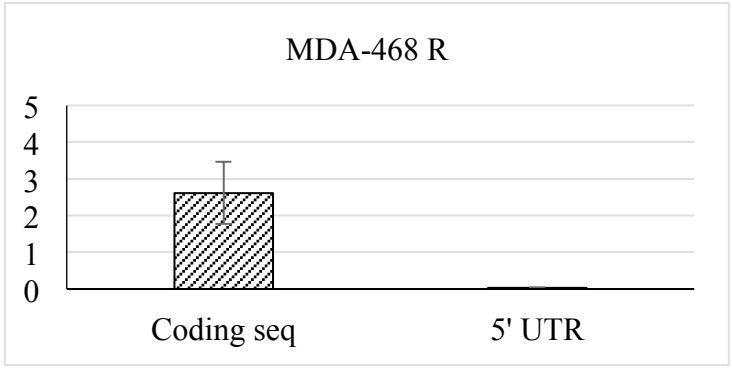

Figure 4.15. The qRT-PCR analysis of deleted and amplified regions in ABCB1 gene. Two pairs of primers were designed targeting amplified (coding sequence) and deleted (5'UTR) region of ABCB1 and the related transcript level for A: BT20R, B: SUM149R, C: MDA-MB-468R cell line was measured by qRT-PCR. Results represent mean values of three independent replicates ± SD

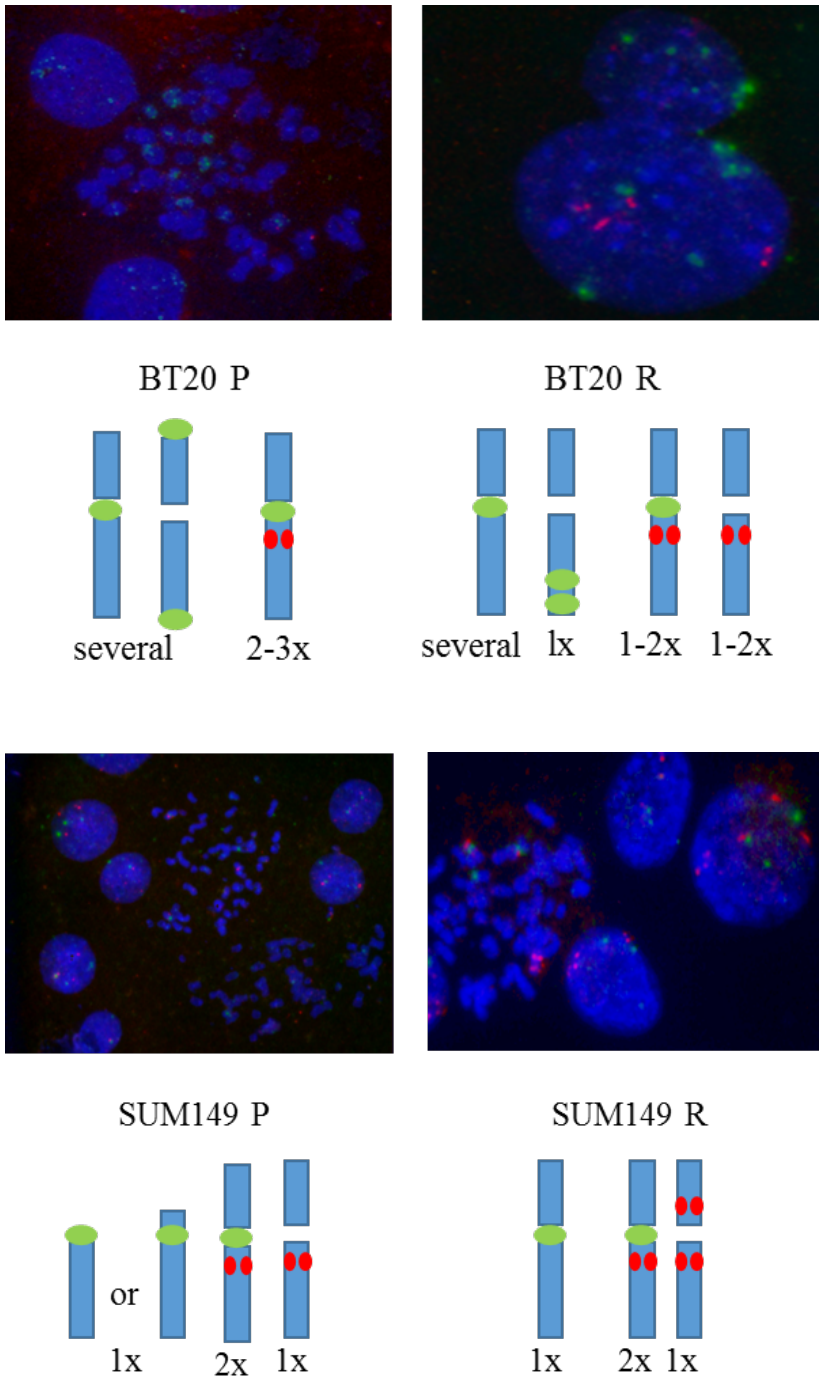

Figure 4.16. Validation of ABCB1 gene copy number gain using FISH. Representative FISH images for BT20P, BT20 R, SUM149P and SUM149R are depicted. Orange-labeled ABCB1 specific probe and chromosome-7 centromeric probe (CEP7) labeled with spectrum green was used. A schematic of a possible amplification structures are shown.

4.8. ABCB1 genomic rearrangement

To further investigate the underlying genomic rearrangement in ABCB1, we performed RNA-seq on resistant cell lines and their sensitive counterparts. Analysis of RNA-seq data revealed gene fusion in BT20R and SUM149R cell lines. The ABCB1 hybrid transcript in BT20R is composed of the first two exons of TEKT4P2, a pseudogene originally located on chromosome 21, fused to exon 3 of ABCB1. Sequencing of the ABCB1 transcript in SUM149 unveiled SLC25A40 and C17orf42 as 5′ fusion partners of ABCB1. In MDA-MB-468 cells, the result showed a truncated ABCB1 transcript with a full deletion of exon 1 and partial deletion of exon 2. The genomic rearrangement in ABCB1 in BT20R, SUM149R and MDA-468R occurred in 5' un-translated region (5'UTR). The RNA-seq analysis of ABCB1 in BT20R revealed the deletion of both upstream and downstream promoters of ABCB1 (Figure 4.17). A similar rearrangement was seen in ABCB1-SLC25A40 and ABCB1-C17orf42. These results indicate translocation events in SUM149R and BT20R may have led to a possible juxtaposition of a non-ABCB1 promoter sequence to ABCB1 gene that allows transcription initiation and favours the expression of ABCB1 in these cell lines. However, we also identified an ABCB1-C17orf42 fused transcript in SUM149R containing part of exon 2, including the proximal ABCB1 promoter. The proximal promoter was also present in MDA-MB-468R, suggesting that the expression of the one of the

fused transcript in SUM149R and the truncated ABCB1 transcript in MDA-MB-468R is under the control of ABCB1 proximal promoter.

As mentioned we were not able to knockdown ABCB1 in SUM149. Identification of several ABCB1 fusion partners in SUM149 could explain the complexity of the mechanisms by which ABCB1 is regulated in SUM149.

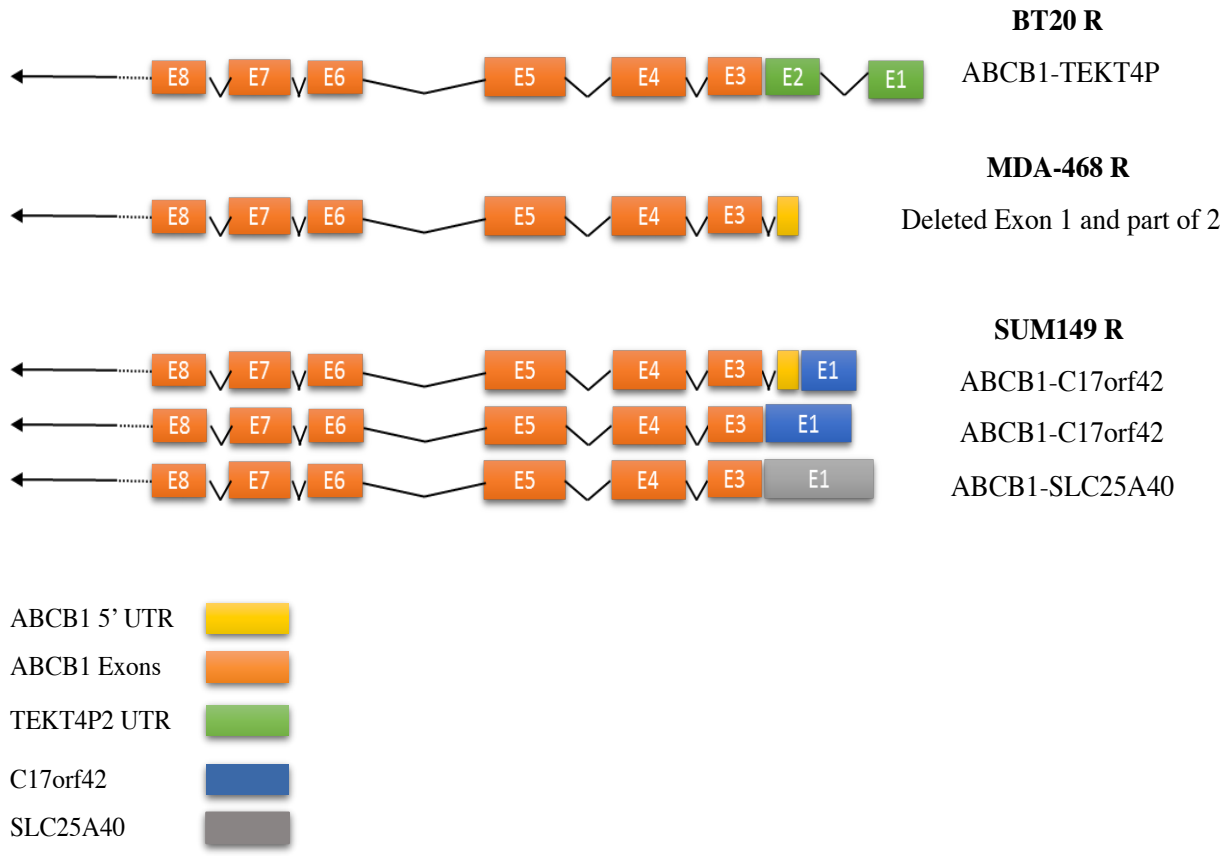

Figure 4.17. Schematic depict the structures of gene fusion in ABCB1 in BT20R, SUM149R and MDA-MB-468R cell lines that was identified by RNAseq analysis. E: exon.

4.9. Down regulation of 4E-BP or overexpression of eIF4E renders the translation of ABCB1

We sought an explanation for the lack of ABCB1 protein overexpression in the other 2 PTX-resistant cell lines that show high levels of ABCB1 RNA but do not contain ABCB1 gene amplification associated with breaks in the 5'UTR of the ABCB1 gene. It has been shown that the highly structured 5' UTR of the ABCB1 transcript in fact inhibits translation of the gene by adopting a highly structured fold that blocks translation [211]. Indeed, the 5' loop of the transcript renders it poorly competitive for eIF4E, the rate-limiting transcription initiation factor. mRNAs containing such complex secondary structures can be translated when eIF4E is over-expressed [212]. Since translation is controlled by the balance between 4E-BP and eIF4E activity at the 5'end of transcripts, we reasoned that silencing 4E-BP could lead to translation of the ABCB1 transcripts in those cell lines without genomic rearrangements (MDA-MB-231 and MDA-MB-436). ShRNA silencing of 4E-BP in both cell lines led to an increase in ABCB1 protein expression as predicted (Figure 4.18). ABCB1 protein expression was also detected in MDA-MB-436R cell lines transfected with eIF4E vector. These findings suggest that the elimination of the 5' end of the ABCB1 gene by a genomic rearrangement or deletion is critical for ABCB1 protein overexpression in drug resistant TNBC cells.

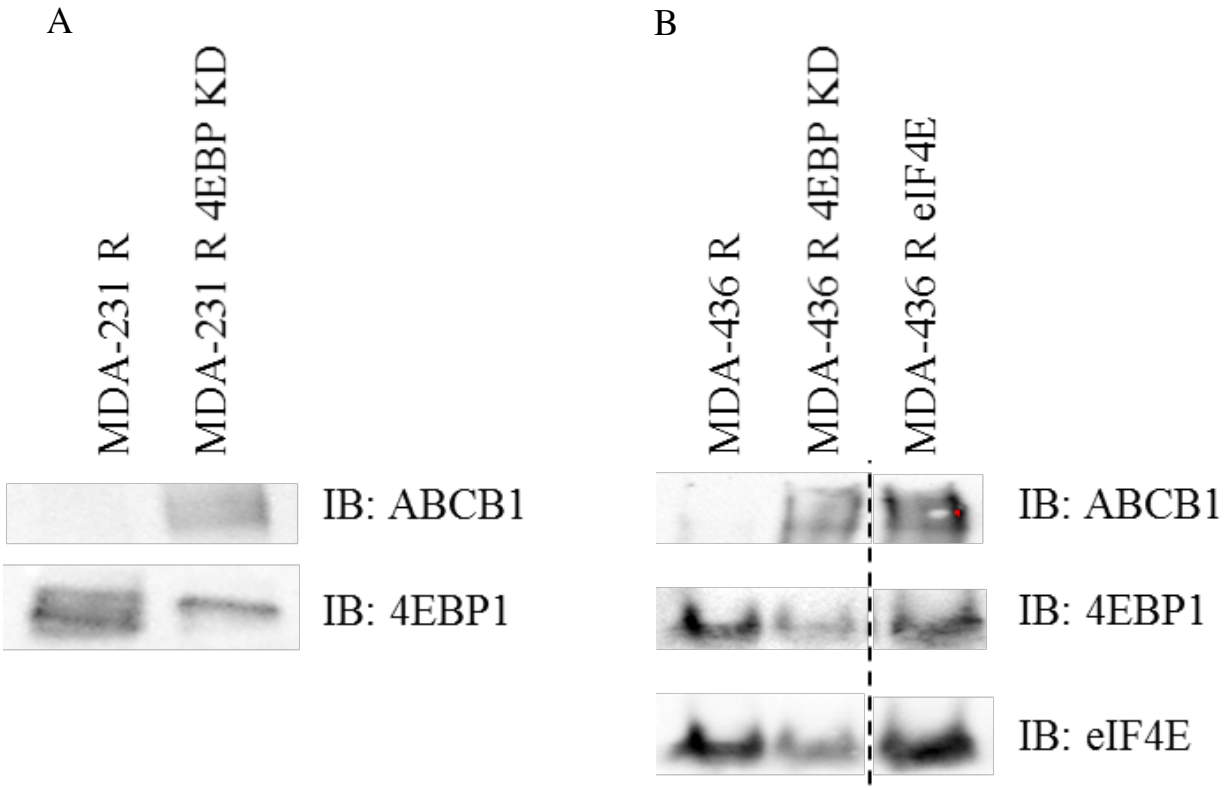

Figure 4.18. Down regulation of 4E-BP or overexpression of eIF4E renders the translation of ABCB1. Western blot analysis of MDA-MB-231R (A) and MDA-MB-436R (B) transfected with shRNA targeting 4EBP1 and 4EBP2. ABCB1 protein expression was detected upon over-expression of eIF4E in MDA-MB-436R

4.10. Summary

The gene expression analysis of resistant cell lines and their sensitive counterparts identified ABCB1 gene as the only gene commonly up-regulated in all resistant cell lines. Using aCGH, we showed that up-regulation of ABCB1 in BT20R, SUM149R and MDA-468R was accompanied by high-level amplification. The evaluation of protein expression of ABCB1 showed up-regulation in BT20R, SUM149R and MDA-468R but not in MDA_MB-231R and MDA-MB-436R, suggesting that changes in ABCB1 copy number results in ABCB1 gene activation. We showed that inhibition of ABCB1 efflux activity by verapamil partially reversed the sensitivity of ABCB1 overexpressing cells, suggesting that ABCB1 overexpression contributes to PTX resistance. To further study the impact of ABCB1 expression in resistant cell lines, we employed TRC lentiviral shRNA targeting ABCB1. However, using puromycin as selective marker of transfected cells, selected for cells expressing higher level of ABCB1. This result is in agreement with a recent finding of Theile et al, showing that puromycin is, in fact, a substrate of ABCB1 [213]. To avoid the use of any selective marker, we used a GIPZ-shRNA system and selected GFP-expressing cells. ABCB1 knockdown re-sensitized the cells to PTX in a dose-dependent manner, indicating that ABCB1 is the main cause of resistance to PTX in these cell lines.

The mechanisms responsible for ABCB1 gene expression are complex and can be controlled by a myriad of factors that contribute to the expression and activity of ABCB1 either pre- or post-transcriptionally. In many multidrug resistant cell lines, overexpression of ABCB1 is accompanied by gene amplification and chromosomal rearrangements. Array CGH analysis of 7q21.12 in BT20R, SUM149R and MDA-468R revealed similar, but not identical, breakpoints in the 5'UTR of ABCB1. These breakpoints, accompanied by focal amplifications, highlight the potential for the occurrence of genomic rearrangement events in ABCB1 in PTX resistant cells. The ABCB1 gene activation driven by chromosomal translocation was first reported in an Adriamycin-selected human colon adenocarcinoma cell line [147]. The activation of ABCB1 occurred after a (4q;7q) translocation in these cell lines that resulted in juxtaposition of ABCB1 gene 3' to a transcriptionally active gene located on chromosome 4 [147]. Additional ABCB1 gene rearrangements within active gene sequences of chromosomes 1, 4, or 16 have been identified in cell lines [147, 152, 162]. In fact, we identified inter-chromosomal translocations of ABCB1 in BT20R and SUM149R cell lines. This genomic rearrangement occurred in 5'UTR of ABCB1. Despite the diversity of the fusion partners, most of the cell lines shared a similar pattern of chromosomal rearrangement, suggesting that chromosomal rearrangements leads to "capture" ABCB1 by a, random, constitutively active promoter resulting in aberrant activation of the gene. Kitada et al. have proposed that ABCB1 chromosomal translocation, mediated by breakage-

fusion-bridge cycle, occurs prior to amplification and activates the ABCB1 gene placed downstream of a constitutively active gene promoter [152]. However, detailed activation mechanisms of ABCB1 by gene fusion remain to be elucidated.

Interestingly, ABCB1 genomic rearrangement in MDA-468R did not lead to formation of a hybrid mRNA, suggesting that ABCB1 gene activation is more complex. Previous reports have shown that the 5' UTR of the ABCB1 mRNA can inhibit translation initiation by preventing the binding of translational machineries [211]. We propose that the deletion of the 5'UTR of ABCB1 in these resistant cell lines overcomes the translation initiation block [211]. Therefore, this genomic rearrangement favours the expression and the activity of ABCB1. To our knowledge, we are the first to report ABCB1 amplification and ABCB1 gene fusion in PTX resistant TNBC cell lines

Chapter 5

Results: Tyrosine kinase inhibitors sensitize resistant cell lines to PTX

5.1. Investigation of the role of EGFR ligands in PTX resistance

Our comparative gene expression analysis identified genes that were differentially expressed in resistant cell lines compared to their sensitive counterparts. In order to understand the biological significance of the observed changes, we performed pathway analysis using the D.A.V.I.D. Bioinformatics Resources web tool. [214]. The DAVID Gene Ontology Molecular Function revealed similarities as well as clear differences between molecular functions over-represented in the resistant cell lines. The only enriched molecular function of up-regulated genes common to all 5 cell line models was that of "growth factor activity". We noted that several epidermal growth factor receptor (EGFR) ligands were up-regulated in the "growth factor activity" list, including EGF, AREG, EREG, TGFA, BTC and HBEGF (Table 5.1).

Members of the EGFR family of trans-membrane receptor tyrosine kinases (HER1/EGFR; HER2; HER3; HER4) and their respective ligands constitute a robust biologic system that trigger a rich network of signaling pathways, that regulates cell proliferation, survival, and differentiation [215]. Ligand binding to a monomeric HER receptors form homo- or heterodimers activates the cytoplasmic catalytic function by promoting receptor dimerization and self-phosphorylation on tyrosine residues, which serves as docking sites for adaptor proteins that activate downstream growth and survival signaling cascades [216, 217]. In many different cancer cell types, the HER

pathway is constitutively active. This can be caused by a range of mechanisms including gene amplification, overexpression of ligands and receptors, activating mutations or constitutive activation of receptors [215].

Human breast cancer cell lines with acquired drug resistance frequently show increased EGFR and TGF-α expression [218]. In addition, overexpression of EGFR in human breast cancer cells resulted in a reduced sensitivity to several cytotoxic drugs, such as doxorubicin, vinblastin, cisplatin and 5-fluorouracil which suggests that EGFR activation influenced the sensitivity of tumour cells to cytotoxic compounds [218, 219].

The aim of this chapter is to first validate the result of comparative gene expression analysis and second to determine the impact of EGFR ligands up-regulation in PTX resistant TNBC cell lines.

Gene Symbol	EREG	AREG	BTC	EGF	HBEGF	NRG1	TGFA
BT20 P	421.03	3306.46	96.87	63.24	146.37	51.98	7708.6
BT20 R	5980.19	1320.90	149.46	195.58	188.75	49.60	7800.1
BT20 R vs P p value	<0.05	<0.05	<0.05	<0.05	0.20	0.77	0.9
BT20 RvsP FC	**14.20**	**-2.50**	**1.54**	**3.09**	**1.29**	**-1.05**	**1.0**
SUM149 P	378.63	24623.03	101.36	41.59	52.05	117.19	7609.1
SUM149 R	1226.21	60618.97	164.56	41.46	110.46	89.11	5887.3
SUM149 R vs P p value	<0.05	<0.05	<0.05	0.98	<0.05	0.09	0.1
SUM149 RvsP FC	**3.24**	**2.46**	**1.62**	**-1.00**	**2.12**	**-1.32**	**-1.3**
MDA231 P	110.84	4013.16	71.80	73.71	2670.27	3873.36	10885.1
MDA231 R	225.82	7072.05	143.55	138.21	2869.46	1071.09	21866.5
MDA231 R vs P p value	<0.05	0.08	<0.05	<0.05	0.71	<0.05	<0.05
MDA231 RvsP FC	**2.04**	**1.76**	**2.00**	**1.88**	**1.07**	**-3.62**	**2.0**
MDA436 P	5259.57	818.08	71.58	51.75	191.08	216.69	7244.1
MDA436 R	866.81	1211.02	94.02	49.54	380.30	874.58	8486.7
MDA436 R vs P p value	<0.05	0.22	<0.05	0.78	<0.05	<0.05	0.3
MDA436 RvsP FC	**-6.07**	**1.48**	**1.31**	**-1.04**	**1.99**	**4.04**	**1.2**
MDA468P	45.04	771.71	181.57	151.26	250.51	48.17	2264.4
MDA468R	37.92	833.89	187.41	51.93	207.03	47.29	3175.3
MDA468 R vs P p value	0.60	0.83	0.78	<0.05	0.40	0.92	<0.05
MDA468 RvsP FC	**-1.19**	**1.08**	**1.03**	**-2.91**	**-1.21**	**-1.02**	**1.4**

Table 5.1 Gene expression values of EGFR ligands in all parental and resistant cell lines. The fold change (FC) of each ligand in each cell line is highlighted in light blue.

5.2. EGFR ligands are up-regulated in TNBC resistant cell lines.

To validate the result of gene expression microarray, we performed quantitative real time PCR on EGFR ligands including EGF, betacellulin (BTC), epiregulin (EREG), amphiregulin (AREG), and heparin-binding EGF-like growth factor (HB-EGF) and Neuregulin 1(NRG1). The result of quantitative RT-PCR confirmed the elevation of most of these EGFR ligand transcript level in several of the resistant cell lines (Figure 5.1). It is important to note that our integrative analysis of array CGH and gene expression data did not show any significant amplification for the up-regulated EGFR ligands.

A

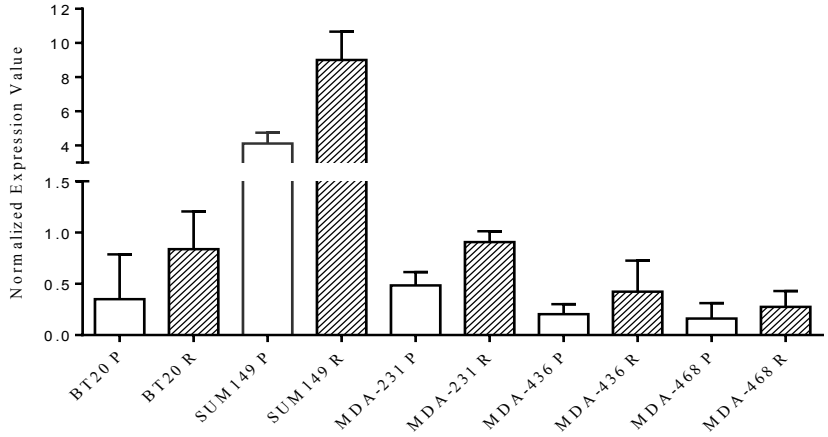
AREG
Normalized Expression Value
12
10
8
6
4
1.5
1.0
0.5
0.0
BT20 P
BT20 R
SUM149 P
SUM149 R
MDA-231 P
MDA-231 R
MDA-436 P
MDA-436 R
MDA-468 P
MDA-468 R

B

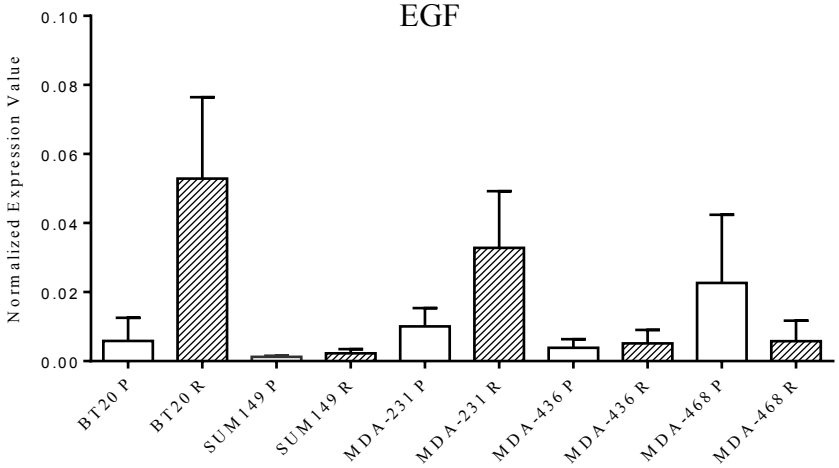
EGF
Normalized Expression Value
0.10
0.08
0.06
0.04
0.02
0.00
BT20 P
BT20 R
SUM149 P
SUM149 R
MDA-231 P
MDA-231 R
MDA-436 P
MDA-436 R
MDA-468 P
MDA-468 R

C

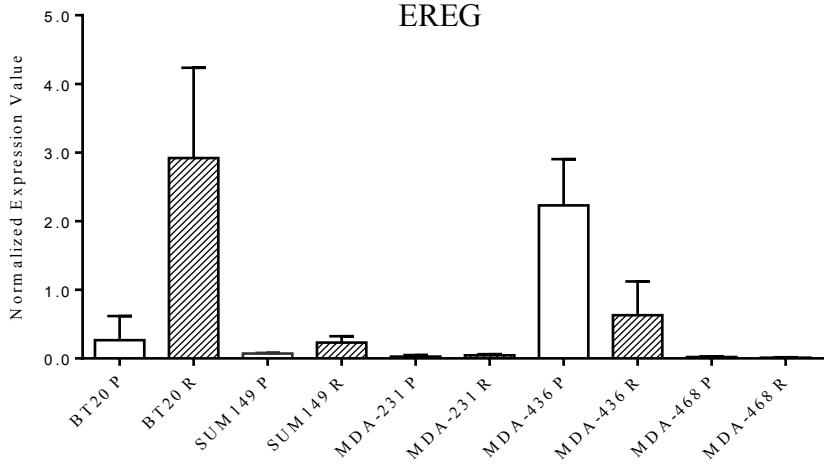
EREG
Normalized Expression Value
5.0
4.0
3.0
2.0
1.0
0.0
BT20 P
BT20 R
SUM149 P
SUM149 R
MDA-231 P
MDA-231 R
MDA-436 P
MDA-436 R
MDA-468 P
MDA-468 R

D

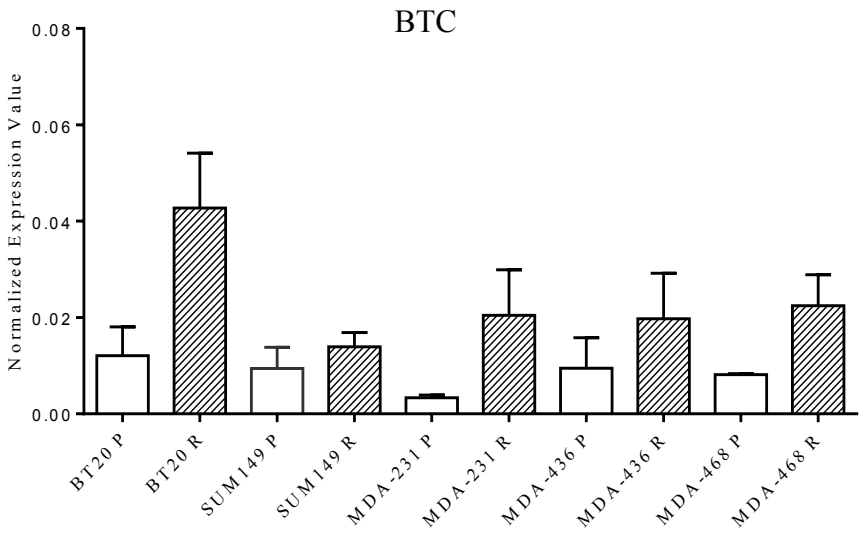

E

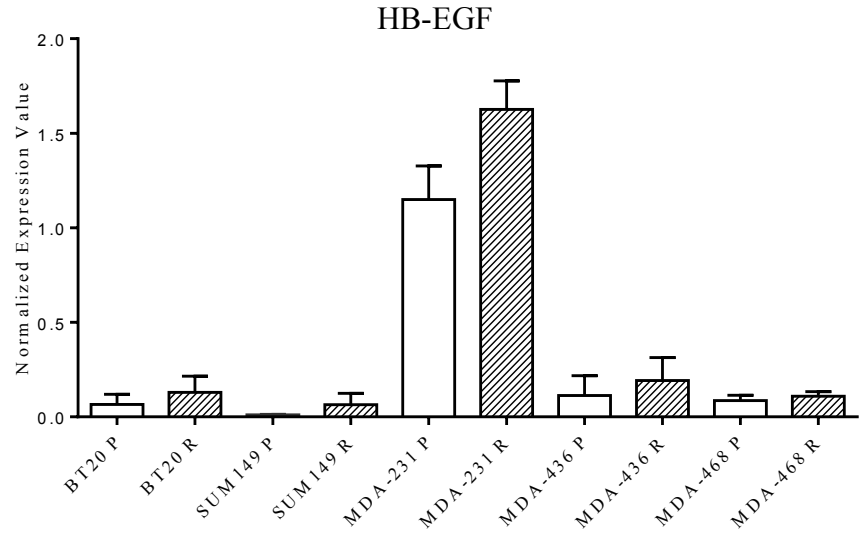

Figure 5.1. qRT-PCR analysis of EGFR ligands. A: AREG, B: EGF, C: EREG, D: BTC and E HB-EGF. The expression values were normalized using HPRT1 gene. Results represent mean values of three independent biological replicates ± SD (experimental error).

5.3. Evaluation of EGFR activity in resistant TNBC cell lines

Considering the up-regulation of EGFR ligands and to investigate the potential mechanisms to confer resistance to PTX, we evaluated the expression of EGFR and downstream signaling pathways in all cell lines (Figure 5.2). EGFR expression was detected in all resistant cell lines and their sensitive counterparts. This expression was more pronounced in BT20 and MDA-MB-468 cell lines. EGFR is highly phosphorylated in MDA-MB-468 parental and resistant cell lines. We did not detect any significant increase in levels of EGFR phosphorylation of resistant cell lines compared to their matching sensitive lines.

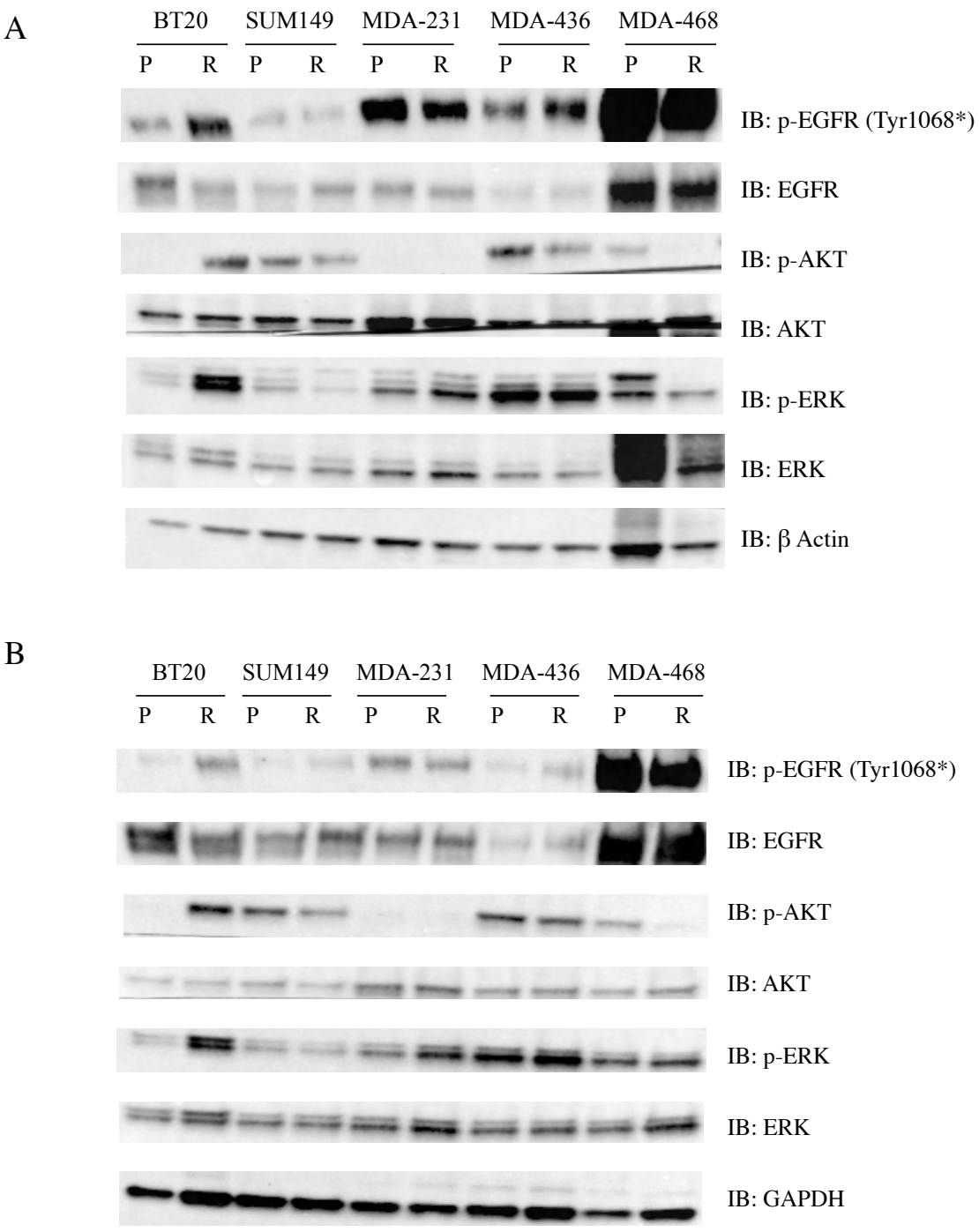

Figure 5.2. Western blot analysis of the expression and activity of EGFR and downstream signaling in resistant cell lines and their sensitive counterparts. Representative of two separate experiments, A: beta actin and B: GAPDH were used as loading control.

5.4. Anti-EGFR therapy re-sensitizes drug resistant TNBC cells to paclitaxel

Given the up-regulation of the RNA expression of EGFR ligands in resistant cell lines, we tested whether blocking the EGFR receptor may overcome PTX resistance. Lapatinib is a reversible dual EGFR and HER2 inhibitor and is currently used in the clinic for the treatment of locally advanced or metastatic breast cancer [181]. We used alamar blue cytotoxicity assay to determine whether lapatinib was able to inhibit the growth of resistant cell lines (Figure 5.3). The result showed that Lapatinib alone did not exert any anti-proliferative activity on resistant cell lines. In addition, parental cells did not show any sensitivity to lapatinib alone.

To elucidate whether lapatinib enhances the cytotoxicity of PTX in resistant cell lines, we tested the cytotoxicity of lapatinib in combination with PTX. Cells were exposed to 100nM lapatinib along with PTX in series of concentration ranging from10 pM to 10 μM. Remarkably, the addition of 100nM of Lapatinib re-sensitized MDA-231R, MDA-436R and MDA-468R cell lines to PTX to significant degrees (Figure 5.4). BT20R cell line was the only cell line that did not show significant sensitivity to cobination of PTX and 100nM lapatinib. It is noteworthy that BT-20 cells carry a PIK3CA mutation, a known factor of resistance to lapatinib [220, 221].

To investigate whether the observed effect is restricted to lapatinib, we tested the sensitivity of the cell lines to another tyrosine kinase inhibitor, neratinib. Neratinib is a pan-ErbB receptor TKI with

activity against epidermal growth factor receptor (EGFR), HER-2, and HER-4. Unlike lapatinib, which is a reversible inhibitor of HER-2 and EGFR, neratinib binds irreversibly to those kinases [222]. Neratinib was tested as single agent and in combination with PTX. Both parental and resistant cell lines were relatively insensitive to neratinib (IC_{50} value > 1 μM) (Figure 5.5). The IC_{50} values for neratinib were lower than those for lapatinib in the resistant cell lines. SUM-149R and MDA-MB-436R cell lines were more resistant to neratinib monotherapy than their parental counterparts while the BT20R, which did not show sensitivity to monotherapy or combination treatment of PTX and lapatinib, displayed sensitivity to neratinib monotherapy. This is particularly interesting since BT20P did not show sensitivity to high concentration of neratinib (10 μM). The combination treatment of PTX and 100nM neratinib was significantly more effective in reducing cell growth compared to neratinib or PTX alone in both resistant cells lines and their sensitive counterparts (Figure 5.6). Interestingly, 100nM neratinib in combination with PTX re-sensitized BT20R cell lines to PTX. It has been shown that, unlike lapatinib, neratinib sensitivity is not associated with PI3K mutation status [188]. This can explain the significant difference observed in sensitivity of BT20R cells to combination of neratinib and PTX compared to lapatinib and PTX. Together, these results suggest that anti-EGFR therapies can re-sensitize PTX-resistant TNBC cells to PTX, providing a viable strategy for overcoming paclitaxel resistance in TNBCs.

Interestingly, in some cases the addition of an anti-EGFR drug also increased the sensitivity of parental cell lines to PTX.

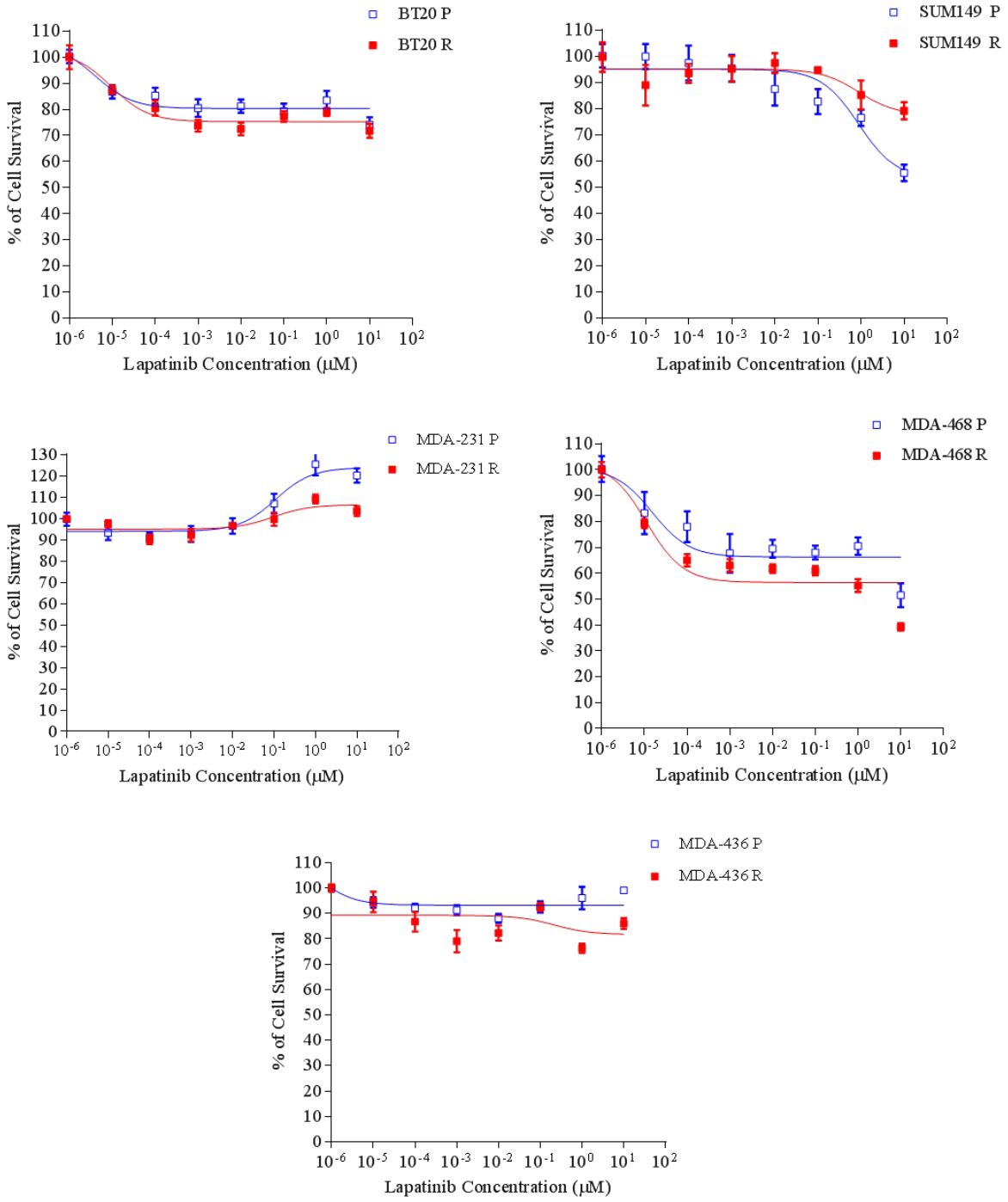

Figure 5.3. Effect of lapatinib on viability of parental and resistant cell lines. Cell viability was measured by alamar blue assay. The data show the mean ± SD (n=3). Cells did not show sensitivity to micro molar concentration of lapatinib.

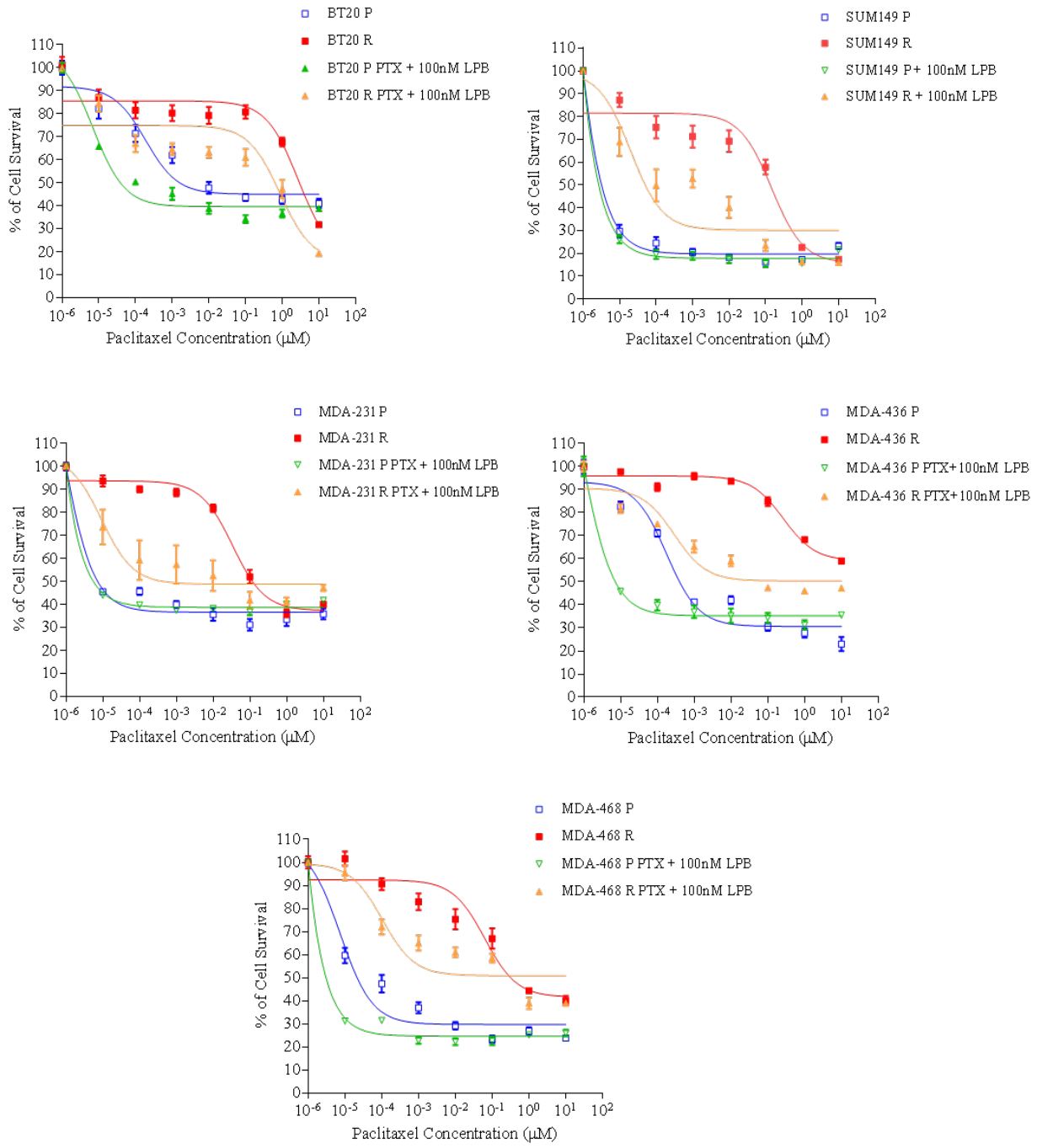

Figure 5.4. Effect of lapatinib and PTX on viability of resistant and parental cell lines. Cells were incubated for 72h with 100nM of lapatinib in combination with increasing concentrations of PTX. Cell viability was measured by alamar blue assay. The data show the mean ± SD (n=3). LPB: lapatinib.

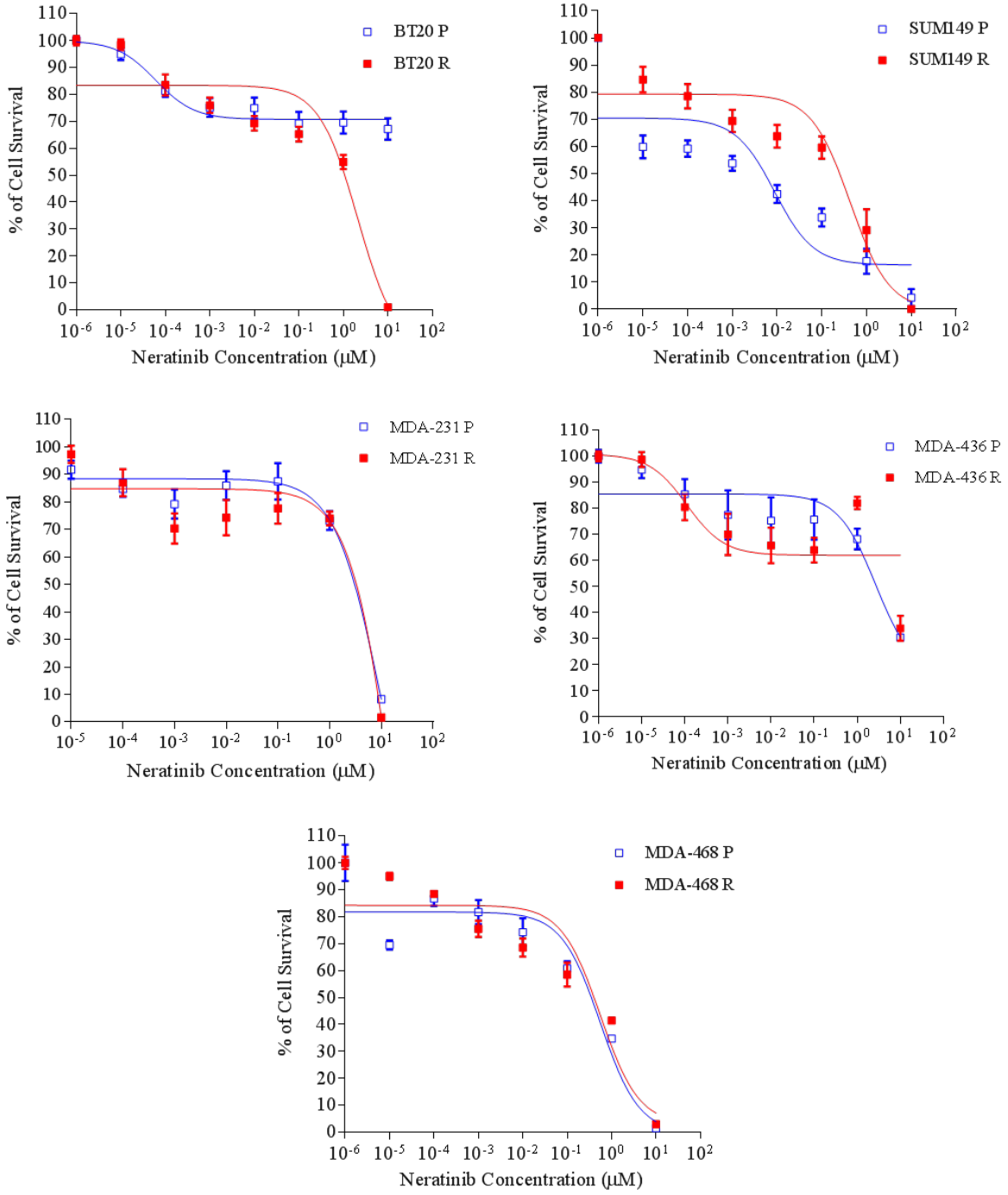

Figure 5.5. Effect of neratinib on viability of parental and resistant cell lines. Cell viability was measured by alamar blue assay. The data show the mean ± SD (n=3). All resistant cell lines showed sensitivity to high concentration of neratinib.

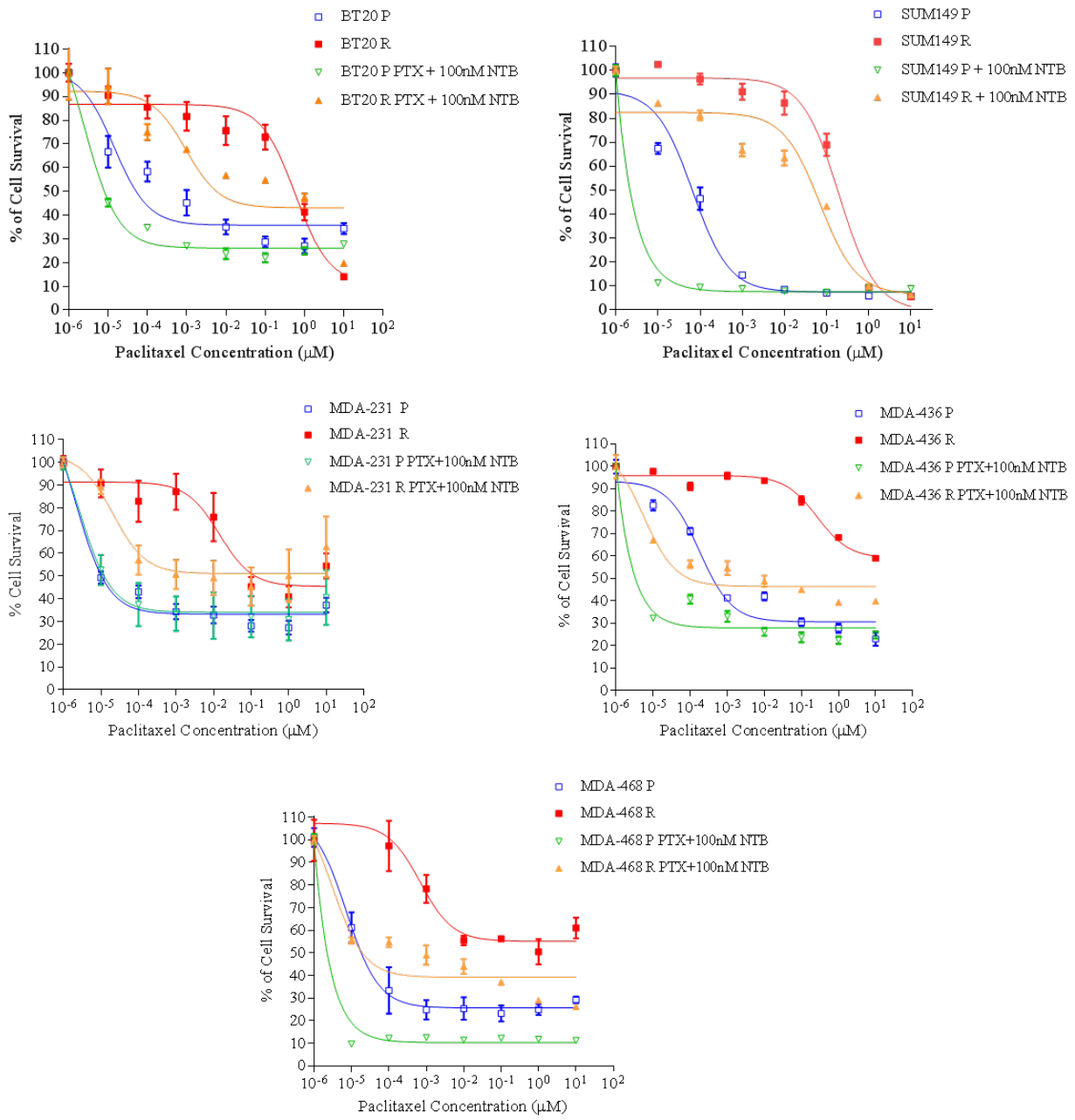

Figure 5.6. Effect of neratinib and PTX on viability of resistant and parental cell lines. Cells were incubated for 72h with 100nM of neratinib in combination with increasing concentrations of PTX. Cell viability was measured by alamar blue assay. The data show the mean ± SD (n=3). NTB: Neratinib.

5.6. Effect of EGFR inhibitors on cell cycle distribution and apoptosis.

It has been shown that lapatinib induces a G0-G1 arrest in HER2 amplified breast cancer cell lines [223]. Having determined the inhibitory effect of lapatinib cell growth in the presence of PTX in the majority of cell lines, we determined the effect of lapatinib on cell cycle distribution in parental and resistant cell lines. The cells were incubated with 100nM lapatinib for 72h and cell cycle distribution were analyzed by flow cytometry (Figure 5.7). No significant modulation of the distribution of cells in the different phases of the cell cycle was observed upon lapatinib treatment.

To better characterize the mechanism of action of lapatinib on resistant cells, we also performed the degree of apoptosis after treatment with lapatinib. Cells were treated with 100nM lapatinib and the percentage of apoptotic cells were compared to non treated cells. Lapatinib did not induce apoptosis in any of the cell lines. To determine the effect of lapatinib in cells treated with PTX, we treated the cells with 100nM lapatinib and 100nM PTX and determined the percentage of apoptotic cells. Again, we did not detect any increase in apoptosis in neither parental or resistant cell lines treated with combination of PTX and lapatinib (Figure 5.8).

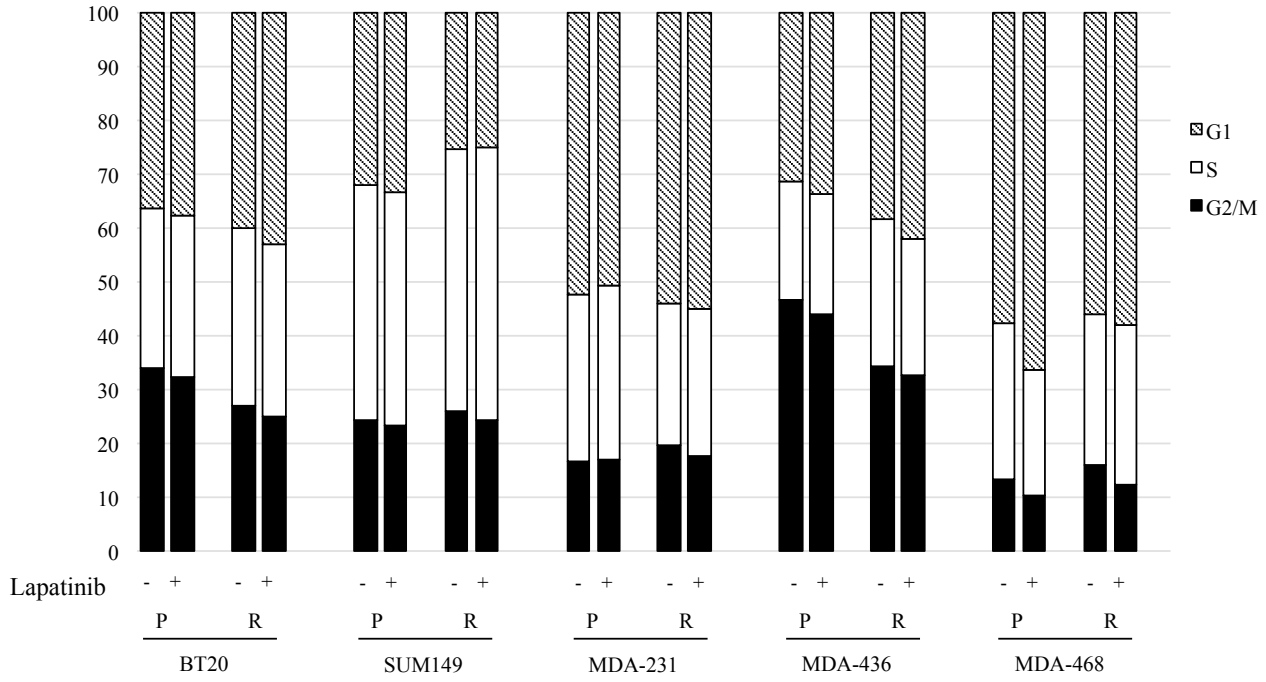

Figure 5.7. Flow cytometry analysis of the effect of lapatinib on cell cycle distribution of resistant cell lines and their sensitive counterparts. Cells were treated with or without 100nM lapatinib and incubated for 72h, stained with propidium iodide and analyzed by flow cytometry. The number of cells in various stages of the cell cycle were quantified measuring the area under each compartments peak and are represented as percentage. Treatment with lapatinib did not have any effect on the cell cycle distribution of the cell lines.

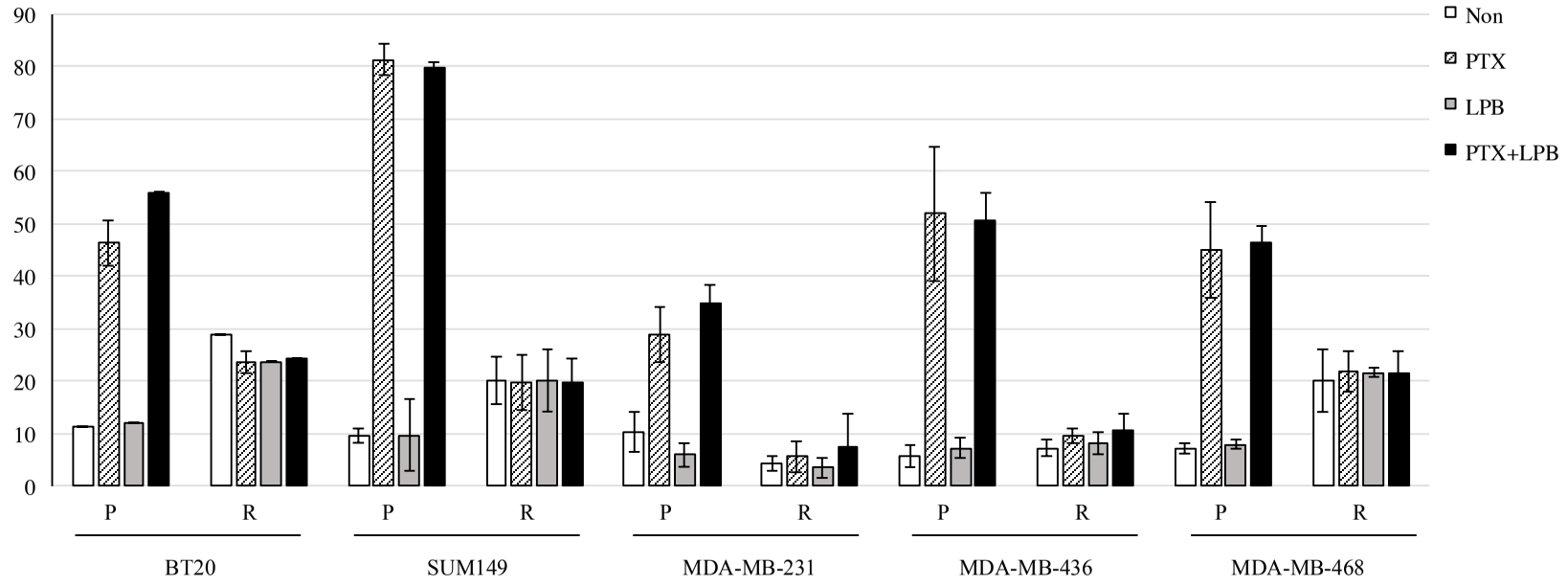

Figure 5.8. Apoptosis analysis of five pairs of resistant cell lines and their matching sensitive cell lines. Cells were treated with 100nM PTX, 100nM lapatinib or combination of 100nM PTX and 100nM lapatinib for 72h and total apoptosis level was

5.7. Effect of EGFR inhibitors on efflux activity and expression of ABCB1

Several studies have shown that tyrosine kinase inhibitors, can significantly attenuate or reverse ABC transporter-mediated drug resistance in cancer cells by binding to their ATP-binding sites [224-227]. Therefore we investigated whether EGFR inhibitors can enhance the efficacy of PTX via interaction with ABCB1 in ABCB1-over expressing resistant cell lines. The efflux activity of ABCB1 is driven by ATP hydrolysis, which is stimulated in the presence of ABCB1 substrates. To assess the effect of EGFR inhibitors on the efflux activity of ABCB1, we measured rhodamine accumulation in resistant cell lines treated with 100nM of either lapatinib or neratinib. Treatment with 100nM of EGFR inhibitors did not reduce the extrusion of rhodamine in BT20R and SUM149R cell lines, suggesting that lapatinib and neratinib did not produce their cytotoxicity effect through inhibition of ABCB1 efflux activity (Figure 5.9). Interestingly, 100nM of EGFR inhibitors increased rhodamine accumulation in MDA-MB-468R cell lines. It is important to note that despite the deletion of 5'UTR in ABCB1 gene, we did not find a fusion partner in ABCB1 in MDA-MB-468R, suggesting that the mechanism of ABCB1 regulation and activation is very complex.

The reversal of ABC transporter-mediated drug resistance can be achieved by either inhibiting of efflux activity or decreasing the expression of the protein. Therefore, we determined the effects of

lapatinib on the expression of ABCB1 protein expression using western blot analyses. Considering the relatively long half-life of ABCB1 (72h), cells were treated with lapatinib , PTX and combination for different time points including 18h and 72h. The results showed a significant decrease in EGFR phosphorylation, however no marked difference in ABCB1 protein expression in BT20R and SUM149R, suggesting that the effect of EGFR inhibitors in combination with PTX on cell growth in BT20R and SUM149R is independent of ABCB1 expression (Figure 5.10). Interestingly, we observed decreased expression of ABCB1 in MDA-MB-468R cells treated with 100nM lapatinib.

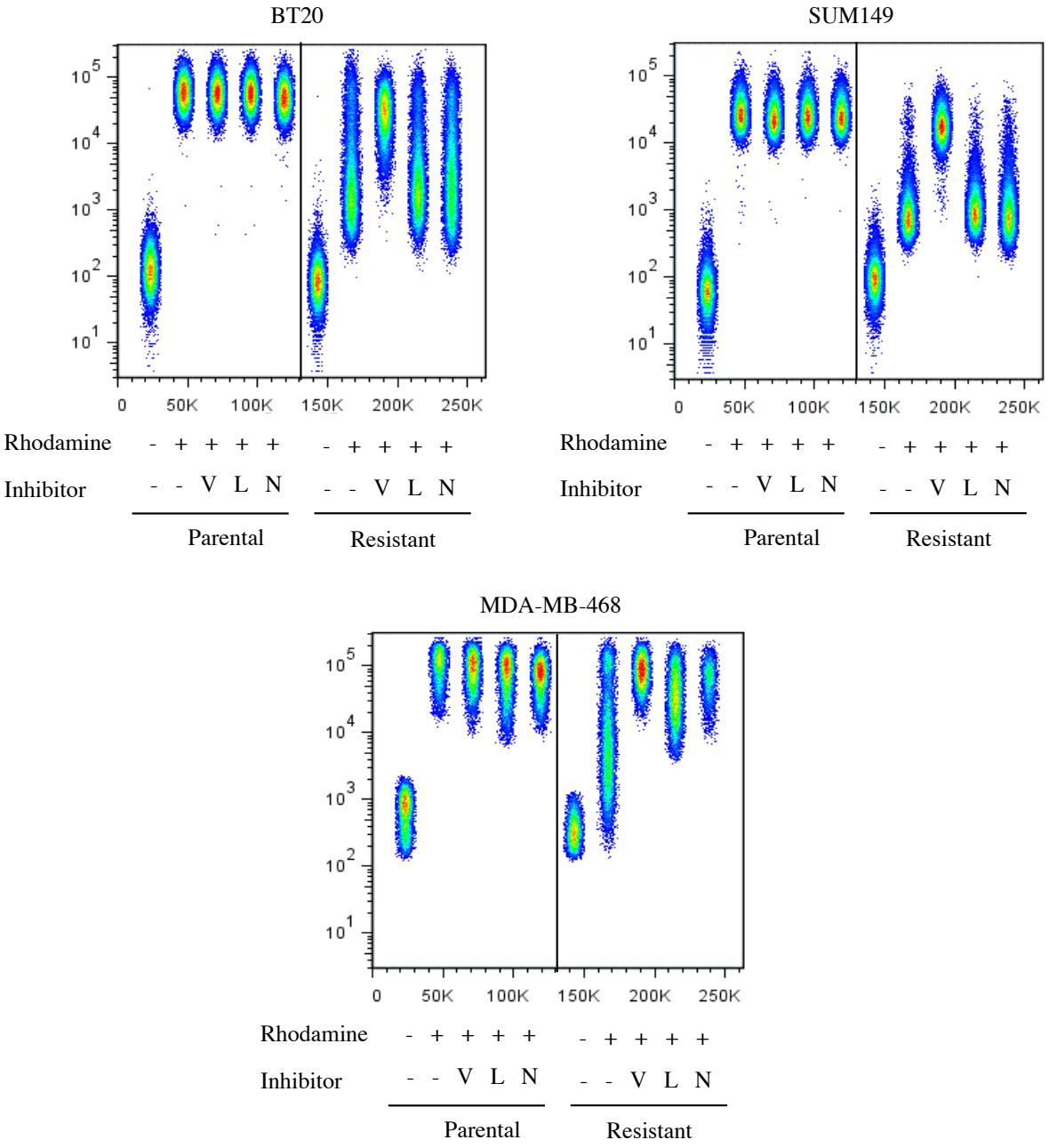

Figure 5.9. Flow cytometry analysis of rhodamine 123 accumulation in ABCB1 over-expressing resistant cell lines and their parental counterparts. The fluorescent intensity of cells treated with or without rhodamine 123 were detected. Rhodamine accumulation was not altered after 30 min incubation of the cells in the presence of 100nM lapatinib or 100nM neratinib.. Verapamil was used as control. V: verapamil, L: lapatinib, N: neratinib

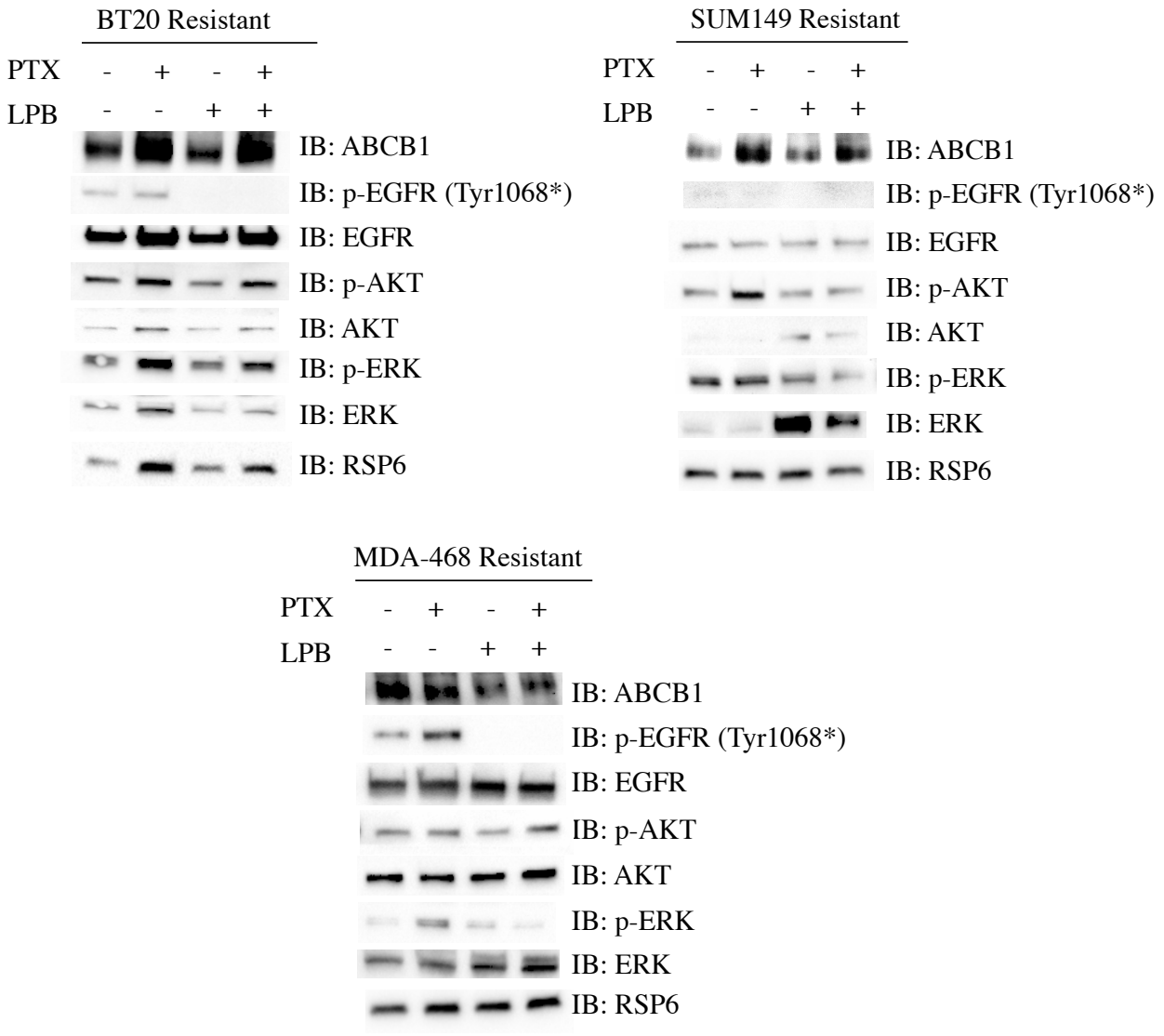

Figure 5.10. The effect of lapatinib on blockade of Akt and Erk phosphorylation and the expression level of ABCB1. A: BT20R, B: SUM149R, C: MDA-MB-468R. Cells were treated with either 100nM lapatinib, 100nM PTX or combination of 100nM lapatinib and 100nM PTX for 18h. 20ng of protein were used for western blot analysis to detect the phosphorylation of EGFR,AKT and ERK and expression of ABCB1. RSP6 were used as loading control. We obtained similar results when cells were treated for 72h.

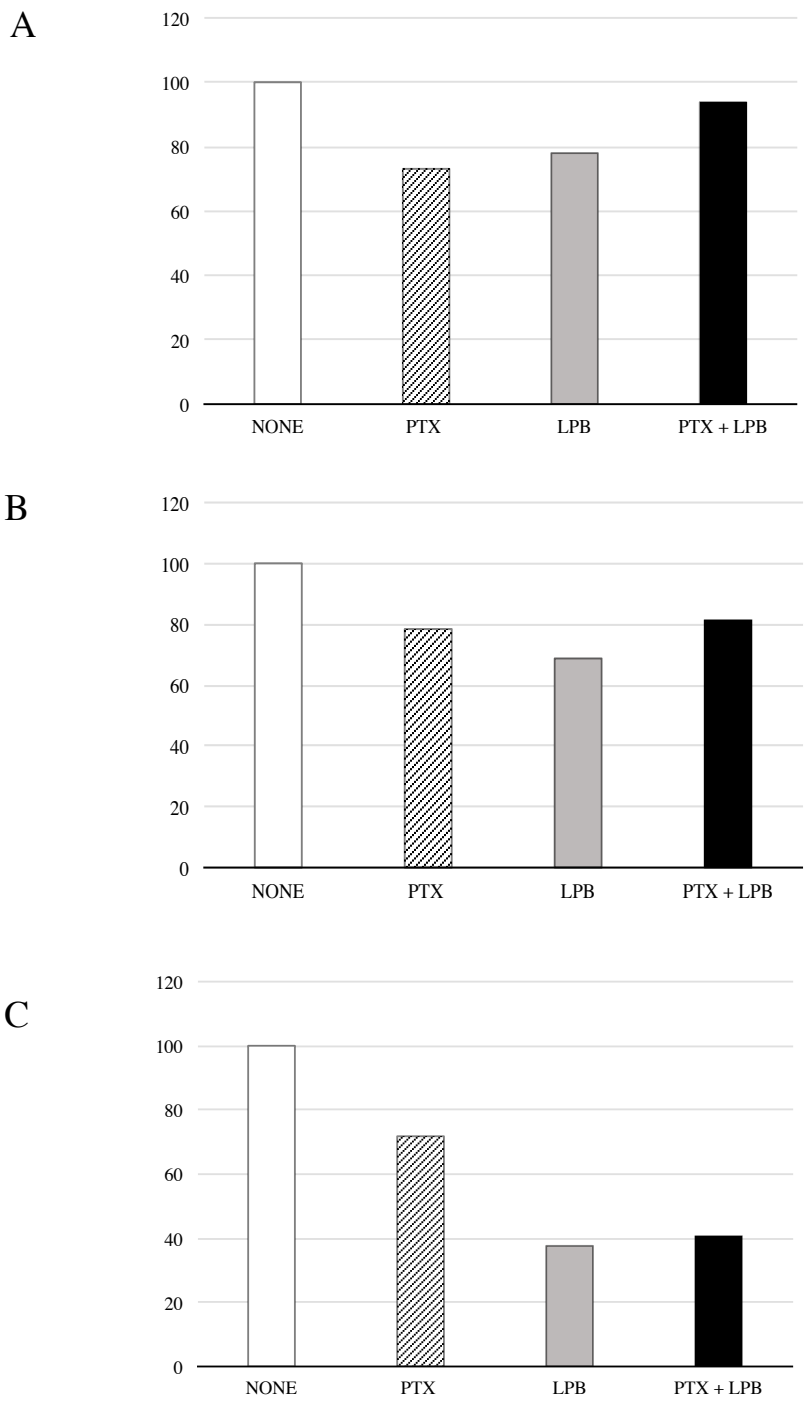

Figure 5.11 The intensity of western blot bands for ABCB1 were quantified by Image lab software (Bio-Rad) and normalized to their respective RSP6. A: BT20R, B:SUM149R, C: MDA-MB-468R

5.8. Summary

The results of pathway analysis performed on differentially expressed genes of each pair revealed enriched molecular function of deregulated genes common in resistant cell line. Of these, the molecular function "growth factor activity" was consistently up-regulated in all 5 resistant cell line models. We noted an overlap of several epidermal growth factor receptor (EGFR) ligands in the "growth factor activity" list, including EGF, AREG, EREG, TGFA, BTC and HBEGF. confirmed by qRT-PCR. We then examined the sensitivity of all five cell line models to two EGFR inhibitors, lapatinib, a dual EGFR and HER2 inhibitor and neratinib, a "pan-HER" inhibitor of EGFR, HER2 and HER3. Unlike lapatinib, neratinib alone showed some growth inhibitory efficacy in most of the cell lines. SUM-149R and MDA-MB-436R cell lines were more resistant to neratinib than their parental counterparts while the BT20R cell line was more sensitive to the drug alone than its sensitive counterpart. These results suggest that acquired resistance to PTX may be accompanied in part by alterations in signaling pathway downstream of EGFR and HER3.

Although over-expression of EGFR can be important as potential target, the ultimate value of inhibition of this pathway may lie in the combined use of EGFR inhibitors with cytotoxic drugs or radiation. Dixit et al. reported that reduced expression of EGFR is associated with increased

resistance to cisplatin in MDA-MB-468 human breast cancer cells [228]. These results seems to conflict with the clinical data and the data obtained by other groups showing that antitumour activity of cisplatin, doxorubicin or paclitaxel were enhanced when administered concomitantly with monoclonal antibody targeting EGFR [229, 230]. Gefitinib enhances taxane activity in bcl-2 overexpressing MCF-7 ADR human breast cancer cell line [231]. A similar contradiction was shown when cancer cells are treated with EGF. Activation of the EGFR signaling pathway, induced by EGF treatment of an ovarian cancer cell line, COLO 316, was reported to enhance their sensitivity to several chemotherapeutic agents. This sensitization was found to be independent of the mitogenic or anti-mitogenic effects of EGF on cell proliferation [232-234]. In contrast, EGF treatment reduced sensitivity to cisplatin in HEY ovarian cancer cell line [235].

Our results revealed that the addition of 100nM of neratinib partially re-sensitized BT-20R, MDA-231R, MDA-436R and MDA-468R cell lines to PTX to various degrees. We observed a similar outcome with lapatinib in combination with PTX, with one difference. BT20R did not show sensitivity to the addition of 100nM lapatinib to increasing concentration of PTX. It is noteworthy that BT-20 cells carry a PIK3CA mutation, a known factor of resistance to lapatinib [220, 221]. These results suggest that anti-EGFR therapies can re-sensitize PTX-resistant TNBC cells to PTX.

The mechanism whereby tyrosine kinase inhibitors enhance the activity of cytotoxic drugs is complex and incompletely understood. Previous studies have shown that lapatinib and neratinib increased rhodamine accumulation in ABCB1-overexpressing cell lines [225, 227]. Contrary to these results, lapatinib or neratinib did not reduce the expression or the efflux activity of ABCB1 in BT20R and SUM149R, suggesting that the effect of neratinib on these cells is independent of efflux activity of ABCB1. Interestingly, we observed decreased expression as well as decreased efflux activity of ABCB1 in MDA-MB-468R cells treated with 100nM lapatinib. Considering the long half-life of the disappearance of ABCB1 (ranges between 15–72 h) [236], the effect of lapatinib on efflux activity in this cell line is likely independent of the decreased expression of ABCB1 since the rhodamine accumulation was measured after one-hour treatment with lapatinib. Therefore, the increased toxicity of PTX in combination with lapatinib can be the result of both effects.

Chapter 6

Conclusions

6.1. Conclusions

The development of resistance to chemotherapeutic agents is the major obstacle to the successful treatment of TNBC patients since it abrogates the response to chemotherapy. The resistance could be acquired through clonal selection of pre-existing resistant cells present at low allelic frequencies, which grow out through the pressure of drug, or development of new genetic events acquired during the course of therapy. The onset of resistance in cancer patients, observed after several months of treatment in most patients, is complex and often not limited to a single genetic alteration. *In vitro* studies on cell lines with acquired resistance provide an important resource, which enable us to better understand and characterize the biological mechanisms of resistance. For this study, we tested seven TNBC cancer cell lines, which were inherently different in their sensitivity to PTX. Such variability may be due to the different treatment regimes that the patients received before surgery and also to the different genetic origin of the cell lines. However, the majority of cell lines used in this study were obtained from primary or metastatic tumours from patients who had received no PTX treatment prior to resection. In fact, they were generated before the FDA approval of PTX. To mimic the condition cancer patients experience during chemotherapy, we generated *in vitro* models of resistance by culturing TNBC cell lines in stepwise increasing concentrations of the drug and thereby selecting for resistant clones. Five

PTX-resistant TNBC cell lines (BT20R, SUM149R, MA-MB-231R, MDA-MB-436R and MDA-MB-468R) were generated by exposing the cells to increasing concentration of PTX.

Although the concentration of PTX in actual breast tumours is not known, it has been shown that a concentration of 5 to 10μM in plasma is achievable after bolus infusion of paclitaxel [237]. Therefore, activity that requires paclitaxel doses higher than 10μM may not be clinically significant. In fact, different concentrations of PTX exerts different effects on cells. Low concentrations of paclitaxel (encompassing 3 to 6 nM) induce a slight inhibition of cell growth and G1/G2 arrest but they do not induce sustained mitotic arrest; clinically relevant concentrations of 5 to 200 nM (also called standard concentration) produce mitotic arrest and cell death; high concentrations, encompassing 3 to 100μM range, induce immediate effects which are not associated with mitotic block, including lipopolysaccharide (LPS)-like activity and tumour necrosis factor (TNF)-like effects [238]. We used 100nM PTX (in the range of standard concentration) in all the experiments performed in this study. We determined the effect of 100nM PTX on cell cycle distribution of parental and resistant cell lines. PTX induced G2/M block in all parental cell lines, but had no such effect in resistant cell lines.

It is generally believed that PTX exerts its anti-tumour effects mainly through interference with the normal function of microtubules, thus preventing mitotic spindle formation, which results in

induction of apoptosis. Paclitaxel-induced apoptosis is p53-independent and lack of wild type p53 does not confer resistance to paclitaxel [239, 240]. It is particularly important because P53 is the most frequently mutated gene in TNBC tumours [30] and all the cells lines used in this study carry P53 mutations. Previous studies have shown that in addition to the induction of apoptosis as a result of mitotic perturbation, paclitaxel can also induce inter-nucleosomal DNA fragmentation and the typical morphological features of apoptosis in a number of tumour cell lines, indicating that paclitaxel also possesses cell-killing activity by direct induction of apoptosis [241]. We showed that PTX-induced apoptosis in resistant cell lines is significantly reduced compared to their sensitive counterparts.

Comparative data analysis of gene expression profiling of resistant cell lines and their sensitive counterparts revealed that on average only 6% of the genes surveyed by microarray analysis showed changes in expression by 2-fold or greater. The PCA analysis revealed a clustering of each of resistant cell lines with their sensitive counterparts**,** suggesting that there are only a small number of genes for which the expression is changed significantly during development of resistance. Although the profiles of gene expression changes were different in the resistant cell lines, we identified a total of 13 genes that were commonly up-regulated and 3 genes that were recurrently down-regulated in 4 of resistant cell lines compared to parental cells, suggesting a

possible common mechanism of resistance in PTX-resistant cell lines.

Using array CGH, we identified regions with significant DNA copy number changes and recurrent chromosomal alterations in resistant cell lines. Our analysis showed that the majority of alterations acquired in MDA-MB-231R and MDA-MB-436R involve entire chromosome arms or extended chromosomal segments whereas BT20R, SUM149R, and MDA-MB-468R exhibit higher number of focal aberrations. This is consistent with characteristics of different subtypes of TNBC introduced by Lehmann et al. in which cell lines that fall into BL1 and BL2 (BT20R, SUM149R, and MDA-MB-468R) subtypes show more genomic instability, displaying significantly more chromosomal rearrangements than M and MSL subtype cell lines such as MDA-MB-231R and MDA-MB-436R.

Genomic copy number alteration can be a random event underlying genomic instability. However, functional amplification which results in increased expression of amplified genes can equip the cancer cells with new molecular machinery that benefits their survival and progression during chemotherapy treatment. As a result, the clone with beneficial functional amplifications expands and ultimately dominates the tumour cell population. Our integrative analysis of aCGH and gene expression revealed deregulated genes whose expression is correlated with their copy number alterations. Although we found a generally positive correlation between ΔCNA and differential

gene expression, our analysis showed a high degree of association between high-level ΔCNA and differential gene expression in resistant cell lines. These results are consistent with previously reported associations of gene copy number with gene expression [205-207]. Our integrative analysis showed that on average more than 20% of high-level ΔCNAs showed positive correction with gene expression. It is important to note that unlike previous studies, which mainly focused on correlation of copy number changes with gene expression, we investigated the differential copy number alterations in resistant cell lines its correlation with differential gene expression. Our finding suggests that the functional CNAs acquired in resistant cell lines may enable the survival of resistant cells in the presence of high concentrations of PTX.

Although both amplifications and deletions can affect gene function, the gain-of-function amplifications make them ideal targets for the development of biomarkers and strategies to overcome resistance. Our integrative analysis of gene expression and array CGH showed that the most highly up-regulated gene in all resistant cell lines, ABCB1, was accompanied by high-level amplification in three resistant cell lines: BT20R, SUM149R and MDA-468. The ABCB1 gene amplification has been previously reported in multidrug resistant cell lines including breast cancer cell line (MCF7) [148, 149], ovarian cancer cell lines [150], lung cancer cell line (NCI-H460) [151, 152], osteosarcoma [153], colon carcinoma cell line (SW620) [154], leukemia [155, 156],

hepatocellular carcinoma cell line (HKCI) [157], neuroblastoma [158], and esophageal cancer [159]. The amplification of 7q21~q22 has been reported in leukemic patients [162]. The evaluation of protein expression of ABCB1 showed up-regulation in BT20R, SUM149R and MDA-468R but not in MDA_MB-231R and MDA-MB-436R, suggesting that changes in ABCB1 copy number may be required for ABCB1 gene over-expression in TNBC resistant cell lines. Interestingly both MDA-MB-231R and MDA-MB-436R belong to MSL subtype of TNBCs. Suggesting that the mechanisms of resistance acquired during development of resistance may be subtype dependent, as is the degree of genomic instability, as reported by Lehmann et al. To our knowledge, we are the first to report an ABCB1 amplification selected for in TNBC cell lines.

Array CGH analysis of 7q21.12 in BT20R, SUM149R and MDA-468R revealed similar, but not identical, breakpoints in the 5'UTR of ABCB1. These breakpoints, accompanied by focal amplifications, highlight the potential for the occurrence of genomic rearrangement events in ABCB1 in PTX resistant cells. Despite the diversity of the fusion partners, most of the cell lines shared a similar pattern of chromosomal rearrangement. In fact, we identified inter-chromosomal translocations in 5'UTR of ABCB1 in BT20R and SUM149R cell lines. It has been suggested before that chromosomal rearrangements leads to "capture" ABCB1 by a, random, constitutively active promoter resulting in aberrant activation of the gene [152]. Interestingly, ABCB1 genomic rearrangement in MDA-468R did not lead to formation of a hybrid mRNA. In addition, the

ABCB1 gene fusion partners identified in this study do not contain strong promoters, suggesting that ABCB1 gene activation is more complex.

Previous reports have shown that 5' UTR of the ABCB1 mRNA is highly structured [211]. Secondary structure of mRNA function as major regulatory tools and has an inhibitory effect on mRNA translation initiation. mRNAs with a highly structured 5 UTR like proto-oncogenes and growth factors use cap-dependent translation initiation and are poorly translated under normal conditions. It has been suggested that the overexpression of components of cap-dependent translation initiation machinery including elf4E can be indicators of tumour progression and poor prognosis in patients with colon, prostate and melanoma cancer [242, 243]. Here we showed that the deletion of the 5'UTR of ABCB1 in BT20R, SUM149R and MDA-MB-468R cells may render these cells independent of eIF4E regulation of ABCB1 translation. In addition, we showed that an increase in the ratio of eIF4E/ 4EBP by either loss of 4E-BP1 or overexpression of eIF4E in cell lines without genomic rearrangements but high expression of ABCB1 transcripts (MDA-MB-231 and MDA-MB-436) can overcome the eIF4E translation block. These findings suggest that the elimination of the 5' end of the ABCB1 gene by a genomic rearrangement or deletion may be necessary for ABCB1 protein overexpression in drug resistant TNBC cells. Also, these finding are particularly important as they can explain the discrepancies observed between mRNA expression of ABCB1 in patients and lack of response to ABCB1 inhibitors. A careful selection of patients

where not only ABCB1 transcript is expressed but also the ABCB1 protein is detectable is critical for positive outcomes, as those deriving benefit from ABCB1 inhibitors may be obscured in trials failing to identify the appropriate target population.

Gene expression profiling can provide important clues of pathways involved in resistance to PTX in TNBC resistant cell lines and help to better understand the biological significance of the observed changes. We used the differentially expressed genes of each pair and performed pathway analysis. The only enriched molecular function of up-regulated genes common to all 5 cell line models was that of "growth factor activity". Interestingly, several EGFR ligands were up-regulated in the "growth factor activity" list. Activation of the EGFR by its ligands stimulates the receptor hetero or homodimerization, which leads to activation of complex intracellular signaling pathways, including RAS-RAF-MAPK and PI3K-PTEN/PTEN/AKT. At the cellular level, the ligands not only induce cell proliferation but also alter adhesion and motility and protect against apoptosis; at the physiological level, the ligands promote invasion and angiogenesis. Though EGFR expression is found in all subtypes of breast cancer, it is more frequently overexpressed in TNBC. Over-expression of EGFR is associated with large tumour size, poor differentiation and [16, 25, 178] and observed to be an independent predictor of poor prognosis in TNBC but not in other subtypes of breast cancer [244, 245]. Over-expression of EGFR in TNBC and the lack of a targeted therapy, together with the availability of a number of approved EGFR inhibitors, provide

a rationale for the study of these agents in TNBC. Several therapies targeting EGFR, including gefitinib, cetuximab, lapatinib, and others, have been developed and tested in clinical trials [246]. However, results of clinical studies of EGFR-targeted therapy in breast cancer have been disappointing [247]. Phase II studies showed very little benefit from gefitinib monotherapy in hormone resistant breast tumours [247, 248]. Unfortunately, results for lapatinib were as disappointing by showing very little clinical benefit, except in HER2-positive tumours [249].

Several predictive biomarker of sensitivity/resistance to anti-EGFR therapy has been proposed, including overexpression and activation of alternative tyrosine kinase receptors that bypass the EGFR pathway, constitutive activation of downstream mediators (e.g. PTEN, KRAS, and others), and the existence of mutations in kinase domain of EGFR and KRAS mutation [250, 251]. Several studies have pointed that EGFR ligands play an important role in response to EGFR inhibitors. Overexpression of NRG1, an EGFR ligand, which could activate the EGFR pathway, increased the sensitivity of MCF7 cells to doxorubicin and this increased sensitivity was accompanied by increase expression of topoisomerase II [252]. Patients with high levels of mRNA for the EREG and AREG, show better respond to an EGFR inhibitor, cetuximab [253]. Therefore, the high expression of EGFR ligand may be a biomarker of sensitivity to EGFR inhibitors as it indicates that the EGFR system may contribute to tumour growth or progression [253].

We showed that the addition of 100nM of neratinib partially re-sensitized BT20R, MDA-231R, MDA-436R and MDA-468R cell lines to PTX to various degrees. We observed similar effects with lapatinib in combination with PTX, with one difference: BT20R did not show sensitivity to the addition of 100nM lapatinib to increasing concentration of PTX. It is noteworthy that BT20 cells carry a PIK3CA mutation, a known factor of resistance to lapatinib [220, 221]. These results suggest that anti-EGFR therapies can re-sensitize PTX-resistant TNBC cells to PTX. The mechanism whereby tyrosine kinase inhibitors enhance the activity of cytotoxic drugs is complex and incompletely understood. Previous studies have shown that although lapatinib and neratinib do not decrease the expression of ABCB1 transcript or protein, they both decrease the efflux activity of ABCB1 [225, 227]. Contrary to these results, neither lapatinib nor neratinib reduced the efflux activity of ABCB1 in BT20R and SUM149R cell lines, suggesting that the effect of these EGFR inhibitors on PTX-resistant cell lines is independent of the efflux activity of ABCB1. However, we found that treatment with 100nM lapatinib increased rhodamine accumulation in MDA-MB-468R: western blot analysis showed ABCB1 protein down-regulation with 18h lapatinib treatment. This observation can be explained by the effect of lapatinib on the ABCB1 proximal promoter: the ABCB1 gene in MDA-MB-468R is truncated through a loss of the first exon, first intron, and part of the second exon; however, the gene retains the part of second exon sequencing the proximal promoter, thereby preserving protein translation. A similar

rearrangement was observed in one of the alleles of ABCB1 in SUM149R, which can explain the slight down-regulation of ABCB1 protein when treated with 100nM lapatinib.

The resistant cell lines generated in this study were not derived from an isolated single cell, and each resistant cell line is a collection of PTX-resistant clones that were pooled prior to analysis, rather than an isolated single clone. Considering the high degree of genomic instability in TNBCs, it is conceivable that established cell lines consist of molecularly and genetically heterogeneous sub-populations that employ different mechanisms to attain drug resistance. It is likely that additional mechanisms of tyrosine kinase inhibition enhancing the activity of cytotoxic drugs are involved.

We showed that lapatinib and neratinib partially inhibited cell proliferation of MDA-MB-231R and MDA-MB-436R when combined with PTX. However, there was no increase in apoptosis in MDA-MB-231 or MDA-MB-436R cells treated with either a single agent or lapatinib in combination with PTX. A similar effect was observed for BT20R, SUM149R and MDA-MB-468R. These results suggest that other inhibition mechanisms may play a role in the observed inhibitory effects induced by the combined treatment.

In this study we demonstrated that lapatinib and neratinib can partially re-sensitize PTX-resistant TNBC cell lines in an ABCB1-independent manner. We also found that ABCB1 gene

rearrangement can serve as a biomarker of PTX resistance in TNBC cell lines. These findings may be useful for individualized therapy and for cancer combination therapy with tyrosine kinase inhibitors.

Chapter 7

Future Directions

7.1 Future directions

Our comparative analysis of gene expression results of all parental and resistant cell lines identified a total of 86 genes that were up-regulated (> 2 fold) in at least 3 of resistant cell lines compared to parental cells. We identified up-regulation of RASGRP2, IGF2, RTP4, CLDN1, CTHRC1, INHBA, TRIM29, IFI27 gene. In addition, genes in SERPINB family, including SERPINB3, SERPINB4 and SERPINB5 showed increased in transcript level in several resistant cell lines. Interestingly, SERPINB5 encode for genes known to be involved in resistance to cytotoxic chemotherapy. It would be interesting to further investigate the role of these genes in resistance to PTX.

Also, our preliminary data showed increased expression of IL-6 transcript and protein in several of resistant cell lines. This up-regulation was also observed in clinical sample. The role of IL-6 in chemo-resistance have been previously studied [254]. The in vitro model of acquired resistance generated in this study, can provide a useful tool to study the mechanisms by which IL-6 confer resistance to chemotherapy.

Our analysis also revealed genes that were commonly down regulated in resistant cell lines, including SPDEF, down-regulated in BT20R, MDA-MB-231R, MDA-MB-468R and SUM149R, UGT1A6 and CFI, that showed down-regulation in BT20R, MDA-MB-436R, MDA-MB-468R

and SUM149R. The fact that some of the identified deregulated genes are common between ABCB1-overexpressing cells and non-ABCB1 over-expressing cells, makes these genes more interesting for further analysis. Further studies could investigate the mechanism of over/underexpression of these genes, which may be unrelated to its presence in an amplified or deleted region, but could potentially be due chromosome rearrangements placing the genes under the control of a different promoter, or near an amplified enhancer.

The increased sensitivity obtained by addition of tyrosine kinase inhibitors to PTX treatment can be further investigated. Further studies could:

1. Determine the effect of PTX, lapatinib and neratinib on gene expression profiling of resistant and parental cell lines to better understand the underlying mechanism of sensitivity of the combination therapy.
2. Perform protein analysis using western blotting on non-ABCB1 expressing cells treated with PTX, lapatinib and neratinib to determine the downstream effect of these tyrosine kinase inhibitors on signaling pathways in the resistant cell lines.
3. Determine the role of EGFR ligands by silencing the gene in resistant cell lines and overexpressing the ligands in the matching parental cells to see whether altering expression of the ligands confer the sensitivity of the cells to PTX.

The *in vitro* model of drug resistance is widely used to study the mechanisms underlying resistance and to test hypotheses to improve the efficacy of treatment. However, results obtained from in vitro analysis need to be further investigated using mouse models and the relevance of the findings in clinical samples needs to be validated.

References

1. Hanahan, D. and R.A. Weinberg, *Hallmarks of cancer: the next generation.* Cell, 2011. 144(5): p. 646-74.
2. Hanahan, D. and R.A. Weinberg, *The hallmarks of cancer.* Cell, 2000. 100(1): p. 57-70.
3. Jesinger, R.A., *Breast anatomy for the interventionalist.* Techniques in vascular and interventional radiology, 2014. 17(1): p. 3-9.
4. Bertos, N.R. and M. Park, *Breast cancer - one term, many entities?* J Clin Invest, 2011. 121(10): p. 3789-96.
5. Gudjonsson, T., et al., *Normal and tumour-derived myoepithelial cells differ in their ability to interact with luminal breast epithelial cells for polarity and basement membrane deposition.* Journal of cell science, 2002. 115(Pt 1): p. 39-50.
6. Sopel, M., *The myoepithelial cell: its role in normal mammary glands and breast cancer.* Folia Morphol (Warsz), 2010. 69(1): p. 1-14.
7. Jemal, A., et al., *Global cancer statistics.* CA Cancer J Clin, 2011. 61(2): p. 69-90.
8. de la Cruz, M.S., M. Sarfaty, and R.C. Wender, *An update on breast cancer screening and prevention.* Prim Care, 2014. 41(2): p. 283-306.
9. Terese Winslow. Available from: http://www.teresewinslow.com/portshow.asp?nxt=1&sid=3CF86AAE-34B9-4DF1-9A0E-F16C90F28454&portfolioid={4B56C61F-9C24-47C6-9F4D-9444E1D75BA2}.
10. Viale, G., *The current state of breast cancer classification.* Ann Oncol, 2012. 23 Suppl 10: p. x207-10.
11. Shah, S.S., et al., *Impact of American Society of Clinical Oncology/College of American Pathologists guideline recommendations on HER2 interpretation in breast cancer.* Hum Pathol, 2010. 41(1): p. 103-6.
12. Perou, C.M., et al., *Molecular portraits of human breast tumours.* Nature, 2000. 406(6797): p. 747-52.
13. Perou, C.M., *Molecular stratification of triple-negative breast cancers.* Oncologist, 2011. 16 Suppl 1: p. 61-70.
14. Perou, C.M., *Molecular stratification of triple-negative breast cancers.* Oncologist, 2010. 15 Suppl 5: p. 39-48.
15. Lu, S., et al., *Analysis of integrin beta4 expression in human breast cancer: association with basal-like tumours and prognostic significance.* Clin Cancer Res, 2008. 14(4): p. 1050-8.
16. Siziopikou, K.P. and M. Cobleigh, *The basal subtype of breast carcinomas may represent*

the group of breast tumours that could benefit from EGFR-targeted therapies. Breast, 2007. 16(1): p. 104-7.

17. Charafe-Jauffret, E., et al., *Gene expression profiling of breast cell lines identifies potential new basal markers.* Oncogene, 2006. 25(15): p. 2273-84.
18. Nielsen, T.O., et al., *Immunohistochemical and clinical characterization of the basal-like subtype of invasive breast carcinoma.* Clin Cancer Res, 2004. 10(16): p. 5367-74.
19. Weigelt, B., et al., *Breast cancer molecular profiling with single sample predictors: a retrospective analysis.* The Lancet. Oncology, 2010. 11(4): p. 339-49.
20. Neve, R.M., et al., *A collection of breast cancer cell lines for the study of functionally distinct cancer subtypes.* Cancer Cell, 2006. 10(6): p. 515-27.
21. Livasy, C.A., et al., *Phenotypic evaluation of the basal-like subtype of invasive breast carcinoma.* Mod Pathol, 2006. 19(2): p. 264-71.
22. Dent, R., et al., *Triple-negative breast cancer: clinical features and patterns of recurrence.* Clin Cancer Res, 2007. 13(15 Pt 1): p. 4429-34.
23. Morris, G.J., et al., *Differences in breast carcinoma characteristics in newly diagnosed African-American and Caucasian patients: a single-institution compilation compared with the National Cancer Institute's Surveillance, Epidemiology, and End Results database.* Cancer, 2007. 110(4): p. 876-84.
24. Badve, S., et al., *Basal-like and triple-negative breast cancers: a critical review with an emphasis on the implications for pathologists and oncologists.* Mod Pathol, 2011. 24(2): p. 157-67.
25. de Ruijter, T.C., et al., *Characteristics of triple-negative breast cancer.* J Cancer Res Clin Oncol, 2011. 137(2): p. 183-92.
26. Tischkowitz, M., et al., *Use of immunohistochemical markers can refine prognosis in triple negative breast cancer.* BMC Cancer, 2007. 7: p. 134.
27. Holstege, H., et al., *High incidence of protein-truncating TP53 mutations in BRCA1-related breast cancer.* Cancer Res, 2009. 69(8): p. 3625-33.
28. Cancer Genome Atlas, N., *Comprehensive molecular portraits of human breast tumours.* Nature, 2012. 490(7418): p. 61-70.
29. Weigman, V.J., et al., *Basal-like Breast cancer DNA copy number losses identify genes involved in genomic instability, response to therapy, and patient survival.* Breast Cancer Res Treat, 2012. 133(3): p. 865-80.
30. Shah, S.P., et al., *The clonal and mutational evolution spectrum of primary triple-negative breast cancers.* Nature, 2012. 486(7403): p. 395-9.
31. Kwei, K.A., et al., *Genomic instability in breast cancer: pathogenesis and clinical implications.* Molecular oncology, 2010. 4(3): p. 255-66.

32. Fulford, L.G., et al., *Specific morphological features predictive for the basal phenotype in grade 3 invasive ductal carcinoma of breast.* Histopathology, 2006. 49(1): p. 22-34.
33. Gralow, J.R., et al., *Preoperative therapy in invasive breast cancer: pathologic assessment and systemic therapy issues in operable disease.* J Clin Oncol, 2008. 26(5): p. 814-9.
34. Lehmann, B.D., et al., *Identification of human triple-negative breast cancer subtypes and preclinical models for selection of targeted therapies.* J Clin Invest, 2011. 121(7): p. 2750-67.
35. Lehmann, B.D. and J.A. Pietenpol, *Identification and use of biomarkers in treatment strategies for triple-negative breast cancer subtypes.* J Pathol, 2014. 232(2): p. 142-50.
36. Carey, L.A., et al., *The triple negative paradox: primary tumour chemosensitivity of breast cancer subtypes.* Clin Cancer Res, 2007. 13(8): p. 2329-34.
37. Rouzier, R., et al., *Breast cancer molecular subtypes respond differently to preoperative chemotherapy.* Clin Cancer Res, 2005. 11(16): p. 5678-85.
38. Keam, B., et al., *Ki-67 can be used for further classification of triple negative breast cancer into two subtypes with different response and prognosis.* Breast cancer research : BCR, 2011. 13(2): p. R22.
39. Isakoff, S.J., *Triple-negative breast cancer: role of specific chemotherapy agents.* Cancer J, 2010. 16(1): p. 53-61.
40. Liedtke, C., et al., *Response to neoadjuvant therapy and long-term survival in patients with triple-negative breast cancer.* J Clin Oncol, 2008. 26(8): p. 1275-81.
41. Huober, J., et al., *Effect of neoadjuvant anthracycline-taxane-based chemotherapy in different biological breast cancer phenotypes: overall results from the GeparTrio study.* Breast Cancer Res Treat, 2010. 124(1): p. 133-40.
42. Schmadeka, R., B.E. Harmon, and M. Singh, *Triple-negative breast carcinoma: current and emerging concepts.* Am J Clin Pathol, 2014. 141(4): p. 462-77.
43. Amos, K.D., B. Adamo, and C.K. Anders, *Triple-negative breast cancer: an update on neoadjuvant clinical trials.* Int J Breast Cancer, 2012. 2012: p. 385978.
44. Byrski, T., et al., *Pathologic complete response rates in young women with BRCA1-positive breast cancers after neoadjuvant chemotherapy.* J Clin Oncol, 2010. 28(3): p. 375-9.
45. Byrski, T., et al., *Response to neoadjuvant therapy with cisplatin in BRCA1-positive breast cancer patients.* Breast Cancer Res Treat, 2009. 115(2): p. 359-63.
46. Kwei, K.A., et al., *Genomic instability in breast cancer: pathogenesis and clinical implications.* Mol Oncol, 2010. 4(3): p. 255-66.
47. Fong, P.C., et al., *Inhibition of poly(ADP-ribose) polymerase in tumours from BRCA mutation carriers.* N Engl J Med, 2009. 361(2): p. 123-34.

48. Jordan, M.A. and L. Wilson, *Microtubules as a target for anticancer drugs.* Nat Rev Cancer, 2004. 4(4): p. 253-65.
49. Rohena, C.C. and S.L. Mooberry, *Recent progress with microtubule stabilizers: new compounds, binding modes and cellular activities.* Nat Prod Rep, 2014. 31(3): p. 335-55.
50. Stanton, R.A., et al., *Drugs that target dynamic microtubules: a new molecular perspective.* Med Res Rev, 2011. 31(3): p. 443-81.
51. Lodish, H.F. and J.E. Darnell, *Molecular cell biology*. 4th ed2000, New York: W.H. Freeman. xxxix, 1084, G-17, I-36 p.
52. Westermann, S. and K. Weber, *Post-translational modifications regulate microtubule function.* Nat Rev Mol Cell Biol, 2003. 4(12): p. 938-47.
53. Dehmelt, L. and S. Halpain, *The MAP2/Tau family of microtubule-associated proteins.* Genome Biol, 2005. 6(1): p. 204.
54. Bernard-Marty, C., et al., *Microtubule-associated parameters as predictive markers of docetaxel activity in advanced breast cancer patients: results of a pilot study.* Clin Breast Cancer, 2002. 3(5): p. 341-5.
55. Rouzier, R., et al., *Microtubule-associated protein tau: a marker of paclitaxel sensitivity in breast cancer.* Proc Natl Acad Sci U S A, 2005. 102(23): p. 8315-20.
56. Bhat, K.M. and V. Setaluri, *Microtubule-associated proteins as targets in cancer chemotherapy.* Clin Cancer Res, 2007. 13(10): p. 2849-54.
57. Miceli, C., et al., *Cell cycle inhibition therapy that targets stathmin in in vitro and in vivo models of breast cancer.* Cancer Gene Ther, 2013. 20(5): p. 298-307.
58. Pasquier, E. and M. Kavallaris, *Microtubules: a dynamic target in cancer therapy.* IUBMB Life, 2008. 60(3): p. 165-70.
59. Wani, M.C., et al., *Plant antitumour agents. VI. The isolation and structure of taxol, a novel antileukemic and antitumour agent from Taxus brevifolia.* J Am Chem Soc, 1971. 93(9): p. 2325-7.
60. Horwitz, S.B., *Personal recollections on the early development of taxol.* J Nat Prod, 2004. 67(2): p. 136-8.
61. Downing, K.H., *Structural basis for the interaction of tubulin with proteins and drugs that affect microtubule dynamics.* Annu Rev Cell Dev Biol, 2000. 16: p. 89-111.
62. Diaz, J.F., et al., *Molecular recognition of taxol by microtubules. Kinetics and thermodynamics of binding of fluorescent taxol derivatives to an exposed site.* J Biol Chem, 2000. 275(34): p. 26265-76.
63. Derry, W.B., L. Wilson, and M.A. Jordan, *Substoichiometric binding of taxol suppresses microtubule dynamics.* Biochemistry, 1995. 34(7): p. 2203-11.
64. Blagosklonny, M.V., *Mitotic arrest and cell fate: why and how mitotic inhibition of*

transcription drives mutually exclusive events. Cell Cycle, 2007. 6(1): p. 70-4.

65. Andreassen, P.R., et al., *Tetraploid state induces p53-dependent arrest of nontransformed mammalian cells in G1.* Mol Biol Cell, 2001. 12(5): p. 1315-28.
66. Giannakakou, P., et al., *Low concentrations of paclitaxel induce cell type-dependent p53, p21 and G1/G2 arrest instead of mitotic arrest: molecular determinants of paclitaxel-induced cytotoxicity.* Oncogene, 2001. 20(29): p. 3806-13.
67. Bacus, S.S., et al., *Taxol-induced apoptosis depends on MAP kinase pathways (ERK and p38) and is independent of p53.* Oncogene, 2001. 20(2): p. 147-55.
68. Lin, H.L., et al., *Comparison of 2-methoxyestradiol-induced, docetaxel-induced, and paclitaxel-induced apoptosis in hepatoma cells and its correlation with reactive oxygen species.* Cancer, 2000. 89(5): p. 983-94.
69. Dumontet, C. and B.I. Sikic, *Mechanisms of action of and resistance to antitubulin agents: microtubule dynamics, drug transport, and cell death.* J Clin Oncol, 1999. 17(3): p. 1061-70.
70. Lanni, J.S., et al., *p53-independent apoptosis induced by paclitaxel through an indirect mechanism.* Proc Natl Acad Sci U S A, 1997. 94(18): p. 9679-83.
71. Fauzee, N.J., *Taxanes: promising anti-cancer drugs.* Asian Pac J Cancer Prev, 2011. 12(4): p. 837-51.
72. Torres, K. and S.B. Horwitz, *Mechanisms of Taxol-induced cell death are concentration dependent.* Cancer Res, 1998. 58(16): p. 3620-6.
73. Perera, P.Y., N. Qureshi, and S.N. Vogel, *Paclitaxel (Taxol)-induced NF-kappaB translocation in murine macrophages.* Infection and immunity, 1996. 64(3): p. 878-84.
74. Burkhart, C.A., et al., *Relationship between the structure of taxol and other taxanes on induction of tumour necrosis factor-alpha gene expression and cytotoxicity.* Cancer Res, 1994. 54(22): p. 5779-82.
75. Smoter, M., et al., *The role of Tau protein in resistance to paclitaxel.* Cancer Chemother Pharmacol, 2011. 68(3): p. 553-7.
76. Kavallaris, M., et al., *Taxol-resistant epithelial ovarian tumours are associated with altered expression of specific beta-tubulin isotypes.* The Journal of clinical investigation, 1997. 100(5): p. 1282-93.
77. Derry, W.B., et al., *Taxol differentially modulates the dynamics of microtubules assembled from unfractionated and purified beta-tubulin isotypes.* Biochemistry, 1997. 36(12): p. 3554-62.
78. Kavallaris, M., *Microtubules and resistance to tubulin-binding agents.* Nat Rev Cancer, 2010. 10(3): p. 194-204.
79. Gan, P.P., E. Pasquier, and M. Kavallaris, *Class III beta-tubulin mediates sensitivity to*

chemotherapeutic drugs in non small cell lung cancer. Cancer Res, 2007. 67(19): p. 9356-63.

80. Goncalves, A., et al., *Resistance to Taxol in lung cancer cells associated with increased microtubule dynamics.* Proc Natl Acad Sci U S A, 2001. 98(20): p. 11737-42.
81. Kamath, K., et al., *BetaIII-tubulin induces paclitaxel resistance in association with reduced effects on microtubule dynamic instability.* J Biol Chem, 2005. 280(13): p. 12902-7.
82. Dennis, K., et al., *Cloning and characterization of the 5'-flanking region of the rat neuron-specific Class III beta-tubulin gene.* Gene, 2002. 294(1-2): p. 269-77.
83. Cochrane, D.R., et al., *MicroRNA-200c mitigates invasiveness and restores sensitivity to microtubule-targeting chemotherapeutic agents.* Mol Cancer Ther, 2009. 8(5): p. 1055-66.
84. Lobert, S., B. Jefferson, and K. Morris, *Regulation of beta-tubulin isotypes by micro-RNA 100 in MCF7 breast cancer cells.* Cytoskeleton (Hoboken), 2011. 68(6): p. 355-62.
85. Monzo, M., et al., *Paclitaxel resistance in non-small-cell lung cancer associated with beta-tubulin gene mutations.* J Clin Oncol, 1999. 17(6): p. 1786-93.
86. Giannakakou, P., et al., *A common pharmacophore for epothilone and taxanes: molecular basis for drug resistance conferred by tubulin mutations in human cancer cells.* Proc Natl Acad Sci U S A, 2000. 97(6): p. 2904-9.
87. Hari, M., et al., *Mutations in alpha- and beta-tubulin that stabilize microtubules and confer resistance to colcemid and vinblastine.* Mol Cancer Ther, 2003. 2(7): p. 597-605.
88. Mandelkow, E. and E.M. Mandelkow, *Microtubules and microtubule-associated proteins.* Curr Opin Cell Biol, 1995. 7(1): p. 72-81.
89. Orr, G.A., et al., *Mechanisms of Taxol resistance related to microtubules.* Oncogene, 2003. 22(47): p. 7280-95.
90. Kanakkanthara, A. and J.H. Miller, *MicroRNAs: novel mediators of resistance to microtubule-targeting agents.* Cancer Treat Rev, 2013. 39(2): p. 161-70.
91. Zhou, M., et al., *MicroRNA-125b confers the resistance of breast cancer cells to paclitaxel through suppression of pro-apoptotic Bcl-2 antagonist killer 1 (Bak1) expression.* J Biol Chem, 2010. 285(28): p. 21496-507.
92. Shi, X.B., et al., *An androgen-regulated miRNA suppresses Bak1 expression and induces androgen-independent growth of prostate cancer cells.* Proc Natl Acad Sci U S A, 2007. 104(50): p. 19983-8.
93. Chen, Y., et al., *Inhibitory effects of miRNA-200c on chemotherapy-resistance and cell proliferation of gastric cancer SGC7901/DDP cells.* Chin J Cancer, 2010. 29(12): p. 1006-11.
94. Li, J., et al., *Overexpression of miR-22 reverses paclitaxel-induced chemoresistance*

through activation of PTEN signaling in p53-mutated colon cancer cells. Mol Cell Biochem, 2011. 357(1-2): p. 31-8.

95. Li, J., et al., *miR-203 reverses chemoresistance in p53-mutated colon cancer cells through downregulation of Akt2 expression.* Cancer Lett, 2011. 304(1): p. 52-9.
96. Ambudkar, S.V., et al., *P-glycoprotein: from genomics to mechanism.* Oncogene, 2003. 22(47): p. 7468-85.
97. Saraswathy, M. and S. Gong, *Different strategies to overcome multidrug resistance in cancer.* Biotechnol Adv, 2013. 31(8): p. 1397-407.
98. Choudhuri, S. and C.D. Klaassen, *Structure, function, expression, genomic organization, and single nucleotide polymorphisms of human ABCB1 (MDR1), ABCC (MRP), and ABCG2 (BCRP) efflux transporters.* Int J Toxicol, 2006. 25(4): p. 231-59.
99. Loo, T.W. and D.M. Clarke, *Recent progress in understanding the mechanism of P-glycoprotein-mediated drug efflux.* J Membr Biol, 2005. 206(3): p. 173-85.
100. Fojo, A., et al., *Molecular biology of drug resistance.* Breast Cancer Res Treat, 1987. 9(1): p. 5-16.
101. Fojo, A.T., et al., *Amplification of DNA sequences in human multidrug-resistant KB carcinoma cells.* Proc Natl Acad Sci U S A, 1985. 82(22): p. 7661-5.
102. Inaba, M. and R.K. Johnson, *Uptake and retention of adriamycin and daunorubicin by sensitive and anthracycline-resistant sublines of P388 leukemia.* Biochem Pharmacol, 1978. 27(17): p. 2123-30.
103. Yusa, K. and T. Tsuruo, *Reversal mechanism of multidrug resistance by verapamil: direct binding of verapamil to P-glycoprotein on specific sites and transport of verapamil outward across the plasma membrane of K562/ADM cells.* Cancer Res, 1989. 49(18): p. 5002-6.
104. Naito, M., et al., *Enhancement of cellular accumulation of cyclosporine by anti-P-glycoprotein monoclonal antibody MRK-16 and synergistic modulation of multidrug resistance.* J Natl Cancer Inst, 1993. 85(4): p. 311-6.
105. Naito, M., et al., *Enhancement of reversing effect of cyclosporin A on vincristine resistance by anti-P-glycoprotein monoclonal antibody MRK-16.* Jpn J Cancer Res, 1993. 84(5): p. 489-92.
106. Tanigawara, Y., et al., *Transport of digoxin by human P-glycoprotein expressed in a porcine kidney epithelial cell line (LLC-PK1).* J Pharmacol Exp Ther, 1992. 263(2): p. 840-5.
107. Ueda, K., et al., *Human P-glycoprotein transports cortisol, aldosterone, and dexamethasone, but not progesterone.* J Biol Chem, 1992. 267(34): p. 24248-52.
108. Wall, D.M., et al., *Rapid functional assay for multidrug resistance in human tumour cell*

lines using the fluorescent indicator fluo-3. J Natl Cancer Inst, 1991. 83(3): p. 206-7.

109. Loo, T.W. and D.M. Clarke, *The transmembrane domains of the human multidrug resistance P-glycoprotein are sufficient to mediate drug binding and trafficking to the cell surface.* J Biol Chem, 1999. 274(35): p. 24759-65.
110. Loo, T.W. and D.M. Clarke, *Covalent modification of human P-glycoprotein mutants containing a single cysteine in either nucleotide-binding fold abolishes drug-stimulated ATPase activity.* J Biol Chem, 1995. 270(39): p. 22957-61.
111. Walker, J.E., et al., *Distantly related sequences in the alpha- and beta-subunits of ATP synthase, myosin, kinases and other ATP-requiring enzymes and a common nucleotide binding fold.* EMBO J, 1982. 1(8): p. 945-51.
112. Loo, T.W. and D.M. Clarke, *Identification of residues in the drug-binding domain of human P-glycoprotein. Analysis of transmembrane segment 11 by cysteine-scanning mutagenesis and inhibition by dibromobimane.* J Biol Chem, 1999. 274(50): p. 35388-92.
113. Hennessy, M. and J.P. Spiers, *A primer on the mechanics of P-glycoprotein the multidrug transporter.* Pharmacol Res, 2007. 55(1): p. 1-15.
114. Jones, P.M. and A.M. George, *A new structural model for P-glycoprotein.* J Membr Biol, 1998. 166(2): p. 133-47.
115. Sharom, F.J., et al., *Exploring the structure and function of the P-glycoprotein multidrug transporter using fluorescence spectroscopic tools.* Semin Cell Dev Biol, 2001. 12(3): p. 257-65.
116. Wang, B., et al., *The promoter region of the MDR1 gene is largely invariant, but different single nucleotide polymorphism haplotypes affect MDR1 promoter activity differently in different cell lines.* Mol Pharmacol, 2006. 70(1): p. 267-76.
117. Madden, M.J., et al., *Identification of 5′ and 3′ sequences involved in the regulation of transcription of the human mdr1 gene in vivo.* J Biol Chem, 1993. 268(11): p. 8290-7.
118. van Groenigen, M., L.J. Valentijn, and F. Baas, *Identification of a functional initiator sequence in the human MDR1 promoter.* Biochim Biophys Acta, 1993. 1172(1-2): p. 138-46.
119. Bodor, M., E.J. Kelly, and R.J. Ho, *Characterization of the human MDR1 gene.* AAPS J, 2005. 7(1): p. E1-5.
120. Raguz, S., et al., *Production of P-glycoprotein from the MDR1 upstream promoter is insufficient to affect the response to first-line chemotherapy in advanced breast cancer.* Int J Cancer, 2008. 122(5): p. 1058-67.
121. Goldsmith, M.E., et al., *A Y-box consensus sequence is required for basal expression of the human multidrug resistance (mdr1) gene.* J Biol Chem, 1993. 268(8): p. 5856-60.
122. Cornwell, M.M. and D.E. Smith, *SP1 activates the MDR1 promoter through one of two*

distinct G-rich regions that modulate promoter activity. J Biol Chem, 1993. 268(26): p. 19505-11.

123. Xie, Y., et al., *Pim-1 kinase protects P-glycoprotein from degradation and enables its glycosylation and cell surface expression.* Mol Pharmacol, 2010. 78(2): p. 310-8.
124. Baker, E.K. and A. El-Osta, *MDR1, chemotherapy and chromatin remodeling.* Cancer Biol Ther, 2004. 3(9): p. 819-24.
125. Gottesman, M.M. and I. Pastan, *Biochemistry of multidrug resistance mediated by the multidrug transporter.* Annu Rev Biochem, 1993. 62: p. 385-427.
126. Fojo, A.T., et al., *Expression of a multidrug-resistance gene in human tumours and tissues.* Proc Natl Acad Sci U S A, 1987. 84(1): p. 265-9.
127. Scotto, K.W., *Transcriptional regulation of ABC drug transporters.* Oncogene, 2003. 22(47): p. 7496-511.
128. Johnson, R.A., T.A. Ince, and K.W. Scotto, *Transcriptional repression by p53 through direct binding to a novel DNA element.* J Biol Chem, 2001. 276(29): p. 27716-20.
129. Katayama, K., et al., *Inhibition of the mitogen-activated protein kinase pathway results in the down-regulation of P-glycoprotein.* Mol Cancer Ther, 2007. 6(7): p. 2092-102.
130. Bell, D.R., et al., *Detection of P-glycoprotein in ovarian cancer: a molecular marker associated with multidrug resistance.* J Clin Oncol, 1985. 3(3): p. 311-5.
131. Schneider, J., et al., *P-glycoprotein expression in treated and untreated human breast cancer.* Br J Cancer, 1989. 60(6): p. 815-8.
132. Bourhis, J., et al., *Expression of a human multidrug resistance gene in ovarian carcinomas.* Cancer Res, 1989. 49(18): p. 5062-5.
133. Roninson, I.B., *From amplification to function: the case of the MDR1 gene.* Mutat Res, 1992. 276(3): p. 151-61.
134. Silva, R., et al., *Modulation of P-glycoprotein efflux pump: induction and activation as a therapeutic strategy.* Pharmacol Ther, 2014.
135. Chen, G.K., et al., *CCAAT/enhancer-binding protein beta (nuclear factor for interleukin 6) transactivates the human MDR1 gene by interaction with an inverted CCAAT box in human cancer cells.* Mol Pharmacol, 2004. 65(4): p. 906-16.
136. Comerford, K.M., et al., *Hypoxia-inducible factor-1-dependent regulation of the multidrug resistance (MDR1) gene.* Cancer Res, 2002. 62(12): p. 3387-94.
137. Chen, Q., Y. Bian, and S. Zeng, *Involvement of AP-1 and NF-kappaB in the up-regulation of P-gp in vinblastine resistant Caco-2 cells.* Drug Metab Pharmacokinet, 2014. 29(2): p. 223-6.
138. Kim, R. and W.T. Beck, *Differences between drug-sensitive and -resistant human leukemic CEM cells in c-jun expression, AP-1 DNA-binding activity, and formation of*

Jun/Fos family dimers, and their association with internucleosomal DNA ladders after treatment with VM-26. Cancer Res, 1994. 54(18): p. 4958-66.

139. Tang, P.M., et al., *Photodynamic therapy inhibits P-glycoprotein mediated multidrug resistance via JNK activation in human hepatocellular carcinoma using the photosensitizer pheophorbide a.* Mol Cancer, 2009. 8: p. 56.
140. Henrique, R., et al., *Epigenetic regulation of MDR1 gene through post-translational histone modifications in prostate cancer.* BMC Genomics, 2013. 14: p. 898.
141. Reed, K., et al., *The temporal relationship between ABCB1 promoter hypomethylation, ABCB1 expression and acquisition of drug resistance.* The pharmacogenomics journal, 2010. 10(6): p. 489-504.
142. Zhu, H., et al., *Role of MicroRNA miR-27a and miR-451 in the regulation of MDR1/P-glycoprotein expression in human cancer cells.* Biochem Pharmacol, 2008. 76(5): p. 582-8.
143. Kovalchuk, O., et al., *Involvement of microRNA-451 in resistance of the MCF-7 breast cancer cells to chemotherapeutic drug doxorubicin.* Mol Cancer Ther, 2008. 7(7): p. 2152-9.
144. Bao, L., et al., *Increased expression of P-glycoprotein and doxorubicin chemoresistance of metastatic breast cancer is regulated by miR-298.* Am J Pathol, 2012. 180(6): p. 2490-503.
145. Zhu, X., et al., *miR-137 restoration sensitizes multidrug-resistant MCF-7/ADM cells to anticancer agents by targeting YB-1.* Acta Biochim Biophys Sin (Shanghai), 2013. 45(2): p. 80-6.
146. Wang, F., et al., *MicroRNA-19a/b regulates multidrug resistance in human gastric cancer cells by targeting PTEN.* Biochem Biophys Res Commun, 2013. 434(3): p. 688-94.
147. Mickley, L.A., et al., *Gene rearrangement: a novel mechanism for MDR-1 gene activation.* J Clin Invest, 1997. 99(8): p. 1947-57.
148. Davies, R., et al., *Regulation of P-glycoprotein 1 and 2 gene expression and protein activity in two MCF-7/Dox cell line subclones.* Br J Cancer, 1996. 73(3): p. 307-15.
149. Turton, N.J., et al., *Gene expression and amplification in breast carcinoma cells with intrinsic and acquired doxorubicin resistance.* Oncogene, 2001. 20(11): p. 1300-6.
150. Wang, Y.C., et al., *Regional activation of chromosomal arm 7q with and without gene amplification in taxane-selected human ovarian cancer cell lines.* Genes Chromosomes Cancer, 2006. 45(4): p. 365-74.
151. Yabuki, N., et al., *Gene amplification and expression in lung cancer cells with acquired paclitaxel resistance.* Cancer Genet Cytogenet, 2007. 173(1): p. 1-9.
152. Kitada, K., T. Yamasaki, and S. Aikawa, *Amplification of the ABCB1 region accompanied by a short sequence of 200bp from chromosome 2 in lung cancer cells.* Cancer Genet

Cytogenet, 2009. 194(1): p. 4-11.
153. Hattinger, C.M., et al., *Mechanisms of gene amplification and evidence of coamplification in drug-resistant human osteosarcoma cell lines.* Genes Chromosomes Cancer, 2009. 48(4): p. 289-309.
154. Chao, C.C., C.M. Ma, and S. Lin-Chao, *Co-amplification and over-expression of two mdr genes in a multidrug-resistant human colon carcinoma cell line.* FEBS Lett, 1991. 291(2): p. 214-8.
155. Struski, S., et al., *Cytogenetic characterization of chromosomal rearrangement in a human vinblastine-resistant CEM cell line: use of comparative genomic hybridization and fluorescence in situ hybridization.* Cancer Genet Cytogenet, 2002. 132(1): p. 51-4.
156. Zhou, D.C., et al., *Sequential emergence of MRP- and MDR1-gene over-expression as well as MDR1-gene translocation in homoharringtonine-selected K562 human leukemia cell lines.* Int J Cancer, 1996. 65(3): p. 365-71.
157. Pang, E., et al., *Karyotypic imbalances and differential gene expressions in the acquired doxorubicin resistance of hepatocellular carcinoma cells.* Lab Invest, 2005. 85(5): p. 664-74.
158. Flahaut, M., et al., *Molecular cytogenetic characterization of doxorubicin-resistant neuroblastoma cell lines: evidence that acquired multidrug resistance results from a unique large amplification of the 7q21 region.* Genes Chromosomes Cancer, 2006. 45(5): p. 495-508.
159. Obara, K., et al., *Comparative genomic hybridization study of genetic changes associated with vindesine resistance in esophageal carcinoma.* Int J Oncol, 2002. 20(2): p. 255-60.
160. van Dekken, H., et al., *Genomic array and expression analysis of frequent high-level amplifications in adenocarcinomas of the gastro-esophageal junction.* Cancer Genet Cytogenet, 2006. 166(2): p. 157-62.
161. Struski, S., M. Doco-Fenzy, and P. Cornillet-Lefebvre, *Compilation of published comparative genomic hybridization studies.* Cancer Genet Cytogenet, 2002. 135(1): p. 63-90.
162. Knutsen, T., et al., *Cytogenetic and molecular characterization of random chromosomal rearrangements activating the drug resistance gene, MDR1/P-glycoprotein, in drug-selected cell lines and patients with drug refractory ALL.* Genes Chromosomes Cancer, 1998. 23(1): p. 44-54.
163. Cohen, S., *The epidermal growth factor (EGF).* Cancer, 1983. 51(10): p. 1787-91.
164. Brand, T.M., et al., *The nuclear epidermal growth factor receptor signaling network and its role in cancer.* Discov Med, 2011. 12(66): p. 419-32.
165. Jura, N., et al., *Structural analysis of the catalytically inactive kinase domain of the human*

EGF receptor 3. Proc Natl Acad Sci U S A, 2009. 106(51): p. 21608-13.
166. Lax, I., et al., *Noncontiguous regions in the extracellular domain of EGF receptor define ligand-binding specificity.* Cell Regul, 1991. 2(5): p. 337-45.
167. Grant, S., L. Qiao, and P. Dent, *Roles of ERBB family receptor tyrosine kinases, and downstream signaling pathways, in the control of cell growth and survival.* Front Biosci, 2002. 7: p. d376-89.
168. Burgess, A.W., *EGFR family: structure physiology signalling and therapeutic targets.* Growth Factors, 2008. 26(5): p. 263-74.
169. Okines, A., D. Cunningham, and I. Chau, *Targeting the human EGFR family in esophagogastric cancer.* Nat Rev Clin Oncol, 2011. 8(8): p. 492-503.
170. Schulze, W.X., L. Deng, and M. Mann, *Phosphotyrosine interactome of the ErbB-receptor kinase family.* Mol Syst Biol, 2005. 1: p. 2005 0008.
171. Klein, P., et al., *A structure-based model for ligand binding and dimerization of EGF receptors.* Proc Natl Acad Sci U S A, 2004. 101(4): p. 929-34.
172. Chong, C.R. and P.A. Janne, *The quest to overcome resistance to EGFR-targeted therapies in cancer.* Nat Med, 2013. 19(11): p. 1389-400.
173. Martinazzi, M., et al., *Relationships between epidermal growth factor receptor (EGF-R) and other predictors of prognosis in breast carcinomas. An immunohistochemical study.* Pathologica, 1993. 85(1100): p. 637-44.
174. Lo, H.W., et al., *Novel prognostic value of nuclear epidermal growth factor receptor in breast cancer.* Cancer Res, 2005. 65(1): p. 338-48.
175. Nakajima, H., et al., *Protein expression, gene amplification, and mutational analysis of EGFR in triple-negative breast cancer.* Breast Cancer (Dove Med Press), 2014. 21(1): p. 66-74.
176. Gumuskaya, B., et al., *EGFR expression and gene copy number in triple-negative breast carcinoma.* Cancer Genet Cytogenet, 2010. 203(2): p. 222-9.
177. Reis-Filho, J.S., et al., *EGFR amplification and lack of activating mutations in metaplastic breast carcinomas.* J Pathol, 2006. 209(4): p. 445-53.
178. Park, H.S., et al., *High EGFR gene copy number predicts poor outcome in triple-negative breast cancer.* Mod Pathol, 2014. 27(9): p. 1212-22.
179. Glover, K.Y., R. Perez-Soler, and V.A. Papadimitradopoulou, *A review of small-molecule epidermal growth factor receptor-specific tyrosine kinase inhibitors in development for non-small cell lung cancer.* Semin Oncol, 2004. 31(1 Suppl 1): p. 83-92.
180. Janmaat, M.L. and G. Giaccone, *Small-molecule epidermal growth factor receptor tyrosine kinase inhibitors.* Oncologist, 2003. 8(6): p. 576-86.
181. Liao, J., et al., *Lapatinib: new opportunities for management of breast cancer.* Breast

Cancer (Dove Med Press), 2010. 2: p. 79-91.
182. Wang, X., et al., *The Potential of panHER Inhibition in Cancer.* Front Oncol, 2015. 5: p. 2.
183. Chu, Q.S., et al., *A phase I and pharmacokinetic study of lapatinib in combination with letrozole in patients with advanced cancer.* Clin Cancer Res, 2008. 14(14): p. 4484-90.
184. Burstein, H.J., et al., *A phase II study of lapatinib monotherapy in chemotherapy-refractory HER2-positive and HER2-negative advanced or metastatic breast cancer.* Ann Oncol, 2008. 19(6): p. 1068-74.
185. Chen, Y.J., et al., *Lapatinib-induced NF-kappaB activation sensitizes triple-negative breast cancer cells to proteasome inhibitors.* Breast Cancer Res, 2013. 15(6): p. R108.
186. Liu, T., et al., *Combinatorial effects of lapatinib and rapamycin in triple-negative breast cancer cells.* Mol Cancer Ther, 2011. 10(8): p. 1460-9.
187. http://www.drugbank.ca/drugs/db01259.
188. Canonici, A., et al., *Neratinib overcomes trastuzumab resistance in HER2 amplified breast cancer.* Oncotarget, 2013. 4(10): p. 1592-605.
189. http://pubchem.ncbi.nlm.nih.gov/compound/Neratinib#section=Top.
190. Joshi, A.D., et al., *Evaluation of tyrosine kinase inhibitor combinations for glioblastoma therapy.* PLoS One, 2012. 7(10): p. e44372.
191. Bauer, J.A., et al., *RNA interference (RNAi) screening approach identifies agents that enhance paclitaxel activity in breast cancer cells.* Breast Cancer Res, 2010. 12(3): p. R41.
192. Greshock, J., et al., *Molecular target class is predictive of in vitro response profile.* Cancer Res, 2010. 70(9): p. 3677-86.
193. Kao, J., et al., *Molecular profiling of breast cancer cell lines defines relevant tumour models and provides a resource for cancer gene discovery.* PLoS One, 2009. 4(7): p. e6146.
194. Lasfargues, E.Y. and L. Ozzello, *Cultivation of human breast carcinomas.* J Natl Cancer Inst, 1958. 21(6): p. 1131-47.
195. Lebeau, J. and G. Goubin, *Amplification of the epidermal growth factor receptor gene in the BT20 breast carcinoma cell line.* Int J Cancer, 1987. 40(2): p. 189-91.
196. Ignatoski, K.M. and S.P. Ethier, *Constitutive activation of pp125fak in newly isolated human breast cancer cell lines.* Breast Cancer Res Treat, 1999. 54(2): p. 173-82.
197. Filmus, J., et al., *MDA-468, a human breast cancer cell line with a high number of epidermal growth factor (EGF) receptors, has an amplified EGF receptor gene and is growth inhibited by EGF.* Biochem Biophys Res Commun, 1985. 128(2): p. 898-905.
198. Stefansson, O.A., et al., *BRCA1 epigenetic inactivation predicts sensitivity to platinum-based chemotherapy in breast and ovarian cancer.* Epigenetics, 2012. 7(11): p. 1225-9.

199. Biedler, J.L. and H. Riehm, *Cellular resistance to actinomycin D in Chinese hamster cells in vitro: cross-resistance, radioautographic, and cytogenetic studies.* Cancer Res, 1970. 30(4): p. 1174-84.
200. McDermott, M., et al., *In vitro Development of Chemotherapy and Targeted Therapy Drug-Resistant Cancer Cell Lines: A Practical Guide with Case Studies.* Front Oncol, 2014. 4: p. 40.
201. Lee, E.A., et al., *Inactivation of the mitotic checkpoint as a determinant of the efficacy of microtubule-targeted drugs in killing human cancer cells.* Molecular cancer therapeutics, 2004. 3(6): p. 661-9.
202. Wang, X., et al., *Cell-cycle synchronization reverses Taxol resistance of human ovarian cancer cell lines.* Cancer cell international, 2013. 13(1): p. 77.
203. Perou, C.M., *Molecular stratification of triple-negative breast cancers.* The oncologist, 2011. 16 Suppl 1: p. 61-70.
204. Noah, T.K., et al., *SPDEF functions as a colorectal tumour suppressor by inhibiting beta-catenin activity.* Gastroenterology, 2013. 144(5): p. 1012-1023 e6.
205. Pollack, J.R., et al., *Microarray analysis reveals a major direct role of DNA copy number alteration in the transcriptional program of human breast tumours.* Proc Natl Acad Sci U S A, 2002. 99(20): p. 12963-8.
206. Phillips, J.L., et al., *The consequences of chromosomal aneuploidy on gene expression profiles in a cell line model for prostate carcinogenesis.* Cancer Res, 2001. 61(22): p. 8143-9.
207. Ulger, C., et al., *Comprehensive genome-wide comparison of DNA and RNA level scan using microarray technology for identification of candidate cancer-related genes in the HL-60 cell line.* Cancer Genet Cytogenet, 2003. 147(1): p. 28-35.
208. Hyman, E., et al., *Impact of DNA amplification on gene expression patterns in breast cancer.* Cancer Res, 2002. 62(21): p. 6240-5.
209. Liu, B., et al., *Cross-reactivity of C219 anti-p170(mdr-1) antibody with p185(c-erbB2) in breast cancer cells: cautions on evaluating p170(mdr-1).* J Natl Cancer Inst, 1997. 89(20): p. 1524-9.
210. Chan, H.S. and V. Ling, *Anti-P-glycoprotein antibody C219 cross-reactivity with c-erbB2 protein: diagnostic and clinical implications.* J Natl Cancer Inst, 1997. 89(20): p. 1473-6.
211. Randle, R.A., et al., *Role of the highly structured 5'-end region of MDR1 mRNA in P-glycoprotein expression.* Biochem J, 2007. 406(3): p. 445-55.
212. Koromilas, A.E., A. Lazaris-Karatzas, and N. Sonenberg, *mRNAs containing extensive secondary structure in their 5′ non-coding region translate efficiently in cells overexpressing initiation factor eIF-4E.* EMBO J, 1992. 11(11): p. 4153-8.

213. Theile, D., B. Staffen, and J. Weiss, *ATP-binding cassette transporters as pitfalls in selection of transgenic cells.* Anal Biochem, 2010. 399(2): p. 246-50.
214. Huang da, W., B.T. Sherman, and R.A. Lempicki, *Systematic and integrative analysis of large gene lists using DAVID bioinformatics resources.* Nat Protoc, 2009. 4(1): p. 44-57.
215. Yarden, Y. and M.X. Sliwkowski, *Untangling the ErbB signalling network.* Nat Rev Mol Cell Biol, 2001. 2(2): p. 127-37.
216. Ferguson, K.M., et al., *Extracellular domains drive homo- but not hetero-dimerization of erbB receptors.* The EMBO journal, 2000. 19(17): p. 4632-43.
217. Rubin, I. and Y. Yarden, *The basic biology of HER2.* Annals of oncology : official journal of the European Society for Medical Oncology / ESMO, 2001. 12 Suppl 1: p. S3-8.
218. Wosikowski, K., et al., *Altered gene expression in drug-resistant human breast cancer cells.* Clin Cancer Res, 1997. 3(12 Pt 1): p. 2405-14.
219. Dickstein, B.M., K. Wosikowski, and S.E. Bates, *Increased resistance to cytotoxic agents in ZR75B human breast cancer cells transfected with epidermal growth factor receptor.* Mol Cell Endocrinol, 1995. 110(1-2): p. 205-11.
220. Eichhorn, P.J., et al., *Phosphatidylinositol 3-kinase hyperactivation results in lapatinib resistance that is reversed by the mTOR/phosphatidylinositol 3-kinase inhibitor NVP-BEZ235.* Cancer Res, 2008. 68(22): p. 9221-30.
221. Junttila, T.T., et al., *Ligand-independent HER2/HER3/PI3K complex is disrupted by trastuzumab and is effectively inhibited by the PI3K inhibitor GDC-0941.* Cancer Cell, 2009. 15(5): p. 429-40.
222. Rabindran, S.K., et al., *Antitumour activity of HKI-272, an orally active, irreversible inhibitor of the HER-2 tyrosine kinase.* Cancer Res, 2004. 64(11): p. 3958-65.
223. Wainberg, Z.A., et al., *Lapatinib, a dual EGFR and HER2 kinase inhibitor, selectively inhibits HER2-amplified human gastric cancer cells and is synergistic with trastuzumab in vitro and in vivo.* Clin Cancer Res, 2010. 16(5): p. 1509-19.
224. Shi, Z., et al., *Erlotinib (Tarceva, OSI-774) antagonizes ATP-binding cassette subfamily B member 1 and ATP-binding cassette subfamily G member 2-mediated drug resistance.* Cancer Res, 2007. 67(22): p. 11012-20.
225. Dai, C.L., et al., *Lapatinib (Tykerb, GW572016) reverses multidrug resistance in cancer cells by inhibiting the activity of ATP-binding cassette subfamily B member 1 and G member 2.* Cancer Res, 2008. 68(19): p. 7905-14.
226. Dai, C.L., et al., *Sensitization of ABCG2-overexpressing cells to conventional chemotherapeutic agent by sunitinib was associated with inhibiting the function of ABCG2.* Cancer Lett, 2009. 279(1): p. 74-83.
227. Zhao, X.Q., et al., *Neratinib reverses ATP-binding cassette B1-mediated chemotherapeutic*

drug resistance in vitro, in vivo, and ex vivo. Mol Pharmacol, 2012. 82(1): p. 47-58.

228. Dixit, M., et al., *Abrogation of cisplatin-induced programmed cell death in human breast cancer cells by epidermal growth factor antisense RNA.* J Natl Cancer Inst, 1997. 89(5): p. 365-73.
229. Baselga, J., et al., *Antitumour effects of doxorubicin in combination with anti-epidermal growth factor receptor monoclonal antibodies.* J Natl Cancer Inst, 1993. 85(16): p. 1327-33.
230. Sirotnak, F.M., et al., *Efficacy of cytotoxic agents against human tumour xenografts is markedly enhanced by coadministration of ZD1839 (Iressa), an inhibitor of EGFR tyrosine kinase.* Clin Cancer Res, 2000. 6(12): p. 4885-92.
231. Ciardiello, F., et al., *ZD1839 (IRESSA), an EGFR-selective tyrosine kinase inhibitor, enhances taxane activity in bcl-2 overexpressing, multidrug-resistant MCF-7 ADR human breast cancer cells.* Int J Cancer, 2002. 98(3): p. 463-9.
232. Basu, A. and R.W. Evans, *Comparison of effects of growth factors and protein kinase C activators on cellular sensitivity to cis-diamminedichloroplatinum(II).* Int J Cancer, 1994. 58(4): p. 587-91.
233. Christen, R.D., et al., *Epidermal growth factor regulates the in vitro sensitivity of human ovarian carcinoma cells to cisplatin.* J Clin Invest, 1990. 86(5): p. 1632-40.
234. Kwok, T., et al., *Analysis of an Escherichia coli mutant TyrR protein with impaired capacity for tyrosine-mediated repression, but still able to activate at sigma 70 promoters.* Mol Microbiol, 1995. 17(3): p. 471-81.
235. Frankel, A. and G.B. Mills, *Peptide and lipid growth factors decrease cis-diamminedichloroplatinum-induced cell death in human ovarian cancer cells.* Clin Cancer Res, 1996. 2(8): p. 1307-13.
236. Richert, N.D., et al., *Stability and covalent modification of P-glycoprotein in multidrug-resistant KB cells.* Biochemistry, 1988. 27(20): p. 7607-13.
237. Huizing, M.T., et al., *Pharmacokinetics of paclitaxel and metabolites in a randomized comparative study in platinum-pretreated ovarian cancer patients.* J Clin Oncol, 1993. 11(11): p. 2127-35.
238. Blagosklonny, M.V. and T. Fojo, *Molecular effects of paclitaxel: myths and reality (a critical review).* Int J Cancer, 1999. 83(2): p. 151-6.
239. Wu, G.S. and W.S. El-Deiry, *Apoptotic death of tumour cells correlates with chemosensitivity, independent of p53 or bcl-2.* Clin Cancer Res, 1996. 2(4): p. 623-33.
240. Bhalla, K., et al., *Taxol induces internucleosomal DNA fragmentation associated with programmed cell death in human myeloid leukemia cells.* Leukemia, 1993. 7(4): p. 563-8.
241. Fan, W., *Possible mechanisms of paclitaxel-induced apoptosis.* Biochem Pharmacol, 1999.

57(11): p. 1215-21.
242. Khosravi, S., et al., *eIF4E is an adverse prognostic marker of melanoma patient survival by increasing melanoma cell invasion.* J Invest Dermatol, 2015. 135(5): p. 1358-67.
243. Zheng, J., et al., *Phosphorylated Mnk1 and eIF4E are associated with lymph node metastasis and poor prognosis of nasopharyngeal carcinoma.* PLoS One, 2014. 9(2): p. e89220.
244. Burness, M.L., T.A. Grushko, and O.I. Olopade, *Epidermal growth factor receptor in triple-negative and basal-like breast cancer: promising clinical target or only a marker?* Cancer J, 2010. 16(1): p. 23-32.
245. Nogi, H., et al., *EGFR as paradoxical predictor of chemosensitivity and outcome among triple-negative breast cancer.* Oncol Rep, 2009. 21(2): p. 413-7.
246. Masuda, H., et al., *Role of epidermal growth factor receptor in breast cancer.* Breast Cancer Res Treat, 2012. 136(2): p. 331-45.
247. von Minckwitz, G., et al., *A multicentre phase II study on gefitinib in taxane- and anthracycline-pretreated metastatic breast cancer.* Breast Cancer Res Treat, 2005. 89(2): p. 165-72.
248. Green, M.D., et al., *Gefitinib treatment in hormone-resistant and hormone receptor-negative advanced breast cancer.* Ann Oncol, 2009. 20(11): p. 1813-7.
249. Burris, H.A., 3rd, et al., *A phase I and pharmacokinetic study of oral lapatinib administered once or twice daily in patients with solid malignancies.* Clin Cancer Res, 2009. 15(21): p. 6702-8.
250. Dienstmann, R., et al., *Drug development to overcome resistance to EGFR inhibitors in lung and colorectal cancer.* Mol Oncol, 2012. 6(1): p. 15-26.
251. Shaib, W., R. Mahajan, and B. El-Rayes, *Markers of resistance to anti-EGFR therapy in colorectal cancer.* J Gastrointest Oncol, 2013. 4(3): p. 308-18.
252. Harris, L.N., et al., *Induction of sensitivity to doxorubicin and etoposide by transfection of MCF-7 breast cancer cells with heregulin beta-2.* Clin Cancer Res, 1998. 4(4): p. 1005-12.
253. Oliveras-Ferraros, C., et al., *Cross-suppression of EGFR ligands amphiregulin and epiregulin and de-repression of FGFR3 signalling contribute to cetuximab resistance in wild-type KRAS tumour cells.* Br J Cancer, 2012. 106(8): p. 1406-14.
254. Pu, Y.S., et al., *Interleukin-6 is responsible for drug resistance and anti-apoptotic effects in prostatic cancer cells.* Prostate, 2004. 60(2): p. 120-9.